2. SITE 585[1]

Shipboard Scientific Party[2]

HOLE 585

Date occupied: 1122Z, 18 October 1982

Date departed: 1805Z, 26 October 1982

Time on hole: 8 days, 6 hr., 43 min.

Position: 13°29.00′N; 156°48.91′E

Water depth (sea level; corrected m, echo-sounding): 6109

Water depth (rig floor; corrected m, echo-sounding): 6119

Bottom felt (m, drill pipe): 6122.3

Penetration (m): 763.7

Number of cores: 55

Total length of cored section (m): 514.6

Total core recovered (m): 164.5

Core recovery (%): 32

Oldest sediment cored:
Depth sub-bottom (m): 763.7
Nature: Volcanogenic turbidites
Age: late Aptian
Measured velocity (km/s): 2.5

Basement: Not reached

HOLE 585A

Date occupied: 1805Z, 26 October 1982

Date departed: 1709Z, 2 November 1982

Time on hole: 6 days, 23 hr., 4 min.

Position: 13°29.00′N; 156°48.91′E

Water depth (sea level; corrected m, echo-sounding): 6109

Water depth (rig floor; corrected m, echo-sounding): 6119

Bottom felt (m, drill pipe): 6122.3

Penetration (m): 892.8

Number of cores: 22

Total length of cored section (m): 208.8

Total core recovered (m): 101.5

Core recovery (%): 48.6

Oldest sediment cored:
Depth sub-bottom (m): 892.8
Nature: Volcanogenic turbidites
Age: late Aptian
Measured velocity (km/s): 3.2–3.5

Basement: Not reached

Principal results (Hole 585): Hole 585 (13°29.00′N, 156°48.91′E) was drilled as a single-bit attempt to reach the Jurassic basalt crust that presumably underlies the East Mariana Basin. Drilling extended from 18 to 26 October 1982, in a water depth of 6109 corrected meters. The total thickness of the section penetrated was 763.7 m. Fifty-five cores were taken from a total cored section of 514.6 m. Total core recovered was 164.5 m, giving a recovery rate of 32%. Core 1 was taken from 0.0 to 6.8 m and Wash Core H1 was taken from 6.8 to 255.9 m; thereafter the hole was continuously cored. Six lithologic units were recognized.

Unit I. From 0.0 to 6.8 m, this unit consists of Recent to lower Pleistocene brown clay and nannofossil ooze. Next is the unknown interval that was washed.

Unit II. From 256 to 399 m, middle Eocene to upper Campanian nannofossil chalk, silicified limestone, chert, and zeolitic claystone were recovered. A lower Eocene altered ash bed was cored in this unit.

Unit III. From 399 to 426 m, Maestrichtian to upper Campanian zeolitic claystone and nannofossil-bearing clayey chalk and chert were recovered.

Unit IV. Poor recovery occurred from 426 to 485 m, but apparently this unit consists of abundant chert in Campanian zeolitic claystone.

Unit V consists of three subunits: *Subunit VA* extends from 485 to 504 m and is made up of Campanian zeolitic claystone, moderately bioturbated with silty laminae marking turbidite layers. *Subunit VB* ranges from 504 to 550 m and is dark gray claystone with variable amounts of radiolarians in sandy laminae. This subunit spans the middle Cenomanian to Santonian. *Subunit VC:* extends from 550 to 590 m; it is made up of interbedded claystone, nannofossil-bearing claystone, radiolarian-rich limestone and siltstone; laminated and graded intervals are common. The subunit is middle Albian to middle Cenomanian.

Unit VI. This unit extends from 590 to 763.7 m and is composed of graded sequences of volcanogenic siltstones, sandstones, and breccias made up largely of hyaloclastite debris; reworked ooids and skeletal carbonate debris of echinoids and mollusks are common. The unit is upper Aptian to middle Albian.

The fossil assemblages and sedimentary structures indicate that almost the entire section is the product of the redeposition of sediment through the action of turbidity currents directed into the East Mariana Basin. The presence of abyssal benthic foraminifers shows that the Basin was deep as early as the late Aptian; bathyal and particularly neritic foraminifers, the latter of which are common in the Albian and Aptian strata, point to the presence of neighboring shallower slopes. Aptian and Albian volcaniclastic debris accumulated at a rate of at least 40 m/m.y.: this high rate and the abundance of carbonate debris derived from shallow-water platforms indicate that a major volcanic edifice building phase, during which islands formed, took place around the Basin during the Aptian and perhaps the Albian; these edifices have been subsiding since

[1] Moberly, R., Schlanger, S. O., et al., *Init. Repts. DSDP*, 89: Washington (U.S. Govt. Printing Office).

[2] Ralph Moberly (Co-Chief Scientist), Hawaii Institute of Geophysics, University of Hawaii, Honolulu, HI; Seymour O. Schlanger (Co-Chief Scientist), Department of Geological Sciences, Northwestern University, Evanston, IL; Miriam Baltuck, Deep Sea Drilling Project, Scripps Institution of Oceanography, La Jolla, CA (present address: Geology Department, Tulane University, New Orleans, LA); James A. Bergen, Department of Geology, Florida State University, Tallahassee, FL (present address: UNOCAL, P.O. Box 76, Brea, CA 92631); Walter Dean, U.S. Geological Survey, Denver Federal Center, Denver, CO; Peter A. Floyd, Department of Geology, University of Keele, Keele, Staffordshire, United Kingdom; Naoyuki Fujii, Department of Earth Sciences, Kobe University, Kobe, Japan; Janet A. Haggerty, Department of Geosciences, University of Tulsa, Tulsa, OK; James G. Ogg, Department of Geology and Geophysics, University of Wyoming, Laramie, WY; Isabella Premoli Silva, Istituto di Paleontologia, Milan, Italy (present address: Dipartimento di Scienze della Terra, Università di Milano, Milan, Italy); André Schaaf, Institut de Geologie, Strasbourg, France (present address: Université de Bretagne Occidentale, GIS Océanologie et Géodynamique, 29287 Brest Cedex France); Rainer G. Schaefer, Institut für Erdöl und Organische Geochemie, KFA Jülich, Federal Republic of Germany; William V. Sliter, Branch of Paleontology and Stratigraphy, U.S. Geological Survey, Reston, VA (present address: U.S. Geological Survey, Menlo Park, CA); Jill M. Whitman, Geological Research Division, Scripps Institution of Oceanography, La Jolla, CA.

the Late Cretaceous. In the latest Cenomanian to earliest Turonian the Basin was the site of deposition of organic carbon-rich sediments resulting from a marked oxygen deficiency in the water column. This oxygen deficiency is taken to be a manifestation of the global Cenomanian-Turonian "oceanic anoxic event." Paleomagnetic measurements show that the site was at about 5.1°S during the Turonian and about 8.2° during deposition of middle and early Albian volcaniclastic turbidites.

Principal results (Hole 585A): Hole 585A (13°29.00'N, 156°48.91'E) was drilled in a second single-bit attempt to reach basalt basement below the East Mariana Basin from 26 October to 2 November 1982, in a water depth of 6109 m. Twenty-two cores were taken, but the largest part of the section was washed to a depth of 772 m to save the bit and exceed the penetration achieved in Hole 585. The cores taken above that depth, however, did indicate that the sedimentary section was indeed highly resedimented in nature. The total length of the cored section was 208.8 m; total core recovery was 101.5 m, 48.6% of the cored section. The lithologic units in Hole 585A are identical to those in Hole 585. A series of continuous cores—585A-5 through -10—were taken between 502.6 and 561.8 m in Coniacian to Cenomanian strata in an attempt to recore the organic carbon-rich sediments found in Core 585-32. The attempt was successful and a thin sediment layer rich in organic carbon was recovered in Sample 585A-8,CC at or a few centimeters above the Cenomanian/Turonian boundary. The sediments in 585A from 772.1 to 892.8 m are graded sequences of hyaloclastite-rich volcaniclastic breccias, sandstones, and siltstones; the coarser portions contain basalt fragments of cobble size. Ooids and skeletal debris of algae, bryozoans, gastropods, and rudists are abundant; orbitolinid foraminifers are also common, as are fragments of calcite-cemented, sorted, ooid- and orbitolinid-bearing grainstone. This shallow-water carbonate debris is more diverse in nature than the debris in Hole 585. The deepest part of the section is upper Aptian. The section of 585A below the total depth of 763.7 m of Hole 585 thus records redeposition of coarser and more diverse volcanic and biogenic carbonate debris than that seen in the upper Aptian and lower Albian in Hole 585.

Acoustic velocity measurements show an increase in V_p from an average of 2.18 to 3.2 km/s at a depth of 800 m in the volcaniclastic section; perhaps this level is the "9-second" reflector of the site survey, which was believed to be the top of the Jurassic strata.

BACKGROUND AND OBJECTIVES

Introduction

As of October 1982 deep-sea drilling carried out by the JOIDES-IPOD program had not succeeded in sampling Jurassic sediments that could reveal paleoenvironmental conditions in the Pacific Mesozoic superocean. Remnants of sediment deposited on Jurassic crust presumably remain buried in the western Pacific between the northern Marshall Islands and the Mariana Trench. Leg 89 was designed to recover such sediments of probable Bathonian-Callovian age (150–160 Ma), which would enable us to compare Mesozoic superocean strata to Atlantic and Tethyan sediments of similar age deposited along continental margins. One result of drilling in the Pacific basin has been the discovery that the area between the Line Islands and the western bordering trench system was the site of intensive volcanic activity in middle to Late Cretaceous. Therefore a second objective of Leg 89 was to attempt to investigate further the timing and extent of Cretaceous midplate volcanism.

Paleoenvironmental Objectives

Major paleoceanographic changes are thought to have occurred when the configuration of the continents and oceans evolved from a pattern dominated by a single supercontinent and a single superocean to one of fragmented continents and several oceans.

The Middle Jurassic pelagic sediment record comes primarily from sections outcropping in the Tertiary fold belts where they correspond to Tethyan continental margins in various stages of evolution; sediments that contain this record have never been sampled from any deep oceanic basin. A major controversy centers on whether or not these sections can be regarded as truly representative of the early Mesozoic world ocean. A consequence of this enormous gap in our knowledge is that all biostratigraphic data from the early Mesozoic remain biased toward fossil assemblages from nearshore and marginal areas of ocean basins in the early stages of their evolution.

There is ample evidence from magnetic data (Fig. 1) that portions of the oceanic crust in the western Pacific are at least as old as Middle to possibly Early Jurassic, but no complete record of the sediment sequence overlying oceanic crust in this area has been obtained so far. Geophysical data and Deep Sea Drilling Project cores also suggest that these portions of the seafloor were actually generated at moderate to low latitudes in the Southern Hemisphere away from any large continental landmass. We expected that this Mesozoic sediment record could be recovered at Site MZP-6 in the deep East Mariana Basin (Fig. 2).

The specific paleoenvironmental questions to be addressed on Leg 89 included the following:

1. How did the early evolution and radiation of the oceanic plankton (coccoliths, radiolarians, benthic and planktonic foraminifers) influence the composition of pelagic sediments and how do these fauna and flora reflect Mesozoic ocean chemistry?
2. Did the opening of the North Atlantic Ocean affect the circulation and chemistry of the world ocean in a manner similar to that which has been proposed for the opening of the South Atlantic?
3. Are "pelagic" sediments exposed in Tertiary fold belts (ribbon radiolarites, ammonitico rosso, etc.) characteristic of open ocean environments?
4. Can we establish an early Mesozoic pelagic bio- and magnetochronology?
5. Were the mid-Cretaceous sedimentary environments in the deep Pacific better oxygenated than those in the Atlantic and Indian oceans?

Although numerous outstanding Mesozoic paleoenvironmental objectives, such as the nature of the Tertiary/Cretaceous boundary, the mechanisms behind mid-Cretaceous oceanic anoxic events, the occurrence of water exchange with partially or completely isolated basins, the structure and stability of deep water masses, and the chemical fractionation between major ocean basins, remain important problems in other oceanic basins, the basic paleoenvironmental objective of Leg 89 was the recovery of a truly oceanic Jurassic sediment record, which could only have been preserved in the western Pacific.

Midplate Volcanism

One of the major results of DSDP drilling has been the discovery in the central and western Pacific basin of

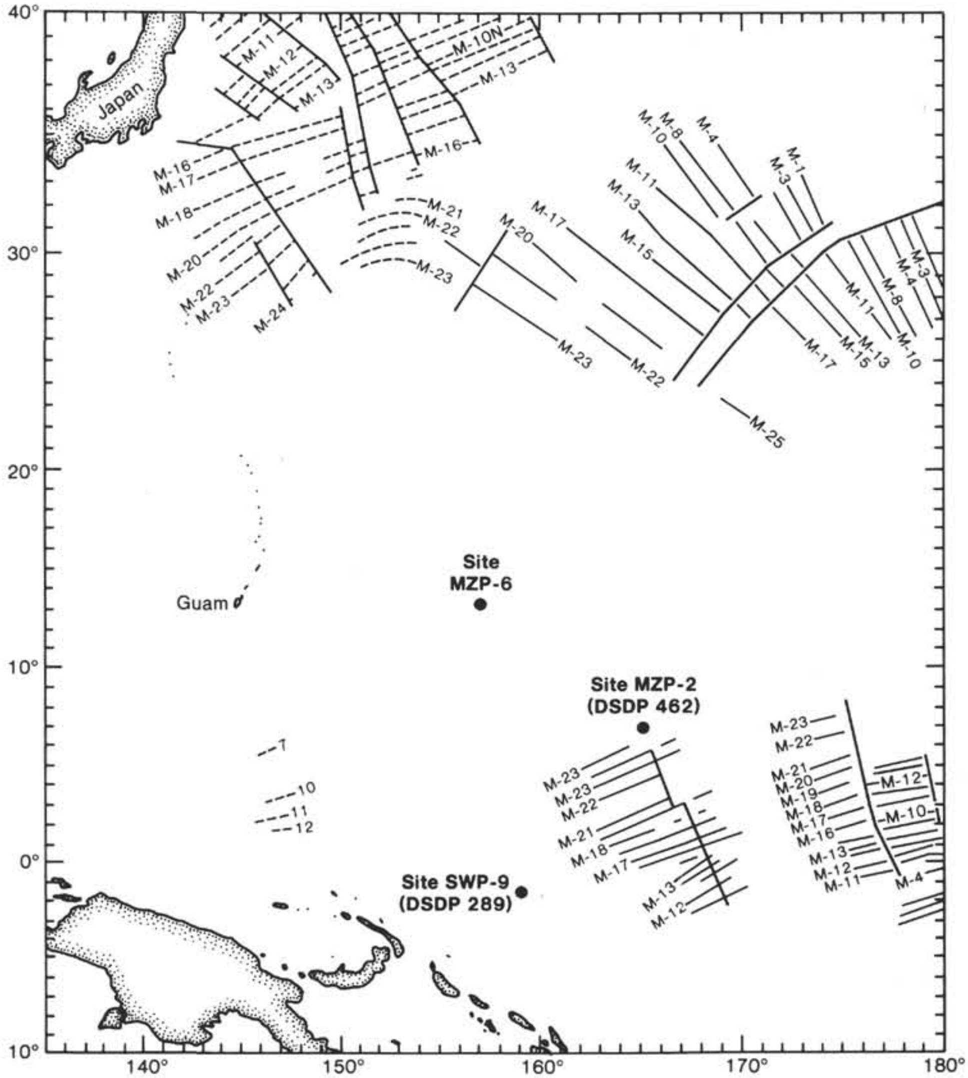

Figure 1. Magnetic lineations in the western Pacific in relation to Sites MZP-2, MZP-6, and SWP-9.

large amounts of volcanic rock that were emplaced on the lithospheric plate in an off-ridge, intraplate setting. Off-ridge volcanism, referred to as midplate volcanism here, resulted in the formation not only of linear island chains but also clusters of seamounts and deep-water sill-flow complexes. Dating of this midplate volcanism by isotopic and biostratigraphic methods indicates that in the western Pacific, widespread volcanism took place between about 110 or 115 and 70 Ma. The widespread nature of this midplate volcanism (Watts et al., 1980; Schlanger and Premoli Silva, 1981) and its apparent restriction to the middle and Late Cretaceous, although evidence from Enewetak (Ladd et al., 1953; Kulp, 1963) and the Line Islands (Haggerty et al., 1982) indicates that Eocene volcanism also took place, has made it difficult to reconcile hot spot theory with such volcanic activity.

Until quite recently the vertical component of plate motion was considered largely in terms of lithospheric cooling, thickening, and subsidence as a function of the age of the oceanic lithosphere. It has now been suggested by a number of workers that the subsidence path of a large portion of the Pacific oceanic lithosphere has diverged significantly over long periods of time from an ideal Parsons-Sclater curve because of reheating of the lithosphere subsequent to its formation at a ridge crest. We need to quantify the vertical component of plate motion resulting from this reheating effect and to determine the temporal and spatial extent of thermally induced bathymetric highs. In order to address the problem of midplate volcanism in the Mariana Basin, we proposed to collect biostratigraphic and petrologic information in the mid-Cretaceous turbidite section expected at MZP-6 above the principal Jurassic sedimentary objectives. Fossil indicators of ages and of depths of water and of surrounding seamounts, and the types and products of volcanism could be used to interpret the history of volcanism and subsidence.

Secondary Objectives at MZP-6

Leg 89 had a number of scientific objectives subordinate to the primary one of retrieving a section of Jurassic midocean sedimentary rocks at MZP-6, and the lesser one of obtaining a mid-Cretaceous record of volcanism

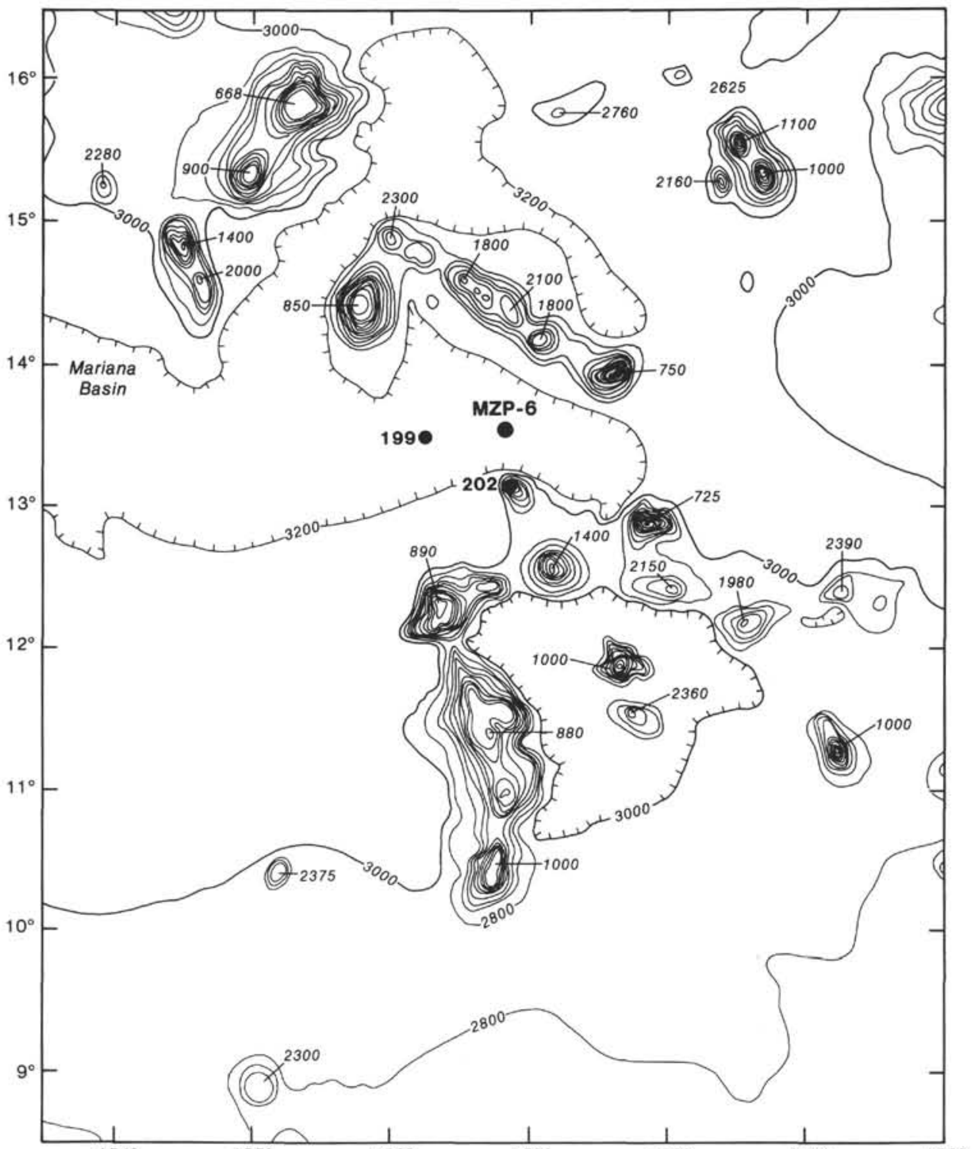

Figure 2. Bathymetric chart showing location of proposed Site MZP-6 and DSDP Sites 199 and 202 (bathymetry in fathoms) (after Chase et al., 1970).

there. Planning of the leg had to take into account those additional objectives. At MZP-6, as at most sites planned by JOIDES, we intended to penetrate into basement and log the hole. The petrology and physical properties of such old midoceanic crust are unknown, and good logs of midocean sites are rare. Committees planning for the leg also recommended continuous coring in the Paleogene and Cretaceous in the hope of extending the available biostratigraphic and geochemical sample of those rocks. Certain engineering studies of the behavior of the drill string were also planned for MZP-6.

Selection of Site MZP-6

As stated earlier, the search for Jurassic strata in the western Pacific has been largely guided by magnetic anomaly patterns (Figs. 1 and 3). Orthogonals (large arrows in Fig. 3) to Anomaly M-29, considered to be about 146 m.y. old, indicate that the plate age in the East Mariana Basin should be about 150 or 160 m.y. Drilling at Site 199 (Heezen, MacGregor, et al., 1973a) showed that Campanian and Maestrichtian chalks were present at a depth of 460 m sub-bottom in the Basin. Deeper reflectors were not reached at Site 199 but a significant sediment section, presumably Early Cretaceous and Jurassic, appeared to be present. Drilling at Site 462 in the Nauru Basin (Larson, Schlanger, et al., 1981) penetrated an Aptian basalt sill and flow complex interbedded with Aptian sediments. The Nauru Basin was known to be shallow with a depth of 5190 m, instead of a depth of 6120 m predicted by a Parsons-Sclater curve for the ca. 150-m.y. age of the crust at Site 462, which was between Anomalies M-26 and M-27. This depth anomaly was, after the discovery of the mid-Cretaceous sill and flow volcanism, interpreted to be the result of thermal rejuvenation and uplift of the Jurassic plate in the Marshalls area (Schlanger and Premoli Silva, 1981; Larson and

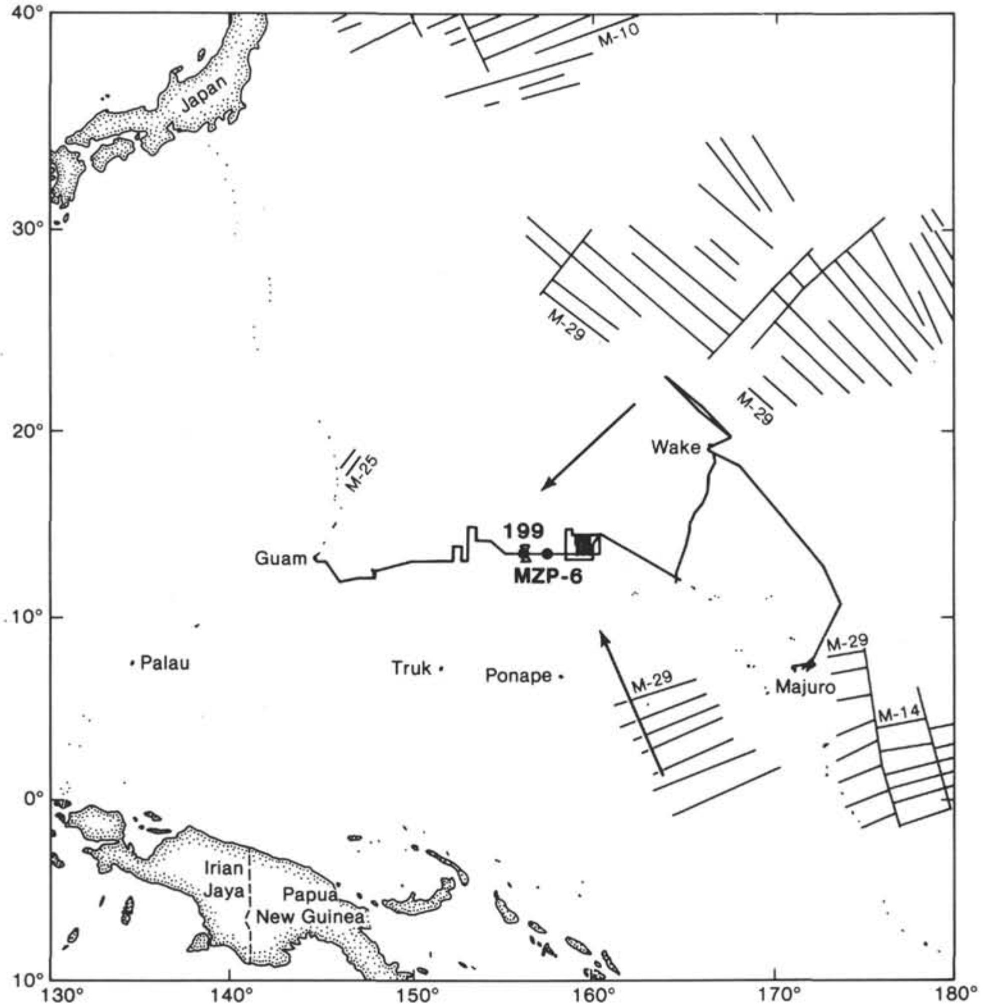

Figure 3. *Kana Keoki* KK810626 Leg 4 cruise track and some magnetic lineations in the western Pacific. Large arrows point to the location of probably the oldest crust in the Pacific basin. MZP-6 was selected because it lies near the center of the basin (from Duennebier and Petersen, 1982).

Schlanger, 1981) as deduced by Detrick and Crough (1978) from their study of subsidence rates at Enewetak Atoll. Therefore we believed that the search for a suitable basin should center on one that has the "correct" depth, about 6100 m, for its age. The Mariana Basin fulfilled this requirement.

A site survey of the Mariana Basin (Duennebier and Petersen, 1982; Duennebier et al., this volume; Shipley et al., 1983) was carried out for JOIDES by the Hawaii Institute of Geophysics and the Scripps Institution of Oceanography in 1981 (Fig. 3). A new type of source—a water gun—was used and the data were digitally recorded for processing ashore. MZP-6 was selected to be drilled into a presumed sedimentary section between 8.1 and 9.1 s two-way traveltime (Fig. 4). An interpretation of the section is shown on Figure 5. Based on this and earlier interpretations, a minimum sub-bottom depth of 1000 m was proposed, with appropriate basement drilling to 200-m penetration or bit destruction, as set forth by the Planning Committee. In view of the Mesozoic objectives the requirement to continuously core the upper section was waived for Leg 89 in order to conserve time. Reentry and logging were planned.

OPERATIONS

After its dry-docking and port call in Yokohama, Japan, the *Glomar Challenger* left for Leg 89 at 0055 hr. local time on 11 October 1982.

En route to Site MZP-6, which was to become Site 585, we deployed a magnetometer, a 12-kHz echo sounder for bathymetry, a 3.5-kHz reflection profiler for discrimination of shallow sub-bottom sediment reflectors, and an air-gun system for reflection profiling with deeper penetration. The system normally used two simultaneously triggered air guns of 60- and 120-in.^{3} (983 and 1966 cm^3) capacity, and two recorders operating at different scales and with various delays but with identical filter settings of 40 to 320 Hz. Approximately 8 hr. before reaching the proposed site the filter settings were changed to 20 to 160 Hz in order that our records might better match those obtained during the precruise site survey. Our track carried us across the Bonin Trench and the Magellan Seamounts en route to the Mariana Basin.

Moderate headwinds and swells retarded our progress during the first part of the transit. After 16 October, when tropical storm Owen passed about 300 mi. south-

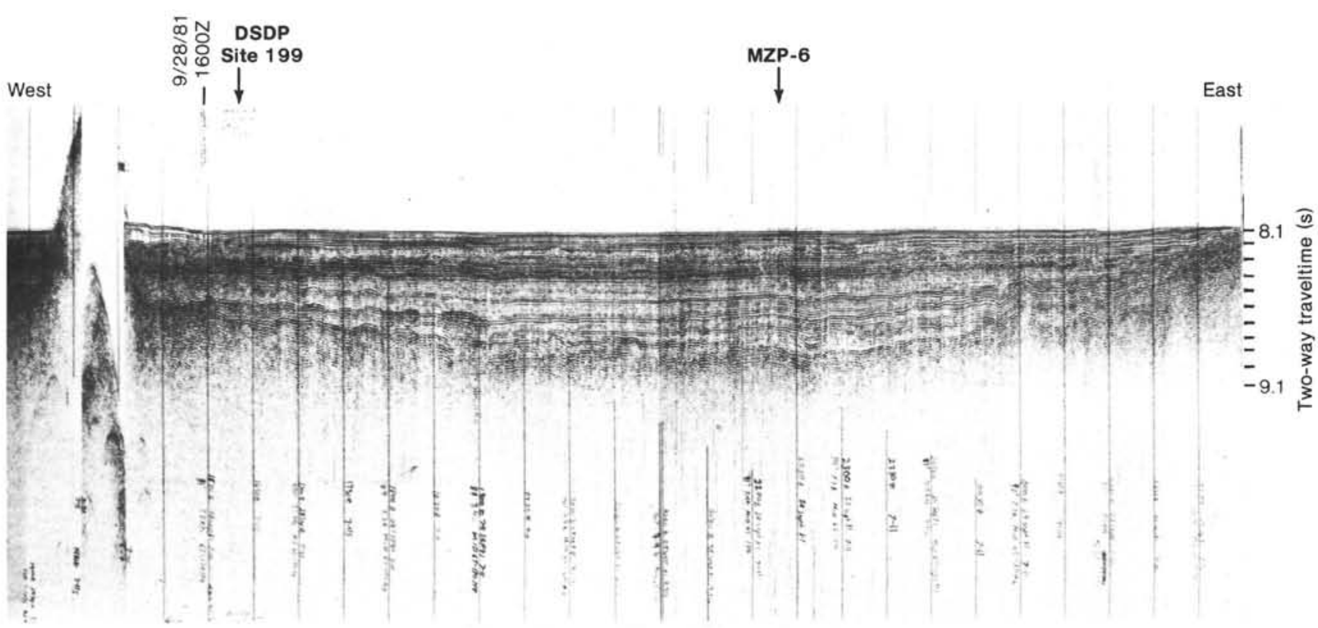

Figure 4. Seismic profile across the East Mariana Basin made using an 80-in.^{3} water gun with a 65–130 Hz bandpass filter. DSDP Site 199 and proposed Site MZP-6 are shown. Water depth at MZP-6 is 6077 m uncorrected (*Kana Keoki*, 28 September 1982). MZP-6 was drilled into a presumed sedimentary section between 8.1 and 9.1 s two-way traveltime (from Shipley et al., 1983).

west of us en route to becoming typhoon Owen, seas and winds moderated and an unexpected following current aided our progress. At 1534 hr. (0534Z) on 18 October we turned south, crossing a guyot of the Magellan Seamounts to approach the Mariana Basin site at right angles to the reflection profile from which the site had been selected.

On our approach to MZP-6 (Fig. 6), we made moderate adjustments of heading based on three satellite navigation fixes. We reduced speed to about 7 knots at 1936 hr. (0936Z) to improve the quality of our reflection profile across the flat-floored Mariana Basin. The record (Fig. 7) resembled the one on the site survey, and, as no small seamounts or other undesirable features appeared, we launched the 16-kHz transducer beacon as we crossed Site MZP-6 at 2122 hr. (1122Z) on 18 October. Depth of water from the 12-kHz transducer was recorded as 6049 m corrected to 6112 m, and our hydrophone depth to 6109, or 6119 m at the drill floor. Site 585 is at 13°29.00′N, 156°48.91′E; our transit was 1642 n. mi. at an average speed of 9.0 knots.

JOIDES planning for MZP-6 had always been in terms of reentry, and the plan by the scientific party had been to set a reentry cone after a short wash-in test and not waste time with a long pilot hole. As a result of drill string losses within the past year off Central America and Japan, however, DSDP engineers were loathe to lower the weight of a reentry cone to the depth of the Mariana Basin. Their proposal, announced to the scientific party only after our arrival in Yokohama, was to make a single-bit attempt, followed by additional single-bit attempts until success was achieved or leg time expired. That program jeopardized not only the MZP-6 Jurassic objectives but also all secondary leg objectives. The controversy between the scientific party and DSDP both on board and with La Jolla before departing Yokohama resulted in the compromise drilling program that called for a reasonable attempt at drilling an extended pilot hole. At bit destruction or earlier, if in the pilot hole the drilling rate or apparent bit condition should indicate probable bit failure before penetrating Jurassic, we would terminate the pilot hole and start reentry.

The drilling crews commenced rigging the piccolo upper drill string support as we maneuvered back over the beacon. A Smith type-F93CK four-cone bit of 9 and 7/8-in. diameter was chosen to strike the balance between a bit that could perform rapid drilling in friable sedimentary rock and one that could penetrate and maintain tooth life in harder rock. The standard DSDP bottom-hole assembly of drill collars, bumper subs, and heavy drill pipe included a sub for hydraulic release of the bit to allow logging through the drill string.

We expected that running the drill string would consume more than the normal time for such depths, because the drill string would be made up mainly of new pipe that had been purchased and loaded in Japan. Each length had to be measured and recorded to insure accuracy in depth, and each joint made, broken, and made a second time to insure tight connections. Malfunctioning air tongs and pipe stabber added to the time. As the drill string reached the approximate depth of the seafloor, two attempts to obtain a mudline or seafloor core failed because of a faulty new design of the flapper valve at the top of the core barrel. It was not until 0716 hr. on 20 October that our first core arrived on deck. Its length of sediment compared to drill string length established the depth of the seafloor from the drill floor to be 6122.3 m (Table 1).

After a wash-in or jetting test, to determine bearing conditions should a reentry cone be set, we drilled and washed to 255.9 m, and recovered a modest amount of sediment in Wash Core 585-H1. The time constraints

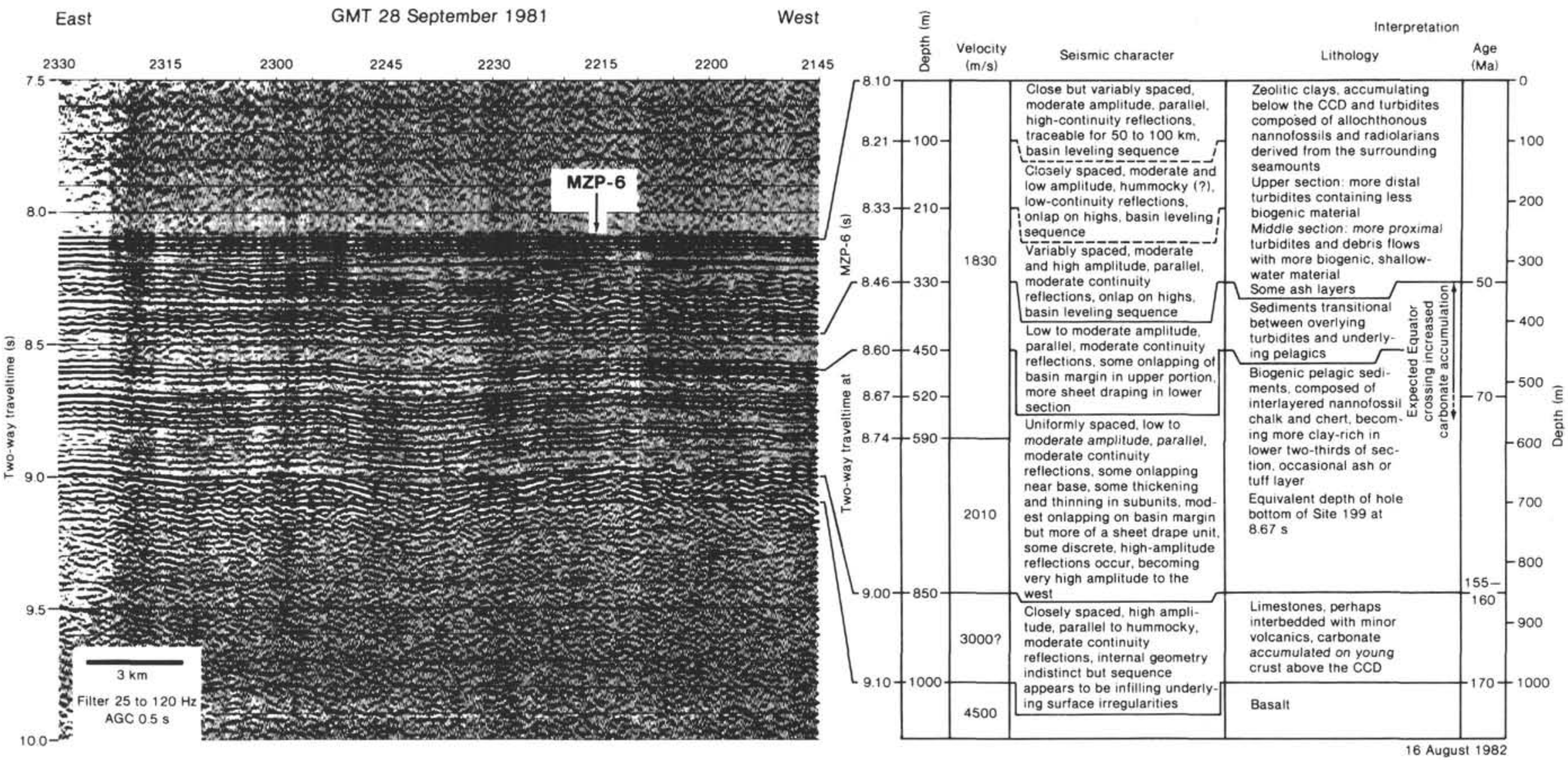

Figure 5. Seismic reflection section with predrilling lithologic interpretations of the basin east of Site 199. Location of proposed MZP-6 drill site is shown. This figure is from Shipley et al. (1983).

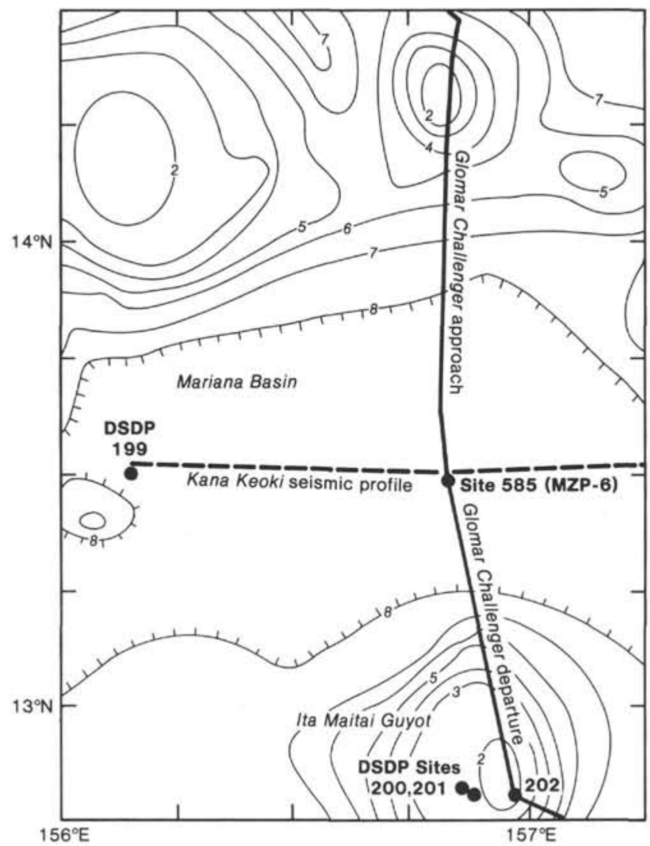

Figure 6. *Glomar Challenger* track near Site 585. Bathymetry, contoured in seconds of two-way traveltime, from Duennebier and Petersen (1982), Chase et al., (1970), Heezen, MacGregor, et al., (1973a), and Figure 3 (this chapter). One second is about 750 m depth; therefore the abyssal plain of the Mariana Basin is slightly deeper than 6000 m.

and the small chance of obtaining useful stratigraphic information from the uppermost section had caused JOIDES to forgo its standing policy of continuously coring in all holes. We were to core continuously only from the Eocene downward. Firmness of the sediment, including porcellaneous chert fragments recovered in Core 2, forced us to core continuously below 255.9 m. Detailed descriptions of the cores recovered at this site as well as their scientific interpretation are reported elsewhere in this chapter and volume.

The Neogene section of claystones and cherty nannofossil chalk between about 256 and 399 m (Cores 2 through 17) was cored in about 41 hr. Drilling times were as slow as 5.1 to 9.8 min. m^{-1} (11.8–6.1 m $hr.^{-1}$ rates) in the cherty section from 275 to 294 m depth, but generally were faster from there to about 358 m depth, averaging about 2 min. m^{-1} (30 m $hr.^{-1}$). Between 358 and 399 m, drilling times increased from 2.7 to 4.8 min. m^{-1} (22.2–12.5 m $hr.^{-1}$). Recovery of Neogene cores was fair to poor (32 to 2%), and probably can be attributed to the alternation of harder porcellanites, cherts, and silicified limestones with softer oozes and clays. Pump pressures sufficient to clear chert chips from the bottom of the hole presumably blew away the friable sediment. On seven instances 20 to 30 barrels of drilling mud was pumped to help in cleaning out the hole.

Comparable drilling times prevailed in the Maestrichtian and Campanian section from about 399 to 494 m depth, ranging from 1.1 to 8.1 min. m^{-1} (55–7.4 m $hr.^{-1}$), but except for fair recoveries in Cores 18, 20, and 27 (21, 44, and 60%), we obtained a very poor sampling of the rocks (0–9% in other cores; 14% overall average for the interval). During this 27-hr. period the heave compensator was removed because its maximum air pressure had been set so low, as a result of a new safety regulation, that it would not operate. Seas remained calm. Except for the recovery, and for periodic shifting of the heavy walled "knobby" joints at the top of the string to keep that pipe in the piccolo, we made good, even progress in these zeolitic claystones and cherty chalks.

That progress of about 100 m day^{-1} continued into the middle Cretaceous claystones and other sediments, with 590 m reached by 1117 hr. on 24 October. Typhoon Owen, which had continued to curve clockwise, north toward Japan, than east, and finally and uncharacteristically southeast, was once again within a few hundred miles of the ship. Owen, northeast of us at about 25°N, 164°E, caused a few gusty squalls, which with the current rendered the vessel unable to maintain its heading into the swell, estimated at about 3 to 5 ft. Maximum isolated rolls of 7° resulted; according to the driller, maximum weight fluctuations of 70,000 lb., in addition to the drill string weight, occurred once or twice near 0400 on 24 October. Unfortunately, the TOTCO recording is blank for that period. In general for the site, 5-ft swells gave 50,000-lb. maximum weight fluctuations. For the interval, recoveries were poor to good, ranging from 9 to 70% and averaging 34%. Drilling times were longest for Core 35 and shortest for Core 32, of 5.6 and 3.1 min. m^{-1}, or rates of 11 to 19 m $hr.^{-1}$, respectively. By noon on 24 October the bit had been used only 20 hr., torquing of the drill string had been minimal, one episode of bit plugging had been cleared relatively easily, and seas were again calm. We began to be optimistic that our objectives below 800 m might be obtained by this single-bit hole.

Below 590 m are middle Cretaceous volcanogenic sediments, mainly hyaloclastites redeposited as turbidites. For the most part these were cored quickly (2–3 min. m^{-1}, or 30–20 m $hr.^{-1}$). Three cores between 668 and 695 m depth were cored more slowly at 4.5 to 4.9 min. m^{-1} (about 13 m $hr.^{-1}$), and the lowest two cores were cut even more slowly at 7.9 and 7.4 min. m^{-1} (about 8 m $hr.^{-1}$).

After retrieving Core 55 at 0840 hr. on 26 October, the next core barrel dropped into the drill string wedged into the liner of the landing subassembly. It was impossible to circulate, and although four runs of the sand line were attempted to pull the barrel from the liner, we were unsuccessful. Pull on the sand line was limited because of the weight of the line itself at these depths.

Modification of the landing subs to allow for the hydraulic piston core, extended core barrel, and hydraulic bit release reduced the area of shoulder that contacts

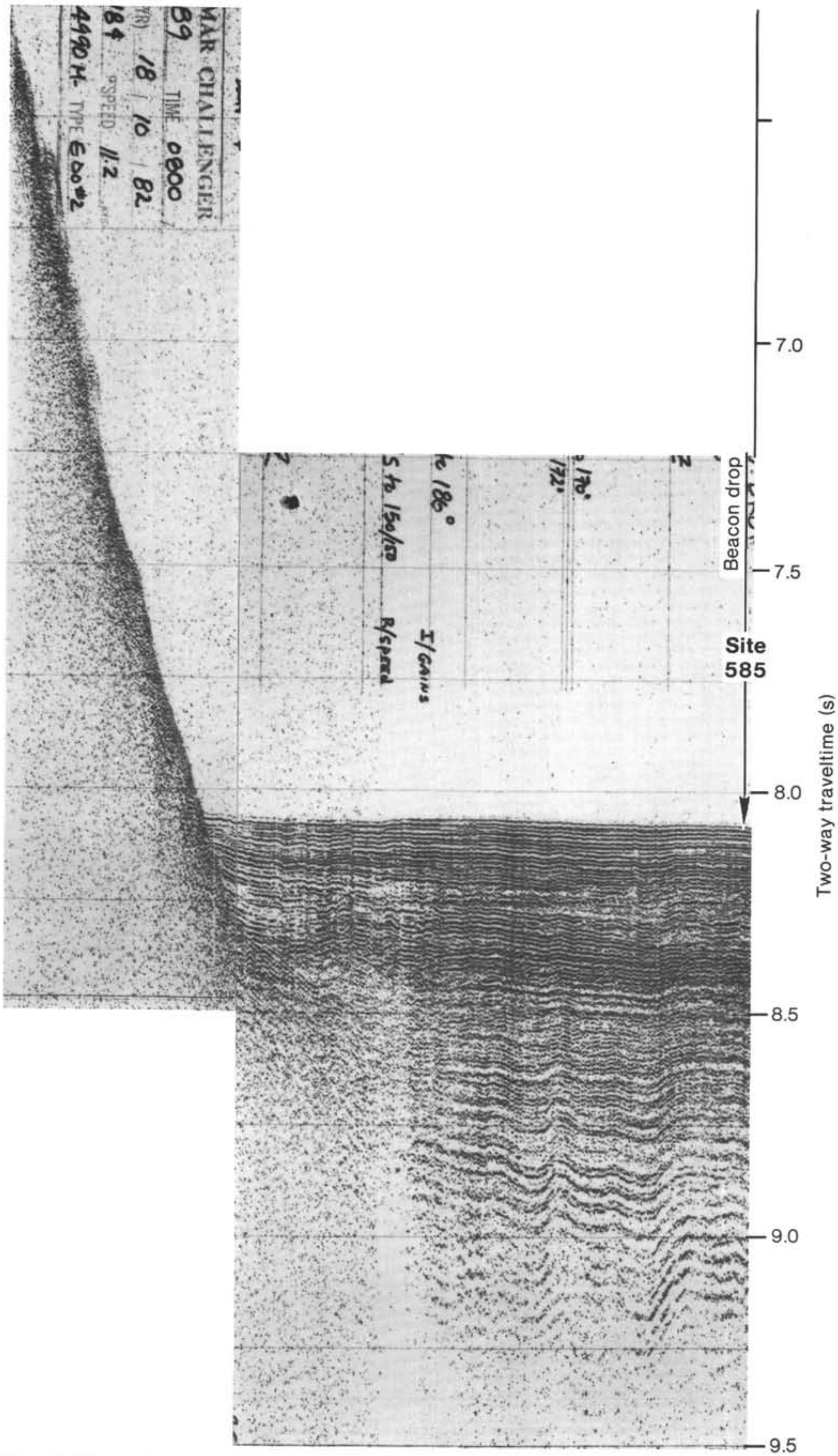

Figure 7. Air gun seismic profile approaching MZP-6, which is Site 585, Mariana Basin.

Table 1. Coring summary, Site 585.

Core no.	Date (Oct., 1982)	Time	Depth from drill floor (m) top bottom	Depth below seafloor (m) top bottom	Length cored (m)	Length recovered (m)	Percent recovered
Hole 585							
1	20	0716	6122.3-6129.1	0.0-6.8	6.8	6.60	97.0
H1	20	1410	6129.1-6378.2	6.8-255.9	Wash core		—
2	20	1621	6378.2-6387.8	255.9-265.5	9.6	0.35	3.6
3	20	1838	6387.8-6397.4	265.5-275.1	9.6	1.05	10.9
4	20	2150	6397.4-6401.4	275.1-279.1	4.0	0.40	10.0
5	21	0118	6401.4-6406.9	279.1-284.6	5.5	0.35	6.4
6	21	0431	6406.9-6416.0	284.6-293.7	9.1	2.38	26.2
7	21	0644	6416.0-6425.2	293.7-302.9	9.2	0.19	2.1
8	21	0912	6425.2-6434.3	302.9-312.0	9.1	3.11	34.2
9	21	1120	6434.3-6443.5	312.0-321.2	9.2	0.84	9.1
10	21	1339	6443.5-6452.6	321.2-330.3	9.1	0.88	9.7
11	21	1540	6452.6-6461.8	330.3-339.5	9.2	2.76	30.0
12	21	1740	6461.8-6470.9	339.5-348.6	9.1	2.26	24.8
13	21	1952	6470.9-6480.1	348.6-357.8	9.2	2.01	21.8
14	21	2212	6480.1-6489.2	357.8-366.9	9.1	2.89	31.8
15	22	0155	6489.2-6502.7	366.9-380.4	13.5	1.85	13.7
16	22	0430	6502.7-6511.8	380.4-389.5	9.1	1.46	16.0
17	22	0730	6511.8-6521.0	389.5-398.7	9.2	2.54	27.6
18	22	0934	6521.0-6530.1	398.7-407.8	9.1	1.88	20.7
19	22	1200	6530.1-6539.3	407.8-417.0	9.2	0.82	8.9
20	22	1410	6539.3-6548.4	417.0-426.1	9.1	3.96	43.5
21	22	1701	6548.4-6557.6	426.1-435.3	9.2	0.56	6.1
22	22	2020	6557.6-6566.7	435.5-444.4	9.1	0.00	0.0
23	22	2240	6566.7-6575.9	444.4-453.6	9.2	0.17	1.8
24	23	0055	6575.9-6585.0	453.6-462.7	9.1	0.16	1.8
25	23	0511	6585.0-6598.6	462.7-476.3	13.6	0.15	1.1
26	23	0745	6598.6-6607.7	476.3-485.4	9.1	0.70	7.7
27	23	1005	6607.7-6616.9	485.4-494.6	9.2	5.57	60.5
28	23	1215	6616.9-6626.0	494.6-503.7	9.1	6.44	70.8
29	23	1412	6626.0-6635.2	503.7-512.9	9.2	3.03	32.9
30	23	1631	6635.2-6644.3	512.9-522.0	9.1	1.65	18.1
31	23	1849	6644.3-6653.5	522.0-531.2	9.2	5.72	62.2
32	23	2053	6653.5-6662.6	531.2-540.3	9.1	6.31	69.3
33	23	2313	6662.6-6671.8	540.3-549.5	9.2	1.00	10.9
34	24	0144	6671.8-6680.9	549.5-558.6	9.1	3.59	39.5
35	24	0614	6680.9-6694.4	558.6-572.1	13.5	2.51	18.6
36	24	0858	6694.4-6703.5	572.1-581.2	9.1	0.85	9.3
37	24	1117	6703.5-6712.7	581.2-590.4	9.2	1.24	13.5
38	24	1329	6712.7-6721.8	590.4-599.5	9.1	0.70	7.7
39	24	1550	6721.8-6731.0	599.5-608.7	9.2	2.33	25.3
40	24	1745	6731.0-6740.1	608.7-617.8	9.1	0.65	7.1
41	24	2001	6740.1-6749.3	617.8-627.0	9.2	0.32	3.5
42	24	2205	6749.3-6758.4	627.0-636.1	9.1	4.71	51.8
43	25	0016	6758.4-6767.6	636.1-645.3	9.2	6.98	75.9
44	25	0239	6767.6-6776.7	645.3-654.4	9.1	7.42	81.5
45	25	0647	6776.7-6790.1	654.4-667.8	13.4	4.82	36.0
46	25	0912	6790.1-6799.2	667.8-676.9	9.1	5.79	63.6
47	25	1148	6799.2-6808.4	676.9-686.1	9.2	6.62	72.0
48	25	1418	6808.4-6817.5	686.1-695.2	9.1	3.20	35.2
49	25	1620	6817.5-6826.7	695.2-704.4	9.2	8.63	93.8
50	25	1817	6826.7-6835.8	704.4-713.5	9.1	5.35	58.8
51	25	2034	6835.8-6845.0	713.5-722.7	9.2	7.30	79.3
52	25	2239	6845.0-6854.1	722.7-731.8	9.1	6.62	72.7
53	26	0051	6854.1-6863.3	731.8-741.0	9.2	2.88	31.3
54	26	0351	6863.3-6872.4	741.0-750.1	9.1	3.65	40.1
55	26	0840	6872.4-6886.0	750.1-763.7	13.6	8.30	61.0
					514.6	164.50	32.0
Hole 585A							
H1	28	0313	6122.3-6486.0	0.0-363.7	Wash core		—
1	28	0526	6486.0-6495.6	363.7-373.3	9.6	1.79	18.6
2	28	0800	6495.6-6505.1	373.3-382.8	9.5	1.28	13.5
3	28	1022	6505.1-6514.6	382.8-392.3	9.5	1.98	20.8
H2	28	1329	6514.6-6560.5	392.3-438.2	Wash core		—
4	28	1543	6560.5-6570.0	438.2-447.7	9.5	0.18	1.9
H3	28	2031	6570.0-6624.9	447.7-502.6	Wash core		—
5	28	2236	6624.9-6634.1	502.6-511.8	9.2	3.58	38.9
6	29	0051	6634.1-6643.2	511.8-520.9	9.1	2.64	29.0
7	29	0558	6643.2-6654.7	520.9-532.4	11.5	4.71	41.0
8	29	0930	6654.7-6665.8	532.4-543.5	11.1	4.11	37.0
9	29	1156	6665.8-6674.9	543.5-552.6	9.1	1.73	19.0
10	29	1400	6674.9-6684.1	552.6-561.8	9.2	1.28	13.9
H4	29	2345	6684.1-6780.3	561.8-658.0	Wash core		—
H5	30	1028	6780.3-6894.4	658.0-772.1	Wash core		—
11	30	1307	6894.4-6903.6	772.1-781.3	9.2	6.90	75.0
12	30	1545	6903.6-6912.7	781.3-790.4	9.1	9.99	+100.0
			6912.7-6921.9	790.4-799.6	Washed		—
13	30	1946	6921.9-6931.0	799.6-808.7	9.1	6.40	70.3
14	30	2256	6931.0-6940.2	808.7-817.9	9.2	7.07	76.8
15	31	0205	6940.2-6949.3	817.9-827.0	9.1	7.59	83.4
16	31	0805	6949.3-6960.9	827.0-838.6	11.6	6.91	59.6
17	31	1122	6960.9-6970.0	838.6-847.7	9.1	8.27	90.9
18	1	0956	6870.0-6980.0	847.7-857.7	10.0	9.93	99.3
19	1	1333	6980.0-6989.1	857.7-866.8	9.1	5.89	64.7
20	1	1648	6989.1-6998.3	866.8-876.0	9.2	3.83	41.6
21	1	1934	6998.3-7007.4	876.0-885.1	9.1	3.06	33.6
22	2	0254	7007.4-7015.1	885.1-892.8	7.7	2.41	31.3
					208.8	101.53	48.6

Note: Material recovered in washed intervals is listed as H1, H2, and so on.

and supports the core barrel, and so those contact surfacings had been deforming. They had been built back by beads of welding rod and machined round, but the final dimensions had not been checked on a second batch and the oversized landing sub wedged.

As there was no reentry cone set, the hole had to be abandoned at a total depth of 6886 m of drill string, 763.7 m below the seafloor. The drilling crews tripped out of the hole, having the last of the bottom-hole assembly on board at 0410 hr. on 27 October. Thus, 8 days, 6 hr., 43 min. were expended in this hole. The core barrel was cut from the assembly and examined, confirming the cause of wedging.

The bit was also examined closely. It had been in use 29 hr., 53 min. No teeth had broken, and few teeth showed more than modest wear. Seals of two sets of bearings were still good, one seal was leaking, but the fourth seal and bearings had failed. The cone using those bearings was wobbly and was estimated to have only 10 to 15 more hours of useful life. If the wedged barrel had not occurred the bit may have gotten us into the upper part of the section of interest.

During the time of tripping the drill string out of the water we received DSDP message 89D21 that reentry must not be attempted at this site. More than two weeks had elapsed since we had been assured before leaving Yokohama that reentry could be attempted if a single-bit hole failed. The highest priority of Leg 89 was to reach Jurassic sediment and crust. After weighing the likelihood of reaching this objective in another single-bit attempt at this site against achieving the other leg objectives of lesser priority, and in consideration of the interests of the scientific party, we decided to try again here.

Hole 585A was therefore planned to be similar to 585 in the rigging of bit type, bottom-hole assembly, new drill string, knobby pipe, and piccolo. We planned to wash and drill to the old total depth as rapidly as possible, with strong pumping, removing core barrels with the sand line wherever drilling characteristics indicated they may be full. Spot cores near 380 to 400 and 500 to 540 m would be taken, as those represented the probable intervals of most scientific value.

During the trip into the hole on 27 October the seas and weather remained excellent, with light airs to 6-knot winds, 3-ft. swells, and rolls and pitch of 2°. By 0313 hr. on 28 October we had washed to 363.7 m and pulled the first wash core, a rubble of broken pieces of mudstone with some short cored pieces of gray mudstone and chalk.

Three cores between 364 and 392 m drilled somewhat faster than they had in the first hole, and recovery was slightly improved through this uppermost Mesozoic–lowermost Cenozoic interval. After washing to about 438 m, an attempt to spot core at a level where drilling was slow and recovery was poor in Hole 585 met with little success. Core 585A-5 was drilled rapidly, but less than 2% of the interval was recovered (compared to none in 585). Next we washed to about 503 m.

Our purpose in taking six cores between 503 and 562 m in 585A was to improve our sedimentological and paleontological control in the lower Upper Cretaceous section that showed evidence of an oceanic anoxic event in

Hole 585, and in many other locations. In the section of greatest interest we slowed our drilling rates somewhat in an attempt to optimize recovery, but our percentage of recovery actually was less than in the first hole. We next washed to 772 m, one joint of pipe beyond the total depth of Hole 585. At that point near noon on 30 October, the bit had rotated 20 hr., 20 min. From that point, except for one washed interval of 9 m, we cored continuously to the total depth of Hole 585A.

Cores 585A-11 through -22 remained in a dominantly volcaniclastic section that generally resembled the lower part of 585. These firm sandstones, mudstones, and breccias were cored slowly, especially below 800 m depth, but gave good recovery, compared to most of Hole 585 and the upper part of 585A. Our average recovery was 70.2% but that was obtained only at an average of 8.3 min. m^{-1} (7.2 m $hr.^{-1}$). For the section below 800 m (top of Core 585A-13 at 799.6 m), the average penetration was 9.6 min. m^{-1} (only 6.3 m $hr.^{-1}$). Possibly the drilling rate below 800 m may identify that depth as being equal to the 9.0-s reflector in the site survey seismic reflection profile. Further petrographic work ashore, of cements or composition or other aspects of these rocks, can test that possible explanation. Alternatively, perhaps 800 m is the depth at which the bit began to fail to cut well.

During 31 October the ship's motion increased in a rising wind and swell. Occasional excursions of the drill string weight to the operating limits named for this site resulted from the 6970 m of drill string and the ship's motion. After Core 585A-17 was recovered at 1122 hr. on 31 October, the drill string was raised from 848 to about 243 m, to remove sufficient weight for the safety of the drill string. By the early morning of 1 November the swell and wind diminished sufficiently so that we could lower the drill string and commence coring again. We cut the final six cores on 1 November.

Two events took place simultaneously late on 1 November. Penetration while cutting Core 585A-22 stopped at 7.7 of the planned 9.2 m and the drilling crew reported that the torquing or rotational behavior of the drill string indicated to them that the bit had failed. Meanwhile the swell and wind had increased, and because it was night the ship's officers could not observe the direction of the swell to attempt to improve the heave by trying a better ship's heading. Loss of the bit meant that Hole 585A would have to be abandoned, but we could not at that moment ready ourselves for logging by dropping the bit at the total depth of 892.8 m, because the core barrel with Core 585A-22 was still within the lower subassembly of the bottom-hole assembly. The increased ship's motion, which exposed the drill string to its posted limit, would not allow the drilling crew the time to run the sand line to recover the barrel. Rather, the ship's motion resulted again in a decision to pull the drill string up several hundred meters to 280 m, to relieve its weight. Core 585A-22 was retrieved only after the string had been shortened. The decreased diameter of the core in 585A-22 was additional evidence that the bit had failed. Compared to a normal diameter of about 61 mm at the maximum diameter, the diameters of the three thickest pieces of core were 53, 48, and 45 mm, and the three thinnest cores had diameters of 36, 33, and 31 mm.

We intended to wait until the weather improved in order to rerun pipe to drop the bit at the bottom of the hole so we could then pull up and log. We could not pull out to drop the bit on the seafloor because there was no cone to allow reentry, nor could we leave for a nearby site of low priority, such as Ita Maitai Guyot, and drill there until the weather cleared and return and reenter 585A to deepen or log the hole.

We did not believe that dropping the bit while high in the hole would be successful. Almost certainly the bit and its release sub would wedge at one of the harder ledges part way down and thus block the logging runs. By noon on 2 November we reviewed the forecasts for sea state and weather. No significant change except possibly a worsening could be expected in the 5-ft swells and 20-knot winds for the next 48 hr. The oceanographic atlases gave scant hope for any general improvement in November. Without such a limit as was imposed on our string length, which reached 7015.1 m at total depth, one might have characterized the weather and sea as mild. A current estimated by the Master as up to 2 knots was now running from the southeast, and as the 5-ft. swell was now from the northeast, maintenance of position in the current would put the swell on the beam. That configuration, in fact, caused us to pull up an additional 115 m closer to the seafloor shortly before noon. Faced with a delay of at least 48 hr. and no good chance of improvement even after that, we reluctantly decided to leave the site without logging. Also, we could not waste additional JOIDES time waiting to attempt yet another futile single-bit hole at this site. Thus we accomplished neither our primary leg objective of penetrating Lower Cretaceous and Jurassic sedimentary rocks and oceanic crust in the Mariana Basin, nor one of our lesser objectives—of logging there.

By 0025 hr. on 3 November the last of the bottom-hole assembly was on board. The bit had lost all four cones, showing battered bearing races and their mounts where the cones had been. The bit had operated 33 hr., 47 min. At Hole 585A it had drilled and washed 684 m and cored 208.8 m, of which we recovered 101.5 m (48.6% overall recovery).

After securing the bottom-hole assembly components and the piccolo, we got under way at 0211 hr. on a northern course while streaming the underway geophysical gear. Initially the larger air gun failed but soon was repaired. We then turned south, crossing within 50 m of the beacon at 0309 hr. on 3 November (1709Z, 2 November), and headed on course 165° for Ita Maitai Guyot at the south edge of the Mariana Basin. From there we turned southeast for MZP-2 in the Naura Basin (DSDP Site 462). We expended 15 days, 5 hr., 47 min. at Site 585 (Fig. 8). Figure 9 is our air gun record as we departed Site 585.

LITHOLOGIC SUMMARY

Lithologic Subdivision

Site 585 is located in the East Mariana Basin at a water depth of 6112 m. A 6.8-m surface core was collected in Hole 585, which was then washed to 256 m; from 256 m coring was continuous to a total sub-bottom depth

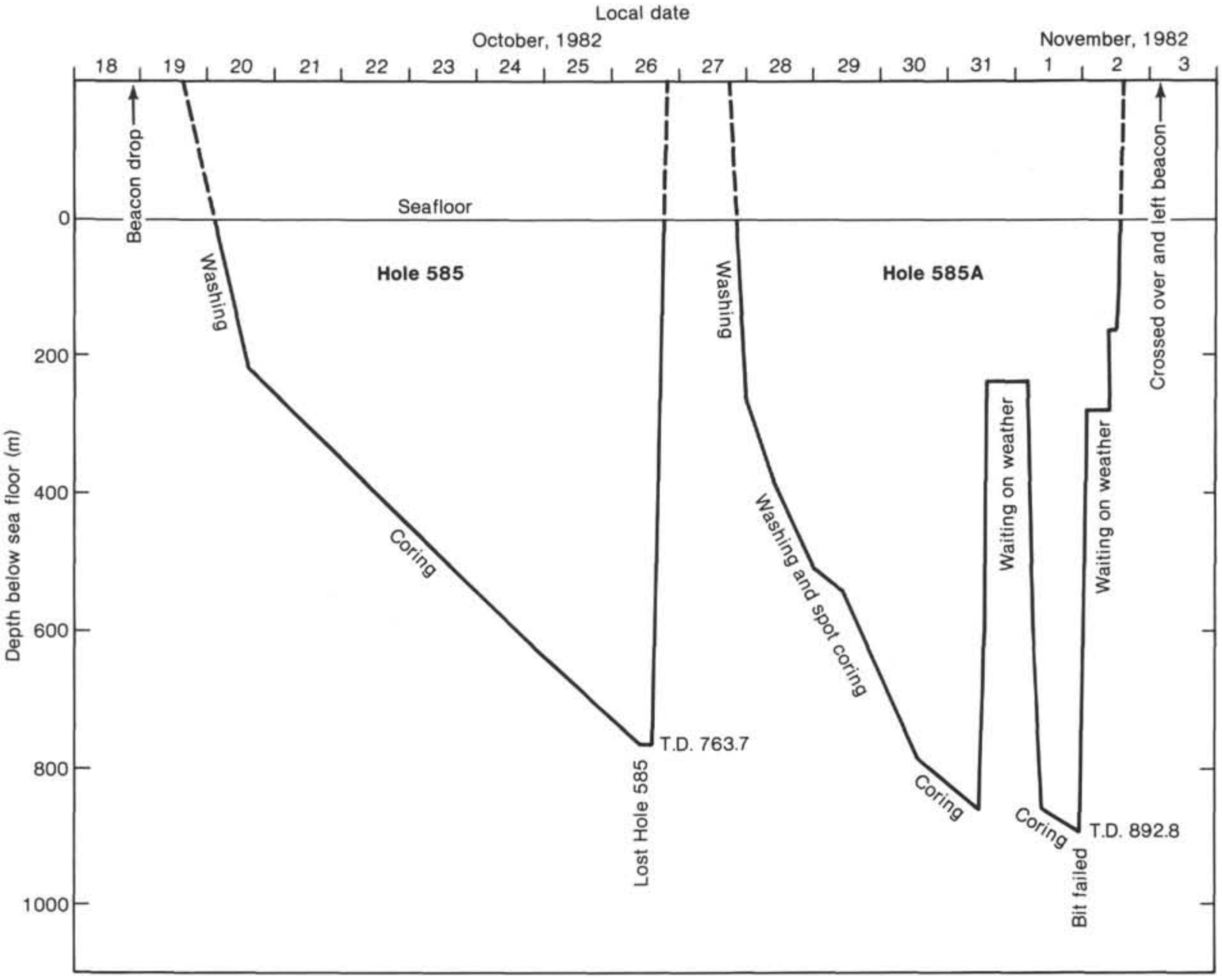

Figure 8. Schematic presentation of drilling operations at Site 585.

of 764 m, with poor to moderate recovery. Hole 585A was spot cored to 772.7 m sub-bottom in order to obtain better recovery of certain key intervals, particularly the Cretaceous/Tertiary boundary and Cenomanian–Turonian claystone containing organic carbon-rich layers. Hole 585A was then cored continuously to a total depth of 893 m. We subdivided the sedimentary section recovered at Site 585 into six lithologic units (I through VI) on the basis of composition and degree of diagenesis and lithification (Fig. 10; Table 2). The lithologic classification used is given in the Introduction and Explanatory Notes chapter (this volume).

Lithologic Unit I (0–6.8 m) consists of 1.5 m of brown clay overlying 5.3 m of nannofossil ooze at the top of Hole 585A. Unit II (256–399 m) was poorly recovered but appears to consist mainly of nannofossil chalk, silicified limestone, chert, and zeolitic claystone. Unit III (399–426 m) contains about equal proportions of zeolitic claystone and nannofossil-bearing claystone, and minor amounts of nannofossil chalk and chert. Recovery of Unit IV (426–485 m) also was very poor because of abundant chert, but the dominant lithology interbedded with the chert appears to be brown zeolite-bearing claystone. Unit V (485–590 m) consists mainly of claystone with varying amounts of zeolites, carbonate, and radiolarians; we subdivided the unit into three subunits based on relative proportions of these latter three components. Unit VI (590–893 m) consists of a thick section of graded volcanogenic sandstones, siltstones, and claystones deposited from turbidity currents and debris flows.

Unit I is composed of nannofossil ooze, clay-bearing nannofossil ooze, and clay (Core 585-1; 0–6.8 m; lower Pleistocene to Recent). The top of Unit I consists of a 1.5-m-thick bed of brown (5YR 3/4) homogeneous clay. Other very minor components observed in smear slides include zeolites and nannofossils (see Appendix to this chapter). Most of the unit, however, consists of about 5 m of light yellowish brown to brown (10YR 8/2–10YR 3/2) nannofossil ooze and clay-bearing nannofossil ooze. Concentrations of $CaCO_3$ in two samples from this part of the unit are 51 and 83% (Table 3).

Unit II consists of nannofossil chalk, silicified limestone, chert, and zeolitic claystone (Cores 585-2 to -17, and 585A-1 to -3; 256–399 m; middle Eocene to Upper Cretaceous [Maestrichtian]). Because of abundant chert and silicified limestone in this unit, recovery was poor, particularly in the upper part of the unit, and knowledge of interbedded softer units in most cores of this unit is based only on a few recovered fragments. Most material recovered from the Unit II interval consists of

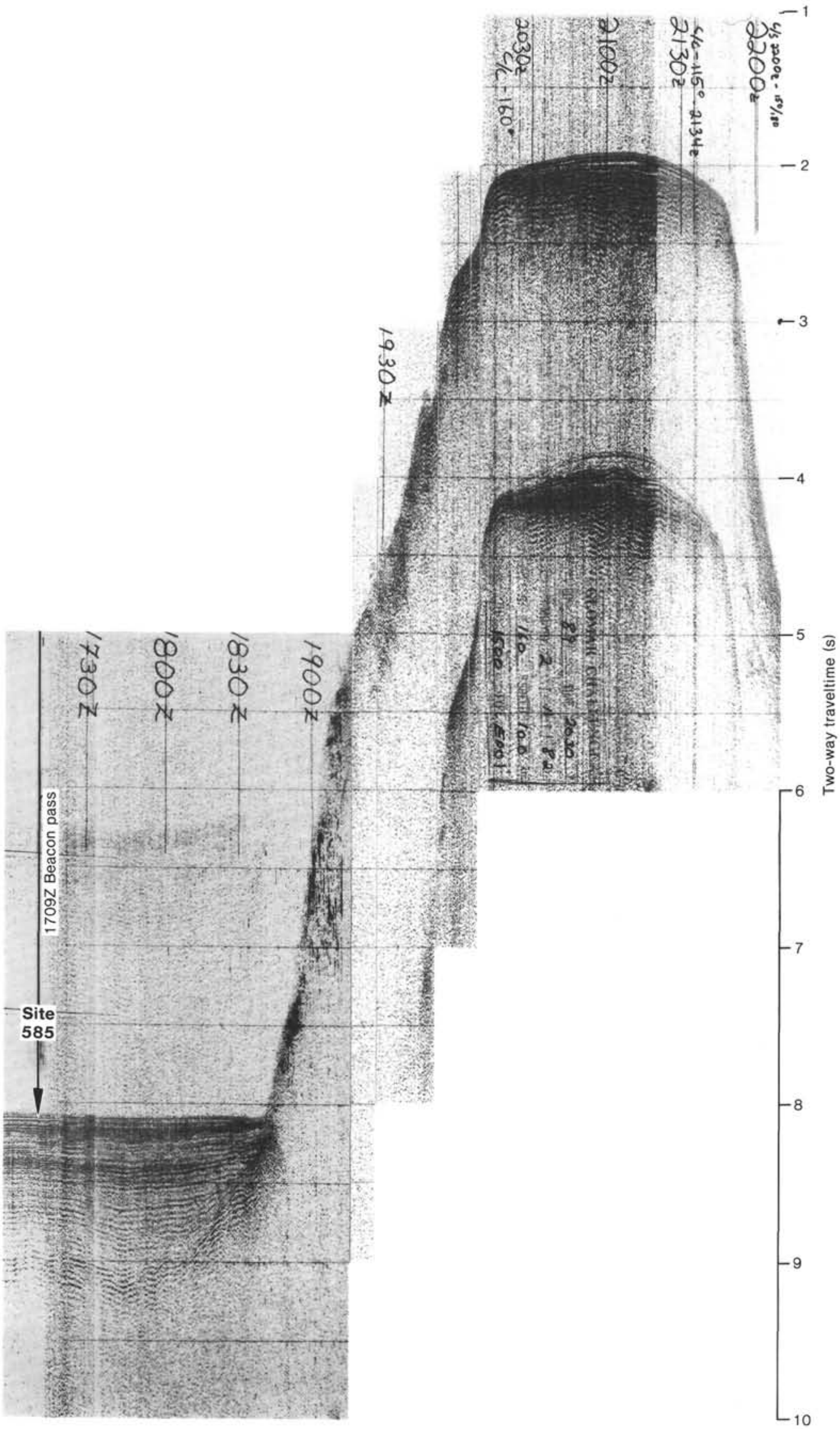

Figure 9. Air-gun-record upon leaving Site 585, showing Mariana Basin at left and the northern slope of Ita Maitai Guyot at right (south); c/s = change of scale; c/c = change of course.

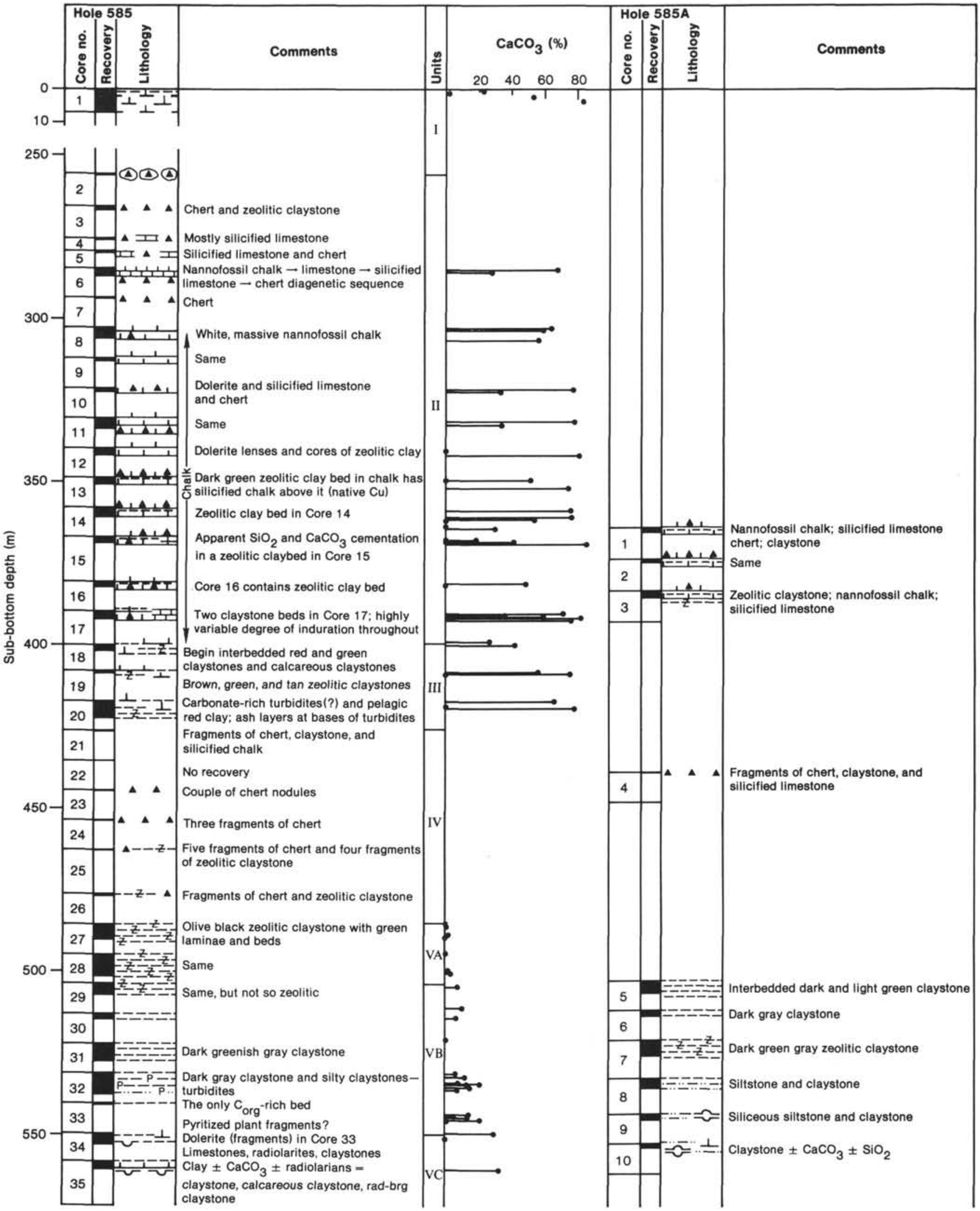

Figure 10. Summary of lithologic column for Holes 585 and 585A.

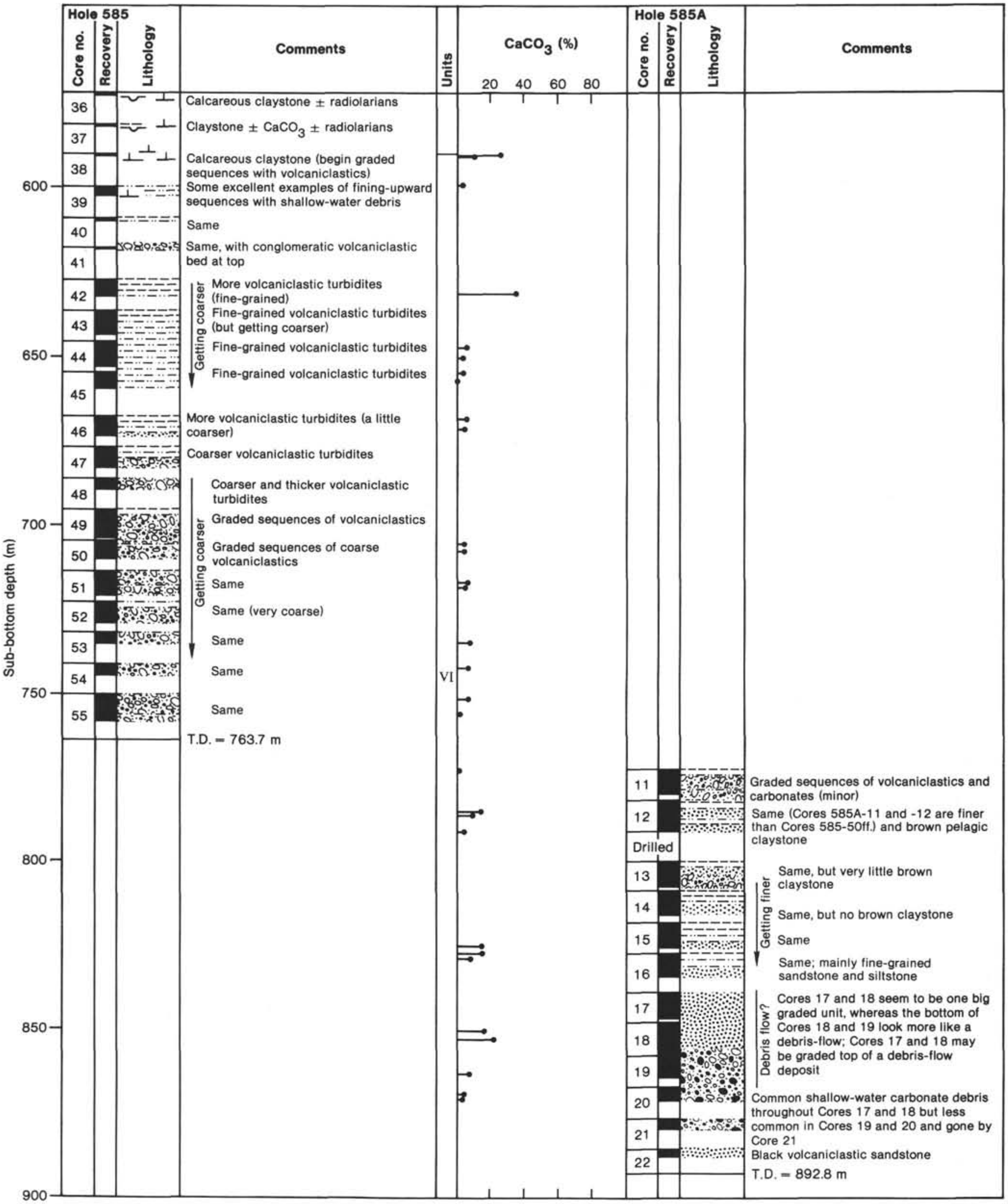

Figure 10 (continued).

Table 2. Lithologic units at Site 585.

Unit	Lithology	Cores	Sub-bottom depth (m)	Thickness (m)	Age
I	Nannofossil ooze, clay-bearing nannofossil ooze, and clay	585-1	0–6.8	6.8	Recent to early Pleistocene
II	Nannofossil chalk, silicified limestone, chert, and zeolitic claystone	585-2 to 17 585A-1 to 3	256–399	143	Middle Miocene to Maestrichtian
III	Zeolitic claystone, nannofossil claystone, and clayey nannofossil chalk and chert	585-18 to 20	399–426	27	Maestrichtian to late Campanian
IV	Chert and claystone	585-21 to 26 585A-4	426–485	59	Campanian
VA	Brown and olive black claystone	585-27 to 28	485–504	19	Campanian
VB	Dark gray claystone	585-29 to 33 585A-5 to 9	504–550	46	Coniacian to late Cenomanian
VC	Calcareous claystone, radiolarian claystone, and clayey limestone	585-34 to 37 585A-9,CC to 10	550–590	40	Cenomanian to middle Albian
VI	Graded sequences of volcanogenic sandstones, siltstones, and claystones	585-38 to 55 585A-11 to 22	590–893	303	Middle Albian to late Aptian

white to light gray (N9–10YR 8/2) nannofossil chalk with varying degrees of $CaCO_3$ and SiO_2 diagenesis between chalk, limestone, silicified limestone, and chert. Interbeds of brown zeolite-bearing claystone are common and increase in abundance below about 360 m (Core 585-13). Above 360 m, zeolite-bearing claystone apparently occurs mainly in thin beds, but also occurs as lenses subparallel to stratification in chalk and as subrounded cores of many fragments of chert and silicified limestone.

Diagenetic silicification of carbonate ooze has resulted in a highly variable percentage of $CaCO_3$, which ranges from less than 20% in silicified limestones to at least 85% in chalks. X-ray diffraction (XRD) results from samples of zeolitic claystones from Cores 585-13 and -14 (Table 4) show that the most abundant minerals identified on XRD diffractograms are smectite, clinoptilolite, quartz, and calcite; less abundant minerals identified are celadonite, siderite, and nontronite(?). Within the zeolitic claystone bed in Core 585-13 there is a thin (ca. 0.5 mm) layer of black material with a light green reduction "halo" around the layer (Fig. 11). Small pieces of native copper were observed in a sample from this layer in preparing the sample for XRD analysis. The black layer is not rich in organic carbon; the black color is probably due to fine-grained iron sulfides. Dendritic black veins having similar green halos also were observed in Core 585-14.

Unit III comprises zeolitic claystone, nannofossil claystone, and minor clayey nannofossil chalk and chert (Cores 585-18 to -20; 399–426 m; Maestrichtian to upper Campanian). The dominant lithology of Unit III is dark brown (7.5YR 4/4) zeolite-bearing to zeolitic claystone with variable amounts of $CaCO_3$ as nannofossils and unspecified carbonate that is presumably present as cement. As a result, the recovered section contains about 50% zeolitic claystone, 42% calcareous (nannofossil-bearing) claystone, and 8% clayey nannofossil chalk with a few pieces of chert appearing in each core of Unit III. Grading is apparent in many of the units, but it is usually very subtle. The bases of several carbonate-rich layers have thin laminae of silty, redeposited hyaloclastic material (see smear slide from Sample 585-20-3, 60 cm), which usually are accompanied by thin, light green reduction halos around the laminae. XRD results from samples of brown claystone from Core 585-18 (Table 4) show that the most abundant minerals on diffractograms are quartz, clinoptilolite, smectite, celadonite, calcite, and siderite.

Unit IV contains chert and claystone (Cores 585-21 to -26 and 585A-4; 426–485 m; Campanian). Recovery of Unit IV was very poor because of abundant chert, but on the basis of a few sediment fragments in Cores 585-21, -25, and -26, it appears that the most common material interbedded with the chert is brown (7.5YR 3/2–4/2) zeolite-bearing claystone. The dominant colors of chert fragments recovered are dark brown (7.5YR 3/2 and 10YR 3/2), very dark brown (7.5YR 5/2), brown (10YR 4/3), and yellowish brown (10YR 5/4). Textures and fabrics observed in the larger chert fragments suggest that the chert formed by silicification of carbonate grainstones that were graded, both in terms of number of sand-size grains and in terms of fining upward of grain size.

Chert and silicified limestone were recovered in lithologic Units II and IV. The texture and fabric of these silicified sediments and of their host lithology are indicators of the sequence of postdepositional processes and are the subject of a special study (see Baltuck, this volume).

Unit V consists of claystone with minor limestone and radiolarian sandstone (Cores 585-27 to -37 and 585A-5 to -10; 485–590 m; Campanian to middle Albian). The dominant lithology of Unit V is claystone, with varying amounts of zeolites, $CaCO_3$, and radiolarians; we subdivided Unit V into three subunits on the basis of color and the relative abundances of these three components.

Subunit VA is composed of brown and olive black claystone (Cores 585-27 and -28; 485–504 m; Campanian). This subunit consists of dark reddish brown (5YR 2.5/2) and olive black (5Y 2/1) zeolite-bearing claystone that is very low in carbonate; analyses of four samples of claystone from Cores 585-27 and -28 for $CaCO_3$ range from 0 to 2% $CaCO_3$ (Table 3). Other minor components observed in smear slides include feldspar, altered volcanic glass, and iron oxides (see Appendix). Plant frag-

Table 3. Carbonate bomb results, Site 585.

Sample (core-section, cm interval)	Sub-bottom depth (m)	% $CaCO_3$	Lithology
Hole 585			
1-1, 21	0.21	1	Brown clay
1-2, 61	2.11	51	Nannofossil ooze
1-3, 61	3.61	83	Nannofossil ooze
6-1, 28-32	284.88	63	Nannofossil chalk
6-1, 119-120	285.79	27	Laminae from nannofossil limestone
8-1, 16-17	303.06	64	Nannofossil chalk
8-2, 12-14	303.52	57	Nannofossil chalk
8,CC	306.50	56	Nannofossil ooze
10-1, 39-42	321.59	77	Nannofossil chalk
10,CC (3-5)	322.00	32	Nannofossil chalk
11-1, 98-100	331.30	78	Nannofossil chalk
11-2, 110-112	332.90	34	Silicified limestone
12-2, 57-58	341.57	83	Nannofossil chalk
13-1, 94-95	349.54	0	Zeolitic clay
13,CC (3-7)	351.50	74	Nannofossil chalk
13-1, 53-56	349.10	52	Silicified limestone
14-1, 64-67	358.44	76	Nannofossil chalk
14-2, 75-79	360.05	77	Nannofossil chalk
14-2, 92-94	360.97	53	Silicified nannofossil limestone
14-2, 105-108	361.10	0	Zeolitic claystone
15-1, 34-36	367.24	18	Silicified limestone
15-1, 61-62	367.51	0	Claystone
15-1, 86-88	367.76	0	Claystone
15-1, 98-100	367.90	0	Zeolitic claystone
15-1, 113-114	368.03	41	Silicified limestone
15-1, 129-130	368.19	85	Nannofossil chalk
16-1, 22-23	380.62	49	Clayey nannofossil chalk
16-1, 69-70	381.09	0	Zeolite-bearing claystone
17-1, 67-73	390.17	72	Nannofossil chalk
17-1, 104-105	390.54	36	Silicified limestone
17-1, 140-141	390.90	60	Nannofossil chalk
17-2, 18-23	391.18	51	Chalk
17-2, 7-9	391.07	83	Chalk
17-2, 52-53	391.52	0	Claystone
17-2, 75-79	391.75	77	Chert(?)
18-1, 13-15	398.83	27	Claystone
18-1, 53-56	399.23	43	Calcareous claystone
19-1, 38-40	408.18	57	Nannofossil chalk
19-1, 48-49	408.28	76	Nannofossil chalk
19-1, 56-57	408.36	0	Claystone
20-1, 8-16	417.08	66	Nannofossil-bearing clay
20-2, 12-18	418.62	0	Claystone
20-3, 20-26	418.70	79	Nannofossil-bearing claystone
27-1, 13-19	485.53	1	Zeolitic claystone
27-3, 20-24	488.60	2	Claystone
28-1, 38-40	494.98	0	Zeolite-bearing claystone
28-4, 76-78	499.86	2	Claystone
30,CC (19-21)	514.59	6	Claystone
32-1, 57-59	531.77	6	Claystone
32-2, 35-39	533.00	12	Claystone
32-3, 41-48	534.61	7	Claystone
32-3, 13-18	534.33	11	Silty claystone
32-3, 72-73	534.92	2	Silty claystone
32-3, 73-74	534.93	0	Black gritty layer
34-1, 11-12	549.61	29	Nannofossil-bearing clayey limestone
34-2, 92-93	551.92	0	Clayey radiolarite
34-1, 91-92	559.51	6	Claystone
34,CC (3-5)	560.76	32	Clayey limestone
38-1, 24-28	590.64	25	Calcareous claystone
38-1, 32-38	590.72	9	Calcareous claystone
39-1, 25-27	599.75	3	Clay-bearing radiolarite
39-1, 42-44	599.92	0	Silty claystone
42-3, 140-142	631.40	34	Claystone
44-2, 84-85	647.64	5	Claystone
44-5, 50-51	651.80	3	Claystone
45-1, 54-55	654.94	3	Claystone
45-3, 18-19	657.58	0	Claystone
46-1, 82-83	668.62	5	Claystone
46-3, 24-25	671.04	3	Claystone
50-1, 128-130	705.68	3	Claystone
50-3, 31-32	707.71	3	Claystone
51-3, 87-88	717.37	5	Claystone
51-4, 37-38	718.37	4	Silty claystone
53-2, 105-106	734.35	7	Claystone
54-1, 119-120	742.19	5	Sand
55-2, 36-37	751.86	6	Clayey volcanic siltstone
55-4, 119-120	755.79	18	Silty claystone
Hole 585A			
3-1, 21-26	363.91	0	Zeolitic clay
3-1, 40-43	364.10	29	Clayey nannofossil chalk
5-1, 80-81	503.40	3	Claystone-gray
5-2, 59-60	504.69	7	Claystone-green
6-1, 54-57	512.34	10	Red-bearing silty claystone
7-1, 94-100	521.84	0	Clayey siltstone
Hole 585A (Cont.)			
8-2, 75-76	534.65	21	Slightly calcareous silty claystone
8-2, 95-96	534.85	13	Slightly calcareous silty claystone
8-3, 32-33	535.72	15	Slightly calcareous silty claystone
8-3, 80-81	536.20	8	Slightly calcareous silty claystone
8,CC (19-20)	536.46	1	Organic-bearing radiolarite
9-1, 27-29	543.77	14	Slightly calcareous siliceous claystone
9-1, 82-83	544.32	0	Chert
9-1, 93-94	544.43	4	Siltstone
9-1, 140-141	544.90	14	Siltstone
9,CC (17-19)	545.17	21	Claystone
11-4, 84-85	772.94	1	Claystone
12-3, 68-74	784.98	13	Claystone
12-4, 27-28	786.07	8	Volcanogenic siltstone
12,CC (3-4)	791.07	3	Claystone
15-5, 135-137	825.25	14	Calcareous claystone
16-1, 8-9	827.08	15	Calcareous-rich claystone
16-2, 31-34	828.81	7	Claystone
18-4, 79-80	852.99	21	Volcanogenic sandstone
18-2, 81-82	850.01	16	Volcanogenic sandstone
19-4, 71-72	862.91	6	Volcanogenic sandstone
20-2, 102-103	870.47	3	Volcaniclastic debris
20-3, 67-68	869.32	3	Volcaniclastic debris
21,CC (10-11)	878.97	0	Volcanogenic sandstone

ments were found in a foraminifer preparation of a sample of a 0.5-cm dark band in Sample 585-27-3, 138 cm. The claystone is mostly massive-appearing, but some parts of it are moderately bioturbated, with most burrows flattened by compaction so that they are subparallel to stratification. Burrows commonly are filled with chemically more reduced claystone (usually green or black). Laminations and thin beds of light green (5G 7/4) occur at several horizons and appear to be reduction halos around coarser, silty laminae that form the bases of graded sequences.

Subunit VB contains dark gray claystone with variable calcareous, siliceous, and organic components (Cores 585-29- to -33 and 585A-5 to -9; 504–550 m; Coniacian to upper Cenomanian). Consisting mainly of dark gray (5Y 4/1 to N4) claystone, this subunit also has variable concentrations of recrystallized radiolarians, $CaCO_3$, and silica. As a result, most of the rocks are somewhat calcareous and contain at least some siliceous cement, and, therefore, are well indurated. The recrystallized radiolarians usually are concentrated in sandy layers, lenses, or stringers. Some fining-upward graded sequences are evident, one being over 3 m thick. Pale green reduction halos are common throughout the subunit as laminae, thin beds, and mottles around silt laminae and burrows that probably contained slightly more organic matter. Common components observed on smear slides (Appendix) include radiolarians (most recrystallized), nannofossils, recrystallized calcite, and zeolites. Twenty samples of claystone from Subunit VB range from 0 to 21% $CaCO_3$ (Table 3). An XRD analysis of a sample of black claystone from Sample 585-32-2, 140 cm shows that the most abundant minerals that can be recognized on the diffractogram are cristobalite, calcite, and smectite, with lower abundances of quartz, celadonite, and clinoptilolite (Table 4).

In Cores 585-32 and 585A-8 the dark gray claystone contains common black flakes of organic-rich material

Table 4. Site 585: summary of XRD shipboard data.

Sample (core-section, interval in cm)	Main lithology	Abundant minerals	Less common minerals
Hole 585			
13-1, 91–92	Olive gray zeolitic clay	Smectite, clinoptilolite, celadonite	Quartz, siderite, nontronite(?)
13-1, 93	Green band with black organic layer	Calcite, clinoptilolite, quartz, smectite	Celadonite, siderite, native copper
14-2, 10	Chalk (nannofossil)	Calcite	Quartz
14-2, 109	Zeolitic claystone	Smectite, clinoptilolite, calcite, quartz	Siderite, celadonite(?), hydrous iron sulfide(?)
18-1, 77	Light brown clay	Calcite, quartz, smectite	Clinoptilolite
18-1, 130	Dark brown clay	Quartz, clinoptilolite, celadonite	Smectite, siderite, phillipsite(?)
18-2, 37	Dark brown clay	Quartz, clinoptilolite, smectite	Celadonite
30,CC	Granular vein in clay	Calcite	Quartz
31-2, 20	White vein in clay	Calcite	Quartz
32-2, 140	Claystone with black flakes	Cristobalite, calcite, smectite	Quartz, celadonite, clinoptilolite(?)
36-1, 54	Chert with green band	Quartz	Calcite, celadonite, clinoptilolite
39-1, 57	Bright yellow "clay" band	Quartz, smectites (nontronite?)	
46-1, 26	White vein in clay	Barite	
47-2, 108	White vein in hyaloclastite	Calcite, quartz	
47-4, 13	White "vein" in turbidite	Quartz, calcite, cristobalite plus unknown (about 2.94 Å)	Phillipsite
48 (paleo residue)	Light and dark green grains	Augite	
48-2, 132	Dark platy vein in turbidite	Natrolite, analcite	Calcite
54-1, 113–115	Pale green material (In volcanic graywacke)	Analcite, saponite	Calcite, hematite
54-2, 123–140	Reddish material (In volcanic graywacke)	Hematite, pyroxene (augite?)	
54-2, 60	White vesicle infilling (In volcanic graywacke)	Analcite, calcite, saponite	
Hole 585A			
3-1, 18–19	Black zone in brown clay	Quartz, cristobalite, smectite (saponite and nontronite?)	Palygorskite, celadonite, clinoptilolite, todorokite (= black coloration)
15-2, 25	White and colorless crystals in vug surrounded by green clay matrix	Analcite, phillipsite	Smectite (saponite)
16-4, 66	Pink crystalline fragments in green clay matrix	Analcite, calcite	Cristobalite, smectite, palygorskite (all in matrix)
18-7, 56	White and pale yellow crystalline material in vug	Heulandite	
19-2, 41	White crystalline material in vug	Heulandite	Analcite
20-2, 109	White crystalline material in vug	Heulandite	

(plant debris?) that are oriented parallel to stratification (Fig. 12). Three thin (several mm to 1 cm) black bands were observed that seemed likely to contain organic matter. Each of the three bands has a different lithologic association (Fig. 13). A 2-cm-thick black pyritic silty claystone containing abundant organic carbon in Sample 585-32-3, 72–74 cm (see section on Organic Geochemistry) occurs at the top of a fining-upward graded sequence, just above bioturbated claystone, and just below parallel- and cross-laminated silty claystone of the overlying graded sequence (Figs. 13A and 14). The concentration of black flecks of organic matter in dark gray siltstone in the core catcher of Core 585A-8 increases downward over an interval of about 1 cm into a 3-mm-thick band of black sandstone consisting mainly of coated recrystallized radiolarians and flecks of black organic matter (Figs. 13B and 15). An analysis of a sample of this black layer showed that it contains 1.4% organic carbon. This band clearly represents a single pulse or influx of both radiolarians and organic debris. The influx of organic debris then continued but at a much reduced rate, manifested as black flecks mixed with the overlying siltstone that decrease in abundance upward (Fig. 15).

A very different occurrence of what we thought was organic matter was observed in Section 585A-9-1 (Figs. 13C and 16). Here, a 4-mm-thick black band occurs within a fragment of laminated radiolarian-bearing siltstone. The siltstone fragment is overlain by fragments of brightly colored yellow, red, and black chert, each of which contain abundant pyrite in blebs and small lenses up to 1 mm in maximum dimension. The stratigraphic sequence here has been badly disturbed by drilling through the chert and subsequently by cutting the core in half in the liner, but the stratigraphic sequence appears to be as illustrated diagrammatically in Figure 13C. An analysis of a sample from the black band showed that it contains only 0.1% organic carbon, therefore it is not particularly rich in organic matter. Unlike the other two black bands, the one in Core 585A-9 is not obviously associated with graded sequences but appears to be associated with chertification. The chert associated with the black band is very different from other cherts recovered at Site

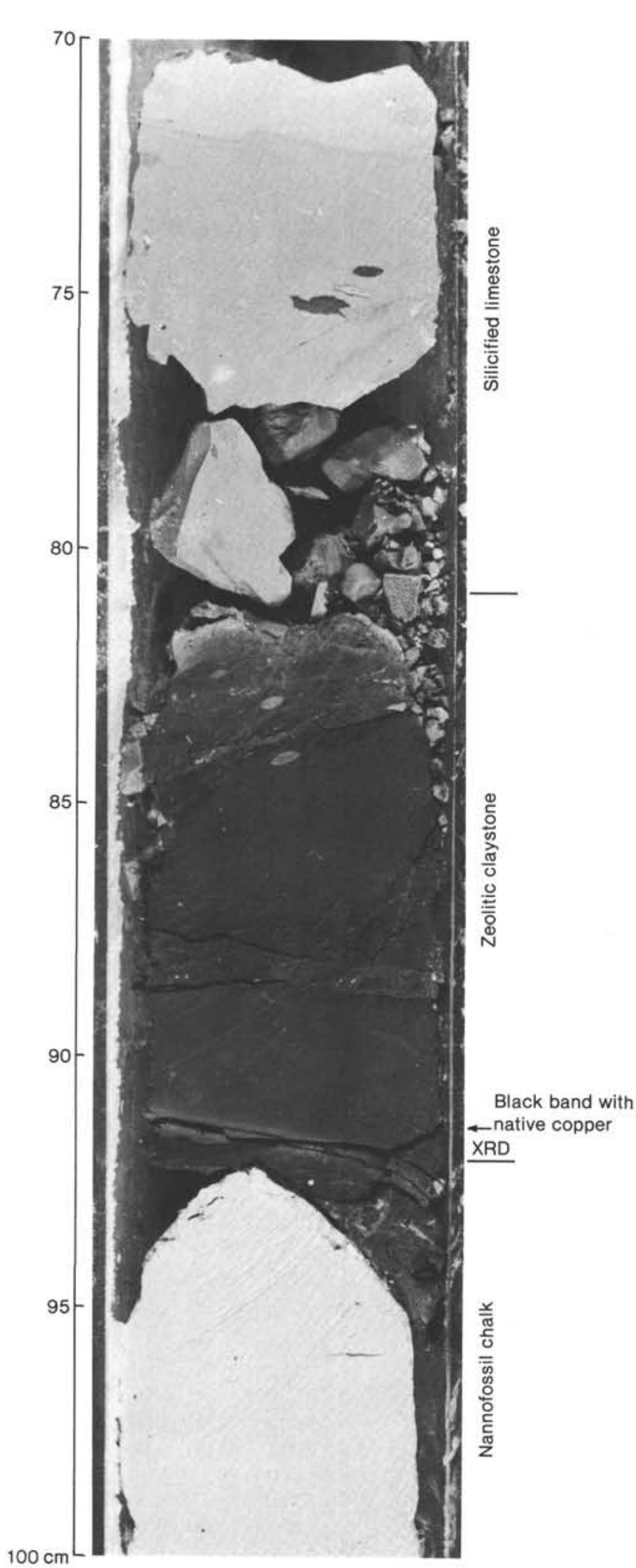

Figure 11. Bed of zeolitic claystone between beds of nannofossil chalk and silicified nannofossil chalk, Sample 585-13-1, 70–100 cm. A black band with a green reduction "halo" around it in the basal part of the claystone bed contains native copper.

585 in that it has a higher specific gravity, contains abundant pyrite (and possibly other sulfides to give it the high specific gravity), and is more brightly colored relative to the other cherts recovered. All three black bands occur between 535 and 545 m sub-bottom depth (upper Cenomanian to lower Turonian) and the two organic carbon-rich bands both occur at about 535 m.

Subunit VC is composed of calcareous claystone, radiolarian claystone, and clayey limestone (Cores 585-34 to -37 and 585A-9,CC to -10; 550–590 m; Cenomanian to middle Albian). This subunit consists of claystone with abundant but highly variable concentrations of radiolarians and $CaCO_3$, which has resulted in interbedding of dark gray claystone, red (5R 6/2) nannofossil-bearing claystone and clayey limestone, radiolarian-bearing limestone and clayey limestone of varying colors but mostly shades of brown, and in the extreme, grayish brown (10YR 5/2–4/2) radiolarian-sandy siltstone (Fig. 17). Parallel laminations are common, and several graded units are apparent. Some thin beds and laminae of pale green (10GY 7/2) occur in some clay-rich units, and these appear to be reduction halos in red claystone around coarser silty layers and laminae.

Unit VI comprises graded sequences of volcanogenic sandstones, siltstones, claystones, and breccias with variable concentrations of $CaCO_3$ and SiO_2 (Cores 585-38 to -55 and 585A-11 to -22; 590–893 m; middle Albian to upper Aptian). Unit VI consists of a thick section of coarse volcaniclastic sediments in fining-upward graded sequences that may be more than several meters thick, and commonly have bases of coarse sandstone or breccia (Fig. 18). The bases of a few of the graded sequences consist of sand-size carbonate clasts or interlaminated or mixed carbonate and volcanogenic clasts (Figs. 19–22). Most of these sequences grade upward into fine-grained tops of claystone or silty claystone. Except for the light gray carbonate bases of some sequences, most lithologies usually are some shade of dark greenish gray, olive black, or dark gray. The tops of some sequences that contain more pelagic components are lighter greenish gray or reddish brown claystone.

Unit VI contains variable amounts of $CaCO_3$ and diagenetic SiO_2. The $CaCO_3$ is derived from both pelagic microfossils and shallow-water carbonate debris. The proportions of these materials vary considerably throughout the unit and they are not always present in every core. Analyses of 32 samples from Unit VI for $CaCO_3$ range from 0 to 34%, but most samples contain less than 10% $CaCO_3$. No shallow-water debris were seen in the two deepest cores at the site (585A-21 and -22). Recognizable shallow-water carbonate components include ooids, benthic foraminifers, algae, bryozoans, and rudist fragments (Fig. 19; for details see Haggerty and Premoli Silva, this volume). SiO_2 is present both as microcrystalline quartz and as spherical masses that are recognizable as recrystallized radiolarians. Other common components recognized in smear slides include altered volcanic glass, zeolites, celadonite, clay minerals, and volcanic lithic and crystal fragments. Additional details about the composition of volcanogenic materials are presented in the following discussion.

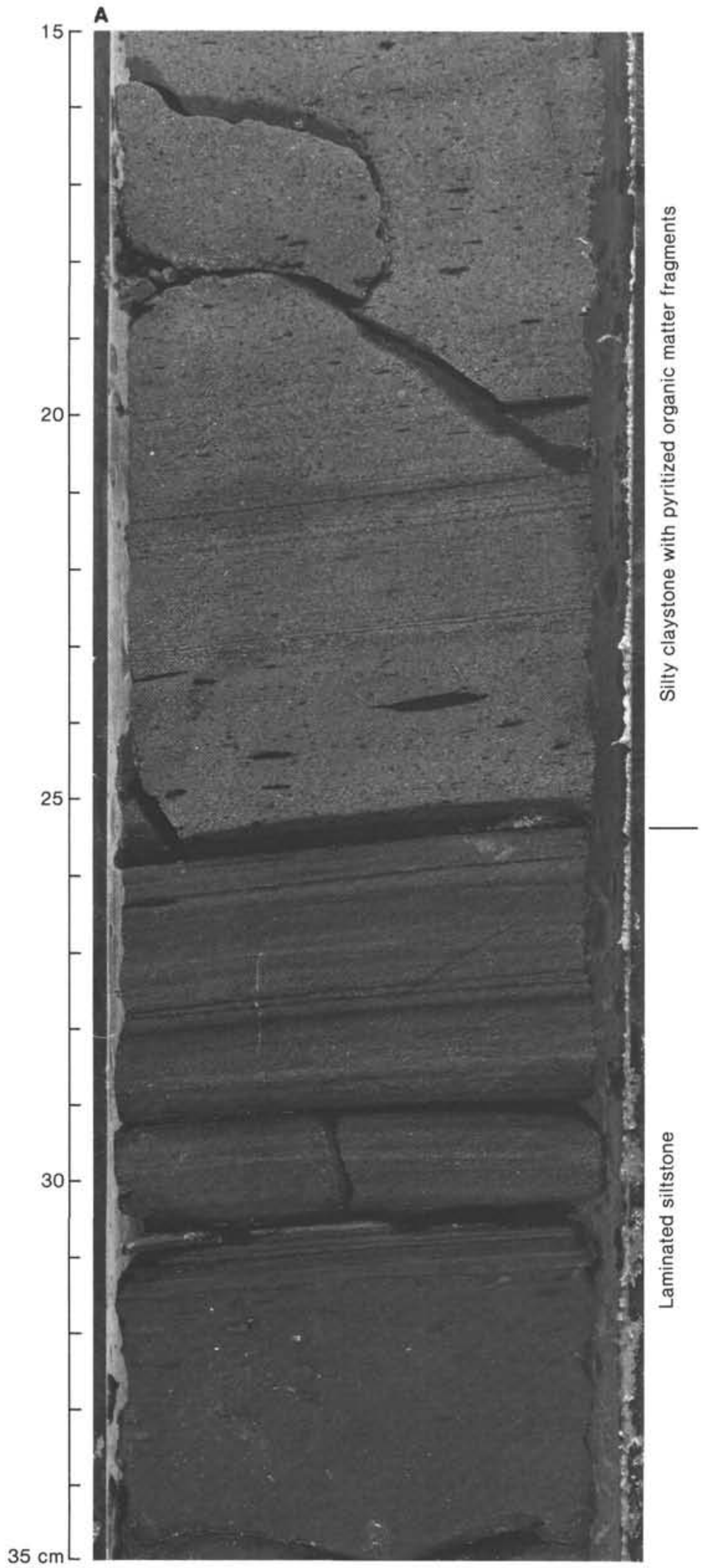

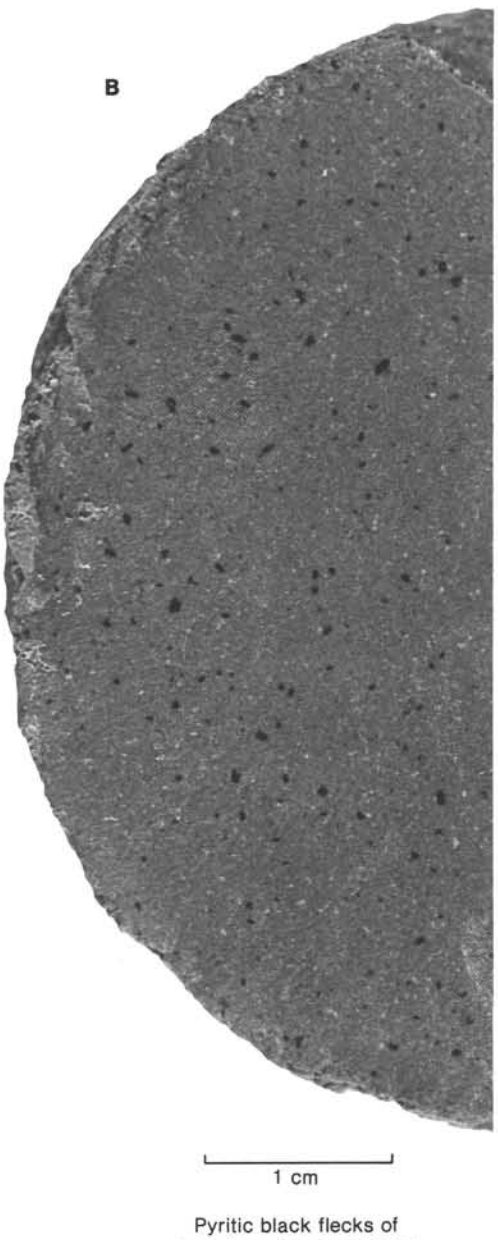

Figure 12. A. Gray silty claystone containing lenses, laminae, and streaks of black pyritized organic matter, Sample 585-32-3, 15–35 cm, cut perpendicular to bedding. B. Sample 585-32-1, 104 cm, along a bedding plane.

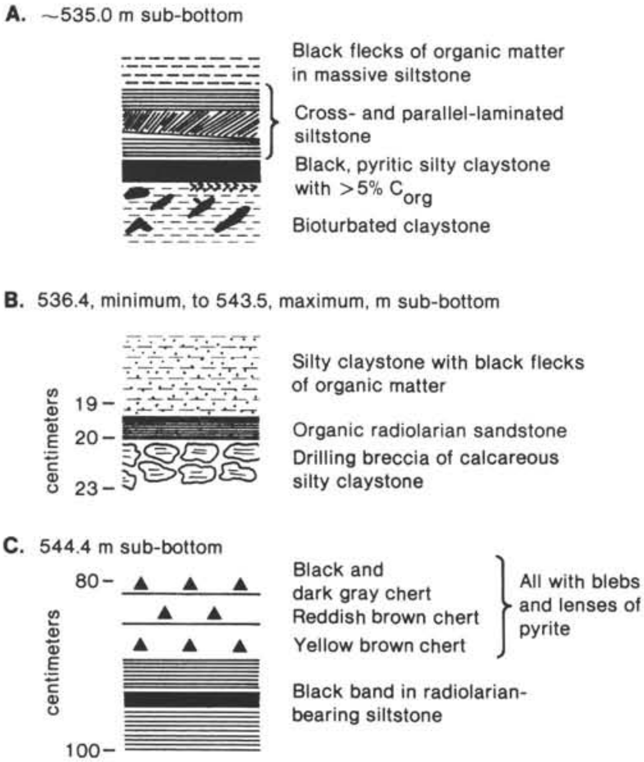

Figure 13. Lithologic associations of black layers originally thought to contain organic matter from (A) Sample 585-32-3, 69–74 cm, (B) Sample 585A-8,CC (19–23 cm), and (C) Sample 585A-9-1, 80–100 cm. Only the black bands in A and B were subsequently found to be rich in organic carbon (i.e., contained more than 1% C_{org}).

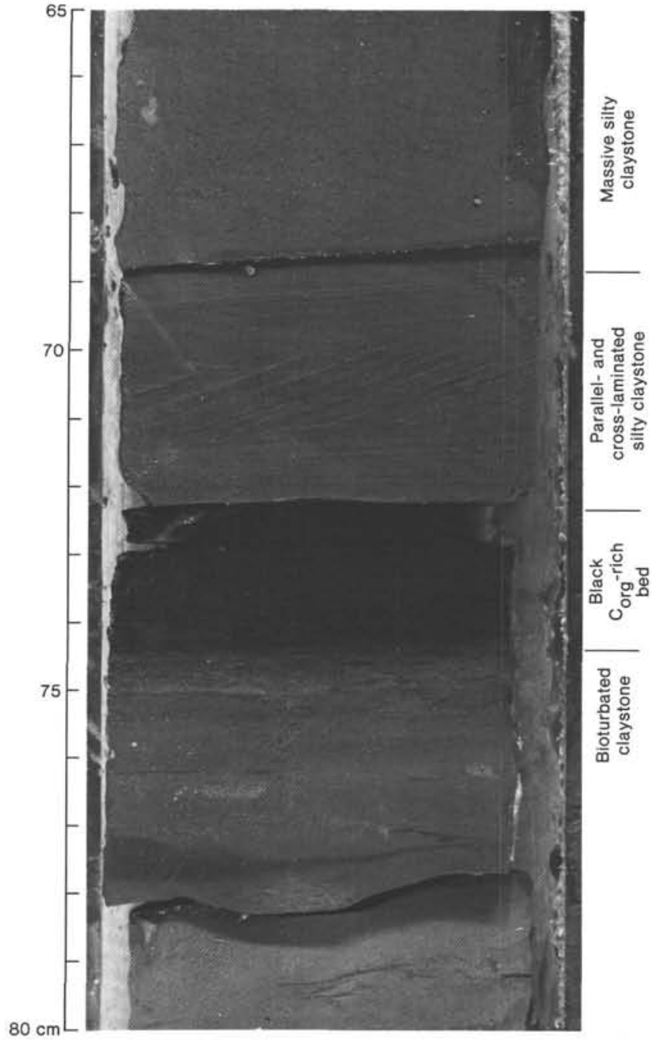

Figure 14. A 2-cm-thick bed of black, organic-carbon-rich claystone occurs at the top of a fining-upward graded sequence, just above bioturbated claystone and just below parallel- and cross-laminated silty claystone of the overlying graded sequence, in Sample 585-32-3, 65–80 cm.

Discussion

Graded Volcaniclastic Sequences

Many of the graded sequences in Unit IV show well-developed and relatively complete Bouma turbidite sequences (Figs. 18, 20–25; Bouma, 1962). Many of the graded sequences, particularly in the lower half of the unit, have coarse sandstone bases. The bases of many of the coarser beds at the bottom of the graded sequences have load casts or have scoured the underlying bed (Fig. 26).

We conclude that the graded sequences of Unit VI, at least into Core 585A-16, are turbidites. Below Core 585A-16 the unsorted nature of the clasts, the extreme size range of clasts, ranging up to boulder-size clasts that have been truncated by the core, and the heterogeneity of clast composition, ranging from volcanic fragments, shallow-water carbonate debris, and subrounded fragments of siltstone and claystone suggest that this material is part of one or more debris flow deposits.

In a complete Bouma turbidite sequence at Site 585, a massive graded basal sandstone (Bouma Unit A; Figs. 18, and 20 through 26), which may be conglomeratic and may extend for several sections, is overlain by a lower unit of laminated sandstone or siltstone (Bouma Unit B), a cross-laminated sandstone or siltstone (Bouma C or ripple-laminated unit), and an upper laminated siltstone or sandstone (Bouma Unit D) (Figs. 21, 23–25) The lower and upper laminated units usually are an interlayering of darker, coarser material (usually olive black sandstone) and slightly lighter, finer material (usually dark greenish gray siltstone or fine sandstone). If the coarse basal layer contains clastic carbonate, the laminated units, particularly the lower unit, may be an intercalation of volcaniclastic material and clastic carbonate material (Figs. 20 through 22). In most of the graded sequences at Site 585, the upper unit is a dark (olive black or dark greenish gray) massive volcaniclastic claystone or silty claystone that probably is mostly fine-grained turbiditic material (Unit E_t of Kuenen, 1964) (Figs. 20, 22, and 26). The upper unit in some graded sequences appears to be more pelagic (Unit E_p of Kuenen); it contains more clay minerals and less obvious volcanogenic material, is generally finer-grained, and is lighter and redder in color (usually lighter olive gray or even reddish brown). In addition, the more pelagic appearing upper units commonly are bioturbated in contrast to the dark-

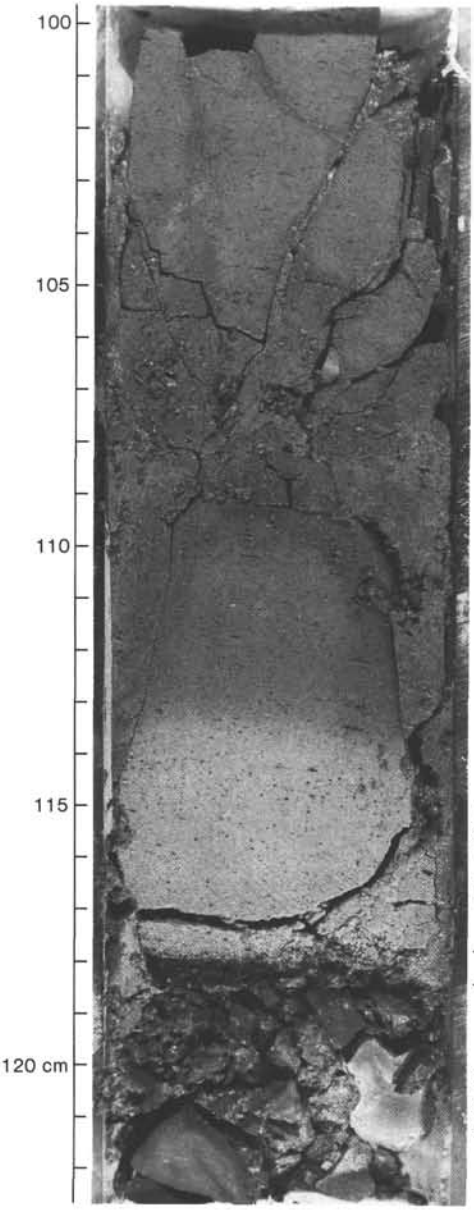

Figure 15. Black organic-carbon-rich band at the base of a gray siltstone bed containing flecks and lenses of pyritized organic matter, Core 585A-8,CC.

er, massive, more volcaniclastic E_t units (Figs. 21, 23, and 24). Some of these graded sequences are more than 1 m thick, and it is not uncommon to have a graded sequence split between two successive cores.

Description of Volcaniclastic Components

Igneous material recovered from Site 585 was restricted to volcaniclastic sediments containing a variety of crystal fragments, altered glass, and basaltic clasts. Because of the polymictic nature of the coarser units and their deposition via turbidity currents, interpretation of the volcanic activity in the source areas can only be tentative.

Table 5 lists occurrences of volcanic material in terms of the relative proportions and types of glass, crystals, and lithic fragments.

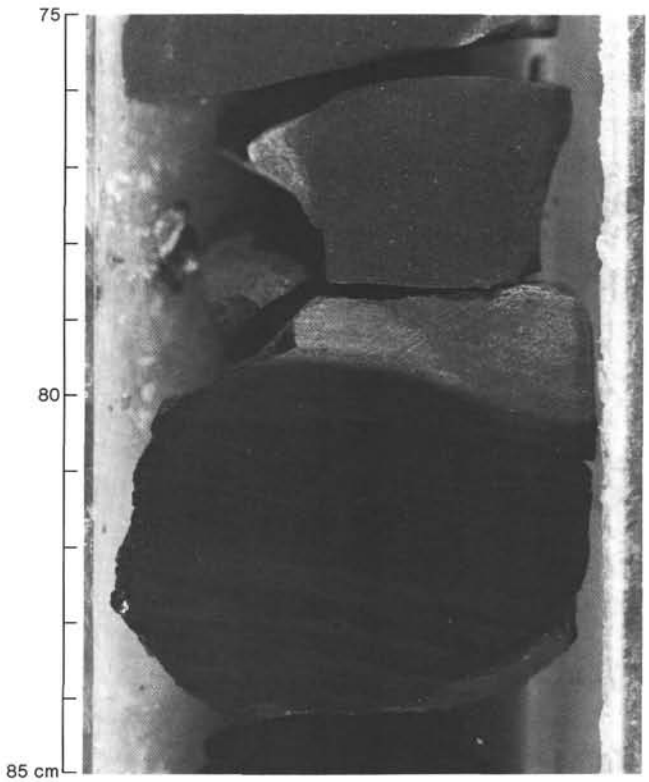

Figure 16. Black band in laminated siltstone underlying multicolored chert, Sample 585A-9-1, 75–85 cm.

Table 6 is a summary of the main clasts in the coarser parts of the volcaniclastic turbidites and reworked hyaloclastite horizons. Microphotographs illustrating some of the main features of glass and basaltic clasts are shown in Figures 27 and 28, respectively.

All the volcanogenic material is pervasively altered and the ubiquitous presence of clinoptilolite, together with other zeolites and analcite, indicate zeolite facies metamorphic grade. Clinoptilolite and phillipsite are generally characteristic of the lower grades of the zeolite facies and probably represent alteration temperatures of well below about 60°C or low-grade submarine weathering of oceanic crust. Other secondary minerals, such as smectites, celadonite, and analcite are stable over the full range of zeolite facies metamorphism.

Alteration minerals found in the volcaniclastic material include: smectites (only saponite identified by XRD), zeolites (clinoptilolite, heulandite, phillipsite, natrolite), analcite, celadonite, calcite, siderite, barite, quartz, and hematite. Natrolite with analcite, barite, and quartz with calcite occur as vein material (2–4 mm wide and generally sparse).

Olivine and glass are nearly always replaced by brown or pale to dark green smectites that appear to be the earliest alteration products. Glass fragments may be white and green zoned with alteration products or totally replaced by dark red smectites with or without hematite. Plagioclase may be fresh or partly replaced by a gray smectite (montmorillonite—not XRD confirmed) or analcite or both. Carbonate replacement is patchy in the matrix of clasts and later in development relative to other

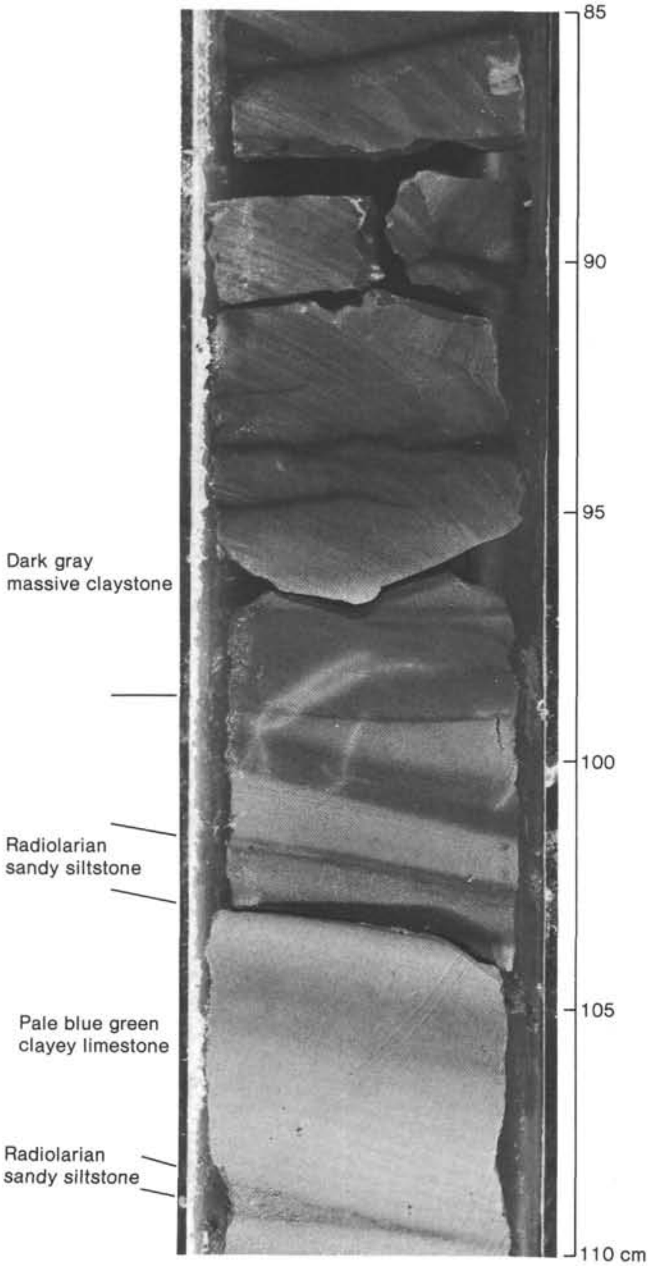

Figure 17. Interbedded radiolarian siltstone, clayey limestone, and massive claystone typical of lithologic Subunit VC, Sample 585-35-1, 85–110 cm.

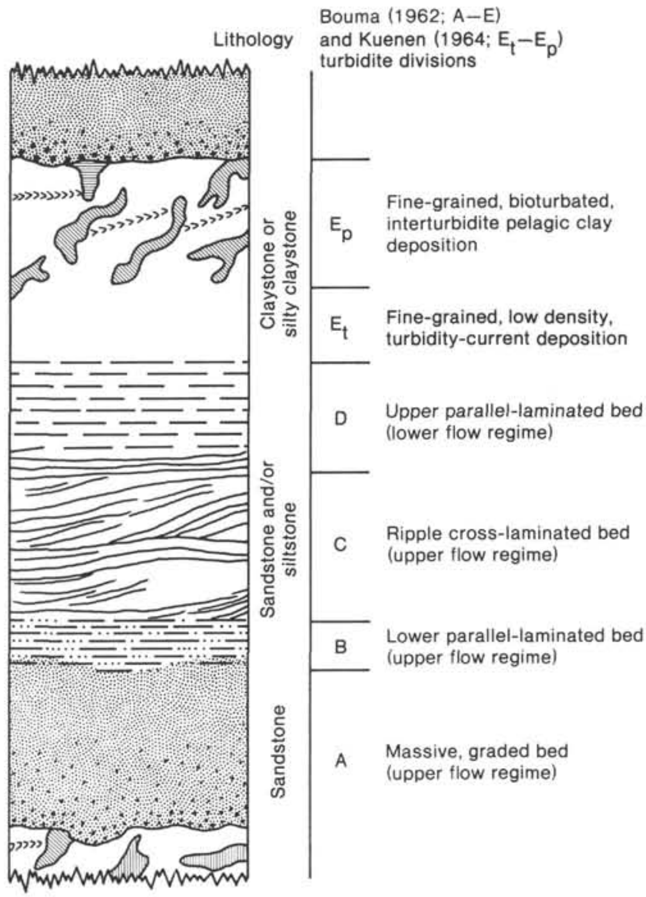

Figure 18. Diagrammatic representation of an idealized complete turbidite sequence showing subdivisions A through E of Bouma (1962) and Kuenen (1964) (modified from Blatt, Middleton, and Murray, 1972).

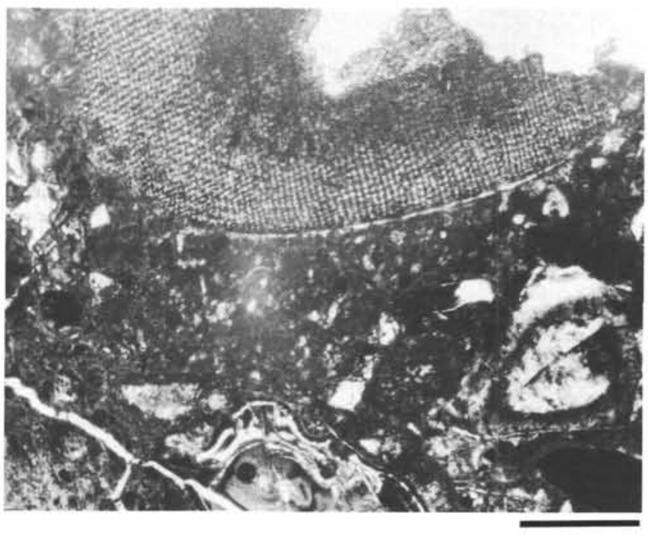

Figure 19. Photomicrograph of an echinoid fragment displaying a reticulate pattern in a volcanogenic sandstone. A poorly preserved ooid is located between two altered glass fragments. Plane-polarized light. Scale is 0.5 mm. Sample 585A-20-3, 62–65 cm.

secondary products. Clinopyroxene is the only primary phase not altered.

Vesicles may be partly or totally filled with radially oriented smectites colored in various shades of green to bright green blue celadonite. A bright red smectite(?) may occupy the center of some vesicles.

Volcanogenic material was assigned an "alteration rating" (Fig. 29) that was utilized in Table 5. Further details appear in Floyd (this volume).

Interpretation of Sedimentary History at Site 585

The single most striking feature of the entire sedimentary section recovered at Site 585 is that most of

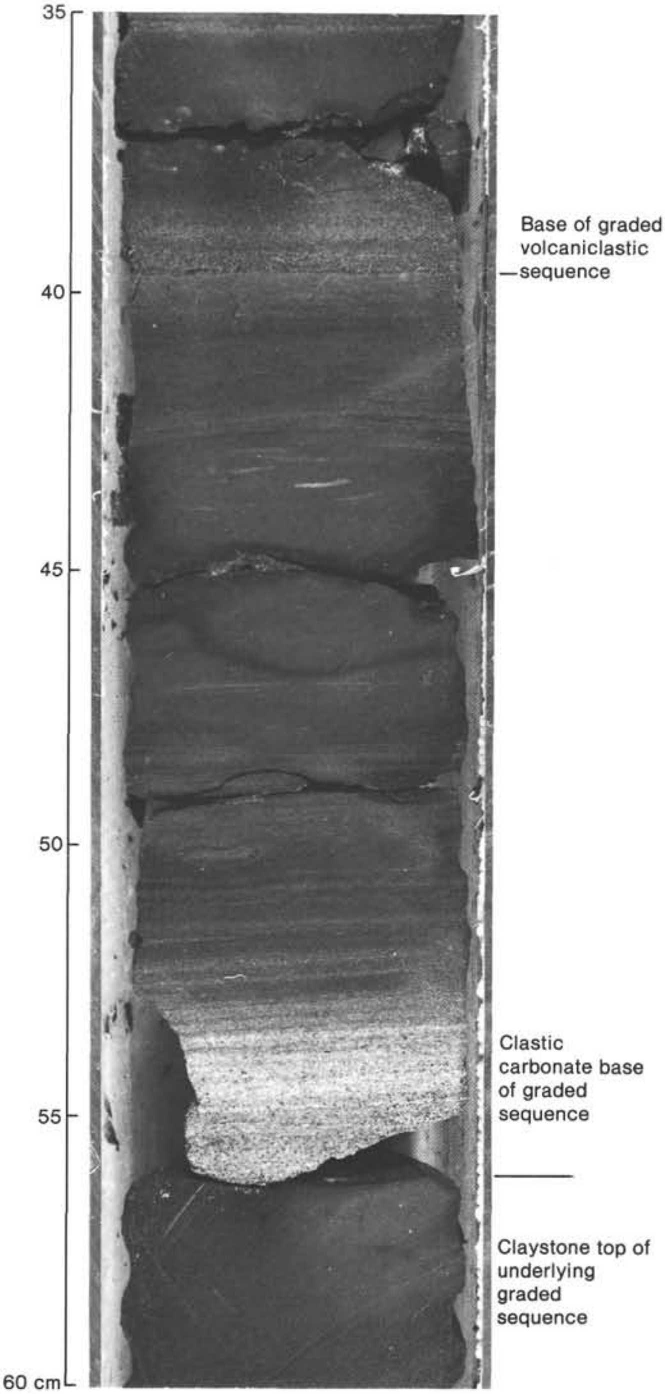

Figure 20. A graded sequence with a coarse clastic carbonate base and claystone top, Sample 585-49-6, 35-60 cm. Also shown are the claystone top of the underlying volcaniclastic graded sequence and the sandstone base of the overlying volcaniclastic graded sequence.

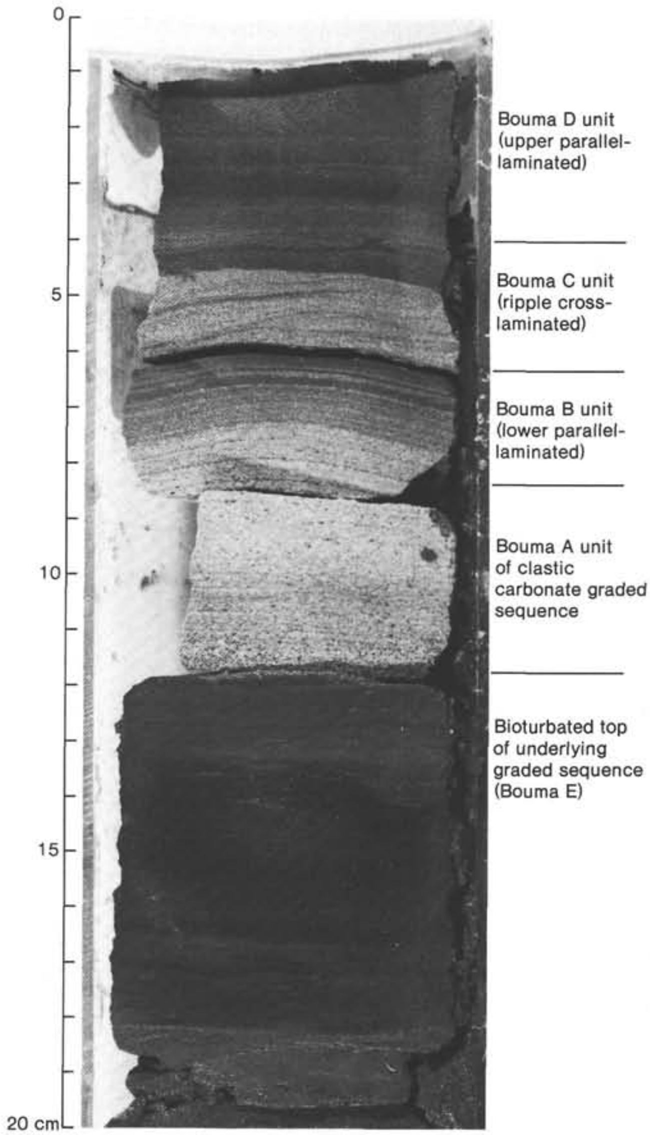

Figure 21. Top of a volcaniclastic graded sequence and bottom of a clastic carbonate graded sequence showing well-developed Bouma turbidite divisions A-E, Sample 585-49-3, 0-20 cm.

the biogenic and volcanogenic components have been reworked, transported, and redeposited from shallower sources. This is most obvious for the volcaniclastic sandstones, siltstones, and claystones at the base of the section that were deposited by turbidity currents and debris flows. The Upper Cretaceous and Tertiary carbonates in the upper part of the section also have been extensively reworked and redeposited, as evidenced first by the fact that they accumulated below the CCD, and second by the winnowed size fractionation and discordant ages of the enclosed microfossils (see Biostratigraphy section). Because of its location in the East Mariana Basin surrounded on three sides by numerous seamounts, it is not surprising that the sediments at Site 585 should contain abundant reworked material. However, we did not anticipate that reworking and redeposition would be so extensive. The section recovered at Site 585 provides an excellent record of the formation, erosion, and subsidence histories of volcanic edifices.

The building of these volcanic edifices during the late Aptian and early Albian is recorded in the coarse volcaniclastic sediments that are the erosional products of differentiated volcanoes. The clasts dominantly are reworked hyaloclastite debris, mixed with clasts that probably were derived from basalt and previously deposited tephra. That the volcanoes were at or near sea level by

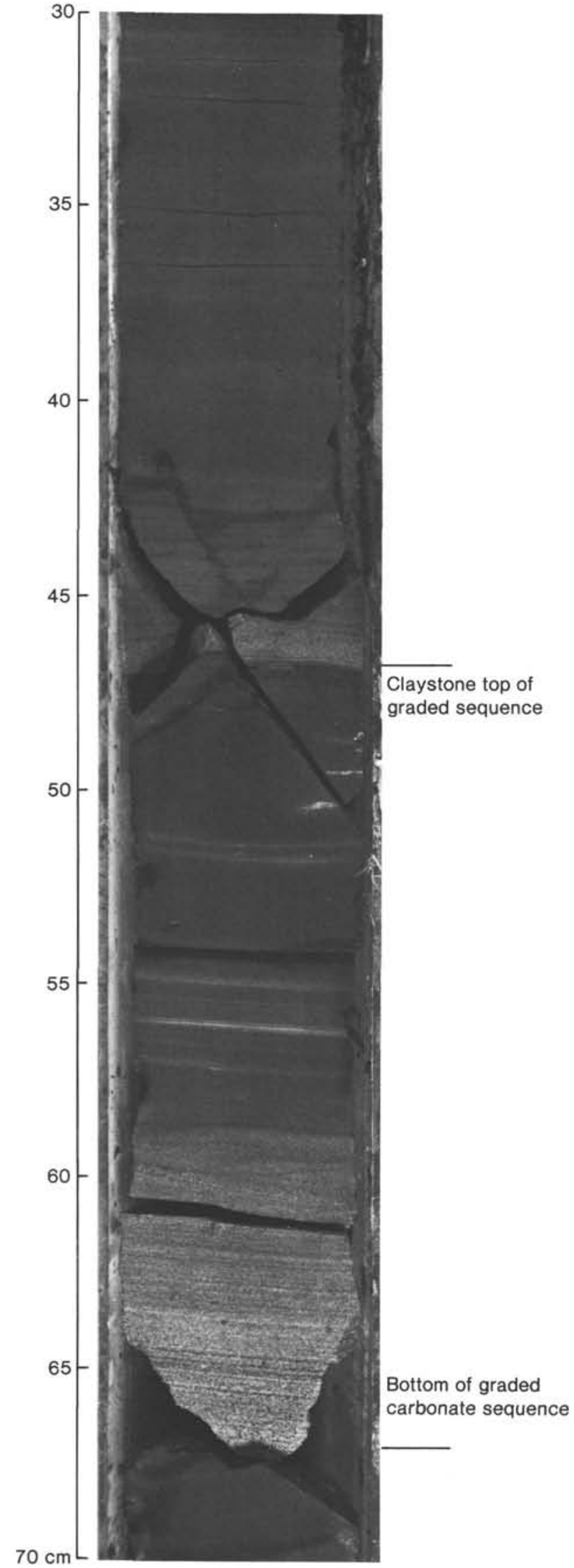

Figure 22. Clastic carbonate graded sequence showing interlamination of volcaniclastics (dark) and carbonate clastics (light), Sample 585-44-1, 30–70 cm.

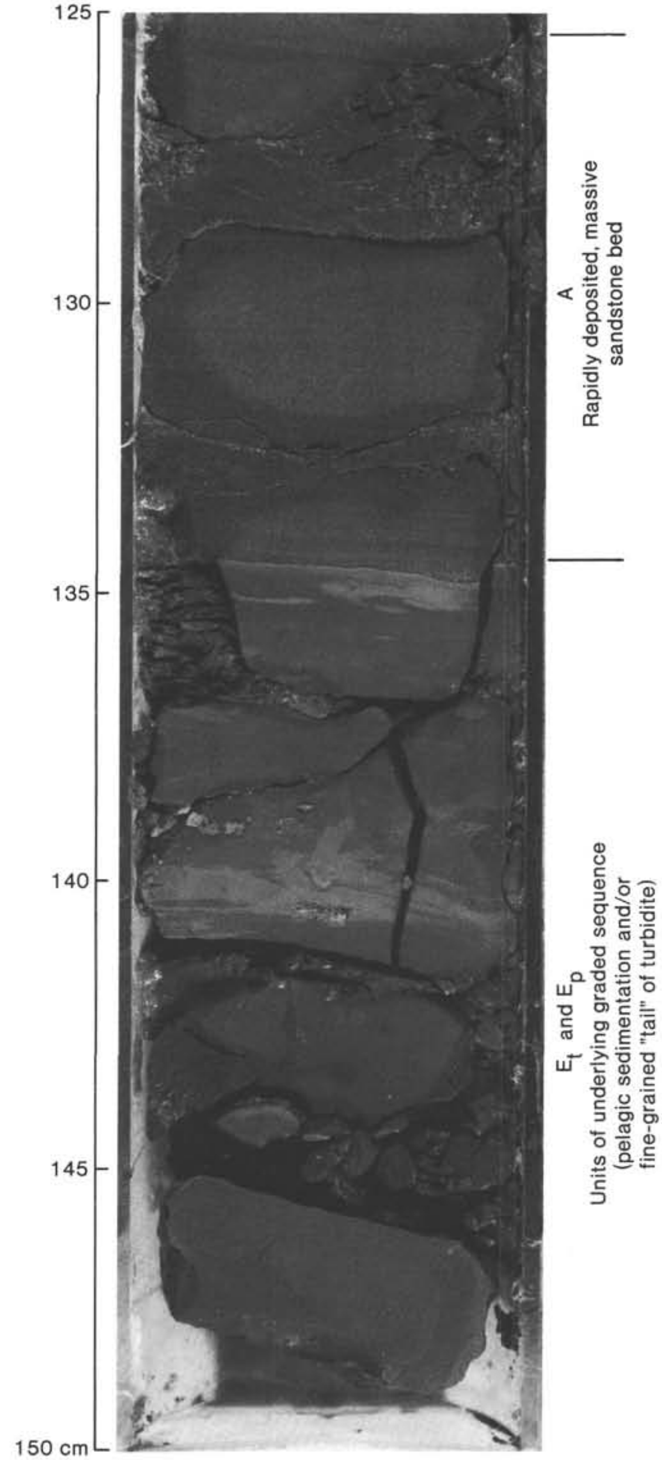

Figure 23. Contact between the bioturbated pelagic clay or fine-grained turbidite top (Bouma E Unit) of one volcaniclastic graded sequence and the rapidly deposited, massive volcaniclastic sandstone base of the overlying graded sequence (Bouma A Unit, Sample 585-42-3, 125–150 cm).

the late Aptian is indicated by the abundant (up to 10%) skeletal carbonate debris that occurs as individual fragments of calcite-cemented, sorted foraminifers in ooid-bearing grainstone in Cores 585A-16 through -20. These volcanoes apparently remained at or near sea level during later stages of edifice building, as indicated by the

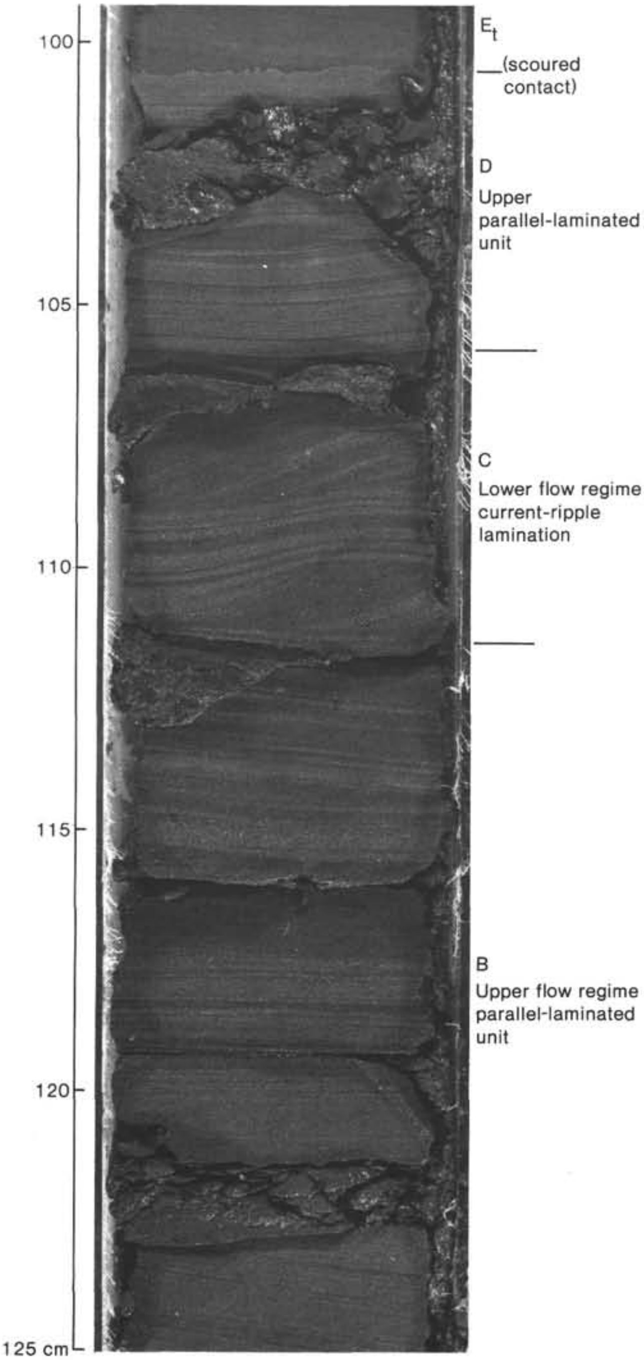

Figure 24. The upper part of the Bouma sequence overlying the sample shown in Figure 23; the graded sequence contains well-developed lower parallel-laminated, ripple cross-laminated, and upper parallel-laminated (Bouma B, C, and D) units, Sample 585-42-3, 100–125 cm.

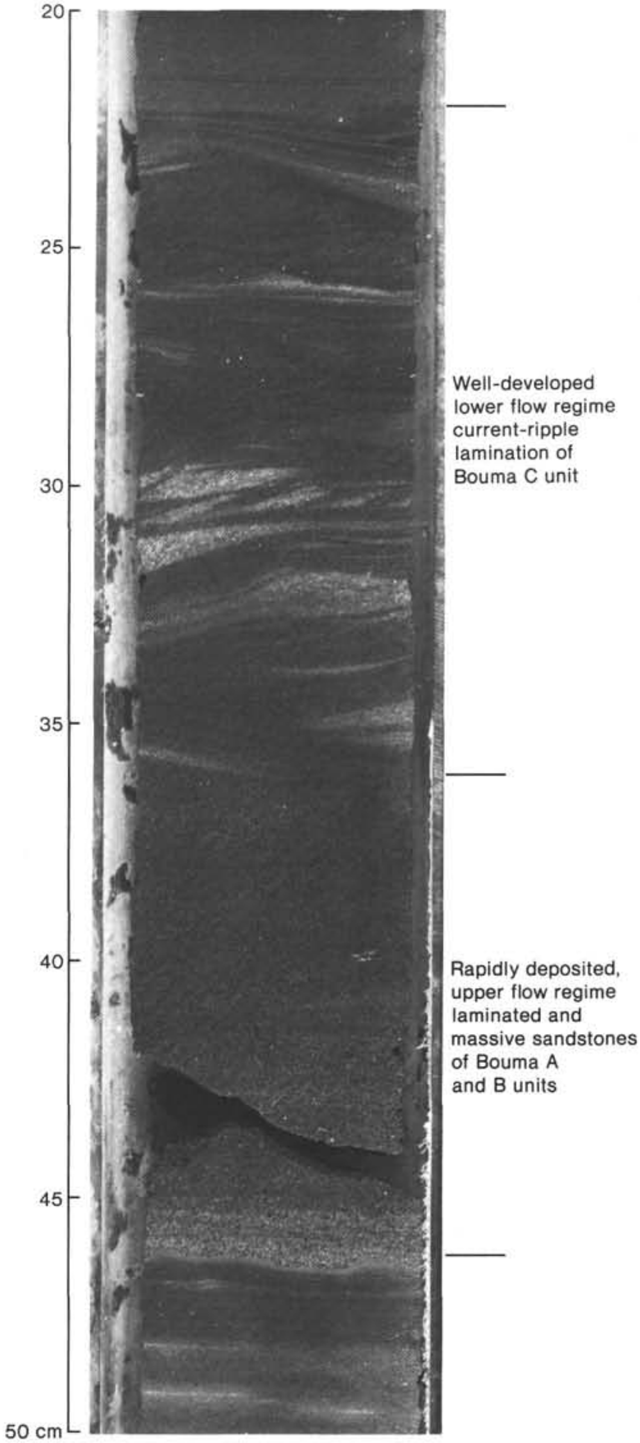

Figure 25. Lower part of a volcaniclastic graded sequence with a massive and laminated sandstone base (Bouma A and B units) and well-developed current-ripple laminations (Bouma C unit), Sample 585A-H5-5, 20–50 cm.

interbedding or mixing of coarse shallow-water carbonate debris at the bases of many of the middle Albian graded sequences (Cores 585-38 to -45).

The claystones of Unit V were mainly deposited as fine-grained distal turbidites during the middle Albian to Campanian. The variable abundances of zeolites and calcareous and siliceous microfossils most likely reflect variations in influx of allochthonous volcanic and biogenic components, but may also reflect variations in surface water productivity. A thin layer of sediment rich in organic carbon of algal origin (see Organic Geochemistry section) was found in latest Cenomanian fine-grained turbidites of Unit V. The presence of this carbon-rich layer can be interpreted as indicating that the submarine

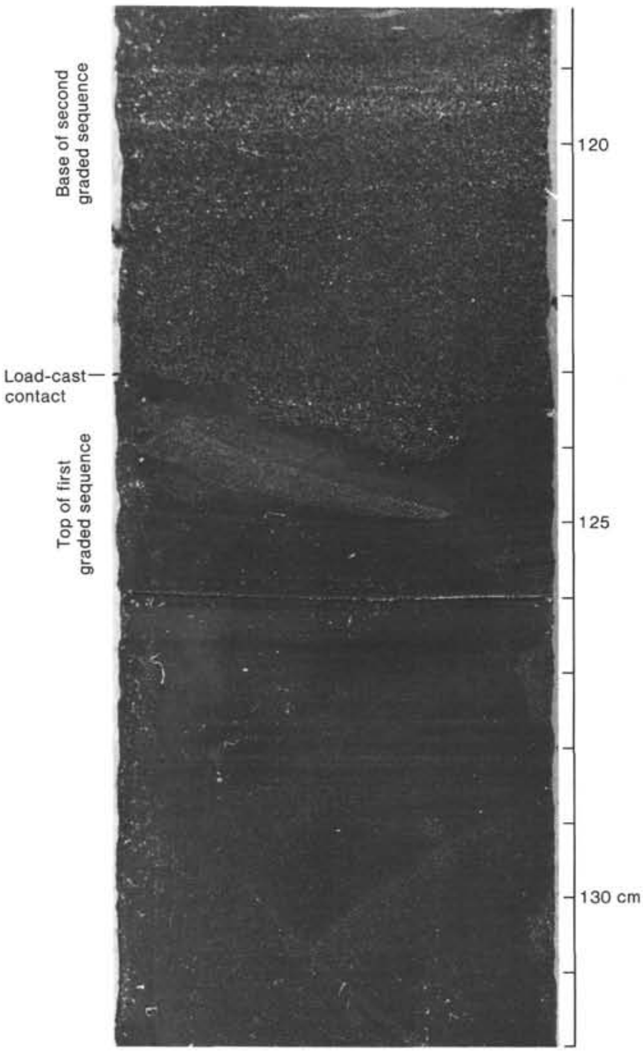

Figure 26. Well-developed load cast at the contact between the claystone top of one volcaniclastic graded sequence and the coarse sandstone base of the overlying graded sequence, Sample 585A-13-1, 120–130 cm.

Table 5. Description of volcanogenic material in Units III, V, and VI, Site 585.

Core	Main lithology	Volcanic components	Alteration rating
585-18 to -20 585-26 to -28	Zeolitic claystones and siltstones	Crystal fragments; altered glass (smectites and zeolite)	C, D
585-38 to -46	Zeolitic and carbonate turbidites	Crystal fragments (plagioclase, clinopyroxene, olivine); altered vesicular glass abundant; basaltic clasts at depth	C
585-47 to -48	Reworked hyaloclastites in turbidite sequence	Mainly altered vesicular clinopyroxene-phyric glass; rare, large basaltic clasts are poorly vesicular	B, C, D
585-49 to -55 and 585A-11 to -17	Volcaniclastic turbidite	Crystal content highly variable; highly vesicular glass common; greater variation in basaltic type of large angular clasts	B, C
585A-18 to -22	Debris flows and reworked hyaloclastites	Poorly vesicular, palagonitized and smectite-replaced glass fragments; various nonvesicular basaltic clasts	B, C, (D)

Note: Alteration ratings are defined in Figure 29.

slopes of the surrounding seamounts were within an oxygen minimum zone. The unoxidized organic matter that accumulated in the slope sediments was subsequently transported to the deep Mariana Basin by turbidity currents. A second interpretation is that the carbon-rich layer is autochthonous, and this demands that the deep basin itself was occupied by oxygen deficient water. Organic carbon-rich strata of the same general mid-Cretaceous age (although they are not synchronous) have been reported from the flanks of a number of other volcanic seamounts and plateaus in the central and western Pacific (Schlanger and Jenkyns, 1976; Thiede, Dean, and Claypool, 1982).

The Late Cretaceous to Tertiary carbonates (and possibly carbonates from the Pleistocene) record the submarine erosion and downslope transport of the pelagic "cap" that had accumulated on the volcanic edifices as they subsided but remained well above the carbonate compensation depth (CCD). These redeposited carbonates are interbedded with brown zeolitic claystones that probably record background pelagic-clay sedimentation below the CCD mixed with some remaining volcanogenic sediments. Several additional minor pulses of volcanic activity are suggested by thin beds and laminae of zeolite-rich material and are found in Cores 585-26 to -38, and in -20. Much of the Late Cretaceous and early Tertiary sedimentary record was not recovered because of abundant chert. However, the abundance of chert, reaching a maximum between Campanian and Eocene, may itself be significant and may reflect increased surface water productivity of radiolarians as the site passed under the equatorial zone of high organic productivity between about 90 and 50 Ma (see Paleomagnetic section).

No record of post-Eocene sedimentation was recovered at Site 585 except for a single core taken at the seafloor. This core is composed of 5.3 m of reworked nannofossil ooze that contains early Pleistocene to Miocene microfossils (see Biostratigraphy section) overlain by 1.5 m of Recent brown clay. The reworked ooze suggests that downslope transport of carbonate sediment from the pelagic "cap" of surrounding seamounts continued at least into the Recent. The Recent brown pelagic clay at the top of the section indicates either that redeposition of carbonate debris has ceased, or, more likely, that Site 585 is awaiting its next influx of reworked carbonate debris.

BIOSTRATIGRAPHY

Summary

Recent sediments at Site 585, deposited at 6109 m and recovered in the uppermost 150 cm of Core 585-1, consist of brown clay rich in manganese nodules and associated commonly with fish remains. Noticeably, they do not contain any abyssal benthic foraminifers. Below that layer, the sediments recovered contain a considerable amount of carbonates, the presence of which is not consistent with the abyssal depth of the East Mariana Basin, where sediments have been deposited well below the CCD since the Early Cretaceous and particularly during the Tertiary.

Table 6. Summary of clast types in the coarser parts of volcaniclastic turbidites, Site 585.

Clast types	Cores 585-38 to -46	585-47 to -48	585-49 to -55 585A-11 to -17	585A-18 to -22	Comments
Glass					Glass generally palagonitized or replaced by smectite; often highly vesicular (up to 40% vesicles), but also many non- or poorly vesicular fragments; quenched plag microlites may be abundant in some cases
Aphyric	C	C	—	A	
Plag-phyric	A	A	—	C	
Cpx-ol-phyric	—	—	C	R	
Cpx-plag-phyric	C	C	—	—	
Basalts					Invariably fine-grained with granular or intersertal textures; some are alkali basalts with titanaugite in groundmass or rarely as microphenocrysts; generally poorly vesicular, with vesicles infilled with smectite
Aphyric basalt	R	—	—	C	
Plag-phyric ol basalt	—	R	A	C	
Ol-phyric alkali basalt	—	—	A	—	
Ol-plag phyric basalt	—	—	C	C	
Differentiates					
Trachyte	—	R	C	R	Good flow orientation of plag laths; abundant Fe ore granules throughout
Ferrobasalt	—	—	R	R	
Amphibolite	—	—	R	—	Nonfoliated, low-pressure amphibolite facies
Clinopyroxene					Often broken, but generally very fresh; released from glassy clasts on transportation
"Megacrysts"	—	R	R	—	

Note: A = abundant; C = common; R = rare; plag = plagiolcase, cpx = clinopyroxene, ol = olivine; — = not present.

The majority of sediments recovered from Site 585 are characteristic of transported and reworked deposits. Indeed, few autochthonous intervals of pelagic clay were recovered throughout the cored sequence. Fossil assemblages recovered reflect the turbiditic nature of the sediments. Younger-aged material typically is masked by the influx of older, often better-preserved fossil material, thus the biostratigraphic signal is commonly obscured. Consequently, the ages reported must be considered maximum ages, and many may in fact be considerably younger. Shape and size sorting are characteristic attributes of the foraminiferal and radiolarian assemblages. The recovered specimens are small-sized adults and juveniles that range in size from 45 to 149 μm. Deposition below the CCD also has strongly altered the character of the calcareous and siliceous fossils as a result of dissolution and recrystallization.

Biostratigraphic schemes for the three fossil groups are based on the following references: Calcareous nannofossils—Martini, 1971; Okada and Bukry, 1980; Perch-Nielsen, 1979; Romein, 1979; Thierstein, 1976; Verbeek, 1977. Foraminifers—Hardenbol and Berggren, 1978; van Hinte, 1976; Sigal, 1977; Premoli Silva and Sliter, 1981. Radiolarians—Riedel, 1974; Foreman, 1973, 1975; Schaaf, 1981.

A synthesis of the biostratigraphic events in Hole 585 based on the three fossil groups, namely, calcareous nannoplankton, foraminifers (both planktonics and benthics), and radiolarians (Fig. 30) shows that some stratigraphic intervals could not be identified. That does not imply that the succession is not continuous. The generally poor recovery, the fact that the autochthonous sediments are devoid of age-diagnostic species, and the turbiditic character of the other sediments that contain index species prevent further biostratigraphic refinement. In particular, most of the Paleocene is not evident: the few nannofossil and planktonic foraminiferal zonal assemblages recorded were either reworked into the Eocene sequence or mixed with younger zones within the Paleocene. Moreover, upper and middle Maestrichtian assemblages occur only mixed within the Tertiary sequence. The Cretaceous/Tertiary boundary is placed within Core 585-16. Cores 585-26 and -30 seem to span the interval from Santonian through upper Turonian. The Cenomanian/Turonian boundary is placed within Core 585-32.

The lower Cenomanian and upper Albian interval may be located between Cores 585-35 and -36, but the poor recovery prevents further resolution. The most complete intervals recorded are from: lower middle Eocene to uppermost Paleocene; Santonian; lower upper Albian to upper Aptian.

A similar synthesis of biostratigraphic events in Hole 585A is shown in Figure 31. Stratigraphic intervals recovered include the lower Eocene, upper Paleocene, and a portion of the Maestrichtian. The Cretaceous/Tertiary boundary is placed in Core 585A-3. Cores 585A-5 to -9 span the Santonian to lower Turonian. The Cenomanian/Turonian boundary appears to occur in Core 9. Portions of the upper Cenomanian and upper Albian were found in Cores 585A-9 and -10, whereas 585A-11 to -22 are identified as upper Aptian.

Nannofossils

Hole 585

Smear slides were prepared for each of the samples taken from cores recovered at Site 585. Although nannofossils are present in samples throughout the section,

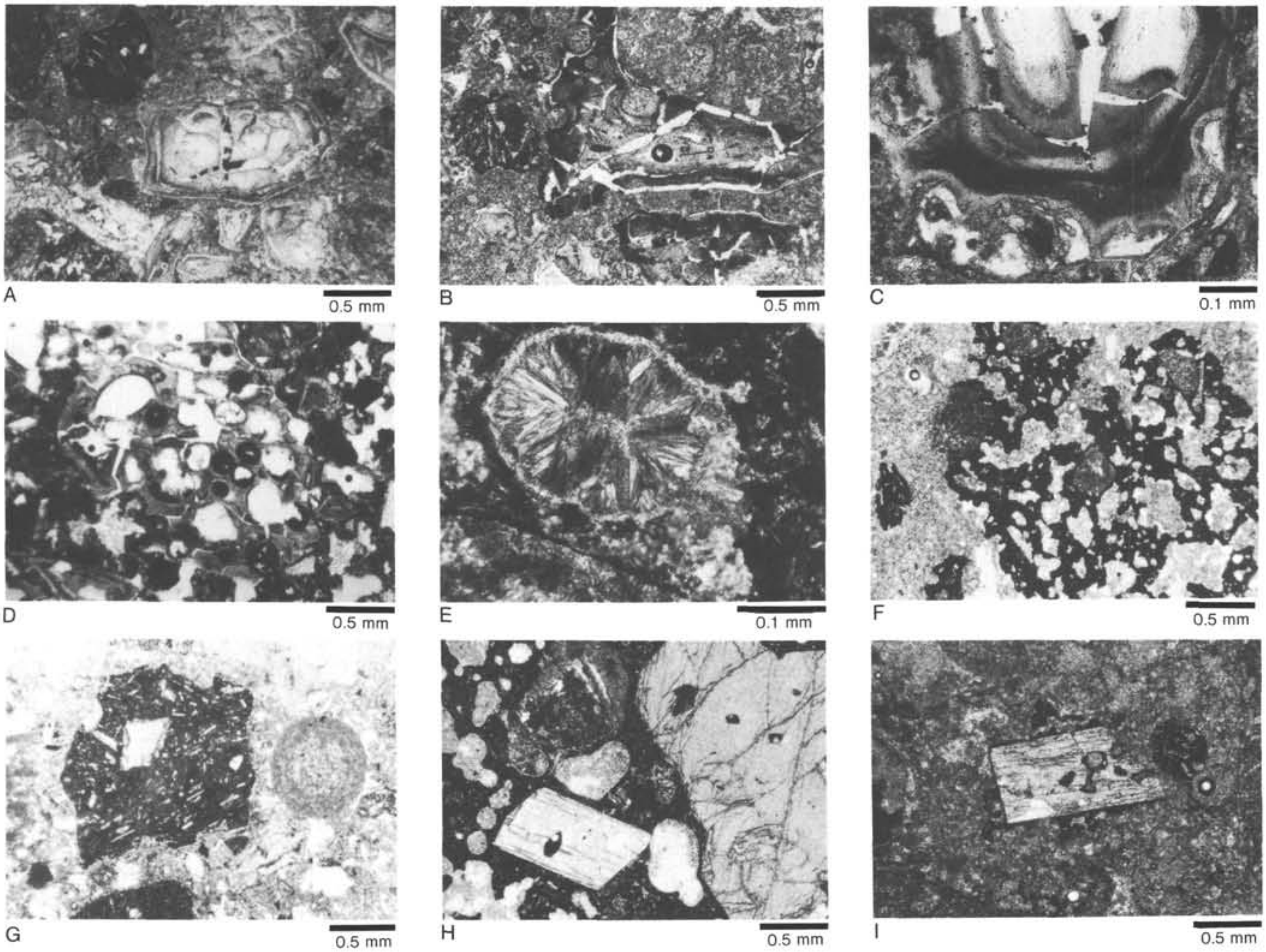

Figure 27. Various features exhibited by glassy fragments in volcaniclastic sediments, Site 585. (A) Subangular, alteration zoned, palagonitized sideromelane fragment (plane polarized light); Sample 585A-18,CC. (B) Vesicular, cuspate palagonite shard with dark smectite-replaced border (plane polarized light); Sample 585-48-1, 81–84 cm. (C) Microfractured and alteration zoned palagonite fragment (plane polarized light); Sample 585A-18,CC. (D) Highly vesicular, subrounded palagonite fragment; vesicles infilled with dark smectite and white zeolite (plane polarized light); Sample 585-14-2, 23–26 cm. (E) Vesicle rimmed by a thin zone of yellow smectite and infilled by radiate fibers of pleochroid green smectite (plane polarized light); Sample 585-54-2, 65–67 cm. (F) Highly vesicular, olivine- (dark and granular, now totally replaced) phyric tachylyte fragment (plane polarized light); Sample 585-48-1, 81–84 cm. (G) Angular, plagioclase-phyric tachylyte fragment and concentrically zoned ooid (plane polarized light); Sample 585A-18-7, 48–50 cm. (H) Large clinopyroxene and (altered) olivine phenocrysts in vesicular tachylyte (plane polarized light); Sample 585-54-2, 65–67 cm. (I) Subhedral clinopyroxene "megacryst" with a thin dark rim of adhering tachylyte (plane polarized light); Sample 585-48-1, 134–137 cm.

assemblages were often difficult to date because of extensive reworking in the top part of the section (Cores 585-1 through -20) and the generally sparse assemblages that were recovered from samples below that.

The occurrence of nannofossil-rich sediments in Cores 585-1 through -20 is suspicious, given that Site 585 is at 6109 m depth. Such evidence as grading observed in thin section, and the absence of larger-sized planktonic foraminifers and abyssal benthic foraminifers in most samples, presented by other members of the scientific party, demonstrates that these sediments have been redeposited. The extreme amount of reworking observed in many of the nannofossil assemblages and the mixing of sediments of apparently different ages support this interpretation. The sparse assemblages recovered from Cores 585-28 through -55 are also out of place, as they occur in sediments that show visible signs of grading. Problems with reworking were not detected in these assemblages.

Shipboard examination of the smear slides yielded the following results: Abundant and moderately well preserved nannofossils occur in samples from the bottom of Core 585-1 and contain *Discoaster quinqueramus*, a species restricted to the upper Miocene. This assemblage is reworked, however, because *Ceratolithus rugosus*, which is very rare in this core, indicates an early Pliocene or younger age.

Cores 585-2 through -14 are dated as early to middle Eocene. All samples from these cores contain reworked upper Campanian to Paleocene species. *Discoaster diastypus, Marthasterites bramlettei*, and *Discoaster kuepperi* are rare in sediments at the base of Core 585-14 and

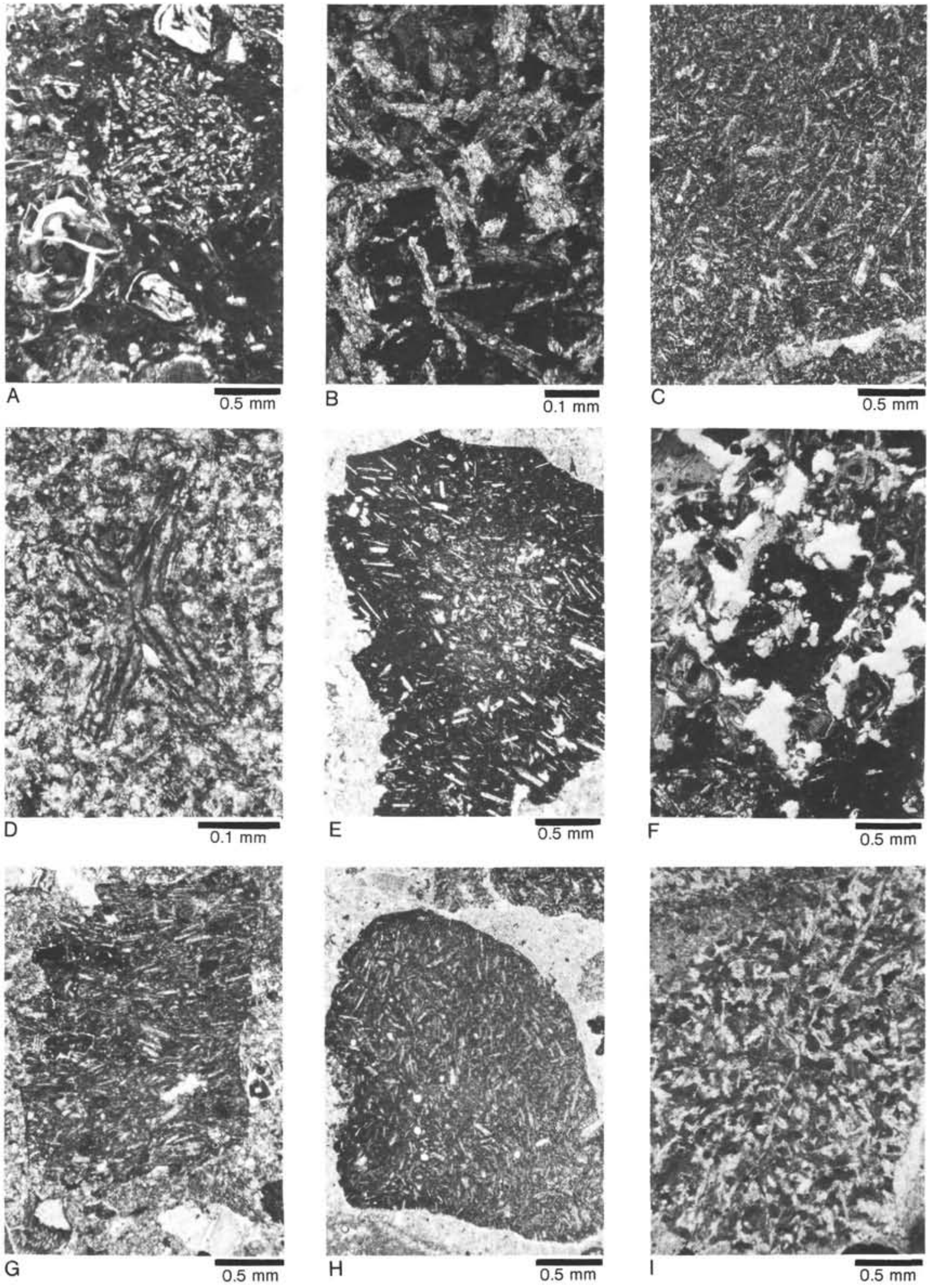

Figure 28. Various features exhibited by basaltic fragments in volcaniclastic sediments, Site 585. (A) Rounded plagioclase-rich basalt clast and palagonitized glass fragments (plane polarized light); Sample 585A-18,CC. (B) Smectite-replaced plagioclase laths in granular-textured alkali basalt (plane polarized light); Sample 585-54-2, 65-67 cm. (C) Close-textured, fine-grained, aphyric basalt; some replacement by carbonate (plane polarized light); Sample 585-48-1, 134-137 cm. (D) Microphenocryst of cruciform-twinned titanaugite in olivine basalt (plane polarized light); Sample 585-54-2, 65-67 cm. (E) Hypocrystalline plagioclase-phyric basalt fragment with dark tachylyte rim. (plane polarized light); Sample 585-48-1, 81-84 cm. (F) Clinopyroxene-glomerophyric hypocrystalline basalt clast (plane polarized light); Sample 585A-14-2, 23-26 cm. (G) Angular, poorly vesicular basalt clast with flow-oriented plagioclase laths (plane polarized light); Sample 585-48-1, 81-84 cm. (H) Subrounded trachyte clast with remnants of dark trachyte rim (plane polarized light); Sample 585-54-2, 65-67 cm. (I) Nonfoliated epidote amphibolite clast (plane polarized light); Sample 585-54-2, 65-67 cm.

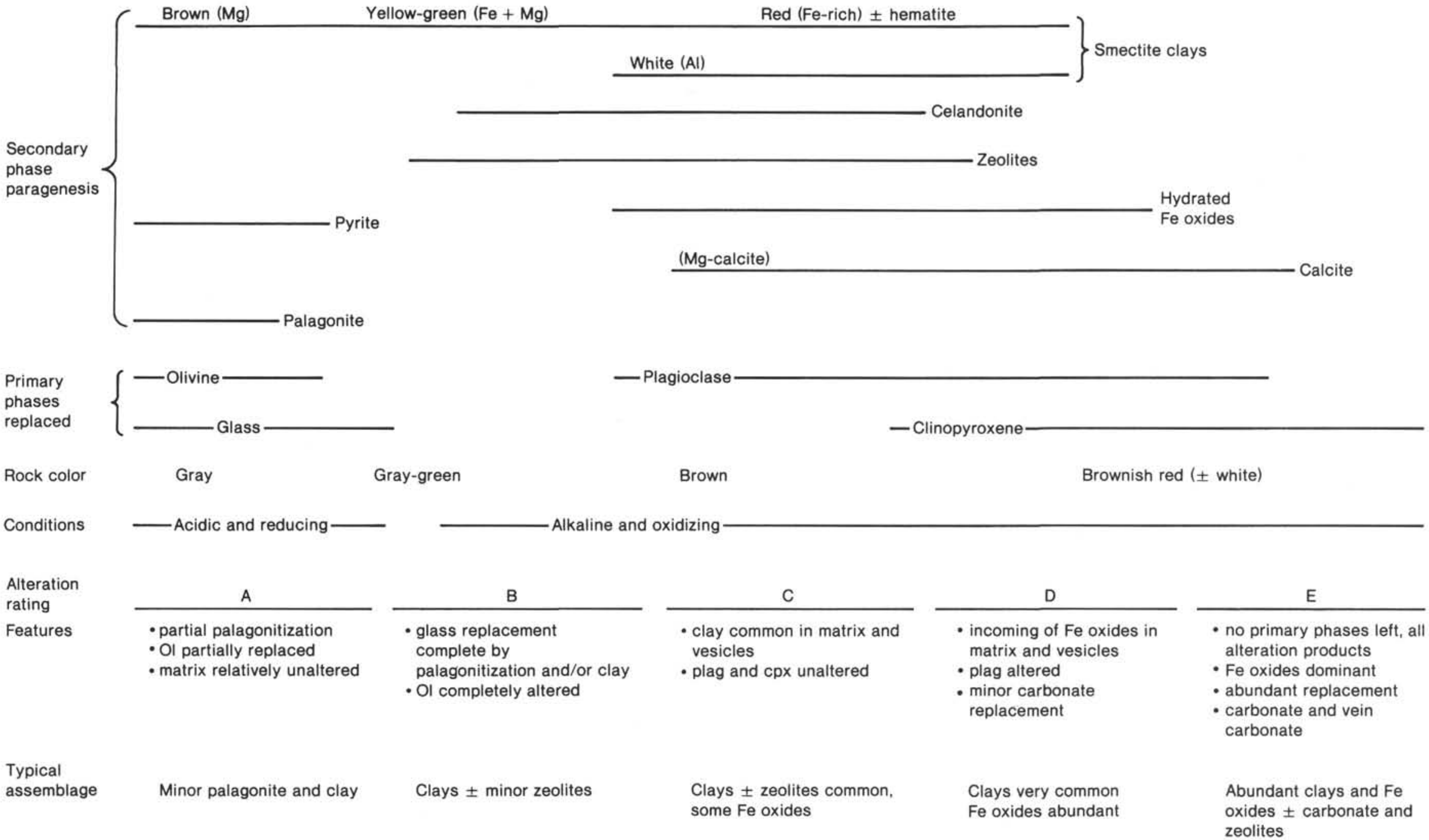

Figure 29. Visual estimate and alteration rating (A–E) in glass and basaltic rocks (fresh rocks = 0). Ol = olivine, plag = plagioclase; cpx = clinopyroxene.

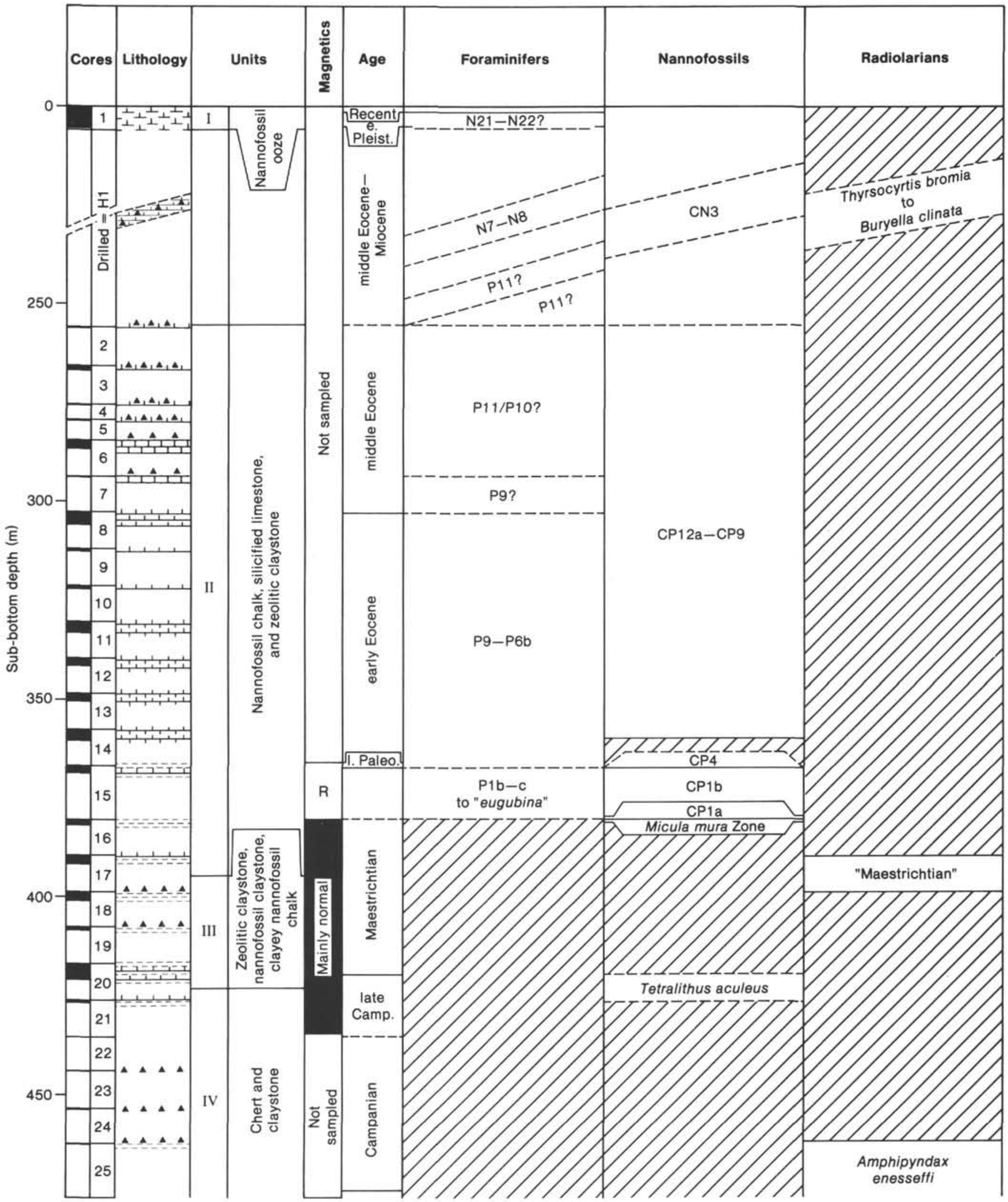

Figure 30. Biostratigraphy of Hole 585 plotted against lithology and magnetic stratigraphy. (In Magnetics column, R or white area indicates reversed polarity, and black area, normal polarity. FAD = first appearance datum.)

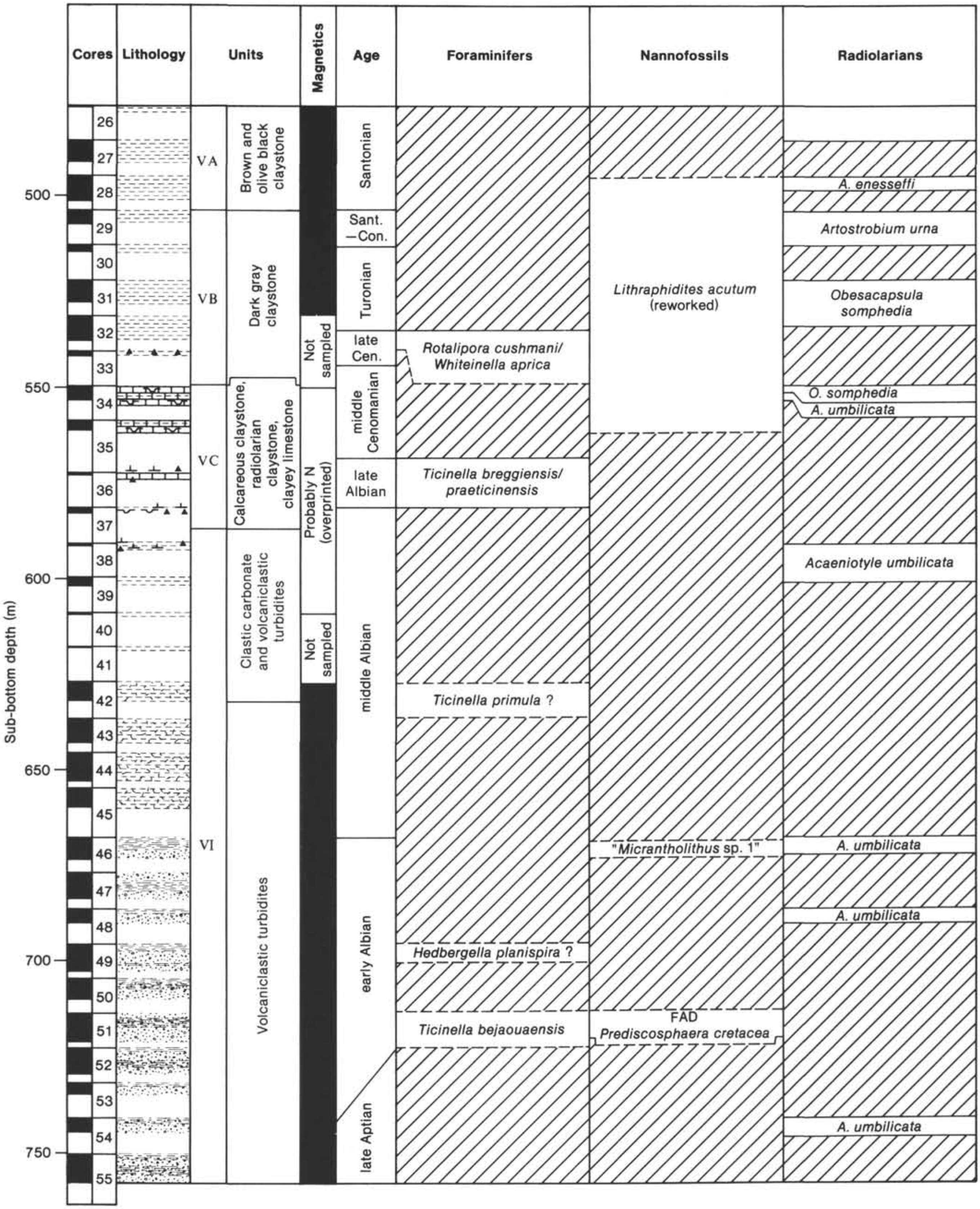

Figure 30 (continued).

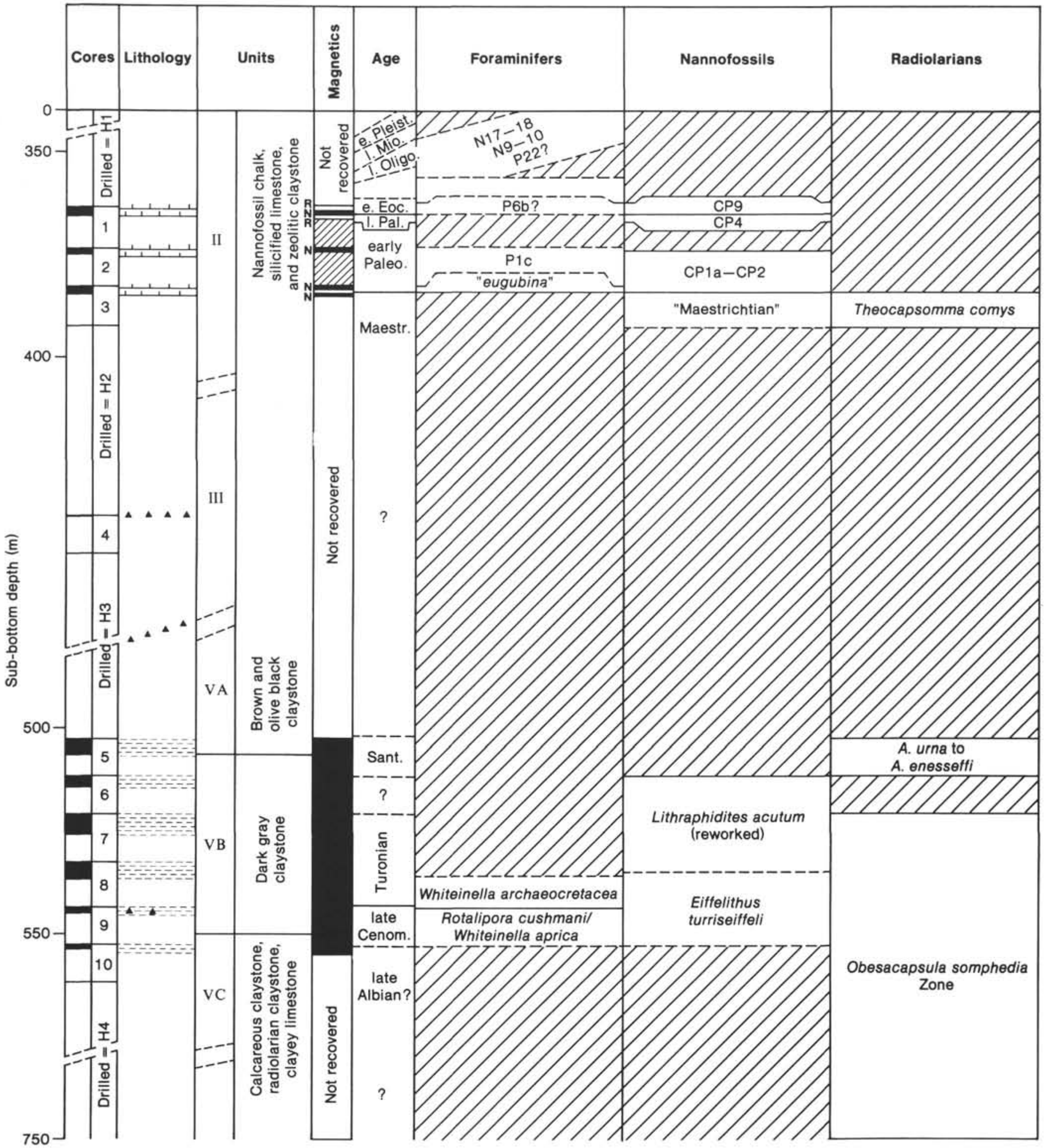

Figure 31. Biostratigraphy of Hole 585A plotted against lithology and magnetic stratigraphy. (In Magnetics column, R or white space indicates reversed polarity, and black space or N, normal polarity. Hachured areas indicate areas for which no fossil zones were assigned.)

indicate an age of earliest Eocene. *Discoaster sublodoensis* and *Discoaster lodoensis* are present in a sample from the top of Core 585-3, and the youngest Eocene sediments are dated in the *Discoaster sublodoensis* Zone. The first occurrences of *Discoaster sublodoensis* and *Discoaster lodoensis* appear to be in Cores 585-7 and -9, respectively, but their rare and inconsistent occurrences make these datums somewhat tentative. These two species commonly are heavily calcified, whereas reworked species in the same sample are more common and moderately well preserved. In addition, some samples above the *Discoaster lodoensis* and *Discoaster sublodoensis* datums appear older. They contain a well-preserved basal Eocene assemblage that includes *Marthasterites contor-*

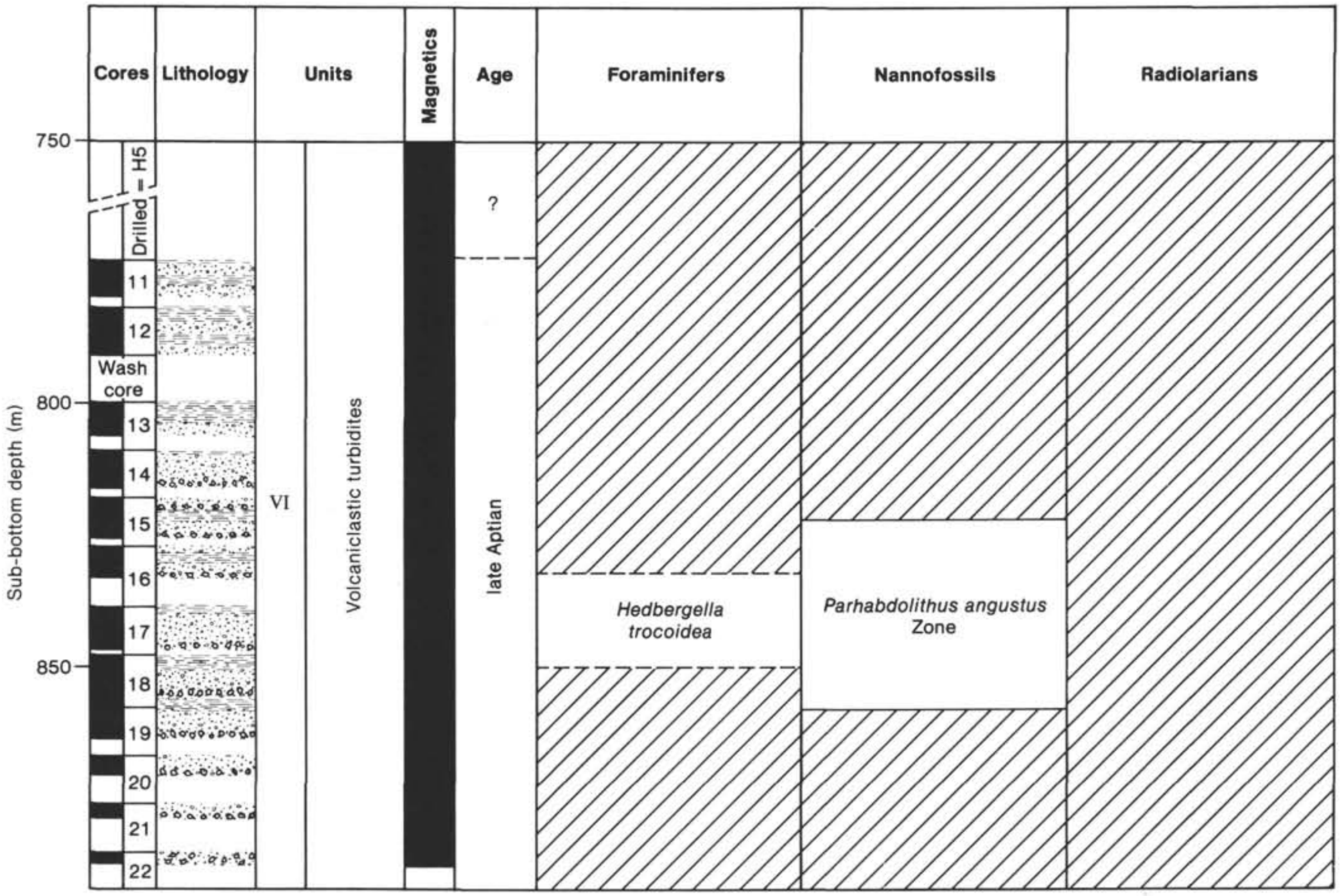

Figure 31 (continued).

tus, Marthasterites bramlettei, Discoaster diastypus, and *Discoaster multiradiatus*, but not *Discoaster lodoensis* and *Discoaster sublodoensis*. Thus it is possible that the sediments in Cores 585-2 through -14 are either a mixture of different age sediments that were redeposited after the middle Eocene (*Discoaster sublodoensis* Zone) or that the poorly preserved specimens of *Discoaster lodoensis* and *Discoaster sublodoensis* are in place and preserved only at a few horizons.

Part of the upper Paleocene is missing between Cores 585-14 and -15, as the top of Core 585-15-1 contains species that date this interval in the *Fasciculithus tympaniformis* Zone. Reworked Cretaceous species make up 10 to 25% of the assemblages in these samples. The remainder of Core 585-15 and the top of Core 585-16 (585-16-1, 8–10 cm) are identified with the lower Paleocene *Cruciplacolithus tenuis* Subzone and contain the eponymous species. Sample 585-16-1, 49–50 cm contains *Thoracosphaera saxea*, but not *Cruciplacolithus tenuis*, and is placed in the *Cruciplacolithus primus* Subzone. Reworked Cretaceous species dominate assemblages from these lower Paleocene sediments (more than 99% of specimens observed) and make it impossible to recognize the mass extinction of flora at the Cretaceous/Tertiary boundary. The flood of *Thoracosphaera* seen at the base of the Tertiary in many parts of the world was also overwhelmed by this reworking, and the boundary had to be placed at the first occurrence of *Thoracosphaera*.

Sample 585-16-1, 88–90 cm contains *Micula mura*, with no Tertiary species, and so appears to be upper Maestrichtian. *Tetralithus trifidus, Tetralithus gothicus*, and *Ceratolithoides aculeus* are in Samples 585-16-1, 101–103 cm through 585-20-1, 52–53 cm. The total range of *Tetralithus trifidus* is upper Campanian to lower Maestrichtian, but this species is reworked into Tertiary sediments in this section and its last occurrence cannot be used as a datum. The sample from Section 585-20-3 contains *Tetralithus gothicus*, but not *Tetralithus trifidus*, and may indicate the uppermost Campanian. Core 585-21 has *Ceratolithoides aculeus* but not *Tetralithus gothicus* or *Tetralithus trifidus* and is dated as early late Campanian.

Nannofossils were not observed in samples from Cores 585-22 through -27. *Eiffellithus turriseiffeli* and *Microstaurus chiastius* occur in samples from Cores 585-28 through -35 and date this interval from late Albian to late Cenomanian. A few specimens of *Lithraphidites acutum* were observed in Samples 585-31-4, 46–47 cm and 585-35-2, 46–47 cm and suggest that Cores 585-28 through -35 may be middle to late Cenomanian. Data from radiolarians indicate a younger age for most of this interval and suggest that these assemblages are reworked.

Nannofossil assemblages in Cores 585-36 to -42 are characterized by low species diversities and poor preservation, and these cores could not be dated. Cores 585-45 through -51 contain Albian assemblages. The lowest dated sample was Sample 585-51-3, 16–18 cm. It contains *Prediscosphaera cretacea*, which has its first occurrence in the lower Albian.

Hole 585A

Several cores in Hole 585A were taken at intervals cored during Hole 585; thus it is no surprise that many of the nannofossil assemblages in samples from this hole are identical to those seen in Hole 585. In Core 585A-1, sediments dated in the basal Eocene *Tribrachiatus contortus* Zone (CP9a) unconformably overlie those of the *Fasciculithus tympaniformis* Zone (CP4). The same hiatus was detected between Cores 585-14 and -15 in Hole 585. Lower Paleocene sediments dated from the *Cruciplacolithus primus* Subzone (CP1a) through the *Chiasmolithus danicus* Zone (CP2) occupy the top of Core 585A-3 and all of Core 585A-2. Although the *Chiasmolithus danicus* Zone was not sampled in Hole 585, the gap in the age of the sediments between Cores 585A-1 and -2 in this hole is similar to that observed in the top of Core 585-15 in Hole 585. The Cretaceous/Tertiary boundary is tentatively placed between Samples 585A-3-1, 73–75 cm and 585A-3-1, 128–130 cm, as the former sample contains *Thoracosphaera* and the latter one does not. This boundary was again hard to recognize because of the large number of reworked Cretaceous species in these cores.

All samples taken below Core 585A-3 are barren or contain few, poorly preserved species. Accurate age determinations could not be obtained for many of these assemblages. Such was the case for all the samples from Cores 585A-4 and -5. Several samples from Cores 585A-6 through -10 contain both *Eiffellithus turriseiffeli* and *Microstaurus chiastius*, which dates these cores between late Albian and late Cenomanian. *Lithraphidites acutum* was found in Sample 585A-8-2, 18–19 cm and indicates an age of middle to late Cenomanian for this sample and those above it through Core 6. These assemblages, as in Hole 585, may be reworked. No ages were determined for Cores 585A-11 through -14. Cores 585-15 through -18 appear to be upper Aptian to Albian. *Lithastrinus floralis* and *Parhabdolithus angustus*, which have their first occurrences in the upper Aptian, are present in samples throughout this interval. *Tranolithus gabalus* and *Rucinolithus irregularis* have not been reported in sediments younger than Albian and are present in Sample 585A-15-3, 24–26 cm. Samples examined from Cores 585A-19 through -21 are barren, except for Sample 585A-21-1, 84–85 cm, which contains only *Watznaueria barnesae*.

Foraminifers

Hole 585

Below the brown clay that represents the Recent and sub-Recent sediments at Site 585, planktonic and calcareous benthic foraminifers occur only as displaced, frequently reworked, assemblages from various water depths, but predominantly from a bathyal setting. The foraminifers occur typically as size-sorted clasts in graded turbidites. In particular, during the Tertiary, the largest fractions recovered never exceeded 250 μm in size and frequently have an average size of about 100 μm. Consequently, most age-diagnostic forms are missing in the recovered sequence, which prevents an accurate dating on the basis of planktonic foraminifers.

In Hole 585, the lower part of Core 585-1 (below 150 cm) is attributed to the lower Pleistocene on the basis of the occurrence of *Streptochilus tokelauae*. Planktonic foraminifers are common to abundant, but (1) they never exceed 150 μm in size, being strongly size sorted, and (2) faunas are strongly mixed with reworked upper Miocene forms dominating the assemblages.

Core 585-H1, from 6.8 to 255.9 m sub-bottom, yielded some planktonic foraminifers attributable to lower Miocene Zone N7–N8 mixed with some Oligocene and middle Eocene faunas.

Core 585-2 (recovery about 5%) contains only very recrystallized radiolarians. Cores 585-3 to -6 consist of a succession of pelagic turbidites, the basal units of which are represented by silicified limestone or chert or both, such as 585-3-1, at 31–33, 63–65, and 83–85 cm. Those layers yielded *Turborotalia boweri, Subbotina yeguaensis*, and *Pseudohastigerina micra*, which suggest the middle Eocene, possibly Zones P11 to P10. Associated with the rare middle Eocene forms are large amounts of reworked lower Eocene, upper Paleocene, and more rarely upper Maestrichtian faunas. Reworked assemblages can constitute up to 98% of the total assemblages in the finer layers within the turbiditic sequence (Core 585-3-1, 7–8 cm). The topmost part of the turbiditic sequence yielded only rare, very poorly preserved radiolarians and nannofloras. The interval from Core 585-7 to Sample 585-14-1, 64–67 cm appears to represent the entire lower Eocene and possibly its lower boundary. As in the interval above, layers with rare, poorly preserved radiolarians alternate with layers rich in planktonic foraminifers. The lack of adult forms prevents the identification of zonal boundaries within this interval. Reworked planktonic foraminiferal faunas include assemblages of late and early Paleocene and late Maestrichtian age.

The ash layer in Sample 585-13-1, 84–87 cm yielded abundant fish remains, and it is bioturbated.

The remaining part of Cores 585-14 and -15 yielded only rare specimens of planktonic foraminifers, also frequently broken. Wall structures of some fragments suggest that Sample 585-15-1, 34–37 cm is late Paleocene in age, possibly Zone P4 (= *Planorotalites pseudomenardii* Zone).

The youngest abyssal agglutinated foraminifers, the only autochthonous fauna, were recovered in Sample 585-15-1, 146–148 cm (see the later text).

Common planktonic foraminifers occur in several layers of Core 585-16, the top of which (585-16-1, 8–10 cm) is attributed to early Paleocene Zone P1b–c (= *Subbotina pseudobulloides* Zone). Common species are *Globoconusa daubjergensis, Subbotina triloculinoides, Planorotalites* aff. *compressus*, and the index species. They are associated with a minor amount of reworked lowest Tertiary "*eugubina*" and Maestrichtian assemblages. Paleocene species decrease rapidly in abundance in Section 585-16-1 and are replaced by Maestrichtian faunas, which make up 100% of the planktonic foraminiferal assemblage in Sample 585-16-1, 110–116 cm. The decrease of Paleocene forms through Core 585-16 is associated with an increase in sorting: the average size of planktonic foraminifers in 585-16-1, 110–116 cm does not exceed 80 to 90 μm. The lowermost Tertiary fauna recovered in Sample 585-16-1, 88–90 cm belongs to the "*eugubina*" Zone. Thus the Cretaceous/Paleocene boundary is placed between Samples 585-16-1, 88–90 cm and 90–110 cm.

The recovery of foraminifers from the Mesozoic sequence of turbiditic claystones, radiolarian claystones, clayey limestones, and volcaniclastic sandstones is particularly sporadic, with the majority of samples being devoid of foraminifers or containing only very rare, poorly preserved specimens. Several samples, however, are useful for biostratigraphic purposes.

Only one layer in Sample 585-17-1, 4–7 cm yielded very rare Maestrichtian forms, whereas abyssal agglutinated benthic foraminifers, fish remains, and radiolarians become more prominent as more autochthonous sediments were recovered.

Fine calcareous turbidites occur once more in Core 585-18. Planktonic foraminifers are strongly size sorted, and assemblages, sometimes rich (Section 585-18-1, 76–79 cm), display an average size of 80 μm. Faunas are dominated by *Heterohelix* and *Globigerinelloides* along with rare representatives of *Globotruncanella, Rugoglobigerina*, and *Globotruncana*. The occurrence of forms attributable to *Globotruncanella havanensis, Globotruncana plummerae*, and *Heterohelix glabrans* suggests the Maestrichtian, but no upper Maestrichtian species could be found. Autochthonous sediments rich in fish debris, abyssal agglutinated benthic forms, and some radiolarians occur in layers interbedded within the turbidites. Those autochthonous sediments become prominent in Core 585-19, which, however, cannot be dated on the basis of planktonic foraminifers. Core 585-20 contains rare, poorly preserved planktonic species of *Hedbergella, Globigerinelloides*, and *Heterohelix* that suggest a possible Maestrichtian age. Cores 585-29, -30, and the upper part of -32 contain species of *Rotalipora, Praeglobotruncana, Whiteinela*, and *Hedbergella* that indicate a possible Turonian assemblage mixed with Cenomanian species. This mixed association is followed in Section 585-32-4 by a moderately diverse and well-preserved planktonic fauna indicative of the upper Cenomanian *Whiteinella aprica* Subzone of the *Rotalipora cushmani* Zone. Species present include *Rotalipora cushmani, R. greenhornensis, Whiteinella aprica, W. baltica*, and *W. brittonensis*, in association with *Praeglobotruncana stephani, P. delrioensis*, and *P. gibba*.

Core 585-36 is assigned to the upper Albian *Ticinella breggiensis/Ticinella praeticinensis* Zone by the occurrence of rare specimens of *Ticinella primula, Hedbergella delrioensis*, and forms that appear to be *Ticinella praeticinensis* and *T. breggiensis*. An upper Aptian–lower Albian benthic foraminiferal association appears in Sample 585-41,CC with forms such as *Osangularia utaturensis, Spiroplectinata complanata, Conorotalites aptiensis, Gaudryina dividens*, and *Dorothia oxycona* among others. A similar assemblage occurs in Sample 585-42,CC with the addition of *Ticinella primula, Gavelinella intermedia*, and *Pleurostomella subnodosa* that indicate the middle to upper Albian. Elements of this assemblage are present in Cores 585-43, -44, and -49. Core 585-49, however, also contains *Favusella washitensis* and *Globigerinelloides* cf. *G. cheniourensis* indicative of lower Albian reworked with Aptian material. The last age-diagnostic sample based on foraminifers from Hole 585 comes from Core 585-51 where an association of *Favusella washitensis, Ticinella bejaouaensis*, and *Gavelinella barremiana bizouardae* indicate the early Albian *Ticinella bejaouaensis* Zone.

Hole 585A

In Hole 585A, the upper 500 m were spot cored and some washed cores were recovered. Among them H1, washed from the seafloor to 363.7 m sub-bottom, recovered dusky green and green siltstone and claystone that yielded few moderately well preserved planktonic foraminifers. The dominant forms suggest the upper Miocene or lower Pliocene mixed with somewhat differently preserved middle Miocene and possibly upper Oligocene faunas. However, a much younger age cannot be ruled out, as the important index species were not recovered.

Three cores (585A-1 to -3) from 363.7 to 392.3 m sub-bottom were recovered in succession. The top of Core 585A-1 yielded a very poorly preserved planktonic foraminiferal fauna composed of rare acarininids and morozovellids, suggesting the lowest Eocene to uppermost Paleocene.

In Core 585A-2, only one sample (585A-2-1, 51–53 cm) contained a relatively rich planktonic foraminiferal assemblage. The species encountered are *Subbotina triloculinoides, Morozovella inconstans*, and *Subbotina pseudobulloides*. On the basis of the evolutionary stage of these species, the assemblage possibly represents the topmost part of the lower Paleocene P1c Zone (= *S. pseudobulloides* Zone). Reworked assemblages of both the "*eugubina*" Zone of the lowermost Tertiary and the Maestrichtian occur in the same sample. Silicified limestone and clayey chalk lithologies in Core 585A-2 are devoid of planktonic foraminifers and contain only size-sorted, poorly to very poorly preserved radiolarians.

Core 585A-3 appears to contain the Paleocene/Cretaceous boundary located within Section 1. The strongly size-sorted planktonic faunule from Sample 585A-3-1, 73–75 cm is dominated by Maestrichtian species but also includes small subbotinids, possibly *Subbotina eobulloides*, and unnamed forms transitional between *Guembelitria* and *Globoconusa daubjergensis* that are characteristic of the lowermost Tertiary "*eugubina*" Zone. The lowermost Tertiary forms are apparently missing in 585A-3-1, 128–130 cm, which yielded only very small Maestrichtian planktonic foraminifers. A few small-sized bathyal benthic foraminifers also occur in the same layers as the planktonic faunules. The chert and zeolitic clay of Core 585A-3 contain only poorly preserved radiolarians, whereas abundant radiolarians were found associated with abyssal benthic foraminifers.

Washed Cores 585A-H2 and -H3 and the intermediate Core 585A-4 do not yield any foraminifers. Only poorly to very poorly preserved, rare to common radiolarians occur in those cores.

Most of Core 585A-5 contains slightly size-selected ghosts of radiolarians, whereas the core-catcher sample at 19–21 cm yielded few poorly preserved planktonic foraminifers, smaller in size than 150 μm. The faunule consists of forms of various ages, specifically late Aptian (*Hedbergella trocoidea*), late Cenomanian (a possible *Whiteinella* and *Heterohelix moremani*), and Turonian to Santonian (*Heterohelix reussi*). No foraminifers were recovered from Cores 585A-6 through -8, which contain only radiolarians and fish debris.

The calcareous siltstones of Core 585A-9 yielded three of the best preserved and abundant planktonic assemblages recovered from both holes at Site 585. The *Whiteinella archaeocretacea* Zone was identified in the upper 50 cm of Section 1 on the basis of the occurrence of the index species associated with *Dicarinella hagni* in the uppermost 10 cm. This zone is equated to the Cenomanian/Turonian boundary. The latest Cenomanian *Whiteinella aprica* Subzone of the *Rotalipora cushmani* Zone occurs below 50 cm in Section 1. All three planktonic assemblages are rich in *Whiteinella aprica, W. baltica, Praeglobotruncana stephani, P. aumalensis*, and *Dicarinella algeriana. Rotalipora brotzeni, R. greenhornensis*, and *Praeglobotruncana delrioensis* are present commonly in the *W. archaeocretacea* zonal assemblages, but their occurrence in that zone is interpreted to be the result of reworking from older layers belonging to the *Rotalipora cushmani* Zone. *Rotalipora greenhornensis* and *R. cushmani* associated with the above species characterize the fauna of the *W. aprica* Subzone. Remarkably, *Whiteinella paradubia, W. brittonensis*, and *Praeglobotruncana gibba* are rare or missing, possibly because of size sorting. Rare Aptian to Albian planktonic foraminifers are reworked in the lower sample. Rare bathyal benthic foraminifers occur associated with the planktonic faunas in all three samples.

Foraminifers are absent in the siliceous claystone recorded in the lower part of Core 585A-9, in -10, and in the washed -H4 and -H5, where poorly preserved radiolarians are abundant.

From Core 585A-11 to total depth (Core 585A-22), planktonic foraminifers are very rare. Nevertheless, a late Aptian age is indicated for this interval by the occurrence of a few specimens of *Hedbergella trocoidea* in Samples 585A-11-5, 43–45 cm and 585A-18-2, 90–93 cm plus the addition of *Globigerinelloides ferreolensis* in Sample 585A-16,CC (22–24 cm). Bathyal benthic foraminiferal assemblages that occur along with the rare planktonic foraminifers further support an Aptian age for the mentioned interval.

The last age-diagnostic foraminifers in Hole 585A were recovered in Cores 585A-18 through -20. A few specimens of the larger foraminifer *Orbitolina* aff. *O. texana*, whose range is upper Aptian–lower Albian, were found scattered throughout this interval. Their occurrence is in agreement with a late Aptian age inferred from the other small foraminifers.

Orbitolinids have been reported from other localities in the western Pacific, but they have never been identified at a specific level. Among the localities, it is worth mentioning the Isakov Guyot (Heezen et al., 1973a), the Nauru Basin at Site 462 where a single specimen was recovered reworked in upper Oligocene layers (Premoli Silva and Brusa, 1981), and some of the Japanese guyots.

Cores 585A-12 through -15 and -17 apparently contain only ooids and mollusk fragments from a shallow-water environment as carbonate components. No foraminifers were found in those cores. Cores 585A-21 and -22 at the bottom of the hole are devoid of any biogenic components.

Paleoecology

Benthic foraminifers recovered from Site 585 sediments consist of three groups: (1) autochthonous abyssal species, (2) transported bathyal species, and (3) transported neritic and shallow-water species (Figs. 32 and 33).

The autochthonous group consists of agglutinated species of *Glomospira, Glomospirella, Ammodiscus, Hyperammina, Bathysiphon, Paratrochamminoides, Saccammina, Haplophragmoides*, and *Trochamminoides* among others that are interpreted to be most characteristic of your water depths between 5000 and 6000 m or closely analogous to the present water depth of the East Mariana Basin. This assemblage is found in the reddish brown zeolitic claystones that represent pelagic sedimentation between turbiditic episodes. Characteristically, the agglutinated fauna is associated solely with fish debris and recrystallized radiolarians, but occasionally rare specimens are found in turbiditic sequences. In Hole 585, the abyssal assemblage is found in Cores 585-15 to -54, which indicates that the entire sequence from the upper Aptian to the Recent was deposited at abyssal water depths (Fig. 32). Below Core 585-54 the assemblage was not recovered because of the heavy influx of volcaniclastic debris in the Aptian to Albian sequence. Above Core 585-15, samples consisted of the planktonic foraminifer- and nannofossil-rich sediments of the Cenozoic sequence. In Hole 585A, the abyssal assemblage is restricted to samples from Core 585A-3. Previously, the elements of this assemblage were recovered from the Pacific Ocean on Legs 20 and 61, from the Indian Ocean on Leg 27, and from the North Atlantic Ocean on Legs 41 and 47B.

The bathyal foraminiferal assemblage consists of small, size-sorted specimens of *Praebulimina, Gavelinella, Gyroidinoides, Stilostomella, Allomorphina, Pleurostomella, Aragonia, Osangularia*, and *Dentalina* among others that are characteristic of water depths above 2500 m. The assemblage is found predominantly in the laminated intervals and coarse basal units of graded sequences that represent distal, gravity-flow deposits. In intervals devoid of shallow-water material, the assemblage is associated with size-sorted radiolarians, planktonic foraminifers, and sponge spicules. In Hole 585, the bathyal assemblage is found in Cores 585-1, to -54. Of special interest are the occurrences of transported bathyal species in Sections 585-32-2 and 585-32-4 that flank the organic layer in Section 3. In the latter case, however, foraminifers are lacking, and the residue larger than 42 μm consists solely of recrystallized radiolarians. In Hole 585A, the bathyal assemblage was found in Cores 585A-3, -9, -11 and -16.

The third group consists of species characteristic of neritic or shallow-water environments. Included are neritic species of genera such as *Patellina, Textularia*, and species of miliolids, polymorphinids, and nodosariids. These smaller forms are listed in Figures 32 and 33 under the neritic column. Also included in this group are specimens of larger, shallower-water foraminifers such as *Orbitolina*, complex agglutinated forms such as Cuneolina, and attached agglutinated species among others shown as larger foraminifers in Figures 32 and 33. The neritic or shallow-water forms occur typically in the coarser basal layers of turbiditic sequences that also contain bioclastic debris of shallow-water origin such as echinoid fragments and spines, ostracodes, bivalve fragments, sponge spicules, fecal pellets, and very rare algal fragments in addition to ooids. In Hole 585, the neritic assemblage is found in Cores 585-36 to -51, whereas the larger forms are restricted to cores 585-36, -49, and -51. Neritic species and bioclastic debris are particularly noticeable in the middle Albian sequence of clastic carbonates and volcaniclastic turbidites (Fig. 32). Noticeably lacking, however, are *Inoceramus* prisms, thick-shelled bivalve and rudist fragments, and shallow-water algal debris typical of reefal environments and recovered from both Cenozoic and Mesozoic sediments of Leg 61 in the Nauru Basin. In Hole 585A, Cores 11 to 20 do contain rudist fragments in association with neritic and shallow-water foraminifers, algal fragments, bryozoans, bivalve fragments, echinoid debris, and ooids.

In summary, the upper Aptian Cores 585A-18 to -20 contain the greatest abundance of shallow-water material in association with volcaniclastic debris flows. This material decreases in abundance, diversity, and coarseness through the upper Aptian–lower Albian section of Hole 585 from total depth up to Core 585-48. In middle and upper Albian Cores 585-36 to -44 the transported material is predominantly neritic in nature, small-sized including the rare bioclastic material, and indicative of distal turbidite deposits. Cenomanian to Santonian Cores 585-29 to -34 contain transported foraminifers that are bathyal in nature. Abyssal foraminifers are particularly in evidence in the Maestrichtian to Paleocene Cores 585-15 to -20 characterized by zeolitic claystones and chert.

Radiolarians

Hole 585

From the 140 samples studied from Hole 585 only 24 (17%) provided stratigraphically useful assemblages, whereas 73 (52%) were barren and 43 (31%) were too poorly preserved to be useful (see Table 7).

In the Cenozoic section only Wash Core H1 provided a well-preserved radiolarian fauna. This fauna extends from the uppermost Eocene to the middle part of the lower Eocene and can be interpreted as a mixing of two Eocene assemblages: *Buryella clinata* (middle part of lower Eocene) and *Thyrsocyrtis bromia* (upper part of upper Eocene). The two assemblages represent 95% of the specimens mixed into a lower Miocene assemblage (*Calocycletta virginis* Zone).

Mesozoic radiolarian assemblages are characterized by two main features: (1) The tests are always recrystallized, usually to quartz, but also sometimes replaced by zeolites; and (2) most of the assemblages are oligospecific.

Based on the specific diversity and on the variable size of tests, only five levels (Samples 585-17-2, 35–36 cm; 585-26-1, 23–25 cm; 585-34-2, 27–29 cm; 585-36-1, 73–74 cm, and 585-48,CC) seem to be autochthonous.

If we consider the morphology and the size of the tests, all other samples seem to be allochthonous. The samples show spherical radiolarian morphology (Spumellarians and essentially cryptocephalic Nassellarians) and very good size sorting (the smallest specimens in clays, larger specimens in silts, and the largest in the coarse fractions).

The *Amphipyndax enesseffi* Zone, however, can be recognized in Cores 585-25, -26, and -28; the *Artostrobium urna* Zone in Core 585-29; the *Obesacapsula somphedia* Zone in Cores 585-31 and -32, and as deep as 585-34-2, 52 cm; and the *Acaeniotyle umbilicata* Zone below 585-34-2, 77 cm.

Actually the calibration of the Upper Cretaceous radiolarian zonation is not very precise. The *Amphipyndax enesseffi* Zone is approximately Campanian and the *Artostrobium urna* Zone corresponds to an interval between the Coniacian and Campanian. The limit between the *Obesacapsula somphedia* Zone and the *Acaeniotyle umbilicata* Zone is very close to the boundary between middle and upper Albian.

Hole 585A

From Hole 585A, 20 samples (42%) were barren, 17 samples (36%) provided faunas too poorly preserved to be useful, and 10 samples (21%) can be used for stratigraphic resolution (see Table 8).

Three intervals can be defined on the basis of radiolarian occurrences and preservation: (1) in Cores 585A-H1 to Sample 585A-3-1, 40–41 cm (Cenozoic), radiolarians are nearly absent; (2) in Samples 585A-3-1, 2–3 cm to 585A-H4-1, 79–80 cm (Upper Cretaceous), radiolarians are confined to sandy layers and the tests are always recrystallized; and (3) in Cores 585A-11 to -22, radiolarians are absent except in Cores 585A-18 and -20, which yielded a fauna too sparse and poorly preserved to be stratigraphically useful.

Three assemblages can be recognized in the second interval: (1) the *Theocapsomma comys* Zone (Maestrichtian) in Core 585A-3; (2) the *Artostrobium urna* to *Amphipyndax enesseffi* Zones (Campanian to Turonian) in core 585A-5; and (3) the *Obesacapsula somphedia* Zone in Cores 585a-7 to -H4.

Correlation, Holes 585 and 585A

Biostratigraphic correlation between Holes 585 and 585A is shown in Figure 34. The key tie points are lim-

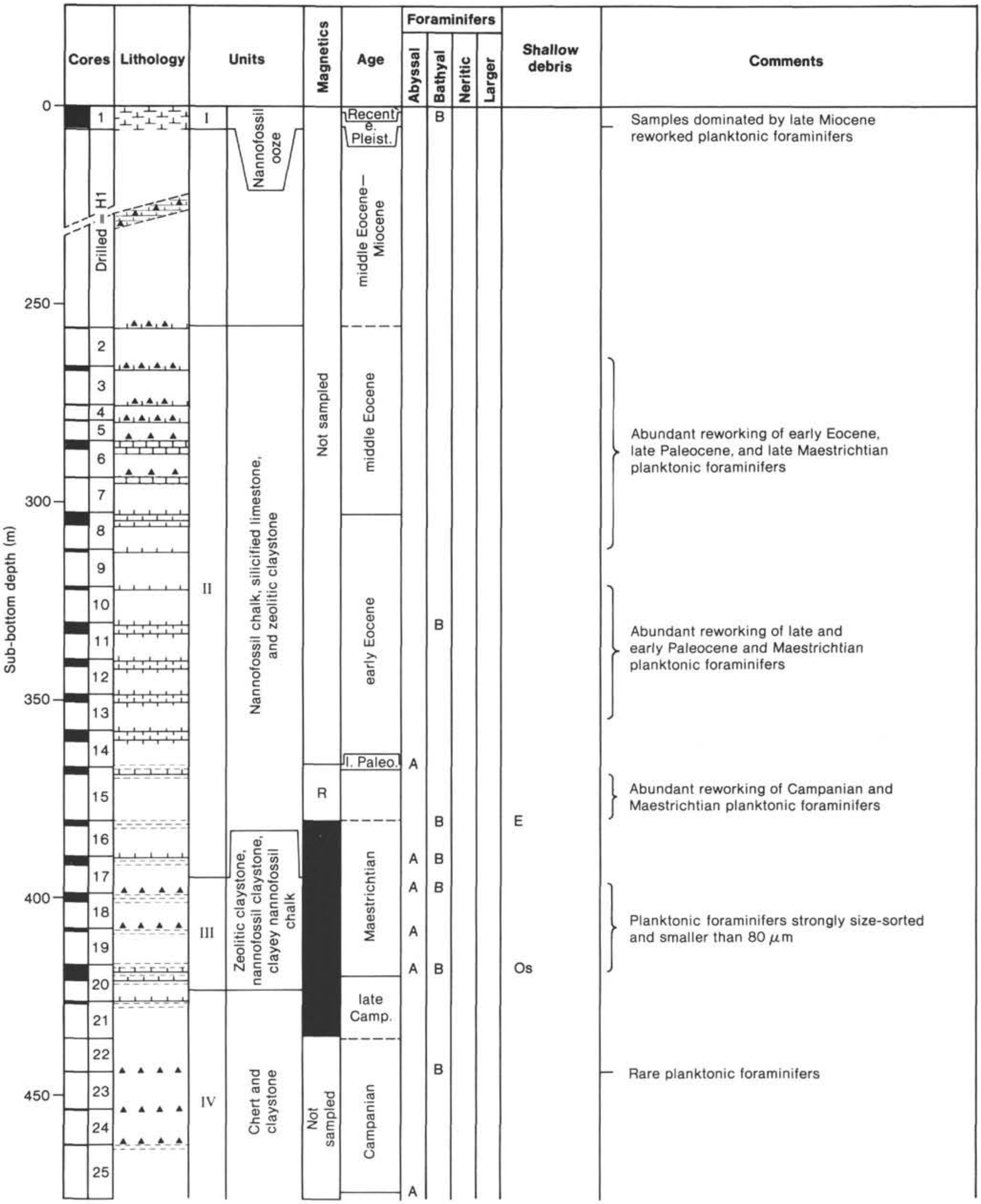

Figure 32. Paleoecologic summary of Hole 585. A = autochthonous abyssal foraminifers; B = transported bathyal foraminifers; N = transported neritic foraminifers; L = transported larger foraminifers; O = ooids; E = echinoid debris; M = bivalve fragments; and Os = ostracodes. (In Magnetics column, R or white area indicates reversed polarity, black area, normal polarity.)

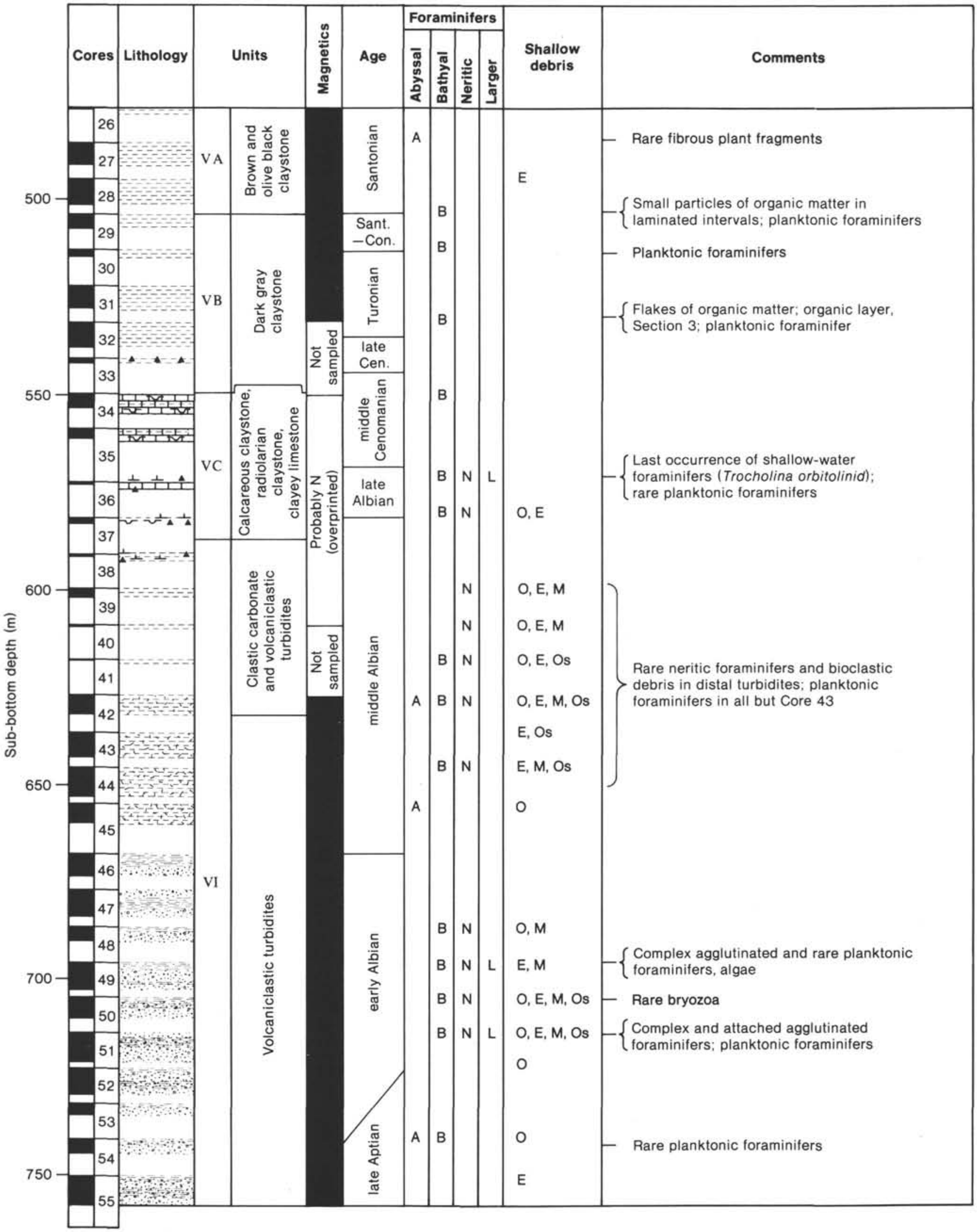

Figure 32 (continued).

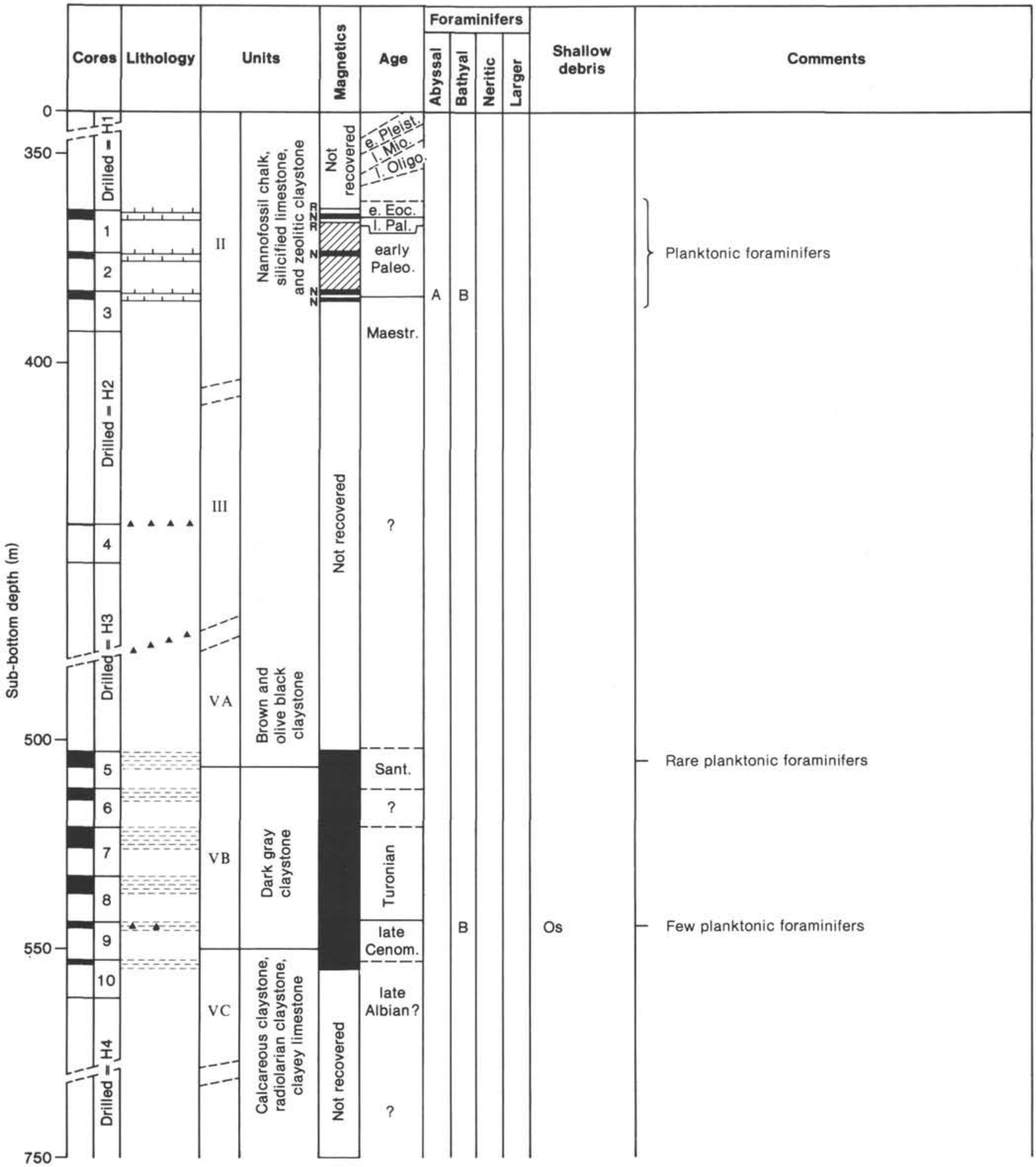

Figure 33. Paleoecologic summary of Hole 585A. A = autochthonous abyssal foraminifers; B = transported bathyal foraminifers; N = transported neritic foraminifers; L = transported larger foraminifers; O = ooids; E = echinoid debris; M = bivalve fragments; and Os = ostracodes. (In the Magnetics column, R or white area indicates reversed polarity, black area or N, normal polarity. Hachured areas indicate intervals without paleomagnetic information.)

ited to a few cores because of the washing and spot coring techniques and the sporadic paleontologic recovery in general. Of particular importance are the Cenomanian/Turonian boundary, the Cretaceous/Tertiary boundary, and the Paleocene and Eocene boundaries. The sub-bottom depths of these tie points are very close but not identical. This difference in depths is believed to have resulted from poor recovery and the different inclination of the two holes as determined from the magnetic measurements.

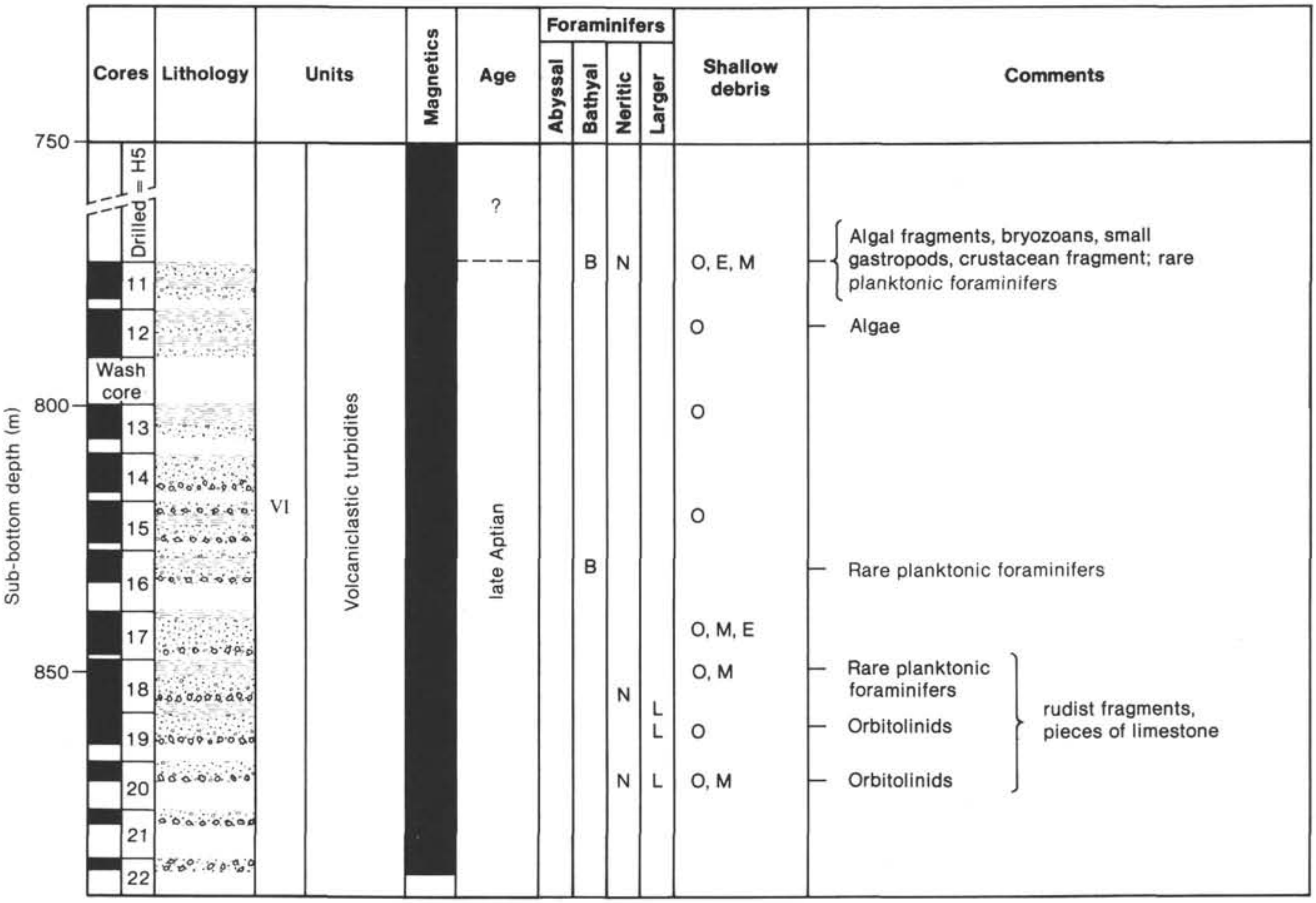

Figure 33 (continued).

SEDIMENTATION RATES

Sedimentation rates for Site 585 are shown in Figure 35. Four pulses of sedimentation are recorded in Hole 585 that are separated by apparent unconformities or reductions in sedimentation. The four pulses occur in the late Aptian to late Albian, middle Cenomanian to Turonian, Santonian to early Paleocene, and latest Paleocene to middle Eocene. Sedimentation rates for the Cenomanian to Eocene pulses range from about 5 to 10 m/m.y. The rate for the initial Aptian to Albian pulse characterized by volcaniclastic debris flows is about 20 m/m.y. Unconformities or much reduced rates of sedimentation were apparently the case during the late Albian to early Cenomanian, the Coniacian to Santonian, and the middle and late Paleocene. Cores 585A-11 to -22 extended the drilled section by nearly 130 m but remain within the late Aptian. The new rate for the volcaniclastic debris flows is about 40 m/m.y.

ORGANIC GEOCHEMISTRY

Introduction

The main objectives of the on-board geochemical studies were: (1) to provide analytical data that would enable the co-chief scientists and the cruise operations manager to make proper safety-oriented decisions regarding the possibility of approaching significant gas and/or crude oil accumulations during the drilling operations; (2) to contribute relevant data to characterize the sedimentary organic matter in terms of amount, type, and maturity by applying various analytical techniques, such as organic carbon determination, pyrolysis measurements, and gas analyses; (3) to take different sample sets for the Organic Geochemistry Advisory Panel, our own detailed shore-based organic geochemical studies, and approved research programs submitted by other geoscientists.

ANALYTICAL METHODS

On-board organic geochemical studies comprise the following analytical techniques.

Gas Chromatography

Initially, two gas chromatographic systems were available for gas and gasoline range hydrocarbon analysis: the Carle Gas Chromatograph, Model 800, equipped with an 1/8-in. O.D., 5-ft.-long packed column with 8% Carbowax 1540 as the stationary phase on Anakrom ABS (90-100 mesh) for the analysis of the light gases (methane, ethane, carbon dioxide, and eventually hydrogen sulfide) using a thermal conductivity detector; and the Hewlett-Packard Gas Chromatograph, Model 5710A, equipped with two sets of two combined 1/8-in. O.D. packed columns (4 ft. packed with Spherosil porous silica beads and 12 ft. packed with 20% methyl silicone OV-101 as the stationary phase on Anakrom AS [100–110 mesh]) for the quantitative analysis of the C_2 to C_6 hydrocarbon fraction. Flame ionization detectors are used for this analysis, usually run in the compensation mode. Sample introduction is performed via a Carle 6-port valve into a gas loop cooled at

Table 7. Absence of or poorly preserved radiolarian fauna from Hole 585 samples (core-section, cm interval).

Radiolarians were not found		Radiolarians were too poorly preserved for biostratigraphy	
1-1, 4-5	30,CC	3-1, 27-28	38-1, 42-44
1-1, 140-141	31-3, 146-147	12-1, 65-66	39-1, 10-12
1-2, 40-41	31-4, 5-6	13-1, 22-23	42-3, 30-32
1-2, 144-145	32-1, 100-103	13-1, 88-89	44-1, 89-91
1-3, 70-71	32-2, 135-137	17-1, 13-14	45-3, 50-52
1-4, 60-61	32-1, 108-109	20-1, 39-40	46-2, 96-98
1-5, 30-31	39-2, 39-41	20-2, 108-109	46-3, 7-9
1,CC	40-1, 3-4	27-3, 22-23	46-3, 15-17
3-1, 108-111	41,CC	27-3, 126-127	49-1, 118-120
6-1, 86-87	42-2, 63-64	28-3, 16-17	49-2, 146-148
6-2, 79-80	43-2, 57-59	28-3, 138-139	49-5, 40-42
7-1, 17-18	43-4, 61-62	28,CC	49-6, 14-15
8-1, 75-76	44-2, 100-102	29-1, 34-35	49-6, 49-51
8-2, 106-107	44-3, 140-142	29-2, 5-6	51-2, 37-38
12-2, 34-35	44-4, 108-110	30-1, 1-2	52-1, 128-130
14-2, 94-95	45-1, 73-75	31-1, 108-109	52-2, 116-118
15-1, 22-23	45-2, 40-42	32-3, 72-74	54-2, 62-64
15-1, 74-75	45-2, 130-132	34-1, 140-142	54-3, 6-7
15-2, 4-5	45-4, 9-11	34-2, 84-96	55-1, 82-83
16-1, 35-36	45,CC	35-1, 30-32	55-2, 34-35
17-2, 47-48	46-1, 44-46	36-1, 36-38	55-4, 44-45
17-2, 69-70	47-2, 31-33		
18-1, 119-120	48-1, 146-147		
18-1, 143-144	48-2, 90-91		
18-2, 28-32	49-3, 19-21		
19-1, 12-14	49-4, 43-45		
19-1, 53-55	50-1, 113-114		
20-3, 73-74	50-2, 6-7		
20-4, 34-35	50-3, 30-32		
27-1, 82-83	50-4, 30-31		
27-4, 59-60	51-3, 28-30		
27,CC	51-4, 62-64		
28-1, 16-17	51-1, 147-148		
28-2, 29-30	53-2, 102-103		
28-4, 8-9	55-2, 82-83		
28-4, 121-122	55-4, 109-110		

Table 8. Absence of or poorly preserved radiolarian fauna from Hole 585A samples (core-section, cm interval).

Radiolarians were not found		Radiolarians were too poorly preserved for biostratigraphy	
H1-1, 4-6	2-1, 76-78	3-1, 38-39	9-1, 45-47
H1-1, 51-52	2-1, 111-117	3-1, 40-41	9-1, 140-141
H1-2, 6-7	H2-1, 12-14	3-2, 2-3	10-1, 36-38
H1-2, 96-98	11-2, 56-57	3,CC (4-5)	H4-1, 3-4
H1,CC (12-13)	11-4, 126-127	5,CC (1-2)	H4-1, 18-20
1-1, 14-16	13-3, 72-73	6-1, 113-115	H4-1, 118-120
1-1, 124-126	13-3, 100-102	7-1, 48-49	11-1, 9-11
1-2, 8-10	16,CC (9-11)	7-3, 127-128	18-6, 17-18
1,CC (10-11)	18-2, 81-82	8-1, 129-131	20-1, 58-59
2-1, 7-9	18-4, 80-81	8,CC (4-6)	

Hole 585 (core or core-section, cm interval)	Hole 585A (core or core-section, cm interval)	Ages
Core 14	1-1, 1–100	earliest Eocene
Core 15	1-1, 132–133	late Paleocene
15-1, 33–34	Core 1	
15-1, 146–148	Core 2	early Paleocene
16-1, 88–90	3-1, 73–75	Cretaceous/Tertiary boundary
16-1, 90–110	3-1, 128–130	
Core 28	Core 5	Santonian
32-2	9-1, 1–50	Cenomanian/Turonian boundary
32-3	9-1, 50–150	

Figure 34. Biostratigraphic correlation between Holes 585 and 585A.

−70°C. First test measurements showed, however, that the compensation (or differential) mode did not work properly: the baseline drift by column bleeding was exactly the same without the second column.

Installation of a Capillary Gas Chromatography System

Owing to the long steaming time from port to Site 585, there was time available to replace the packed column of channel B in the Hewlett-Packard GC 5710A with a 25-m-long, 0.32-mm-I.D. fused silica capillary coated with cross-linked methyl silicone of 0.52-μm film thickness. The initial 5 m of this capillary was coiled to about 5 cm diameter and used as a cold trap in the same cooling bath as for the packed columns. Gas samples were introduced with a syringe via a capillary injection system (Gerstel, Mulheim/Ruhr, F.R.G.) run in the split mode (split ratio 1:10). Inlet pressure was 0.75 bar or 0.50 bar, respectively, and helium was used as the carrier gas. Carrier gas flow was 2 ml/min. at 0.75 bar. The capillary chromatograms were run isothermally (except for the cooling period in the cold trap) at ambient temperature and gave excellent results if thermal focusing was optimal. See the discussion that follows.

Both gas chromatographs are connected to a laboratory integrator (Supergrator 1). Calibration was performed with appropriate gas standards before Hole 585 was spudded in.

Carbon, Hydrogen, and Nitrogen Analysis

A model 185B Hewlett-Packard CHN analyzer linked to digital Mini-Lab Integrator Model CSI 38 was calibrated for the analysis of both (1) carbon in sediment samples, and (2) CO_2 and H_2O^+ (wt.%) in igneous rock samples. Nitrogen was not determined except for two samples. The carbon determined in the sediments was on the residue of an acidified sample (e.g., after Carbonate Bomb analyses) and gave a value for organic carbon content. In addition, one basalt clast extracted from lithologic Unit VI (Core 585-48) was analyzed.

Sample Preparation

Samples were crushed (either by mortar and pestle or shatterbox if very hard) to a powder, heated to 110°C for 2 hr. to remove H_2O^- if igneous and allowed to cool in a desiccator. Twenty milligrams were weighed out on a Cahn Electrobalance and introduced into the CHN analyzer furnace at 1100°C. Blanks were composed of silica powder and oxidizing agent ("catalyst").

Results

1. Organic geochemical data for the sediments are summarized in Tables 9 through 13.

2. CO_2 and H_2O^+ data for the one basalt clast (585-48-1, 141–144 cm) was 0.3 wt.% and about 0.8 wt.%, respectively.

Pyrolysis Measurements

Pyrolysis measurements on whole rock samples were carried out using the Rock-Eval instrument (IFP-LABOFINA process) introduced by Espitalié et al. (1977). Briefly, a small portion of ground sediment (usually about 100 mg, utilizing the Cahn Electrobalance) is placed into a steel crucible and pyrolyzed in a flow of helium by heating the sample from 250 to 550°C at a rate of 25°/min. The Rock-Eval analysis generates a signal from which four types of information can be obtained: (1) The area of peak S_1 (calculated in mg hydrocarbons/g dry sediment weight) related to the quantity of free hy-

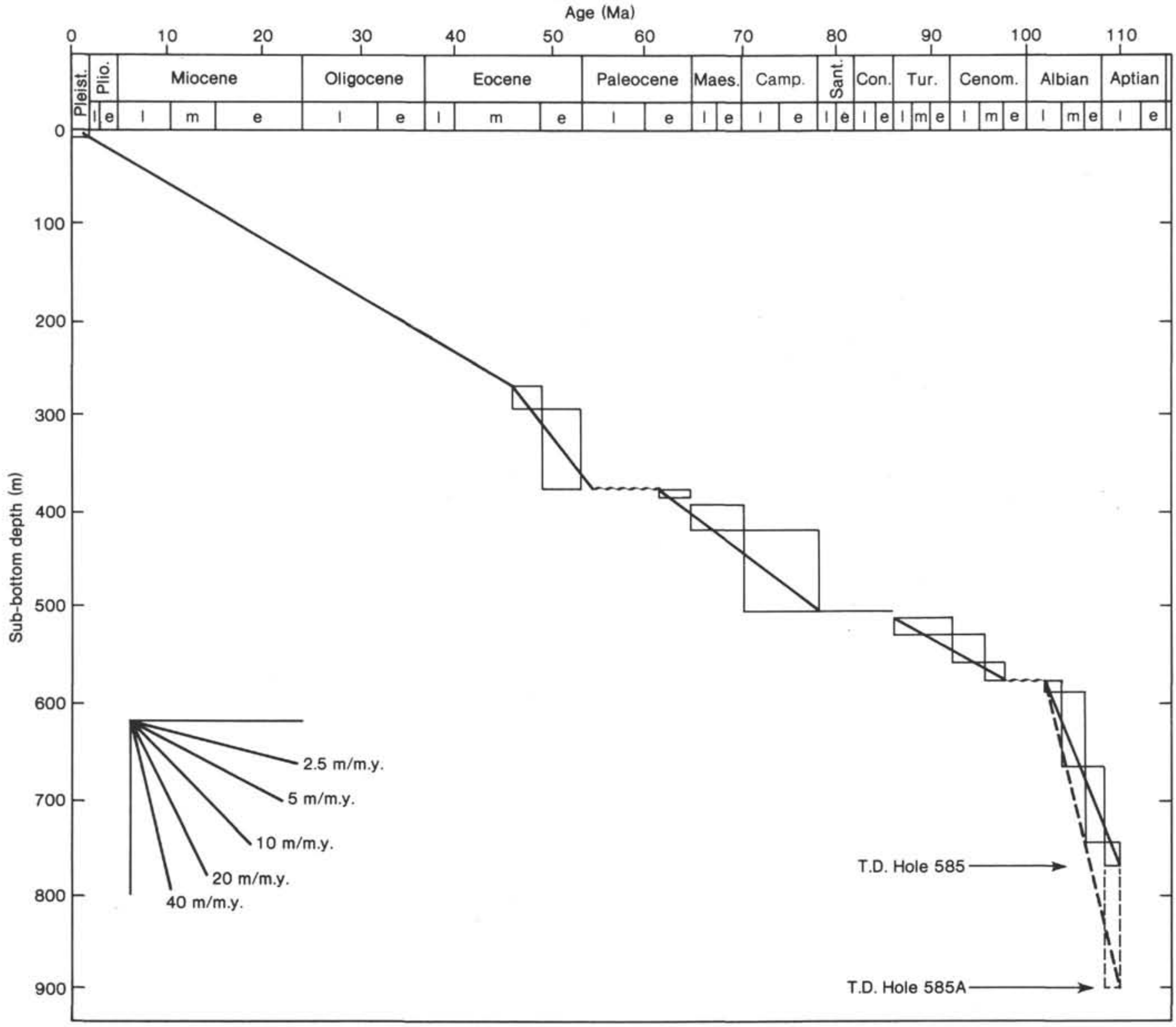

Figure 35. Sedimentation rates for Holes 585 and 585A.

drocarbons present in the sediment; (2) The area of peak S_2 (in mg hydrocarbons/g dry sediment weight) related to the quantity of hydrocarbon-type compounds released by thermal degradation of the kerogen up to 550°C; (3) The temperature T_{max} associated with the maximum of peak S_2 (i.e., where the rate of hydrocarbon formation reaches its maximum at the experimental conditions); (4) The area of peak S_3 (in mg CO_2/g dry sediment weight) related to the CO_2 released by the cracking of the kerogen.

By normalizing S_2 and S_3 to the amount of organic matter present in the sediment, the so-called hydrogen index (I_H in mg hydrocarbons/g of organic carbon) and oxygen index (I_O in mg CO_2/g of organic carbon) can be calculated. These are known to correspond to the elemental composition of the kerogen (H/C and O/C atomic ratios) and can therefore be plotted into a van Krevelen-type diagram. Finally T_{max} and the ratio $S_1/(S_1 + S_2)$, called production index I_p or transformation ratio, are measures of the maturity of the organic matter (both increasing with increasing maturity). I_p, however, also indicates intervals that are enriched by migrated hydrocarbons and can successfully be used for safety considerations (e.g., as proximity indicators for oil and gas accumulations).

The instrument, which is linked to the Supergrator-1 laboratory integrator, was calibrated with the IFP standard sediment from the Toarcian of the Paris Basin regularly with each sample series (at least once per day). This standard has the following characteristic values:

S_1 = 0 (immature sediment)
S_2 = 8.2 mg hydrocarbons/g of rock
S_3 = 0.85 mg CO_2/g of rock
I_H = 330 mg hydrocarbons/g C_{org}

I_O = 34.3 mg CO_2/g C_{org}
T_{max} = 428°C
I_p = 0

The response factors R.F. (in mg hydrocarbons/area count and mg CO_2/area count, respectively) and the observed T_{max} values are summarized in Table 9. Whereas the response factors for the hydrocarbon peaks reveal relatively small variations over the time period considered, the corresponding values for CO_2 show a significant scatter, which is possibly due to the variations in the CO_2 blank values. T_{max} also shows quite a variation (between 412 and 428°C), exceeding those limits usually accepted for the Rock-Eval method (±3°C according to Espitalié, personal communication, 1982). On the average, the T_{max} values measured on board appear to be some 4°C too low.

Two additional sediment standards used at KFA Jülich were brought on board ship and were adequately used for calibration. Their analytical data are as follows:

Parameter	E 38	#320038
C_{org}	8.2%	2.16%
S_1	0.07	0.05 (immature)
S_2	61.5	12.73
S_3	2.05	0.54
I_H	750	589
I_O	25	25
I_p	—	—
T_{max}	429°C	424°C

E 38 represents the Toarcian from southern Germany (Posidonia shale) and may be classified as an oil shale type sediment. Number 320038 represents the same sample, however, it was diluted with bentonite to obtain a lower C_{org} content. This artificial "sediment" was used as a replacement for the IFP Standard #27251, which was nearly used up.

The Rock-Eval data for 40 Site 585 sediment samples are summarized in Tables 10, 11, 12, and 13.

In many cases the peak areas given by the Supergrator turned out to be inaccurate and, therefore, had to be corrected by looking at the individual pyrograms and by manual peak area integration.

Table 9. Measured response factors (R.F.) for Rock-Eval instrument.

Date (day/month/year)	R.F. Hydrocarbon (mg/count)	R.F. CO_2 (mg/count)	T_{max} (°C)	Standard sample
22/10/82	5.0×10^{-7}	1.0×10^{-6}	422	#27251
23/10/82	5.1×10^{-7}	6.2×10^{-7}	426	#27251
23/10/82	6.3×10^{-7}	7.6×10^{-7}	428	#27251
24/10/82	4.0×10^{-7}	4.1×10^{-7}	422	#27251
25/10/82	4.8×10^{-7}	9.0×10^{-7}	420	#27251
27/10/82	4.8×10^{-7}	8.7×10^{-7}	424	#27251
30/10/82	4.1×10^{-7}	7.4×10^{-7}	426	#27251
30/10/82	5.0×10^{-7}	5.7×10^{-7}	419	#320038
31/10/82	3.8×10^{-7}	9.9×10^{-7}	419	#320038
1/11/82	4.5×10^{-7}	9.6×10^{-7}	420	#27251
1/11/82	4.8×10^{-7}	1.1×10^{-6}	420	#320038
2/11/82	4.3×10^{-7}	8.4×10^{-7}	412	#320038

Discussion of Results

Performance of Capillary Gas Chromatographic System

As shown in a test chromatogram (Fig. 36) of a C_1 to C_6 hydrocarbon mixture, the separation efficiency of the system is satisfactory, particularly in the medium and in the higher molecular range (as obvious from, for example, n-butane/2,2-dimethylpropane and 2-methylhexane/3-methylhexane separations, respectively). An improvement of the separation efficiency in the low-molecular-range section of the chromatogram appears possible, as exemplified for methane, ethane, and propane mixtures in Figure 37. The gas chromatogram on the left in Figure 37 was obtained by injecting 100 μl of 1.7% ethane (v/v, volume for volume) in methane (methane/ethane ratio = 60). The chromatogram shows clearly that gases with methane/ethane ratios up to about 1800 (v/v) could be analyzed without problems. The lowest detectable quantity for methane in a 100-μl gas sample is about 2 ppm by volume. The gas chromatogram (GC)

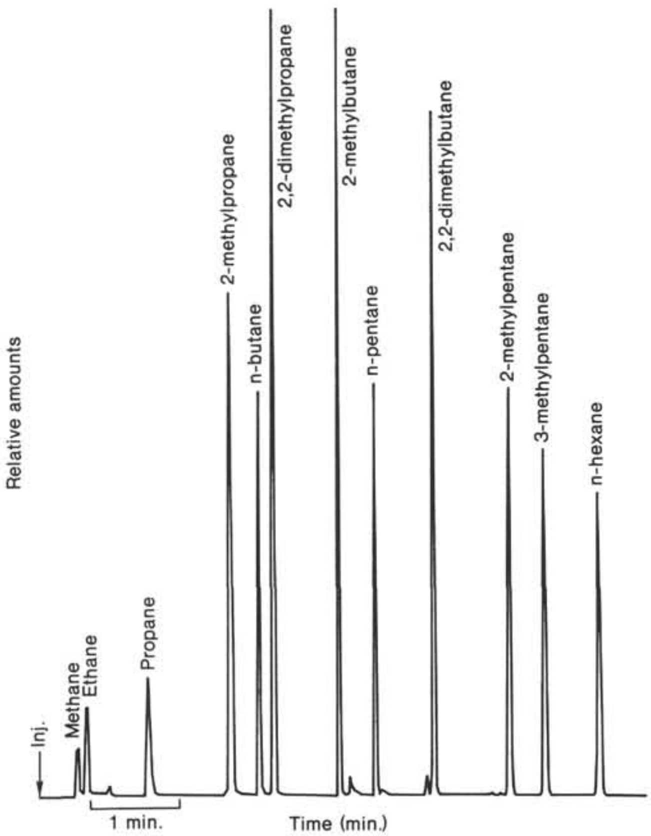

Figure 36. Gas chromatogram of hydrocarbon test mixture using 25 m fused silica capillary (0.32 mm I.D., 0.52 μm film thickness, cross-linked methyl silicone as stationary phase, 60 s trapping time). See text for analytic details.

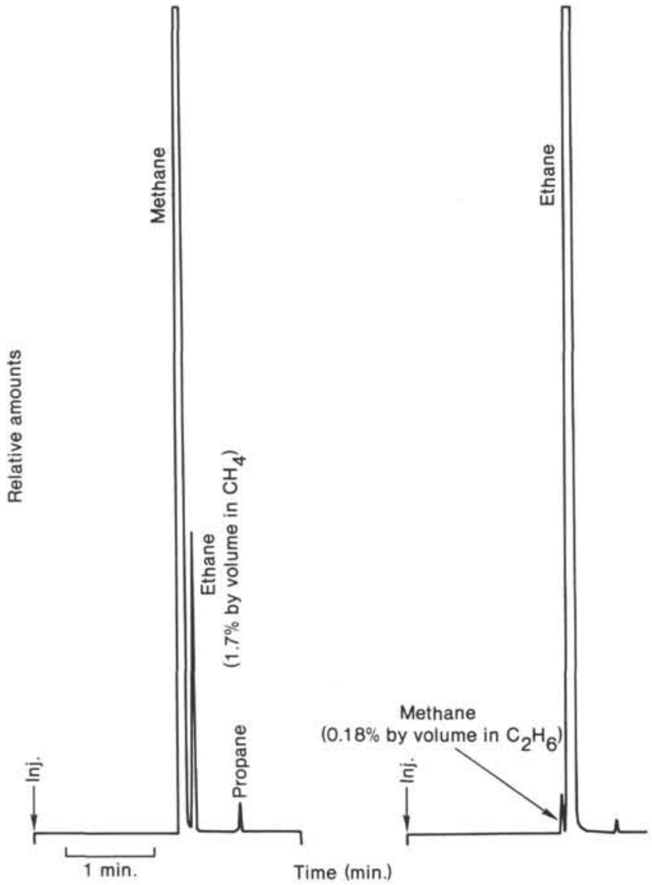

Figure 37. Fused silica capillary gas chromatograms of hydrocarbon mixtures showing separation efficiency and sensitivity of gas chromatographic system (60 s trapping time, helium inlet pressure 0.5 bar).

on the right shows, just for comparison, traces of methane (0.18% by volume) in ethane.

For future Deep Sea Drilling Project applications, it might be advisable to replace the packed columns of the Hewlett-Packard GC by a capillary system, however, with even increased capillary length and film thickness (preferably greater than 1 μm) to achieve a better methane-ethane separation. If successful the Carle GC could then be withdrawn from the gas laboratory. CO_2 analysis could be performed gas chromatographically by a microthermal conductivity detector.

Some capillary GC runs (injection volume 2.5 ml) of Vacutainer blanks (different batches tried) revealed severe contaminations even in the molecular range C_4 and lower (see also Kagami, Karig, Coulbourn, et al., Site 583 report, Leg 87, in press). Butadiene (123 ppm by volume) appears to be a major contaminant in the C_4 range (outgassed from butyl rubber stoppers?), as shown in Figure 38. Gas analyses based on Vacutainer sampling should be considered with great care and perhaps be discontinued.

Organic Geochemistry

No gas occurrences or indications of liquid hydrocarbons or asphalts were observed in sediments from Holes 585 and 585A. Hence, the discussion of the analytical data focuses on the amount and type of organic matter encountered in these sediments.

Hole 585

Organic Carbon Content

The organic carbon content was measured on 79 samples that make up the depth interval 0 to 764 m (Cores 585-1 to -55). The data are summarized in Table 10. On the basis of these data, the following observations can be made. The organic carbon contents measured aboard ship are very low throughout the sampled interval except for one sample (585-32-3, 72–73 cm) in which 5.4% (average of 2 analyses) is reached. The following mean values are measured in the various lithologic units as defined by the shipboard sedimentologists:

Lithologic unit	Core	C_{org} (%)
I	1	0.10
II	2–17	0.06
III	18–20	0.07
IV	21–26	Not determined
V	27–37	0.49
VI	38–41	0.05
	42–55	0.08

The lowest organic carbon values are found in Lithologic Units II and the upper part of VI (0.06 and 0.05%, respectively). They are somewhat higher in lithologic Units III and the lower portion of VI, but still below 0.1%. The value of 0.49% for Lithologic Unit V is biased, insofar as it contains the most organic-carbon-rich sample found (585-32-3, 72–73 cm). However, the layers adjacent to this sample reveal values that are significantly higher (0.2 to 0.3% in parts of Core 585-32) than in all other cores analyzed.

Type of Organic Matter

Pyrolysis data of the 27 samples shown in Table 11 indicate that, in accordance with their low organic carbon values, the hydrocarbon potential of all samples except for Sample 585-32-3, 72–73 cm is very low. Whereas the latter reveals an S_2 value of 51.5 mg hydrocarbons/g dry sediment weight, all other samples remain below 0.6 mg/g, the majority even below 0.2 mg/g. Samples from Lithologic Units II and III and two samples from Unit V and the lower part of VI (one) from Core 585-28 and Core 585-55, respectively) were below the detection limit. Likewise, S_1 peak areas were low throughout the whole sample series, corresponding to 0.02 to 0.27 mg hydrocarbons/g dry sediment weight. The S_3 values appear to be influenced by the carbonate content of the rock samples, a fact that has frequently been observed. Hence the S_3 peaks represent both the CO_2 released by the degradation of the kerogen and a certain fraction due to decomposition of carbonate minerals below 390°C. Only where the carbonate content is low

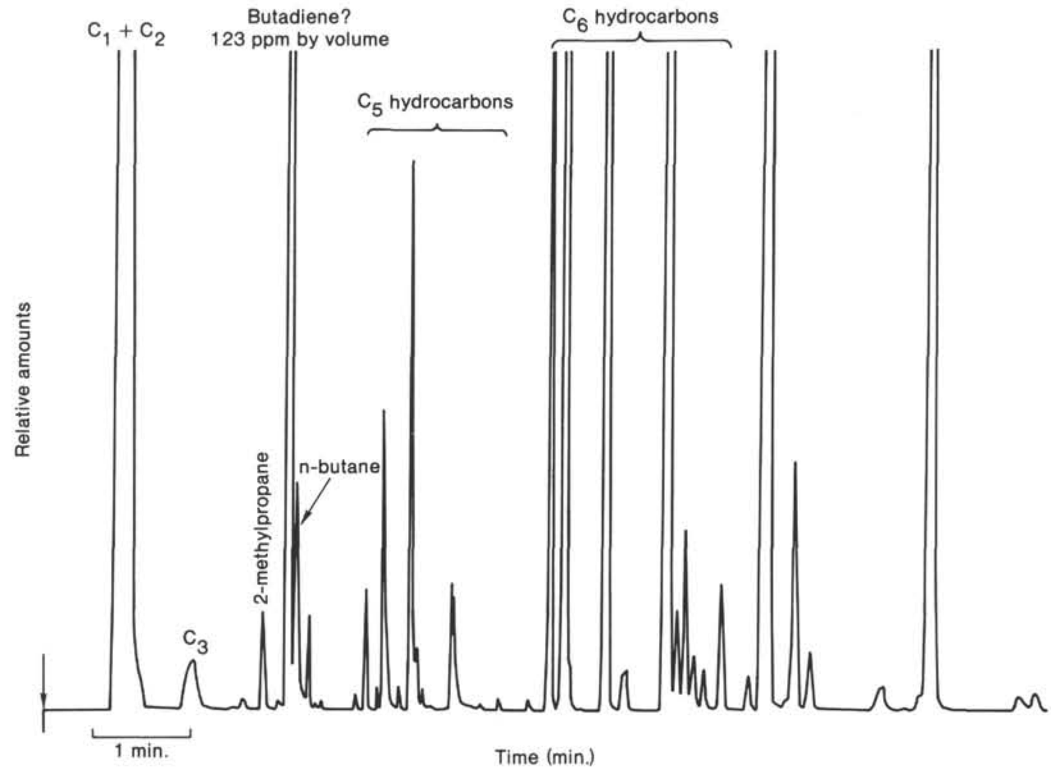

Figure 38. Capillary gas chromatogram of representative Vacutainer blanks (injection volume 2.5 ml, inlet pressure 0.5 bar, T_s = 25°C, split ratio 1:10, 60 s trapping time).

(i.e., about a few percent) does the S_3 value represent the true oxygen content of the organic matter.

From these shipboard measurements the appropriate hydrogen and oxygen indexes were calculated and summarized in Table 10. However, only those data are given where C_{org} values below Core 20 reached a minimum threshold value of 0.1%, above which more or less reliable index values could be expected. As pointed out in the "Shipboard Organic Geochemistry Guide/Handbook" (Deep Sea Drilling Project, 1982), the Rock-Eval results from organic carbon lean samples should not be overinterpreted. Therefore this discussion is focused only on a few selected Hole 585 samples with elevated organic carbon contents. The most interesting one is Sample 585-32-3, 72–73 cm, which has a hydrogen index of 954 mg hydrocarbons/g C_{org} and an oxygen index of 33 mg CO_2/g C_{org}. This sample, if plotted into the van Krevelen-type I_H/I_O diagram (Fig. 39), falls exactly on the initial part of the Type-I kerogen evolution path, suggesting that this sample represents a typical sapropelic oil-shale-type kerogen (i.e., mainly derived from algae). Both the high hydrogen index and the low T_{max} value of 404° (408° if adjusted by comparison with IFP standard) demonstrate the very low maturity of the black shale encountered in Core 585-32. This is also confirmed by the high nitrogen contents of the organic matter (0.33 and 0.20% duplicate measurements).

Also included in Table 10 are, for comparison, organic carbon (measured by a LECO IR 112 carbon determinator) and Rock-Eval pyrolysis data for selected samples determined onshore at the KFA Jülich (F.R.G.) laboratories. Whereas there is no systematic deviation discernible between on-board and onshore measurements for samples containing less than 0.3% C_{org}, the remeasured value for the black shale (585-32-3, 72–73 cm) was 9.9% C_{org}. Accordingly, the hydrogen index was lowered to 383 mg hydrocarbons/g C_{org}. If plotted into the van Krevelen-type diagram (Fig. 39), this sample is then located very close to the Type-II kerogen evolution path. Preliminary microscopic studies by R. Mukhopadhyay (personal communication, 1983, KFA Jülich) on these samples gave the following results. On the basis of transmitted and reflected light (normal and fluorescence mode) microscopy, the organic matter of this sample consists of mostly degraded products of dinoflagellates and small unicellular algae. These macerals are called sapropelinite II or bituminite II, representing an excellent petroleum source rock. The sample in transmitted light shows a fluffy biodegraded mass of brownish yellow color. In normal reflected light it is gray and granular with much framboidal pyrite. The fluorescent light is brownish yellow in color.

A question arises about the origin of this black shale that was deposited at the Cenomanian/Turonian boundary at a water depth of at least 4000 m. We suggest that the deposition of this organic carbon-rich layer is associated with global oxygen deficiency situations in the world ocean (e.g., by an expanded oxygen minimum layer) during the so-called Cenomanian-Turonian "oceanic anoxic event" (Schlanger and Jenkyns, 1976).

Such a high hydrogen index value as in this black shale is not reached or even approached by any other

Table 10. Calcium carbonate and organic carbon contents as well as pyrolysis data (Rock-Eval method) for Hole 585 sediment samples measured on board during DSDP Leg 89.

Sample (interval in cm)	$CaCO_3$ (%)	C_{org} (%)	Measurement onboard				Measurement at KFA				
			I_H	I_O	I_p	T_{max}	C_{org} (%)	I_H	I_O	I_p	T_{max}
585-1-1, 21	1	0.12									
585-1-2, 61	53	0.11									
585-1-3, 61	82	0.07									
585-6-1, 28-32	63	0.01									
585-6-1, 119-120	27	0.03									
585-8-1, 16-17	64	0.04									
585-8-2, 12-14	57	0.01									
585-8,CC	56	0.02									
585-10-1, 39-42	77	0.02									
585-10,CC (3-5)	32	0.01									
585-11-1, 98-100	78	0.02									
585-11-2, 110-112	34	0.06									
585-12-1, 138-139	73	n.d.									
585-12-2, 57-58	83	0.18									
585-13-1, 53-56	52	0.09									
585-13-1, 94-95	0	0.10									
585-13,CC (3-7)	74	0.07									
585-14-1, 64-67	76	0.08									
585-14-2, 75-79	77	0.12									
585-14-2, 92-94	53	0.10									
585-14-2, 105-108	0	0.12									
585-15-1, 34-36	18	0.06									
585-15-1, 61-62	0	0.09									
585-15-1, 86-88	0	0.08									
585-15-1, 98-100	0	0.11									
585-15-1, 113-114	41	0.04									
585-15-1, 129-130	85	0.03									
585-16-1, 22-23	49	0.04									
585-16-1, 69-70	0	0.16									
585-17-1, 67-73	72	0.07									
585-17-1, 104-105	36	0.10									
585-17-1, 140-141	60	0.06									
585-17-2, 7-9	83	0.04									
585-17-2, 18-23	51	0.07									
585-17-2, 52-53	0	0.12									
585-18-1, 13-15	27	0.06									
585-18-1, 53-56	43	0.07									
585-19-1, 38-40	57	0.15									
585-19-1, 48-49	76	0.01									
585-19-1, 56-57	0	0.10									
585-20-1, 8-16	66	0.02					0.08				
585-20-2, 12-18	0	0.09					0.10	34	181	0.51	534
585-20-3, 20-26	79	0.03					0.04				
585-27-1, 13-19	1	0.09					0.06	247	135	0.15	478
585-27-3, 20-24	2	0.14	14	221	*	+	0.08	173	465	0.16	528
585-28-1, 38-40	82	0.02					0.08				
585-28-4, 76-78	2	0.15	31	273	*	+	0.12	84	349	0.40	349
585-30,CC (19-21)	6	0.07					0.08				
585-32-1, 57-59	6	0.13	22	392	*	+	0.10	102	817	0.20	428
585-32-2, 35-39	12	0.33									
585-32-3, 13-18	11	0.24	221	675	0.1	416	0.29	56	371	0.13	428
585-32-3, 41-48	7	0.22	41	291	*	+	0.31	53	366	0.11	425
585-32-3, 72-73	2	5.6	954	33	<0.1	404	9.9	383	38	0.03	414
585-32-3, 72-73	2	5.1									
585-32-3, 73-74	0	0.13	65	115	*	+	0.20	85	47	0.13	406
585-34-1, 11-12	29	0.06									
585-34-2, 92-93	0	0.05									
585-35-1, 6-7	5	0.19	89	236	0.1	+	0.07	45	514	0.41	+
585-35-1, 83-84	5	0.11	145	464	0.1	+	0.07	44	528	0.39	+
585-35-1, 91-92	6	0.05					0.07				
585-35,CC (3-5)	32	0.04									
585-38-1, 24-28	25	0.04									
585-38-1, 32-38	9	0.03									
585-39-1, 25-27	3	0.05									
585-39-1, 42-44	0	0.07									
585-42-3, 140-142	34	0.06									
585-44-2, 84-85	5	0.08					0.08				
585-44-5, 50-51	3	0.06					0.07				
585-45-1, 54-55	3	0.08					0.10	39	230	0.38	+
585-45-3, 18-19	0	0.07					0.07				
585-46-1, 82-83	5	0.12	133	492	*	+	0.08	96	823	0.23	409
585-46-3, 24-25	3	0.10									
585-50-1, 128-130	3	0.10									
585-50-3, 31-32	3	0.10	44	720	*	+	0.08	109	570	0.26	546
585-51-3, 87-88	5	0.09					0.08				
585-51-4, 37-38	4	0.08									
585-53-2, 105-106	7	0.06									
585-54-1, 119-120	18	0.05					0.06				
585-55-2, 36-37	6	0.04					0.08				
585-55-4, 119-120	18	0.04					0.07				

Note: Included for comparison are organic carbon and Rock-Eval pyrolysis data obtained for selected samples in the laboratories at KFA Jülich, F.R.G.; I_H = hydrogen index (mg hydrocarbons/g organic carbon); I_O = oxygen index (mg CO_2/g organic carbon); and I_p = transformation ratio; also, * indicates I_p was insignificant; and + indicates that no clear maximum was discernible. Blank space indicates data were unavailable or unattainable.

Table 11. Rock-Eval data from Hole 585, Leg 89.

Sample (core-section, cm interval)	S_1	S_2	S_3	T_{max}	C_{org}
13-1, 91	0.096	—	2.26	+	n.d.
20-1, 8-16	0.065	—	0.91	+	0.02
20-2, 12-18	0.27	—	0.20	+	0.09
20-3, 20-26	0.21	—	1.41	+	0.03
27-1, 13-19	0.10	0.020	0.20	+	0.09
27-3, 20-24	0.058	0.019	0.31	+	0.14
28-1, 38-40	0.025	—	0.12	+	0.02
28-4, 76-78	0.060	0.047	0.41	+	0.15
30,CC	0.042	0.010	0.42	+	0.07
32-1, 57-59	0.014	0.028	0.51	+	0.13
32-3, 13-18	0.061	0.53	1.62	416	0.24
32-3, 41-48	0.14	0.091	0.64	+	0.22
32-3, 72-73	0.042	51.5	1.78	404	5.4
32-3, 73-74	0.042	0.084	0.15	+	0.13
35-1, 6-7	0.058	0.17	0.45	+	0.19
35-1, 83-84	0.058	0.16	0.51	+	0.11
35-1, 91-92	0.042	0.15	0.48	+	0.05
44-2, 84-85	0.12	0.19	0.75	+	0.08
44-5, 50-51	0.044	0.060	1.13	+	0.06
45-1, 54-55	0.063	0.10	0.17	+	0.08
45-3, 18-19	0.29	0.18	0.56	+	0.07
46-1, 82-83	0.015	0.16	0.59	+	0.12
50-3, 31-32	0.047	0.044	0.72	+	0.10
51-3, 87-88	0.035	0.031	1.33	+	0.09
54-1, 119-120	0.021	0.029	1.19	+	0.05
55-2, 36-37	0.048	0.016	1.96	+	0.04
55-4, 119-120	0.024	—	0.65	+	0.04

Note: — = below detection limit; + = no clear temperature maximum; n.d. = not determined.

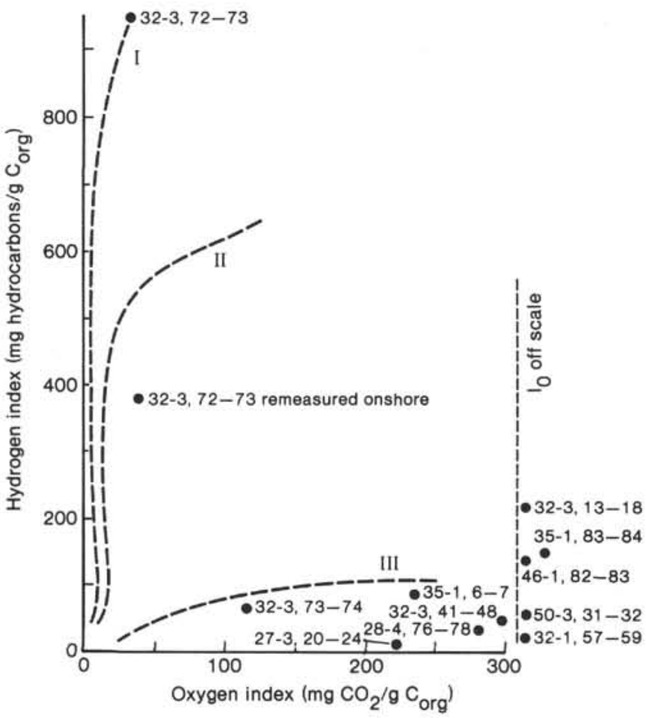

Figure 39. Hydrogen versus oxygen index trends for Type-I to Type-III kerogens showing data for sediment samples from Hole 585 (core-section, cm interval). Included is Sample 585-32-3, 72-73 cm remeasured onshore.

sample analyzed from Hole 585. The next highest hydrogen index is found about 60 cm above the black shale layer (221 mg hydrocarbons/g C_{org}). The kerogen quality in terms of hydrogen content has to be rated fairly low, however. This sample is classified as an immature Type II/III kerogen. The hydrogen index is even lower, on the basis of the shore-based data (C_{org} = 0.31%, I_H = 53 mg hydrocarbons/g C_{org}), indicating a Type-III kerogen. All other kerogens analyzed by the Rock-Eval method have lower hydrogen contents in terms of their I_H values and appear to be more or less oxidized. The fact that these samples plot on or in the vicinity of the Type-III kerogen evolution path does not necessarily mean that they consist of higher terrestrial plant debris.

Hole 585A

Organic Carbon Content

Thirty rock samples were selected from this hole for the determination of organic carbon: 2 from Core 585A-3; and 14 from Cores 585A-7 to -9 (both these sections represent stratigraphic equivalents of Hole 585, Cores 585-16, and -29 to -33, respectively) as well as 14 samples (Cores 585A-11 to -21) from the extended Lithologic Unit VI.

The organic carbon and the $CaCO_3$ contents for the samples are summarized in Table 12. From these data, average values were calculated:

Core	Lithologic unit	C_{org} (%)
3	II	0.08
5-9	V	0.27
11-21	VI	0.19

The highest organic carbon content in Hole 585A (1.45% dry wt., 2.6% according to shore-based analysis) was measured for Sample 585A-8,CC (19-20 cm). Stratigraphically, this organic-rich layer was encountered very close to the black shale from Core 32 of Hole 585. Unfortunately, however, the latter was not recovered in Hole 585A. Nevertheless, the occurrence of the sample with about 2% organic carbon content represents another example of organic carbon-rich sediments deposited at the Cenomanian/Turonian boundary.

The organic carbon values of all other samples are significantly lower. Only in Cores 585A-6, -7, -8, and -12, contents of 0.4 to 0.5% are observed. These values are just below the minimum level commonly required for a clastic petroleum source rock. These relatively high organic carbon contents for deep-sea sediments, however, do not coincide with a corresponding hydrocarbon potential, as shown by pyrolysis data (see the discussion that follows).

Finally, the organic carbon contents for all samples analyzed at Site 585 are plotted against depth in Figures 40 and 41. It is obvious from these figures that there is a strong increase of organic carbon contents from 775 m downward, if compared to the upper part of Lithologic Unit VI penetrated by Hole 585. It is not yet clear if this

Table 12. Calcium carbonate and organic carbon contents as well as pyrolysis data (Rock-Eval method) for Hole 585A sediment samples measured on board during DSDP Leg 89.

Sample (interval in cm)	Measurement onboard						Measurement at KFA				
	$CaCO_3$ (%)	C_{org} (%)	I_H	I_O	I_p	T_{max}	C_{org} (%)	I_H	I_O	I_p	T_{max}
585A-3-1, 21–26	0	0.11									
585A-3-1, 40–43	29	0.05									
585A-5-1, 80–81	3	0.01									
585A-5-2, 59–60	7	0.07									
585A-6-1, 54–57	10	0.48	9	204	*	+	0.09	27	679	0.41	+
585A-7-1, 94–100	0	0.41	12	85	*	+	0.09	137	225	0.29	455
585A-8-2, 75–76	21	0.33	33	482	*	430	0.23	63	428	0.20	424
585A-8-2, 95–96	13	0.04									
585A-8-3, 32–33	15	0.43	40	653	*	425	0.29	86	415	0.15	426
585A-8-3, 80–81	8	0.09				413	0.33	71	50	0.22	418
585A-8,CC (19–20)	1	1.45	807	57	<0.1	419	2.60	423	37	0.04	420
585A-9-1, 27–29	14	0.04									
585A-9-1, 82–83	0	0.01					0.06				
585A-9-1, 93–94	4	0.22	33	123	*	+	0.10	21	79	0.68	+
585A-9-1, 140–141	14	0.10									
585A-9,CC (17–19)	21	0.06									
585A-11-4, 84–85	1	0.25									
585A-12-3, 68–74	13	0.09									
585A-12-4, 27–28	9	0.11	37	945	*	+	0.08	56	895	0.47	+
585A-12-6, 42–43	3	0.25									
585A-12,CC (3–4)	3	0.44	12	230	*	+	0.08	105	767	0.30	537
585A-15-5, 135–137	14	0.10									
585A-16-1, 8–9	15	0.16									
585A-16-2, 31–34	7	0.16									
585A-18-2, 81–82	16	0.21	15	495	*	+	0.08	60	779	0.28	413
585A-18-4, 79–80	21	0.23									
585A-19-4, 71–72	6	0.26	12	581	*	+	0.06	60		0.28	383
585A-20-2, 102–103	3	0.19									
585A-20-3, 67–68	3	0.18									
585A-21,CC (10–11)	0	0.10	23	1460	*	+	0.06	52	971	0.31	417

Note: Included for comparison are organic carbon contents and Rock-Eval pyrolysis data obtained for selected samples in the laboratories at KFA Jülich, F.R.G. I_H = hydrogen index in mg hydrocarbons/g organic carbon; I_O = oxygen index (mg CO_2/g organic carbon; I_p = transformation ratio; also, * indicates I_p was insignificant, and + indicates no clear maximum was discernible. Blank space indicates data unavailable or unattainable.

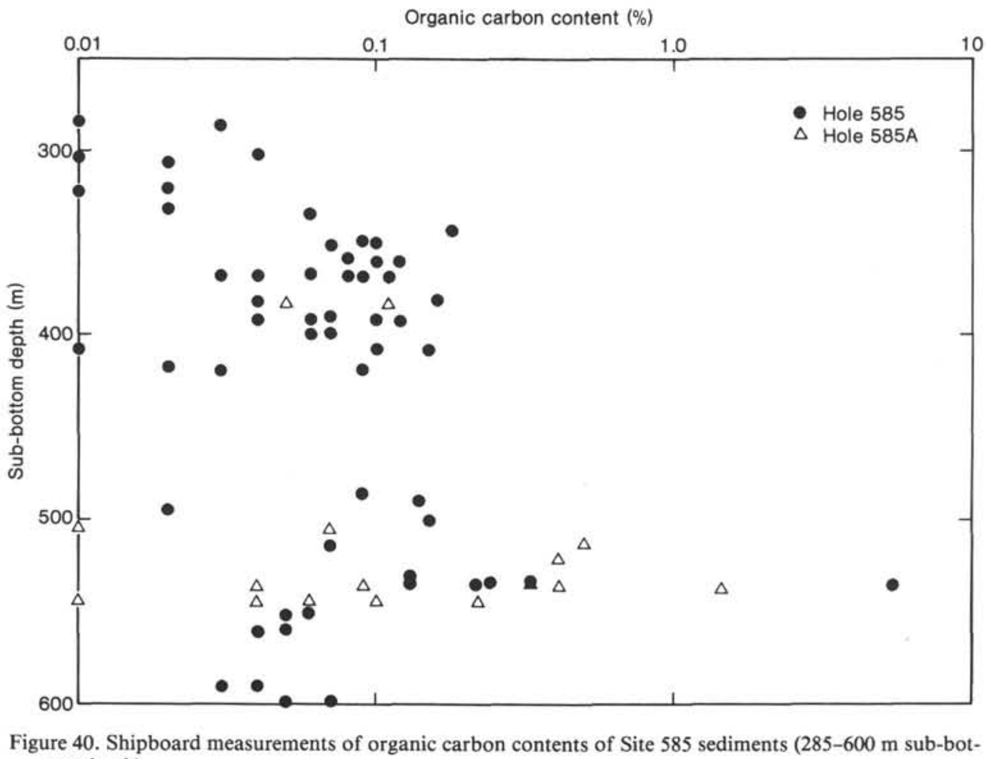

Figure 40. Shipboard measurements of organic carbon contents of Site 585 sediments (285–600 m sub-bottom depth).

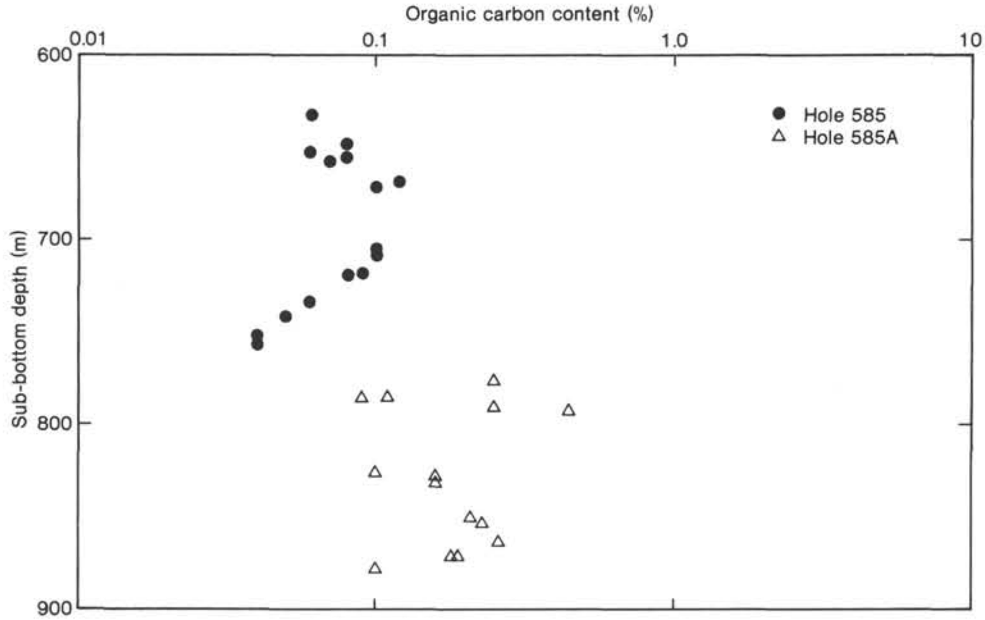

Figure 41. Shipboard measurements of organic carbon contents of Site 585 sediments (600 m sub-bottom depth to T.D.).

difference is geochemically significant or if it is, at least partly, due to a systematic error in the analytical procedure (e.g., by acid resistant carbonates), which could yield too high values for "organic" carbon. All other C_{org} values from Hole 585A fit well into the Hole 585 data.

Type of Organic Matter

Pyrolysis data of 13 selected samples shown in Tables 12 and 13 reveal that the hydrocarbon potential of all samples except for 585A-8,CC (19–20 cm) is very low. Whereas the latter reaches an S_2 value of 11.7 mg hydrocarbons/g dry sediment weight, all other samples remain below 0.3 mg/g, the majority even below 0.1 mg/g. Likewise, the S_1 signals are extremely low, and S_3 peaks reflect more the decomposition of carbonates than the degradation of the kerogen.

For 11 samples (C_{org} exceeding 0.1%), the appropriate I_H and I_O values are plotted in Figure 42. In terms of

Table 13. Rock-Eval data from Hole 585A, Leg 89.

Sample (core-section, cm interval)	S_1	S_2	S_2	T_{max}	C_{org}
6-1, 54–57	<0.001	0.045	0.98	+	0.48
7-1, 94–100	0.005	0.051	0.35	+	0.41
8-2, 75–76	0.003	0.11	1.59	430	0.33
8-3, 32–33	0.014	0.17	2.81	425	0.43
8-3, 80–81	0.019	0.29	1.13	413	0.09
8,CC (19–20)	0.018	11.7	0.83	419	1.45
9-1, 82–83	0.010	0.024	0.37	+	0.01
9-1, 93–94	0.010	0.073	0.27	+	0.22
12-4, 27–28	0.013	0.041	1.04	+	0.11
12,CC (3–4)	—	0.051	1.01	+	0.44
18-2, 81–82	0.022	0.031	1.04	+	0.21
19-4, 71–72	0.032	0.032	1.51	+	0.26
21,CC (10–11)	0.023	0.023	1.46	+	0.10

Note: — = below detection limit; + = no clear maximum.

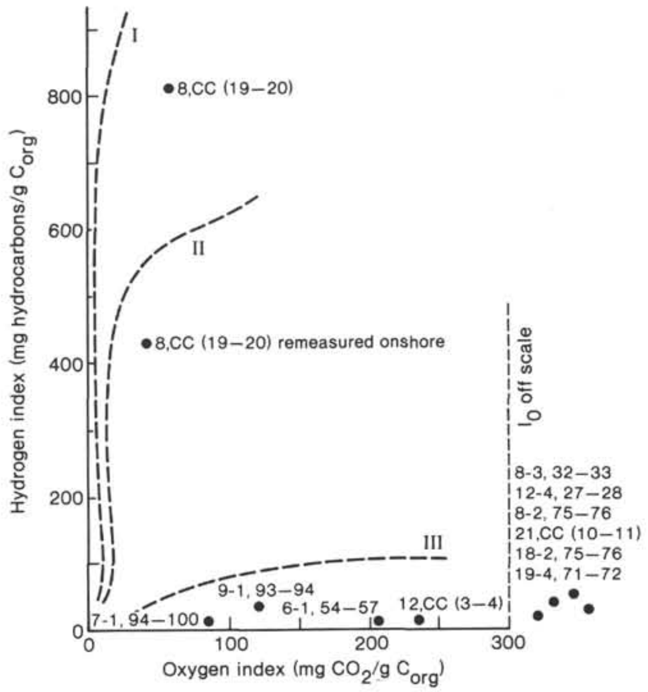

Figure 42. Hydrogen versus oxygen index trends for Type-I to Type-III kerogens showing data for sediments from Hole 585A (core-section, cm interval). Included is Sample 585A-8,CC (19–20 cm), remeasured onshore.

its hydrocarbon potential, organic-matter-rich Sample 585A-8,CC (19–20 cm) is very similar to the black shale of Core 585-32 (I_H = 807 vs. 954, respectively). Its organic matter is therefore an immature Type-I kerogen (i.e., mainly derived from algae). Using the shore-based data, however, the hydrogen index of Sample 585A-8,CC (19–20 cm) is lowered to 423 mg hydrocarbons/g C_{org}, which, again, plots close to the Type-II kerogen evolution path. All other samples analyzed from Hole 585A have very low hydrogen indexes (not exceeding 40 mg hydrocarbons/g C_{org} for the on-board measurements or 140 mg hydrocarbons/g C_{org} for the shore-based data). Provided that the organic carbon measurements are accurate, several samples with elevated organic carbon contents (e.g., from 585A-6-1, 585A-12,CC, and 585A-19-4) give such very low hydrogen indexes that their organic matter appears to consist mainly of so-called "dead carbon" (i.e., organic matter that has been entirely deprived of its effective hydrogen content).

Summary and Conclusions

On-site organic geochemical studies of Site 585 sediments were focused on amount and type of organic matter. Organic carbon contents were generally low, as expected for deep-sea sediments. On the basis of the selected samples the following averaged C_{org} values were obtained for the lithologic units (as defined by the shipboard sedimentologists):

Lithologic unit	C_{org} (%)
I	0.10
II	0.06
III	0.07
IV	Not determined
V	0.37
VI	{ 0.05 0.13

Only very few samples with elevated organic richness were recovered: one black shale sample from Core 585-32 and another relatively organic-rich sample from Core 585A-8 with 5.4 (average of two analyses) and 1.45% organic carbon contents, respectively. The corresponding values for the shore-based measurements were 9.9 and 2.6%, respectively. Both samples were encountered close to the Cenomanian/Turonian boundary. It is assumed that their formation is associated with global oxygen deficiency situations in the world ocean caused by an expanded oxygen minimum layer (i.e., the Cenomanian-Turonian oceanic anoxic event).

Sediments with organic carbon contents ranging from 0.3 to almost 0.5% were found in Core 585-32 as well as in Cores 585A-6, -7, -8, and -12. Whereas the organic matter of the two organic carbon-rich samples mentioned previously consists of an immature, algal-derived, Type-I kerogen (hydrogen indexes of 954 and 807 mg hydrocarbons/g of organic carbon, respectively), all other samples are classified to represent Type-III kerogens, but with strong variations in their hydrogen contents. On the basis of shore-based organic geochemical and microscopic data (determined at KFA Jülich), however, the conclusions are somewhat different. The hydrogen indexes for the two samples were 383 and 423 mg hydrocarbons/g C_{org}, respectively, which are indicative of a Type-II kerogen. The main maceral type of the kerogen was classified to be sapropelinite II and bituminite II. Provided that the organic carbon measurements are correct, several samples with elevated organic carbon contents (e.g., from 585A-6-1, 585A-12,CC, 585A-19-4) reveal such extremely low hydrogen indexes that their organic matter appears to consist mainly of so called "dead carbon" or "residual carbon." "Dead carbon" contents are usually high in those sediments that have been intensely reworked (or oxidized) or that are in the metagenetic stage of hydrocarbon evolution.

Relatively hydrogen-rich Type-III kerogens are observed in Sections 585-32-3, 585-35-1, and 585-46-1. This does not necessarily mean that they consist of organic matter derived from higher land plants. Their occurrence on the Type-III kerogen evolution path in the van Krevelen-type diagrams can also be explained by partial oxidation of their organic matter.

INORGANIC GEOCHEMISTRY

Table 14 constitutes this report; there is no text.

IGNEOUS PETROLOGY

Igneous rocks were not recovered at this site. Petrology of volcaniclastic clasts is included in the Sediment Lithology section.

PALEOMAGNETICS

The main research objective of the paleomagnetic sampling at Site 585 was to determine the northward motion of the Pacific Plate through the Mesozoic. The application of magnetostratigraphy as a dating tool was limited by the poor recovery and condensed sedimentation during the early Tertiary and Late Cretaceous and the lack of magnetic reversals during most of the mid-Cretaceous (Cretaceous long normal interval). A summary of the shipboard and early shore-based analyses at the University of Wyoming is given here; full details and results are reported by Ogg (this volume).

Minicores oriented with respect to the axis of the drill core were drilled in nearly all cores that contained large blocks of sediment. Measurements of NRM (natural remanent magnetization) were performed on board using a Digico fluxgate magnetometer. The samples were remeasured at the University of Wyoming on either a ScT cryogenic magnetometer or Schoenstedt spinner magnetometer, depending on the intensity of magnetization. Progressive thermal and alternating field demagnetization curves were examined for stable intervals. The mean inclination of each sample was determined by line fitting most stable regions (generally three to five measurements at increasing demagnetization levels). The method of Kono (1980a and b) was used to compute the mean inclination and alpha-95 (95% confidence level) for each lithology or age interval. These mean inclinations were adjusted for the deviation of the drill string from vertical as measured by the downhole Kuster tool and apparent dip of laminae in the cores; the direction of this drill string deviation was determined by measuring the apparent magnetic declination on cores with well-developed tilted lamination within the mid-Cretaceous long normal interval (the declination was therefore assumed to be 0°N, and the tilt direction of the drill string computed). The preliminary results are presented in Table 15.

Table 14. Summary of shipboard inorganic geochemical data, Site 585.

Laboratory sample no.	Sample[a] (core-section, cm interval)	pH	Alkalinity (meq/l)	Salinity (‰)	Calcium (mmoles/l)	Magnesium (mmoles/l)	Chlorinity (‰)
	IAPSO	7.91	2.376	34.1	10.55	64.54	19.375
	SSW	8.13	2.565	32.4	10.42	52.28	18.68
Hole 585							
1	28-2, 140-150	7.61	0.640	34.6	39.92	29.97	17.48
2	47-3, 140-150	8.05	0.278	42.4	131.32	202.30	16.41
	SSW	8.23	2.456	34.6	10.57	51.07	18.51
Hole 585A							
1	13-3, 143-150				—		

[a] SSW = surface seawater; IAPSO = International Association for the Physical Sciences of the Ocean seawater standard; no data available for Sample 585A-13-3, 143-150 cm.

Table 15. Northward motion of Site 585 (preliminary results).

Cores	Age	Lithology (dominant)	Demagnetization	Inclination Statistics[a] N	K	Mean incl.	α_{95}	Drift corrected mean[b]	Paleolatitude (α_{95})	Relative to present site
585A-H1	early Miocene	Gray siltstone	Thermal	4	800	10.1°	2.7°	8.1°	4.1°N (1.4°)	9.5°
585A-1 to 585A-3	Eocene and Paleocene	Tan chalk	Thermal	6	70	−6.1°	7.5°	−8.1°	4.1°S (3.8°)	17.7°
585-17 to 585-21	Maestrichtian-late Campanian	Brown claystone	Thermal	17	37	−5.7°	5.8°	−3.7°	1.9°S (2.9°)	15.5°
585A-5 to 585A10	late Cenomanian-Santonian	Dark gray claystone	Thermal	17	45	−15.1°	5.2°	−16.6°	8.5°S (2.7°)	22.1°
585-30 to 585-32	Turonian	Dark gray claystone	Thermal	15	85	−13.1°	4.0°	−10.1°	5.1°S (2.0°)	18.7°
585-34 to 585-39	middle Albian-middle Cenomanian	Brown calcareous claystone	Thermal	15	65	−15.6°	4.6°	−12.6°	6.4°S (2.4°)	20.0°
585-42 to 585-55	early to middle Albian	Volcaniclastics	NRM	49	45	−18.9°	3.0°	−16.0°	8.2°S (1.6°)	21.8°
585A-H5 to 585A-15	late Aptian	Volcaniclastics	NRM	27	80	−21.5°	3.1°	−22.5°	11.7°S (1.7°)	25.3°
585A-16 to 585A-22	late Aptian	Volcaniclastics	Thermal	13	130	−37.9°	3.5°	−38.9°	22.0°S (2.5°)	35.6°

[a] Method of Kono (1980a and b); N = number of samples; K = dispersion parameter, α_{95} = 95% confidence interval.
[b] Drift corrected mean = inclination corrected for apparent deviation of drill string from vertical.

The polarity interpretation of the samples is diagramed in Figures 30 through 32. Nearly all of the samples in the Cretaceous are of normal polarity. An exception is a short reversed or mixed polarity zone in the upper Aptian section. Coeval(?) short reversed intervals occurring within the late Aptian or early Albian have been observed in other DSDP and land sections (Keating and Helsley, 1978a, b; Lowrie et al., 1980; Vandenberg and Wonders, 1980; Pechersky and Khramov, 1973) and seem to have caused a small marine magnetic anomaly (Hilde, Isezaki, et al., 1976; Vogt and Einwich, 1979). It is younger than M0, which suggested M "−1" as a possible name, for lack of a better nomenclature system. However, shore-based demagnification steps removed the reversed or mixed-magnetic component, and the entire section is now recognized as being of normal polarity.

In the lower part of Core 585A-17, an enigmatic vertical contact between greenish black volcaniclastic sandstone (the dominant lithology of the core) and dark greenish gray, clayey siltstone was recovered (Fig. 43). Three minicores were taken from a single block to determine whether this was a part of a very large clast, slump block, or other sedimentary feature; these were from the "host" sandstone, from a similar sandstone below a contact or fault that terminates the fine-grained vertical feature, and from the fine-grained siltstone feature (Samples 585A-17-4, 27, 47, and 43 cm, respectively). The NRM directions are within 10°-declination and 7°-inclination ranges, hence are nearly identical within orientation and analysis precision. This implies that the structure is not a large clast (the very remote possibility of rotation around an axis near the magnetic field direction is eliminated because the inclination relative to the siltstone "bedding" is only −3°, therefore inconsistent with the −15° to −30° range of the other Aptian samples). Therefore, the possibility that this is a sedimentary or neptunian dike was proposed. Recovery of definite sedimentary dikes and filled fractures in later cores supports this interpretation.

The computed paleolatitudes of Site 585 are plotted in Figure 44. During the late Aptian, the site was about 20 to 25° south of the Equator. Rapid northward motion occurred during the Late Cretaceous and the site crossed the Equator near the end of the Cretaceous. The

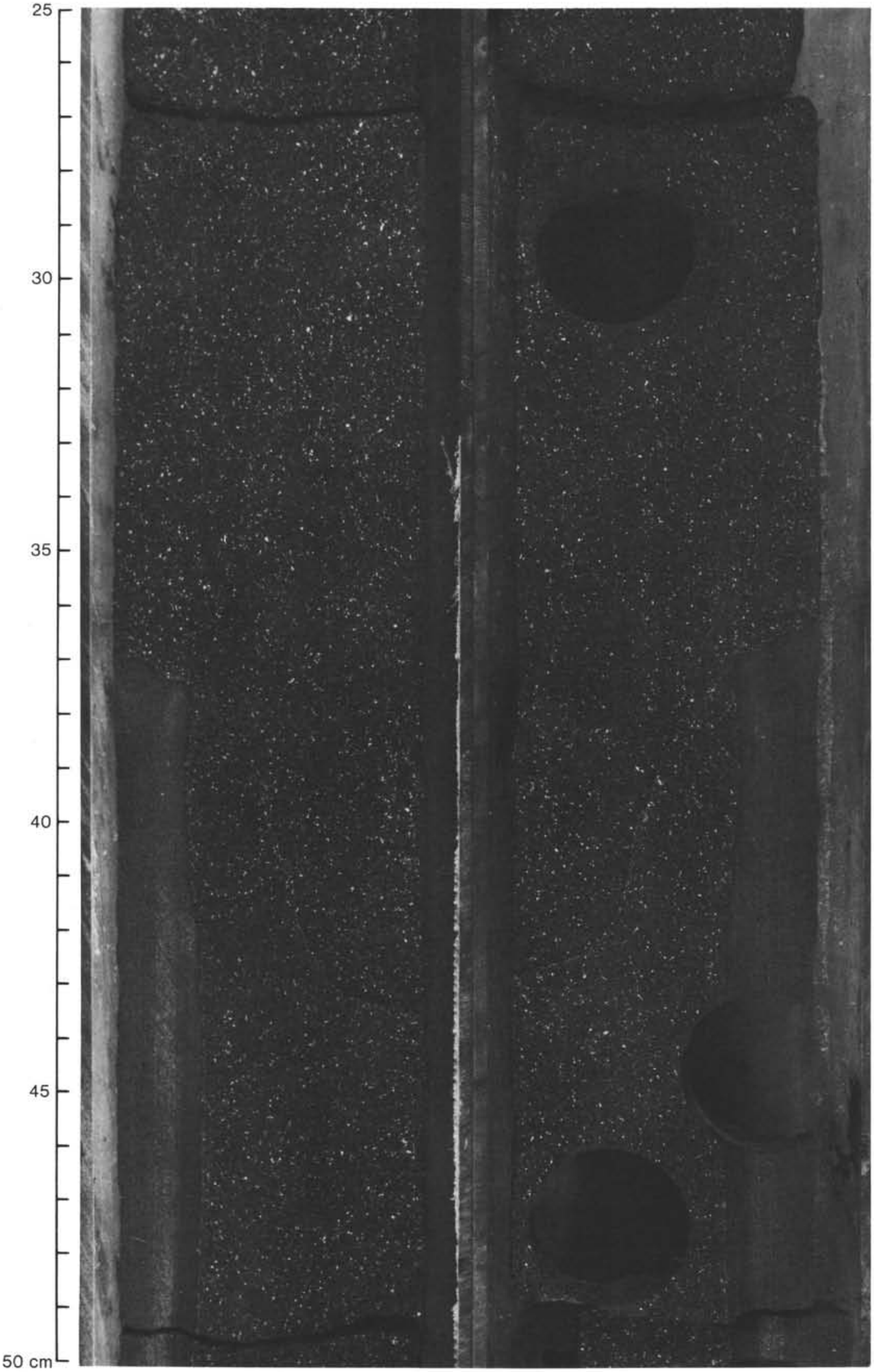

Figure 43. Sedimentary dike in Core 585A-17 (upper Aptian). Paleomagnetic minicores—taken from the greenish black volcaniclastic sandstone above and below the small fault that truncates the fine-grained siltstone dike and from the dike itself—all had similar magnetic directions, indicating that this vertical siltstone feature is probably a sedimentary dike rather than a large rotated block in the debris flow.

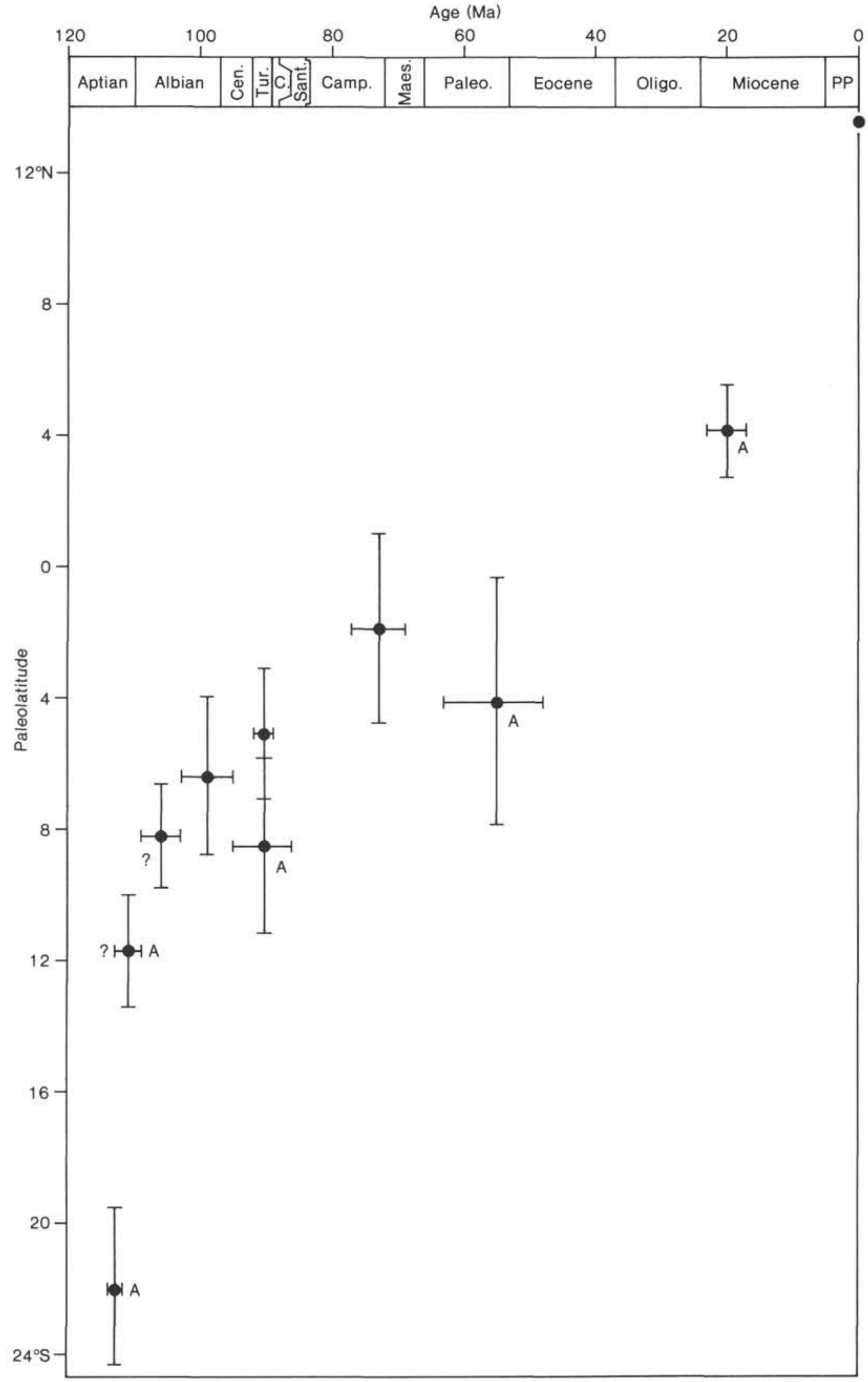

Figure 44. Paleolatitudes of Site 585. Cretaceous time scale is from Lanphere and Jones (1978). Results from Hole 585A are labeled by "A," NRM results, by "?"; error bars are 95% confidence levels.

present location is 13.6°N. This motion is compatible with the paleolatitudes and rate of northward drift of other Pacific sites (Ogg, this volume).

PHYSICAL PROPERTIES

Physical properties measured at Site 585 include wet bulk density, water content, porosity, and compressional sonic velocity. Sampling frequency in each of the holes was basically one minicore per core. However, two or more minicore samples were occasionally taken, depending on recovery rate and homogeneity of the recovered sample. The technique used has been generally described by Boyce (1976). Sonic velocities were measured both in the vertical (V_V) and horizontal (V_H) directions. Wet bulk densities were measured by means of the 2-min. GRAPE and the gravimetric methods. All measured values of sound velocity, wet bulk density, water content, porosity, and impedance are listed in Table 16, and shown in Figure 45.

The wet bulk density values of Cores 585-3 to -32 are very uniform except those measured for limestones (Samples 585-13-1, 38–40 cm; 585-34-1, 91–93 cm; and 585-35-2, 27–29 cm). The scattered values of the sonic velocity in Cores 585-3 to -32 and 585A-5 to -10 result from the variations of hardness among claystones, for example, calcareous or "radiolarian sand" -bearing claystones (Samples 585-18-1, 30–32 cm; 585-29-1, 30–32 cm) and siliceous claystones (Samples 585A-9-1, 106–108 cm and 585A-10-1, 52–54 cm), as indicated by arrows in Figure 45 (see also Sediment Lithology section and the Appendix). However, the scattered values both in the sonic velocity and in the wet bulk density of Cores 585-39 to -55 and 585A-H5 to -22 are caused by the variations in physical properties through the claystone to sandstone transition within a single turbidite layer. Figure 46A and B illustrate the variation of sonic velocities and wet bulk densities with respect to depth for 3-m-thick (Core 585A-H5) and 30-m-thick (Cores 585A-17 to -20) volcanogenic turbidite layers, respectively. Cementing by zeolitic or siliceous minerals considerably increases the sonic velocity. The values of more than 3.5 km/s in compressional sonic velocities are observed in the bottom of a volcanogenic turbidite layer (Cores 585A-18 to -20).

Anisotropy of sonic velocities defined as $2(V_H - V_V)/(V_H + V_V)$ (Carlson and Christensen, 1977) is about 4.8%, a value that is nearly equal to that of Albian to Barremian limestones at the Hess Rise (Fujii, 1981; Bachman, 1983).

The sedimentary column penetrated at Site 585 has been divided into five acoustic units (Table 17), which are related to the lithologic units and seismic-reflection data. The scarcity of sampled data makes it impossible to distinguish the differences among Lithologic Units II, III, and IV. The boundary between Acoustic Units 2 and 3 is less clear than those of 3, 4, and 5.

The averaged values of the compressional sonic velocity in the vertical direction, wet bulk density, and impedance for each acoustic unit are listed in Table 17. As the limestones were seldom recovered, the averaged values excluding those of limestones can be responsible for the representative values of each unit.

LOGGING AND DOWNHOLE MEASUREMENTS

There were no logging and downhole measurements at this site.

SEISMIC STRATIGRAPHY

The seismic profiles across the Mariana Basin run by T. Shipley of the Scripps Institution of Oceanography and F. Duennebier of the Hawaii Institute of Geophysics aboard the *Kana Keoki* during September 1981 appear in Figures 4 and 5 (see the section on Background and Objectives). These profiles were made using an 80-in.^{3} water gun, which does not produce pronounced bubble pulses, and the returns were digitally recorded. Figure 4 is an analog record across the basin, and Figure 5 is a processed record made from the digital data. This was interpreted in terms of the expected lithologic column (see Fig. 5; and Petersen et al., this volume).

Site MZP-6 (Site 585) was selected along the track at 13°30.5′N latitude, 156°48.8′E longitude. The final location of Site 585 is 13°29.00′N latitude, 156°48.91′E longitude. Therefore Site 585 is about 1 mile south of the profile shown on Figure 47. Our approach was from the north and our departure was to the south (Figs. 6, 7, and 9). The reflection stratigraphy on the approach and departure very closely matched that shown on Figure 47 (see also Fig. 7).

Figure 47 represents the postdrilling geologic interpretation of the seismic data. The interpretation is based on (1) the lithology of the cores recovered, (2) acoustic velocities ($\overline{V}$), both vertical and horizontal, rock densities determines by both GRAPE and gravimetric methods as well as the derived impedances ($\overline{I}$) as listed on Table 16, (3) drilling rates, and (4) general geological considerations.

Regional acoustic reflectors in the Basin are shown in Figure 4. The section between 8.1 and 8.4 s (two-way traveltime) extends across the Basin. At Sites 199 and 585, coring and recovery in this section were sparse; it is apparently made up of distal turbidites of middle Eocene to Recent age. The cherts recovered and the continuity of the moderately coherent set of reflectors at about 8.4 s indicate that there are widespread cherts present in the Basin. Cherts of Eocene age are a common occurrence at most western Pacific drill sites. A set of laterally extensive, coherent reflectors at approximately 8.6 s may represent a cherty section at Site 585 of Late Cretaceous age. The Late Cretaceous section at Site 199 is also chert-rich.

The next deeper significant reflector at Site 585 is taken to be the high-amplitude, very coherent one at 8.74 s. Impedances calculated aboard ship suggest that this reflector has a reflection coefficient of 0.125. This is interpreted to be the top, or upper part, of the volcaniclastic section penetrated at Site 585 at 590 m. Within the volcaniclastic section at about 800 m a velocity increase from approximately 2.2 to approximately 3.2 km/s was noted according to shipboard velocity measurements. The reflection coefficient of the 800-m level is calculated at 0.142. Drilling rates showed a marked decrease at about 750 m in Hole 585A. Drilling rates being difficult

Table 16. Physical properties of sediments, Site 585.

Sample (core-section, interval in cm)	Sub-bottom depth (m)	Compressional velocity Vertical (km/s)	Horizontal (km/s)	Anisotropy (%)	Wet bulk density (g/cm^3) GRAPE	Grav.	Wet water content (%)	Porosity (%)	Impedance[a] (10^5 g/cm^2s)	Remarks
Hole 585										
1-3, 50-52	0-6.8		1.49							Nannofossil ooze
1-3, 100-102			1.49							Nannofossil ooze
1-4, 50-52			1.49							Nannofossil ooze
1-4, 100-102			1.50							Clay-bearing nannofossil ooze
3-1, 30-35	265.5-275.1	1.87	2.01	7.5		1.88	27.3	51.3	3.52	Nannofossil chalk
6-1, 22-24	284.6-293.7	1.90	2.06	8.4	1.82	1.78	26.9	47.7	3.42	Nannofossil chalk
8-1, 67-69	302.9-312.0	1.86	1.87	0.6	1.90	1.81	26.0	46.9	3.44	Nannofossil chalk
8-2, 49-51		1.89	1.86	-1.7	1.82	1.76	28.3	49.6	3.38	Nannofossil limestone
9-1, 24-26	312.0-321.2	1.90	1.92	0.8	1.79	1.77	27.0	47.8	3.38	Nannofossil chalk
11-1, 57-59	330.3-339.5	1.90	1.93	1.4	1.77	1.82	27.2	49.4	3.40	Nannofossil chalk
12-1, 16-18	339.5-348.6	1.82	1.85	-1.2	1.78	1.83	27.3	49.8	3.29	Nannofossil chalk
13-1, 38-40	348.6-357.8	2.33	2.52	7.7	1.88	1.95	19.2	37.5	4.45	Silicified nannofossil limestone
14-2, 58-60	357.8-366.9	1.90	1.91	0.6	1.79	1.84	26.6	48.8	3.44	Nannofossil chalk
15-1, 136-138	366.9-380.4	2.03	2.11	3.9	1.77	1.88	24.5	46.6	3.71	Nannofossil chalk
17-1, 131-133	389.5-398.7	1.86	1.88	1.0		1.90	23.8	45.2	3.53	Nannofossil chalk
18-1, 30-32	398.7-307.8	2.17	2.38	9.1	1.78	1.86	23.3	43.3	3.93	Calcareous claystone
20-2, 56-58	417.0-426.1	1.76	1.84	4.5	1.90	1.91	23.4	44.7	3.36	Zeolite-bearing calcareous claystone
21-1, 37-39	426.1-435.3	1.76	1.87	5.7	1.93	1.92	23.3	44.6	3.38	Silicified chalk
27-3, 63-65	485.4-494.6	1.77	1.82	2.7	1.84	1.84	27.2	49.9	3.26	Claystone
28-5, 15-16	494.6-503.7	1.81	1.88	4.0	1.77	1.81	27.8	50.2	3.24	Claystone
29-1, 30-32	503.7-512.9	2.35	2.46	4.8	1.86	1.86	21.5	40.0	4.37	"Red-sand"-bearing claystone
30-1, 32-34	512.9-522.0	1.84	1.96	6.1	1.87	1.85	26.9	49.7	3.42	Claystone
32-1, 46-49	531.2-540.3	1.97	2.14	8.2	1.84	1.84	24.9	45.9	3.62	Claystone
32-4, 29-31		1.95	2.01	3.4	1.86	1.86	24.8	46.0	3.63	Silty claystone
34-1, 91-93	549.5-558.6	2.61	2.79	6.4	2.07	2.06	17.2	35.5	5.40	Limestone
35-2, 27-29	5586.-572.1	2.69	2.86	6.0	2.16	2.15	14.4	31.0	5.81	Limestone
39-2, 28-30	599.5-608.7	2.13	2.28	6.8	1.92	1.95	22.3	43.4	4.11	Volcanic-bearing calcareous siltstone
42-1, 14-16	627.0-636.1	2.41	2.45	2.0	2.07	2.06	21.3	43.8	4.96	Siltstone
43-2, 139-141	636.1-645.3	1.90	2.02	6.5	1.89	1.91	26.4	50.3	3.61	Claystone
44-4, 132-134	645.3-654.4	1.95	2.07	6.3	1.92	1.90	26.3	50.0	3.72	Claystone
45-3, 107-109	654.4-667.8	1.93	2.07	6.8	1.87	1.87	27.0	50.5	3.61	Siltstone
46-2, 100-102	667.8-676.9	1.93	2.11	8.7	1.93	2.05	20.4	41.8	3.84	Claystone
47-1, 91-93	676.9-686.1	2.31	2.46	6.5	1.92	1.94	24.9	48.1	4.46	Coarse sandstone
47-4, 131-133		2.57	2.57	0.3	1.87	1.92	24.0	46.2	4.88	Coarse sandstone
48-2, 62-64	686.1-695.2	2.43	2.57	5.7	2.01	2.00	20.1	40.1	4.86	Volcanic silty sandstone
49-2, 88-90	695.2-704.4	2.37	2.60	9.6	1.98	1.96	23.5	46.0	4.67	Volcanic silty sandstone
50-1, 68-70	704.4-713.5	2.54	2.66	4.4	2.02	2.01	21.3	42.8	5.11	Volcanic silty sandstone
50-3, 72-74		2.03	2.11	4.2	2.02	2.05	20.4	42.0	4.14	Silty claystone
51-3, 43-45	713.5-722.7	2.51	2.84	12.4	2.11	2.11	16.3	34.4	5.30	Sandy siltstone
52-3, 88-90	722.7-731.8	2.34	2.51	6.7	2.11	2.10	18.8	39.5	4.94	Sandy siltstone
53-1, 98-100	731.8-741.0	2.57	2.69	4.3	1.85	1.88	26.0	49.0	4.81	Coarse volcaniclastic sandstone
54-2, 119-121	741.0-750.1	2.95	3.09	4.8	2.20	2.22	15.8	35.1	6.52	Volcaniclastic sandstone
55-3, 52-54	750.1-763.7	2.79	2.82	1.0	2.17	2.17	16.7	36.3	6.05	Volcanic sandstone
Hole 575A										
5-1, 133-135	502.6-511.8	1.78	1.81	1.8	1.54	1.67	37.8	60.7	2.86	Claystone
7-1, 32-34	520.9-532.4	1.80	1.92	6.0	1.75	1.83	28.6	52.5	3.22	Claystone
8-2, 89-91	532.4-543.5	1.81	1.86	2.6	1.64	1.74	33.3	58.0	3.06	Slightly calcareous claystone
9-1, 106-108	543.5-552.6	2.56	2.86	11.1	1.98	2.06	18.6	38.3	5.17	Siliceous claystone
10-1, 52-54	552.6-561.8	2.50	2.73	8.7	1.97	2.05	19.1	39.1	5.03	Siliceous claystone
H5-1, 50-52	658.0-772.1	1.87	2.01	7.6	1.82	1.84	28.4	52.2	3.42	Claystone
H5-1, 56-58		1.86	2.04	9.3	1.85	1.88	26.5	49.8	3.47	Claystone
H5-1, 92-94		1.93	2.09	8.0	1.84	1.87	26.7	50.0	3.58	Interlayer claystone and silty claystone
H5-1, 100-102		2.01	2.16	7.6	1.92	1.88	26.6	49.9	3.82	Interlayer claystone and silty claystone
H5-1, 107-109		1.97	2.17	9.6	1.90	1.94	23.7	45.9	3.78	Interlayer claystone and silty claystone
H5-1, 117-119		1.87	2.04	8.9	1.86	1.88	26.4	49.6	3.50	Claystone
H5-1, 132-134		1.88	2.04	8.1	1.84	1.89	26.9	50.3	3.51	Claystone
H5-1, 141-143		1.90	2.03	6.9	1.82	1.82	29.2	53.2	3.46	Claystone
H5-1, 147-149		1.93	2.08	7.6	1.79	1.83	29.0	52.9	3.49	Silty claystone
H5-2, 3-5		1.95	2.13	8.8	1.84	1.84	28.1	51.8	3.59	Silty claystone (cross bedding)
H5-2, 14-16		1.89	2.04	7.4	1.74	1.82	29.3	53.3	3.36	Silty claystone
H5-2, 25-27		1.91	2.06	7.4	1.80	1.85	28.0	51.7	3.49	Silty claystone
H5-2, 35-37		1.91	2.01	5.4	1.79	1.80	30.1	54.3	3.43	Silty claystone
H5-2, 49-51		1.97	2.05	3.8	1.79	1.77	32.0	56.5	3.52	Silty claystone
H5-2, 60-62		1.98	2.08	5.0	1.80	1.72	29.4	53.5	3.58	Silty claystone
H5-2, 69-71		1.99	2.02	1.9	1.78	1.80	30.3	54.5	3.56	Silty claystone
H5-2, 84-86		1.96	2.05	4.2	1.74	1.80	31.4	55.8	3.47	Silty claystone
H5-2, 95-97		1.95	2.04	4.7	1.75	1.79	31.0	55.4	3.45	Silty claystone
H5-2, 104-106		2.04	2.22	8.2	1.76	1.80	30.5	54.8	3.63	Silty claystone
H5-2, 114-116		2.12	2.21	4.2	1.81	1.83	28.8	52.7	3.86	Silty claystone
H5-2, 126-128	658.0-772.1	2.11	2.19	3.4	1.82	1.84	28.4	52.1	3.86	Volcaniclastic sandstone
H5-2, 132-134		2.09	2.20	5.3	1.79	1.90	25.6	48.6	3.86	Volcaniclastic sandstone
H5-2, 142-144		2.22	2.28	2.5	1.87	1.86	27.4	50.9	4.14	Volcaniclastic sandstone
H5-3, 11-13		2.45	2.47	0.9	1.94	2.00	21.1	42.2	4.83	Volcaniclastic sandstone

Table 16 (continued).

Sample (core-section, interval in cm)	Sub-bottom depth (m)	Compressional velocity: Vertical (km/s)	Compressional velocity: Horizontal (km/s)	Compressional velocity: Anisotropy (%)	Wet bulk density (g/cm³): GRAPE	Wet bulk density (g/cm³): Grav.	Wet water content (%)	Porosity (%)	Impedance[a] (10^5 g/cm²s)	Remarks	
Hole 575A (Cont.)											
H5-3, 20-22		2.73	2.75	0.9	2.02	2.03	19.9	40.4	5.53	Volcaniclastic sandstone	
H5-3, 25-27		2.62	2.66	1.5	1.88	2.00	20.9	41.9	5.08	Volcaniclastic sandstone	
11-1, 60-62	772.1-781.3	2.84	2.91	2.3	2.03	2.12	16.5	34.9	5.89	Sandy siltstone	
12-1, 78-80	781.3-790.4	2.59	2.72	4.8	2.06	2.05	19.2	39.3	5.32	Sandy siltstone	
12-5, 102-104		2.07	2.21	6.5	1.99	2.02	20.4	41.1	4.15	Sandy siltstone	
12-6, 73-75		2.10	2.21	5.1	2.03	2.03	20.0	40.5	4.26	Sandy siltstone	
13-3, 135-137	799.6-808.7	2.83	3.02	6.7	2.09	2.09	17.4	36.4	5.91	Volcanogenic sandstone	
14-1, 146-148	808.7-817.9	3.31	3.53	6.3	1.98	2.11	16.6	35.1	6.77	Volcanogenic sandstone	
14-5, 80-82		2.81	2.97	5.6	1.99	2.04	19.6	39.9	5.66	Volcanogenic sandstone	
15-1, 63-65	817.9-827.0	3.11	3.16	1.7	2.10	1.84	28.4	52.1	6.13	Volcanogenic sandstone	
16-3, 106-108	827.0-838.6	2.87	3.10	7.8	1.96	2.06	18.8	38.7	5.77	Siliceous siltstone	
17-1, 8-10	838.6-847.7	2.90	3.02	4.0	1.97	2.08	18.1	37.5	5.87	Volcanogenic sandstone	
17-1, 77-79		2.80	2.94	4.9	1.93	2.06	18.6	38.4	5.59	Volcanogenic sandstone	
17-1, 107-109		2.88	3.00	4.2	1.95	2.06	18.5	38.1	5.77	Volcanogenic sandstone	
17-2, 22-24		2.89	3.00	3.8	1.94	2.07	18.4	38.0	5.79	Volcanogenic sandstone	
17-2, 116-118		2.95	3.09	4.6	1.95	2.08	17.9	37.2	5.94	Volcanogenic sandstone	
17-3, 23-25		2.91	3.02	3.5	1.97	2.06	18.7	38.5	5.86	Volcanogenic sandstone	
17-3, 119-121		2.98	3.00	0.8	1.99	2.04	19.5	39.8	6.00	Volcanogenic sandstone	
17-4, 21-23		2.83	2.89	2.2	2.00	2.05	18.9	38.8	5.73	Volcanogenic sandstone	
17-4, 86-88		2.82	2.96	5.1	2.02	2.04	19.6	40.0	5.72	Volcanogenic sandstone	
17-5, 120-122		2.98	3.02	1.2	2.02	2.10	17.3	36.2	6.14	Volcanogenic sandstone	
17-6, 53-55	838.6-847.7	3.16	3.17	0.5	2.02	2.14	15.8	33.8	6.57	Volcanogenic sandstone	
18-1, 13-15	847.7-857.7	2.98	3.06	2.7	2.03	2.08	18.0	37.4	6.12	Volcanogenic sandstone	
18-1, 93-95		3.12	3.18	2.0	2.00	2.11	16.9	35.6	6.41	Volcanogenic sandstone	
18-2, 23-25		3.11	3.12	0.4	2.02	2.09	17.4	36.5	6.39	Volcanogenic sandstone	
18-2, 106-108		3.05	3.10	1.7	2.03	2.08	17.8	37.0	6.27	Volcanogenic sandstone	
18-3, 48-50		3.18	3.21	1.1	2.02	2.11	16.9	35.6	6.57	Volcanogenic sandstone	
18-3, 128-130		3.10	3.26	5.0	2.06	2.11	16.7	35.3	6.46	Volcanogenic sandstone	
18-4, 53-55		3.23	3.31	2.4	2.03	2.15	15.1	32.6	6.75	Volcanogenic sandstone	
18-4, 136-138		3.13	3.09	−1.6	1.93	2.10	17.3	36.2	6.31	Volcanogenic sandstone	
18-5, 45-47		3.28	3.38	3.2	2.01	2.12	16.3	34.6	6.77	Volcanogenic sandstone	
18-5, 125-127		3.46	3.55	2.5	2.11	2.22	12.9	28.7	7.49	Volcanogenic sandstone	Clasts up
18-6, 13-15		3.36	3.46	2.7	2.13				7.16	Volcanogenic sandstone	to 3 cm)
18-6, 119-121		3.55	3.57	0.4	2.05	2.15	15.3	32.9	7.46	Volcanogenic sandstone	
18-7, 30-32		3.67	3.77	2.6	2.08	2.17	14.7	31.8	7.80	Volcanogenic sandstone	
19-1, 6-8	857.7-866.8	3.59	3.70	3.1	2.01	2.15	15.4	33.1	7.47	Volcanogenic sandstone	
19-2, 14-16		3.39	3.51	3.3	2.08	2.14	15.7	33.5	7.15	Volcanogenic sandstone	(Grains
19-3, 6-8		3.65	3.70	1.5	2.15	2.14	15.7	33.6	7.83	Volcanogenic sandstone	up to
19-4, 11-13		3.47	3.54	2.0	2.11	2.13	16.1	34.2	7.36	Volcanogenic sandstone	2-3 mm)
20-1, 15-17	866.8-876.0	3.90	3.89	−0.3	2.22	2.24	12.3	27.6	8.70	Volcanogenic sandstone	(Silica
20-2, 13-15		4.03	4.10	1.7	2.26	2.24	12.2	27.3	9.07	Volcanogenic sandstone	cemented)
20-2, 116-118		4.92	4.86	−1.2	2.55	2.43	6.5	15.8	12.25	Basalt (vesicles filled with smectite)	
21-1, 113-115	876.0-885.1	3.08	3.16	2.7	2.03	2.08	17.7	36.9	6.36	Volcaniclastic sandstone	
21-2, 116-118		2.98	3.11	4.2	1.97	2.04	19.4	39.6	5.97	Volcaniclastic sandstone	
22-1, 101-103	885.1-892.8	3.17	3.30	4.0	2.10	2.15	15.4	33.1	6.74	Volcaniclastic sandstone	

[a] Impedance is calculated from the vertical compressional wave (V_V) and the average of wet bulk densities (GRAPE and Grav.).

to interpret, however, we consider the "9.0-s" reflector of the site surveys (8.9-s reflector on Fig. 4) to be the result of the high velocity section of dense, well lithified volcaniclastic rocks present in Hole 585A from 800 m to the total depth of 892.8 m. Thus the "9.0-s" reflector at Site 585 is neither Jurassic limestone nor basement.

SUMMARY AND CONCLUSIONS

Introduction

Site 585, one of several MZP sites considered for the Mesozoic Pacific program of the JOIDES Ocean Paleoenvironment Panel, was selected on the basis of site surveys carried out by the Hawaii Institute of Geophysics and the Scripps Institution of Oceanography. The general area occupied by the East Mariana Basin was considered a favorable one in which to reach Jurassic strata, because the water depth and magnetic anomaly patterns indicated that the Basin was underlain by 150 to 160 m.y. old lithosphere. DSDP Site 199 had been drilled 40 n.mi. to the west of proposed MZP-6 (now 585); Campanian limestone, underlain by lithified tuff, was cored there. Forty nautical miles south of MZP-6, DSDP Sites 200, 201, and 202 were drilled atop Ita Maitai Guyot (for details of Sites 199 through 202 see Heezen, McGregor, et al., 1973a). On Ita Maitai Guyot, lower Eocene to Recent foraminiferal ooze overlies hard oolitic limestone and lagoonal coraliferous mud of indeterminate age. In August 1981 dredge hauls taken from Ita Maitai Guyot by the *Kana Keoki* recovered *Inoceramus*-bearing limestones, which indicated that Ita Maitai Guyot accumulated shallow-water sediment in, probably, the Late Cretaceous (S. Schlanger, unpublished Hawaii Institute of Geophysics data).

The Campanian tuffs found at Site 199 were believed to be the product of Late Cretaceous edifice building volcanism that formed, among other seamounts that lie around the perimeter of the East Mariana Basin, Ita

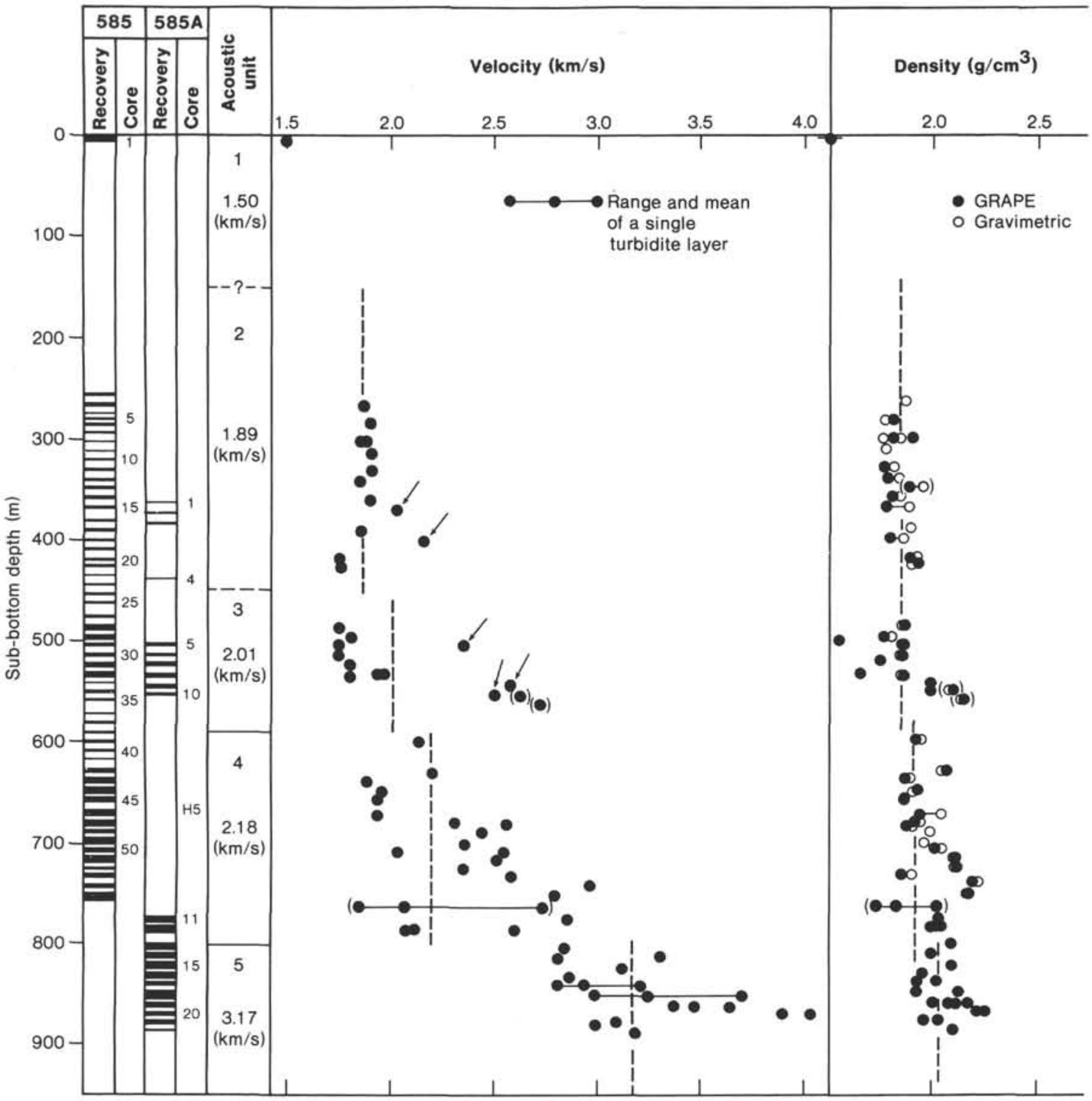

Figure 45. Variations of physical properties with depth at Site 585. Vertical dashed lines indicate average value for that parameter within the particular acoustic unit. Parentheses indicate limestone. See text for an explanation of small arrows.

Maitai Guyot (Heezen, MacGregor, et al., 1973b). The ubiquitous character of Cretaceous midplate volcanism in the western Pacific prepared us for encounters with volcanogenic sediments, but the East Mariana Basin was, it seemed, the best bet for reaching the Jurassic objectives.

Drilling Holes 585 and 585A resulted in a maximum penetration of 763.7 m in 585; a misfit core barrel sub resulted in loss of Hole 585. Hole 585A was terminated at 892.8 m because of complete bit failure. Fifty-five cores were taken from Hole 585, and 22 from 585A. Figure 48 shows the salient data from Site 585 in generalized form.

The sedimentary section that was recovered is dominated by redeposited volcanogenic material in mid-Cretaceous strata and redeposited fossils in Upper Cretaceous and Neogene strata. Compared to most open ocean sites the rocks are relatively unfossiliferous, and the faunal and floral diversity is low. The intensive reworking and general paucity of the autochthonous fossils made the task of assigning a precise zone to each core difficult. Many biostratigraphic zones were recognized, however, and it appears that the section is largely complete from middle Eocene to upper Aptian, with minor hiatuses, although evidence for the presence of most of the Paleocene is lacking and late and middle Maestrichtian assemblages occur only redeposited within Tertiary strata.

Although the Jurassic objectives were not reached, information derived from Holes 585 and 585A revealed the following: (1) Benthic foraminiferal faunas indicate that the East Mariana Basin was at abyssal depths from the Aptian to the present. (2) Intense edifice building volcanism took place in the area during the Aptian through

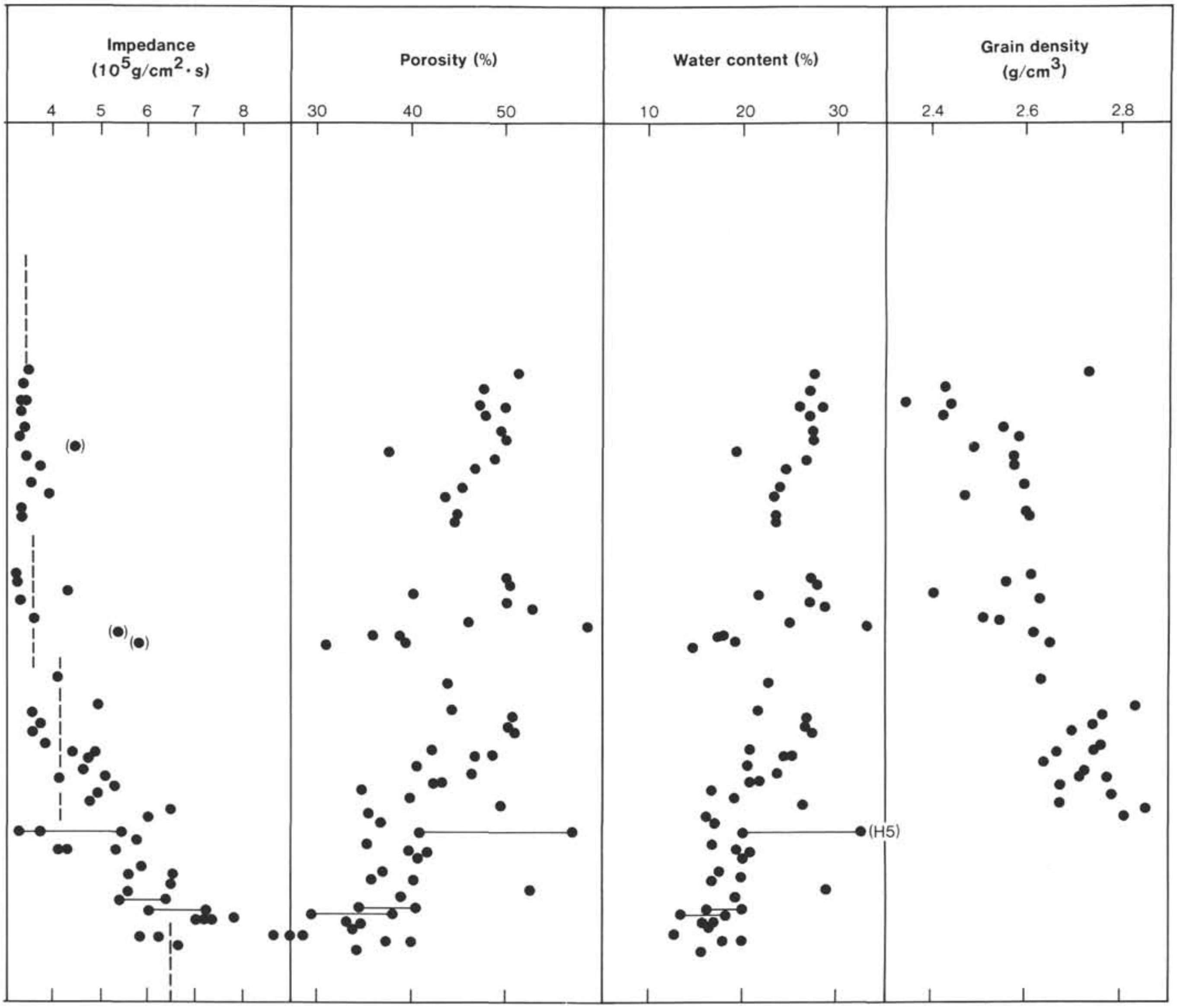

Figure 45 (continued).

middle Albian. The timing of the onset of volcanism is not known. (3) Volcanic edifices around the Basin reached to or above sea level and were capped or fringed by carbonate reefs and banks in the Aptian–Albian. (4) The growth of these edifices provided the bathymetric relief needed for the delivery to the abyssal Mariana Basin of the numerous and thick turbidite sequences that dominate the sedimentary section. (5) Organic carbon-rich sediments formed in the Basin at, or very close to, the Cenomanian/Turonian boundary; these carbonaceous sediments are the local record of a global oceanic anoxic event. (6) The Pacific Plate moved from a paleolatitude of 22.0°S in the late Aptian, through 8.2°S in the Albian, and 5.1°S in the Turonian before reaching its present latitude of 13.5°N at Site 585. (7) The "acoustic basement" in the East Mariana Basin is composed of Aptian midplate volcaniclastic strata—this state of affairs may hold true for much of the western Pacific.

Sedimentology

The sedimentary section recovered at Site 585 was divided into six lithologic units (I through VI) based on composition and degree of diagenesis and lithification (Fig. 10; Table 2). The lithologic classification used is presented in the Introduction and Explanatory Notes chapter (this volume).

Unit I is nannofossil ooze, clay-bearing nannofossil ooze, and clay (Core 585-1, 0–6.8 m sub-bottom depth; lower Pleistocene to Recent). The top of Unit I consists of a 1.5-m-thick bed of brown homogeneous clay. Other very minor components observed in smear slides include zeolites and nannofossils (Appendix). Most of the unit, however, consists of about 5 m of light yellowish brown to brown nannofossil ooze and clay-bearing nannofossil ooze. Concentrations of $CaCO_3$ in two samples from this part of the unit are 51 and 83% (Table 3).

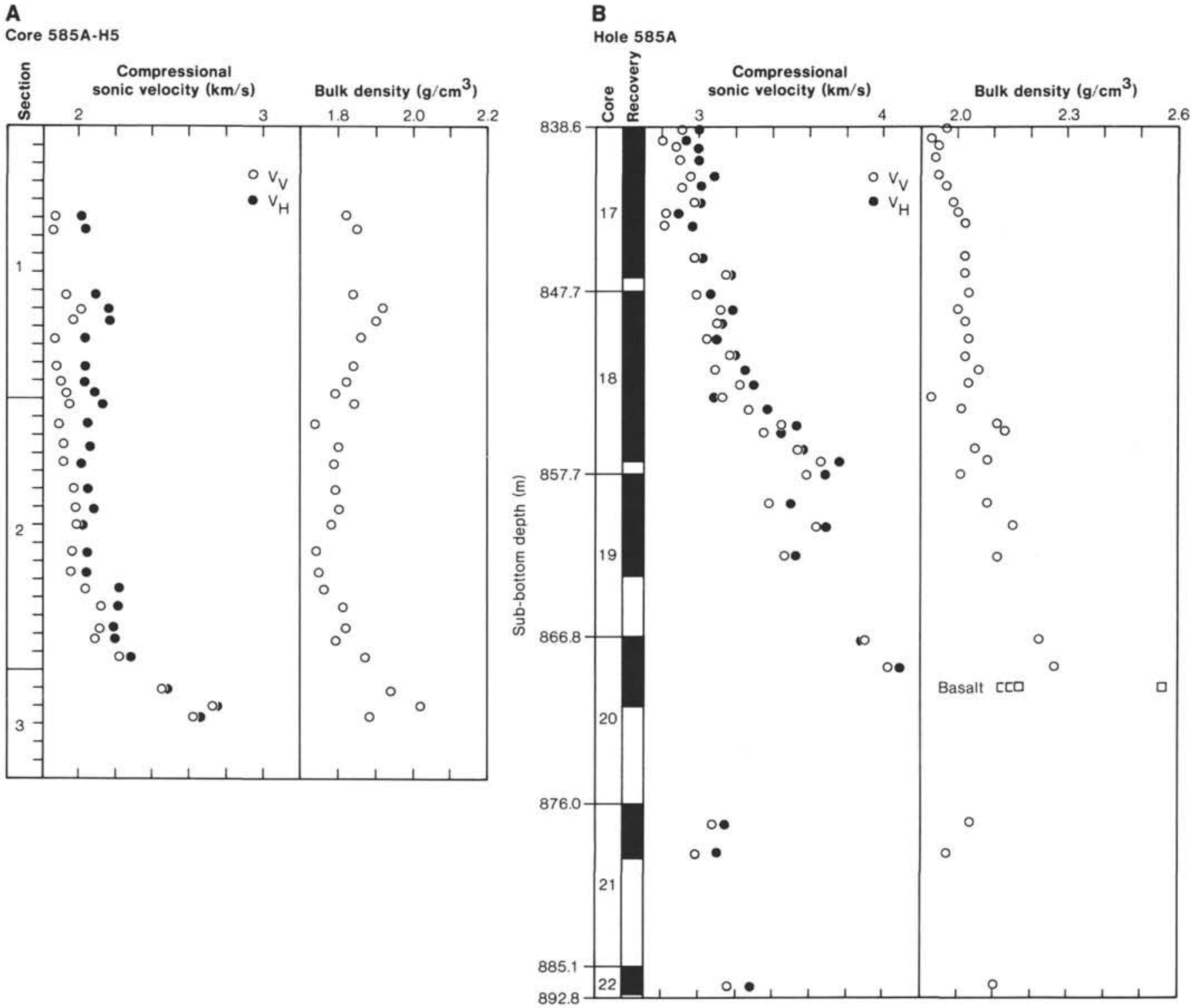

Figure 46. Variations of physical properties with depth for (A) 3-m-thick (Core 585A-H5) and (B) 30-m-thick (Cores 585A-17 to -20) volcanogenic turbidite layers (black areas indicate core recovery).

Table 17. Acoustic units.

Acoustic unit	Core	Sub-bottom depth (m)	Sonic velocity (vertical) (km/s)	Wet-bulk density (g/cm^3)	Impedance (10^5 g/cm^2 · s)
1	1	0–150	1.50	1.40[a]	2.10[a]
2	2 to 21 (1 to 5)[b]	150–450	1.89 (1.93)[c]	1.84 (1.84)[c]	3.48 (3.55)[c]
3	27 to 35 (6 to 10)[b]	450–590	2.01 (2.12)[c]	1.84 (1.91)[c]	3.59 (4.09)[c]
4	39 to 55 (H5 to 12)[b]	590–800	2.18	1.91	4.16
5	(13 to 22)[b]	800–893	3.17	2.03	6.47

[a] Estimated from the data at Site 199 (Heezen, MacGregor, et al., 1973a).
[b] Core numbers in parentheses are from Hole 585A.
[c] Values in parentheses are obtained by including those of limestones.

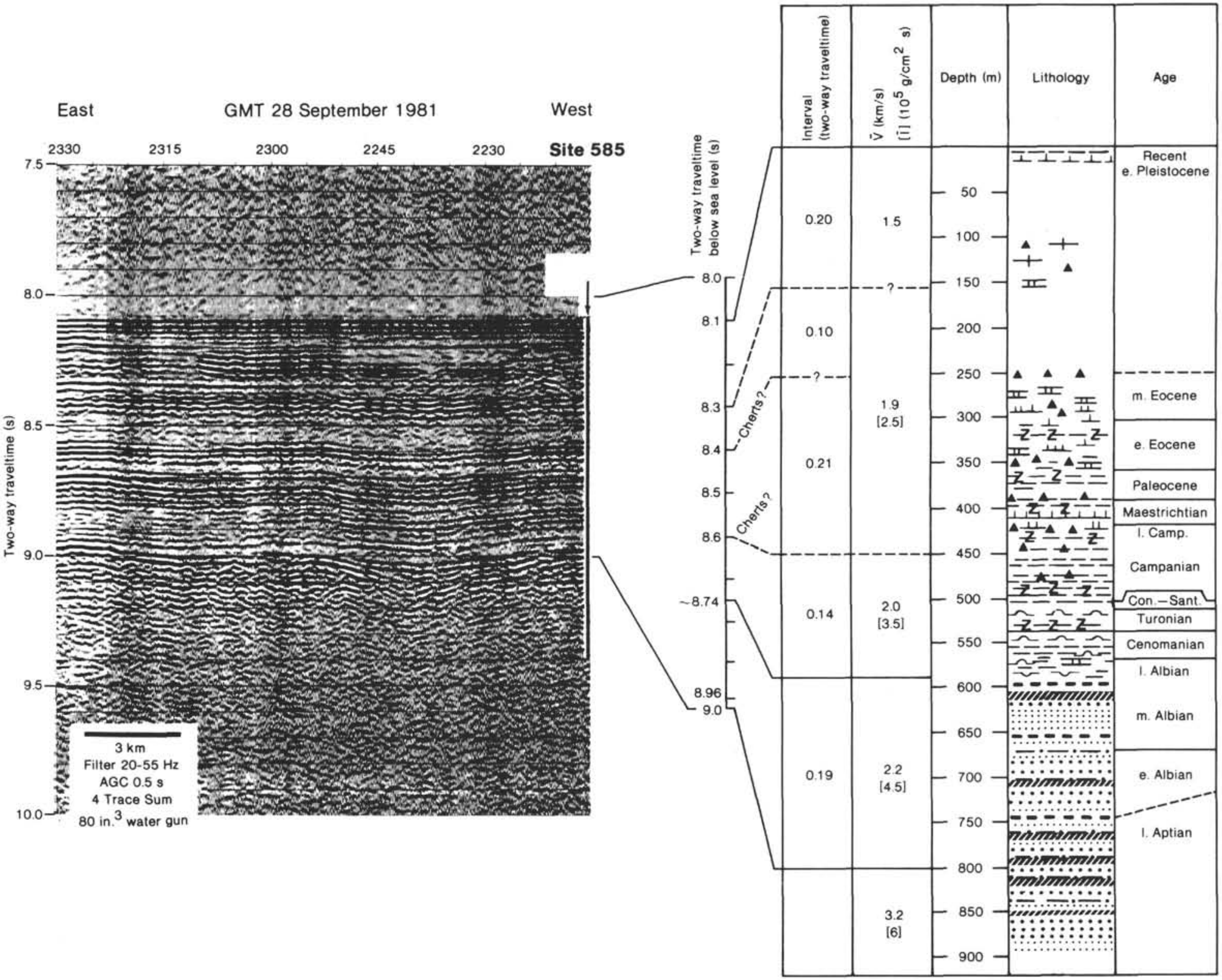

Figure 47. Correlation of seismic profile with the drilled section and shipboard physical properties data at Site 585.

Unit II comprises nannofossil chalk, silicified limestone, chert, and zeolitic claystone (Cores 585-2 to -17, and 585A-1 to -3, 256–399 m sub-bottom depth; middle Eocene to Upper Cretaceous [Maestrichtian]). Most material recovered from Unit II consists of white to light gray nannofossil chalk showing varying degrees of diagenesis by $CaCO_3$ and SiO_2 toward chalk, limestone, silicified limestone, and chert. Interbeds of brown zeolite-bearing claystone are common and increase in abundance below about 360 m (Core 585-13). Above 360 m, zeolite-bearing claystone apparently occurs mainly in thin beds, but also occurs as lenses subparallel to stratification in chalk and as subrounded cores of many fragments of chert and silicified limestone.

Diagenetic silicification of carbonate ooze has resulted in a highly variable percentage of $CaCO_3$, which ranges from less than 20% in silicified limestones to at least 85% in chalks. X-ray diffraction (XRD) results from samples of zeolitic claystones from Cores 585-13 and -14 (Table 4) show that the most abundant minerals identified on XRF diffractograms are smectite, clinoptilolite, quartz, and calcite; less abundant minerals identified are celadonite, siderite, and nontronite(?). Small pieces of native copper were observed in a sample of claystone from Core 585-13. This thin zeolitic claystone may be the product of an Eocene ash fall.

Unit III contains zeolitic claystone, nannofossil claystone, and minor clayey nannofossil chalk and chert (Cores 585-18 to -20, 399–426 m sub-bottom depth; Maestrichtian to upper Campanian). The dominant lithology of Unit III is dark brown zeolite-bearing to zeolitic claystone with variable amounts of $CaCO_3$ as nannofossils and as unspecified carbonate that presumably is present as cement. Grading is apparent in many of the units but it is usually very subtle. The bases of several carbonate-rich layers have thin laminae of silty, redeposited hyaloclastic material. XRD results from samples of brown claystone from Core 18 (Table 4) show that the most abundant minerals are quartz, clinoptilolite, smectite, celadonite, calcite, and siderite.

Unit IV is made up of chert and claystone (Cores 585-21 to -26 and 585A-4, 426–485 m sub-bottom depth; Campanian). The most common material interbedded with the chert is brown zeolite-bearing claystone. Textures and fabrics observed in the larger chert fragments suggest that some chert formed by silicification of graded carbonate grainstones. In some of the silicified limestones undeformed clay-filled burrows are present. In contrast, burrows in the nannofossil chalk surrounding the silicified limestone are flattened. This contrast in burrow preservation is taken as evidence that silicification of the limestone took place before the host chalks were significantly compacted. Further, microfossils in the silicified limestone appear to be less crushed than the fossils in the chalk. The percentage of $CaCO_3$ in the silicified limestones ranges from 20 to 85%; petrographic observations of these $CaCO_3$-rich silicified limestones suggest that silica is added to the limestone as a pore filling rather than as a pervasive replacement. In some specimens pore spaces remain open. Paragenesis of the silica phases is complex. Replacement of silicified limestone by microcrystalline quartz is, in places, controlled by the presence of chalcedony veins; locally the contact between microcrystalline quartz is sharply marked against insoluble clay or Fe-oxides. Silicification and chertification are commonly associated with current-worked laminae or with the basal parts of graded sequences, probably because the greater permeability of these coarser sediments allows easier access to pore-fluid circulation.

Unit V comprises claystone with minor limestone and radiolarian sandstone (Cores 585-27 to -37 and 585A-5 to -10, 485–590 m sub-bottom depth; Campanian to middle Albian). The dominant lithology of Unit V is claystone, with varying amounts of zeolites, $CaCO_3$, and radiolarians. Unit V was subdivided into three subunits based on color and the relative abundances of these three components.

Subunit VA contains brown and olive black claystone (Cores 585-27 and -28, 485–504 m sub-bottom depth; Campanian). Specifically, Subunit VA consists of dark reddish brown and olive black zeolite-bearing claystone that is very low in carbonate content. Other minor components include feldspar, altered volcanic glass, and iron oxides (Appendix). Plant fragments were found in a foraminifer preparation of a sample of a 0.5-cm dark band in Sample 585-27-3, 138 cm. The claystone is mostly massive appearing, but some is moderately bioturbated, with most burrows flattened by compaction so that they are subparallel to stratification. Burrows commonly are filled with green or black claystone, presumably more reduced chemically. Silty laminae form the bases of graded sequences.

Subunit VB is dark gray claystone with variable amounts of calcareous, siliceous, and organic components (Cores 585-29 to -33 and 585A-5 to -9, 504–550 m sub-bottom depth; Coniacian to upper Cenomanian). Subunit VB consists mainly of dark gray claystone with variable concentrations of recrystallized radiolarians, $CaCO_3$, and silica. The recrystallized radiolarians usually are concentrated in sandy layers, lenses, or stringers. Some fining-upward graded sequences are evident, one being over 3 m thick. Common components include radiolarians (most recrystallized), nannofossils, recrystallized calcite, and zeolites.

In Cores 585-32 and 585A-8, dark gray claystone contains common black flakes of organic-rich material (plant debris?) that are oriented parallel to stratification (Fig. 12). A 2-cm-thick black pyritic silty claystone containing organic carbon in Sample 585-32-3, 72–74 cm (see section on Organic Geochemistry) occurs at the top of a fining-upward graded sequence, just above bioturbated claystone, and just below parallel- and cross-laminated siltstone of the overlying graded sequence (Figs. 13A and 14). The concentration of black flecks of organic matter in dark gray siltstone in the core catcher of Core 585A-8 increases downward over an interval of about 1 cm into a 3-mm-thick band of black sandstone consisting mainly of coated recrystallized radiolarians and flecks of black organic matter (Figs. 13B and 15). This band clearly represents a single pulse or influx of both radiolarians and organic debris. The influx of organic debris then continued but at a much reduced rate, manifested as black flecks mixed with the overlying siltstone that decrease in abundance upward (Fig. 15). The nature and origin of these organic carbon-rich layers are discussed later in the section on the Cenomanian–Turonian oceanic anoxic event that follows the section on Biostratigraphy and Paleoecology.

Subunit VC, composed of calcareous claystone, radiolarian claystone, and clayey limestone (Cores 585-34 to -37 and 585A-9,CC to -10, 550–590 m sub-bottom depth; Cenomanian to middle Albian), consists of claystone with abundant but highly variable concentrations of radiolarians and $CaCO_3$. This has resulted in interbedding of dark gray claystone, red nannofossil-bearing claystone and clayey limestone, radiolarian-bearing limestone and clayey limestone of varying colors but mostly shades of brown, and, in extreme, grayish brown radiolarian sandy siltstone (Fig. 17). Parallel laminations are common, and several graded units are apparent. These structures are interpreted as indicating that these rocks are distal turbidites.

Unit VI comprises graded sequences of volcanogenic sandstones, siltstones, claystones, and breccias with variable concentrations of $CaCO_3$ and SiO_2 (Cores 585-38 to -55 and 585A-11 to -22, 590–893 m sub-bottom depth; middle Albian to upper Aptian). Unit VI consists of a thick section of coarse volcaniclastic sediments in fining-upward graded sequences that may be more than several meters thick, and commonly have bases of coarse sandstone or breccia. The bases of a few of the graded sequences consist of sand-size carbonate clasts or interlaminated or mixed carbonate and volcanogenic clasts (Figs. 20 through 22). Most of the graded sequences grade upward into fine-grained tops of claystone or silty claystone. The Albian section in Hole 585 contains scattered skeletal debris of echinoids, mollusks, and ostracodes in addition to individual ooids. The Aptian section in Hole 585A, in contrast, contains an abundance of ooids in association with fragments of calcareous algae, rudists, bryozoans, small gastropods, and tests of orbitolinid foraminifers. In addition to the individual ooids and skeletal fragments, the coarse volcaniclastic units contain fragments of calcite-cemented, sorted, ooid- and orbitolinid-bearing limestone. Although many of the ooids are severely micritized, some can be seen to have cores of volcanic rock fragments suggesting that a subaerial volcanic edifice was being eroded when the ooids were forming (see later section on the Geological History of the East Mariana Basin). Other common components include altered volcanic glass, zeolites, celadonite, clay minerals, and volcanic lithic and crystal fragments. Additional details on the composition of volcanogenic materials are described in following sections.

Many of the graded sequences in Unit VI show well developed and relatively complete Bouma turbidite sequences (Figs. 20–24). Many of the graded sequences, particularly in the lower half of the unit, have coarse sandstone bases. The bases of many of the coarser beds at the bottom of graded sequences are scoured into the underlying bed or have load casts (Fig. 26).

We conclude that the graded sequences of Unit VI, at least as deep as Hole 585A, Core 16, are turbidites. Below Core 585A-16, the unsorted nature of the clasts, the extreme size range of clasts (ranging up to boulder-size clasts that have been truncated by the core), and the heterogeneity of clast composition (ranging from volcanic fragments, shallow-water carbonate debris, and subrounded fragments of siltstone and claystone) suggest that this material is part of one or more debris flow deposits.

Because so much of the sedimentary section at Site 585 is made up of material that originated as volcanic effusive rocks, the igneous petrography and petrology were studied in some detail (see Tables 5 and 6 and Figs. 27–29).

The volcaniclastic sediments in lithologic Units III, V, and VI were described (Table 5) in terms of the nature of lithic clasts in coarse layers and relative proportions of glass, crystals, and lithic clasts.

The volcaniclastic sediments represent reworked debris derived from previously deposited tuffaceous material mixed with the glassy products of submarine volcanism. The two sources are distinct in terms of the degree of erosion and nature of the clasts. Rounded and angular basalt and trachyte clasts probably were derived from differentiated alkaline volcanics. At the base of Hole 585A a debris flow rich in basalt clasts rests on a reworked hyaloclastite deposit. The largest clasts documented at Site 585 are found in the lowest part of the volcaniclastic sequence (below about 850 m depth). Zeolite veining and zeolite-rimmed vugs are relatively common below 820 m depth. Analcite and phillipsite have been found in the upper layers, and heulandite at greater depth.

Biostratigraphy and Paleoecology

Recent sediments at Site 585, deposited at 6109 m and recovered in the uppermost 150 cm of Core 585-1, consist of brown clay rich in manganese nodules and associated commonly with fish remains. Noticeably they do not contain any abyssal benthic foraminifers. Below that depth, the sediments recovered contain considerable carbonate, whose presence is not consistent with the abyssal depth of the East Mariana Basin, where sediments must have been deposited well below the carbonate compensation depth (CCD) since the Early Cretaceous and particularly during the Tertiary.

The majority of sediments recovered from Site 585 are transported and reworked deposits. Indeed, few intervals of autochthonous pelagic clay were recovered throughout the cored sequence. Fossil assemblages recovered reflect the turbiditic nature of the sediments. Younger-aged material typically is masked by the influx of older, often better-preserved fossil material, thus commonly obscuring the biostratigraphic signal. Consequently, the ages reported must be considered maximum ages, and many may in fact be considerably younger. Sorting by shape and size are characteristic attributes of the foraminiferal and radiolarian assemblages. The recovered specimens are small-sized adults and juveniles that range in size from 45 to 149 μm. Deposition below the CCD also has strongly altered the character of the calcareous and siliceous fossils due to dissolution and recrystallization.

Biostratigraphic assignments for the cored sections are shown on Figure 30 (see the Introduction and Explanatory Notes chapter for the biostratigraphic framework used on Leg 89).

A synthesis of the biostratigraphic events in Hole 585 based on the three fossil groups, namely calcareous nannoplankton, foraminifers (both planktonic and benthic), and radiolarians (Fig. 30) shows that some stratigraphic intervals could not be identified. That does not imply that the succession is not continuous. The generally poor recovery, the fact that the autochthonous sediments are devoid of age diagnostic species, and the turbiditic character of the other sediments that contain index species prevent any sort of biostratigraphic refinement. In particular, most of the Paleocene is not evident: the few nannofossil and planktonic foraminiferal zonal assemblages recorded were either reworked into the Eocene sequence or mixed with younger zones within the Paleocene. Moreover, late and middle Maestrichtian assemblages occur only mixed within the Tertiary sequence. The Cretaceous/Tertiary boundary is tentatively placed within Core 585-16-1. Cores 585-26 and -30 seem to span the interval from Santonian through upper Turonian. The Cenomanian/Turonian boundary is placed within Core 585-32 (see the later section on the Cenomanian–Turonian oceanic anoxic event).

The early Cenomanian and late Albian interval may be located between Cores 585-35 and -36, but the poor recovery prevents further resolution. The most complete intervals recorded are from: early middle Eocene to latest Paleocene; Santonian; and early late Albian to late Aptian.

A similar synthesis of biostratigraphic events in Hole 585A is shown in Figure 31. Stratigraphic intervals recovered include the lower Eocene, upper Paleocene, and a portion of the Maestrichtian. The Cretaceous/Tertiary boundary is placed in Core 585A-3. Cores 585A-5 to -9 span the Santonian to lower Turonian. The Cenomanian/Turonian boundary appears to occur in Core 9. Portions of the upper Cenomanian and upper Albian were found in Cores 585A-9 and -10, whereas -11 to -22 are dated as late Aptian.

Benthic foraminifers recovered from sediments of Site 585 consist of three groups: (1) autochthonous abyssal species, (2) transported bathyal species, and (3) transported neritic and shallow-water species (Figs. 32 and 33).

The autochthonous abyssal group consists of agglutinated species that are interpreted to be most characteristic of water depths between 5000 and 6000 m or closely analogous to the present water depth of the East Mariana Basin. This assemblage is found in the reddish brown zeolitic claystones that represent pelagic sedimentation between turbiditic episodes. Characteristically, the agglutinated fauna is associated solely with fish debris and recrystallized radiolarians, but occasionally rare specimens are found in turbiditic sequences. In Hole 585, the abyssal assemblage is found in Cores 585-15 to -54, which indicates that the entire sequence from the upper Aptian to the Recent was deposited at abyssal water depths (Fig. 32). Below Core 585-54 the assemblage was not recovered because of the heavy influx of volcaniclastic debris in the Aptian to Albian sequence. Above Core 585-15, samples consisted of the planktonic foraminifer- and nannofossil-rich sediments of the Cenozoic sequence. In Hole 585A, the abyssal assemblage is restricted to samples from Core 585A-3. Previously, elements of this assemblage were recovered from the Pacific Ocean on Legs 20 and 61, from the Indian Ocean on Leg 27, and from the North Atlantic Ocean on Legs 41 and 47B.

The bathyal foraminiferal assemblage consists of small, size-sorted specimens that are characteristic of water depths above 2500 m. The assemblage is found predominantly in the laminated intervals and coarse basal units of graded sequences that represent distal, gravity flow deposits. In intervals devoid of shallow-water material, the assemblage is associated with size-sorted radiolarians, planktonic foraminifers, and sponge spicules. In Hole 585, the bathyal assemblage is found in Cores 585-1 to -54. Of special interest are the occurrences of transported bathyal species in Sections 585-32-2 and 585-32-4 that flank the organic-carbon-rich layer in Section 585-32-3. In the latter case, however, foraminifers are lacking and the residue larger than 42 μm consists solely of recrystallized radiolarians. In Hole 585A, the bathyal assemblage was found in Cores 585A-3, -9, -11, and -16.

The third group consists of species characteristic of neritic or shallow-water environments. Included are neritic species of genera such as *Patellina*, *Textularia*, and species of miliolids, polymorphinids, and nodosariids. These smaller forms are listed in Figures 32 and 33 under transported neritic foraminifers. Also included in this group are specimens of larger, shallow-water foraminifers such as *Orbitolina*, complex agglutinated forms such as *Cunelina*, and attached agglutinated species among others shown as larger foraminifers in Figures 32 and 33. The neritic or shallow-water forms occur typically in the coarser basal layers of turbiditic sequences that also contain debris of shallow-water origin such as echinoid fragments and spines, ostracodes, bivalve fragments, sponge spicules, fecal pellets, and very rare algal fragments in addition to ooids. In Hole 585, the neritic assemblage is found in Cores 585-36 to -51, whereas the larger forms are restricted to Cores 585-36, -49, and -51. Neritic species and shallow-water fossil debris are particularly noticeable in the middle Albian sequence of clastic carbonates and volcaniclastic turbidites (Fig. 32). Noticeably lacking however, are *Inoceramus* prisms, thick-shelled bivalve and rudist fragments, and shallow-water algal debris typical of reefal environments and recovered from both Cenozoic and Mesozoic sediments of Leg 61 in the Nauru Basin. Cores 585A-11 to -20 do contain rudist fragments in association with neritic and shallow-water foraminifers, algal fragments, bryozoans, bivalve fragments, echinoid debris, and ooids.

In summary, the late Aptian Cores 585A-18 to -20 contain the greatest abundance of shallow-water material in association with volcaniclastic debris flows. This material decreases in abundance, diversity, and coarseness through the upper Aptian–lower Albian section of Hole 585 from total depth up to Core 585-48. In middle and upper Albian Cores 585-36 to -44, the transported material is predominantly neritic in nature, small-sized (including the rare macrofossil fragmented material), and indicative of distal turbidite deposits. Cenomanian to Santonian Cores 585-29 to -34 contain transported foraminifers that are bathyal in nature. Abyssal foraminifers are particularly in evidence in the Maestrichtian to Paleocene Cores 585-15 to -20 characterized by zeolitic claystones and chert.

Sedimentation Rates

Four pulses of sedimentation separated by apparent unconformities or reductions in sedimentation are recorded in the sedimentary section at Site 585. These four are from late Aptian to late Albian, from middle Cenomanian to Turonian, from Santonian to early Paleocene, and from latest Paleocene to middle Eocene. Sedimentation rates for the Cenomanian to Eocene pulses range from about 5 to 10 m/m.y. and apparently reflect the lessening of volcanogenic sediment transported into the basin or the waning of major edifice building volcanism. Unconformities or much reduced rates of sedimentation are apparent during the late Albian or early Cenomanian, the Coniacian to Santonian, and the middle and late Paleocene. The rapidly deposited section represented by the 303 m of volcaniclastic turbidites and debris flows of Unit VI accumulated at a rate of approximately 40 m/m.y. during late Aptian to late Albian. This is a minimum rate, because the base of the late Aptian was not reached.

Paleomagnetics

Preliminary NRM measurements aboard the *Glomar Challenger* were performed on several lithologic units in the lower Tertiary and Cretaceous of Site 585. The Paleocene–Maestrichtian chalks and zeolitic claystones have mixed polarity with a strong normal overprint. Turonian claystones in both holes yield an average paleolatitude of 5.1°S; middle and lower Albian volcaniclastic turbidites yield a paleolatitude of 8.2°S; the lowest upper Aptian volcaniclastic turbidites yield a paleolatitude of 22.0°S. Compilation of Cretaceous paleomagnetic data from DSDP Sites 289, 462, and 585 indicates that the western Central Pacific had a 4.5-cm/yr. northward component of motion (relative to the magnetic dipole or spin axis) between the Aptian and Campanian (Ogg, this volume).

Physical Properties

Measurements made on cores from Holes 585 and 585A include wet bulk density, water content, porosity, and compressional sonic velocity. A somewhat systematic variation in velocity and density with depth allowed the division of the drilled section into acoustic units (see Acoustic velocity column, Fig. 48), which made it possible to correlate the seismic profiles and the lithology of the section (Fig. 47). Of note are the results of closely spaced velocity and density measurements made throughout a single, thick volcaniclastic turbidite unit that spanned Cores 585A-17 through -20; velocities at the top of the unit are approximately 3.0 km/s, whereas those at the base of the unit approach 4.0 km/s. At 800 m sub-bottom depth in Hole 585A a marked increase in velocity and density results in a calculated reflection coefficient of 0.142 at 8.96 s two-way traveltime. We therefore interpret the "9-s" reflector of the site survey to be a high-velocity layer in the Aptian volcaniclastic section rather than a reflection produced by the predicted Mesozoic pelagic sediment section.

The Cenomanian–Turonian Oceanic Anoxic Event

A combination of paleontologic, lithologic, and organic geochemical data indicates that the Cenomanian–Turonian oceanic anoxic event (Schlanger and Jenkyns, 1976) left its record in the sediments cored at Site 585.

In Section 585-32-3, a 2 cm-thick band of black, pyritic silty claystone lies within a turbidite sequence. The sediments directly below the black band are bioturbated claystone; directly above the black band, in very sharp contact (assuming no missing section), are 1 cm of plane-laminated silt overlain by a 2-cm-thick bed of cross-laminated siltstone. Organic carbon percentages from samples studied in Hole 585 are all well below 1.0% except for two replicate analyses of the black band at 72 to 73 cm in Section 585-32-3, which yielded C_{org} values of 5.6 and 5.1%. Rock-Eval data from this interval showed the following: S_1 = 0.042 mg hydrocarbon/g, S_2 = 51.5 mg hydrocarbon/g, S_3 = 1.78 mg CO_2/g, I_H = 954 mg hydrocarbon/g C_{org}, and I_O = 33 mg CO_2/g C_{org}.

The I_H (hydrogen index) and I_O (oxygen index) values plotted on a van Krevelen-type diagram show that this sample falls exactly on the initial part of the Type-I kerogen evolution path; the rock is a typical sapropelic oil shale. The organic carbon in the black band is of marine algal origin. Shore-based measurements of this sample, carried out at KFA Jülich, revealed an organic carbon content of 9.9% and a hydrogen index of 383 mg hydrocarbon/g C_{org}. Based on these data the sample should be classified as a Type-II kerogen, which was also supported by microscopic studies. According to R. Mukhopadhyay (personal communication, 1982), the kerogen consists of mostly degraded dinoflagellates and unicellular algae. The minerals were classified as sapropelinite II and bituminite II, which would make an excellent petroleum source bed. Paleontological data show that in Sections 585-32-2 and 585-32-4, which lie directly above and below Section 585-32-3, transported bathyal species are found. In 585-32-3, however, foraminifers are lacking and the more than 42 μm fraction consists of recrystallized radiolarians. Section 585-32-4 contains a planktonic fauna indicative of the late Cenomanian *W. aprica* Subzone of the *R. cushmani* Zone. The Cenomanian/Turonian boundary is placed between Sections 585-32-2 and 585-32-3. In Sample 585A-8,CC a thin layer (1 cm thick) of a black sediment composed of recrystallized radiolarians coated and encased in a matrix of dark material lies at the base of a light gray section of radiolarian-rich sediment marked by flecks of black, presumably organic, matter. The black lamina in Sample 585A-8,CC contains 1.45% C_{org}. Rock-Eval data for this sample showed the following: S_1 = 0.018 mg hydrocarbon/g, S_2 = 11.7 mg hydrocarbon/g, S_3 = 0.83 mg

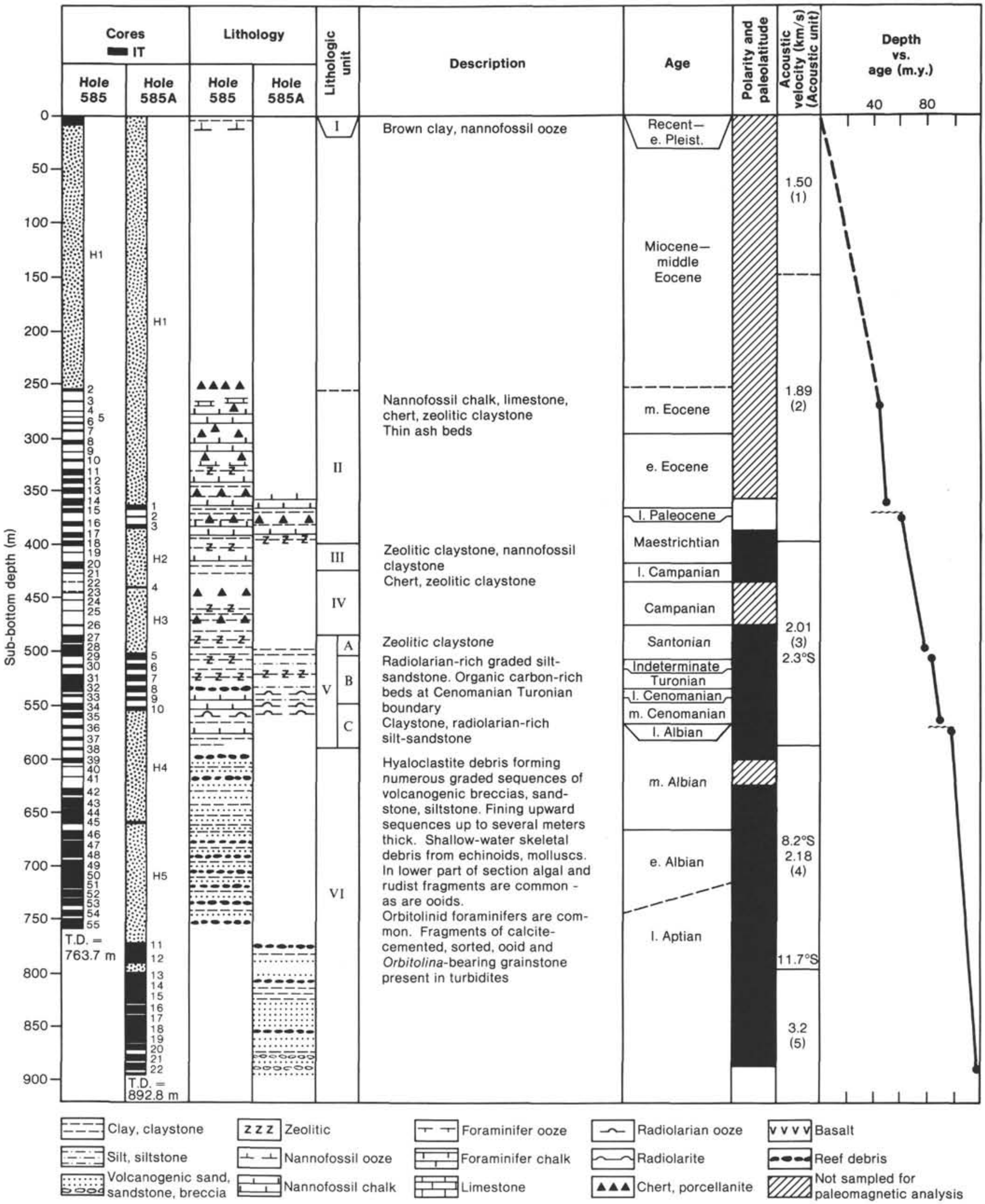

Figure 48. Summary log of Site 585. (Stippled areas in Core Recovery column indicate washed intervals; hachured patterns in Polarity column indicate intervals without paleomagnetic information.

CO_2/g, I_H = 807 mg hydrocarbon/g C_{org}, and I_O = 57 mg CO_2/g C_{org}. The C_{org} in Core 585A-8,CC is also an immature, marine algal-derived Type-I kerogen. The corresponding shore-based data for this sample, however, were 2.6% organic carbon and I_H = 423 mg hydrocarbon/g C_{org}, classifying it also as a Type-II kerogen. This layer, being composed largely of radiolarians, may represent a reworked deposit that was originally similar to the black band in Section 585-32-3 or it may represent a second manifestation of preservation of algal kerogen. In Hole 585A the Cenomanian/Turonian boundary is placed at the level of Sample 585A-9-1, 50 cm (i.e., 50 cm below the C_{org}-rich radiolarian lamina).

The occurrence of these algal kerogen-rich layers at or very close to the Cenomanian/Turonian boundary indicates that they are a product of the preservation of organic carbon during the short-lived but global Cenomanian–Turonian oceanic anoxic event now known to have left its record in sections from the Atlantic basin, the Tethys, the U.S. Western Interior Basin, the northern European shelf, and west African marginal basins as well as the Pacific basin (Schlanger and Jenkyns, 1976; Arthur and Schlanger, 1979; Jenkyns, 1980; Schlanger and Cita, 1982; de Graciansky et al., 1982; Schlanger et al., in press).

Geologic History of the East Mariana Basin

The Mariana Basin is a relatively featureless deep basin bordered on the north by the Magellan Seamounts, on the west by a group of large seamounts along the outer edge of the Mariana Trench, and on the east by a group of seamounts that include Ita Maitai Guyot. Dredge hauls taken from several of these bounding seamounts indicate that they are Cretaceous and have undergone subsidence of approximately 1500 m since the Late Cretaceous. To the south the Mariana Basin is bordered by the Caroline Ridge as well as the Caroline Islands, a chain of volcanic islands that show an age progression from the youngest, Kusaie, which formed 3.5 Ma, through Ponape, which is apparently 12 m.y. old, and Truk, which formed in the early to middle Miocene.

The Mariana Basin (Fig. 2) is enclosed by the 3000-fm contour line (5490 m), with several areas within the Basin lying deeper than the 3200 fm line (5870 m). The flat floor of the East Mariana Basin lies at a depth of 6100 m. This depth corresponds, on the Parsons-Sclater subsidence curve, to a plate age of approximately 150 m.y. The mapped magnetic lineations in the western Pacific (Fig. 1), if projected into the Mariana Basin, predict an age for the Pacific Plate there consistent with the age predicted by the Parsons-Sclater curve. Paleomagnetic data based on cores recovered at several DSDP sites in the area, including Sites 289, 462, and 585, support the idea that the lithosphere underlying the Mariana Basin has been moving to the north since the Aptian at a rate of 4.5 cm/yr.

The following discussions of the geological history of the East Mariana Basin initially assume that the geophysical data can be interpreted as demonstrating that the Basin does indeed have as its basement a segment of lithospheric plate 150 m.y. old. In the interests of objectivity we must point out that not all geologists would accept this assumption; Hilde, Uyeda, and Kroenke (1976) present a scheme in which Cretaceous "intraplate spreading" in the western Pacific produced Late Cretaceous lithosphere in the area of the Mariana Basin. Because well defined magnetic anomaly patterns are not seen in the critical area and because Jurassic sediments have not been drilled in the Mariana Basin, arguments similar to those of Hilde et al. cannot be lightly dismissed. Time limitations aboard *Glomar Challenger*, however, did not allow exhaustive analyses of regional Pacific Mesozoic geology. If our initial assumption is correct, the East Mariana Basin was somewhat south of 11.7°S latitude and was at a depth of 5800 to 5900 m by the late Aptian. By then many of the surrounding edifices had built to sea level and perhaps formed subaerial mountains. Great volumes of hyaloclastic basalt and other fragments were transported by turbidity currents and debris flows for tens of kilometers and deposited on the Basin floor. The volcanic rocks are of normal edifice-basalt types. The carbonate skeletal fragments must have formed on banks or reefs in the photic zone atop the volcanic edifices. Shallow depths would also have provided the water agitation and supersaturation with respect to calcium carbonate necessary to form ooids. As pointed out previously, DSDP Site 202 on Ita Maitai Guyot penetrated lagoonal sediments and hard oolitic limestone of the pre-Eocene. The abundant ooids found on Ita Maitai and in the volcanogenic turbidites at Site 585 pose an intriguing question relating to carbonate petrology. True ooids are unknown in modern atoll environments and were not seen in any of the atolls drilled in the Pacific basin. Nor have any been observed in uplifted reef and associated limestones in the Mariana arc or other arcs bounding the western edge of the Pacific basin. The only Pacific occurrence of oolitic limestone younger than Cretaceous known to us is within the now emergent lagoon of Malden Island (S. O. Schlanger, unpublished U.S. Geological Survey data). These appear to have formed in a hypersaline lagoon environment. The lack of recognizable coral debris and the paucity of algal fragments in Holes 585 and 585A suggest that the ooids formed in an environment less than optimum for vigorous reef growth. Ooids were also found in Cretaceous strata in the Mid-Pacific Mountains (Thiede, Vallier, et al., 1981). The development of these ooid-producing carbonate banks needs to be investigated further. The presence of abyssal benthic foraminifers in strata of late Aptian through Paleocene age shows that the floor of the Mariana Basin was deep throughout this time span and indeed to the present day. The Aptian volcanism that formed the seamounts around the East Mariana Basin correlates with recorded Aptian volcanism in the Mid-Pacific Mountains (Thiede, Vallier, et al., 1981) and the Nauru Basin (Larson, Schlanger, et al., 1981). The undisputed occurrence of Cretaceous midplate volcanism between about 115 and 70 Ma on lithospheric plate segments ranging in age from approximately 100 to 160 m.y. (Haggerty et al., 1982) makes it difficult to reconcile this massive Cretaceous volcanism with simple hot-spot models such as can account for the Hawaiian-Emperor

Chain (see Larson and Schlanger, 1981; Schlanger and Premoli Silva, 1981). Further, the fact that volcanism persisted in particular locations for long periods of time argues against the hot-spot model. In the Nauru Basin, volcanism took place from about 110 to about 70 Ma; with reference to the Mid-Pacific Mountains, Thiede et al. (1982) state that volcanic events built the edifice and platforms there over a period of 40 to 50 m.y.

The next phase in the history of the East Mariana Basin is marked by the rather abrupt change in lithology in Holes 585 and 585A from coarse-grained volcanogenic turbidites rich in shallow-water debris of late Aptian through middle Albian age to finer-grained zeolitic claystones and siltstones rich in radiolarians from late Albian through Cenomanian and Turonian time. These sediments are turbidites and contain bathyal and neritic foraminifers but lack coarse-grained shallow-water carbonate debris. The seamounts around the East Mariana Basin had by this time probably subsided well below sea level but their tops and upper slopes probably lay within a few hundreds of meters of the sea surface.

During latest Cenomanian or earliest Turonian, the water column in the Basin was characterized by a thick and intense midwater O_2 minimum zone or the bottom waters of the Basin were essentially anoxic. These conditions allowed the accumulation of significant amounts of marine algal organic carbon in thin laminae in turbidite sequences. The precise correlation of these organic-rich layers with others described from the Tethys, European shelf sequences, and the Atlantic Basin, as well as the U.S. Western Interior Basin, attest to the globality of the Cenomanian-Turonian oceanic anoxic event, during which time the O_2 minimum layers expanded in many, widespread basins (Schlanger et al., in press).

By Latest Cretaceous and throughout the Tertiary, the East Mariana Basin was receiving turbiditic sediments from the tops and slopes of subsiding seamounts.

A thin ash bed in strata of early Eocene age (about 52 Ma) may be interpreted to be the result of renewed volcanism in the area; the volcanic basement at Enewetak, for example, formed 50 to 59 Ma (Kulp, 1963).

REFERENCES

Arthur, M. A., and Schlanger, S. O., 1979. Cretaceous "Oceanic Anoxic Events" as casual factors in development of reef-reservoired giant oil fields. *Am. Assoc. Pet. Geol. Bull.*, 63:870–885.

Bachman, R. J., 1983. Elastic anisotropy in marine sedimentary rocks. *J. Geophys. Res.*, 88:539–545.

Blatt, H., Middleton, G., and Murray, R., 1972. *Origin of Sedimentary Rocks:* Englewood Cliffs, N.J. (Prentice Hall).

Bouma, A. H., 1962. *Sedimentology of Some Flysch Deposits:* Amsterdam (Elsevier).

Boyce, R. E., 1976. I. Definitions and laboratory techniques of compressional sound velocity parameters and wet-water content, wet-bulk density, and porosity parameters by gravimetric and gamma ray attenuation techniques. *In* Schlanger, S. O., Jackson, E. D., et al., *Init. Repts. DSDP*, 33: Washington (U.S. Govt. Printing Office), 931–958.

Carlson, R. L., and Christensen, N. I., 1977. Velocity anisotropy and physical properties of deep-sea sediments from the western South Atlantic. *In* Supko, P. R., Perch-Nielsen, K., et al., *Init. Repts. DSDP*, 39: Washington (U.S. Govt. Printing Office), 555–559.

Chase, T. E., Menard, H. W., and Mammerickx, J., 1970. Bathymetry of the North Pacific. Scripps Inst. Oceanogr. IMR Tech. Rept. Ser., TR-12, Chart 6.

Deep Sea Drilling Project, 1982. *Shipboard Organic Geochemistry Guide/Handbook*, (B. R. T. Simoneit, ed.). Xeroxed, in-house publication.

de Graciansky, P. C., Brosse, E., Deroo, G., Herbin, J.-P., Montadert, L., Müller, C., Sigal, J., and Schaaf, A., 1982. Les formations d'age Crétacé de l'Atlantique Nord et leur matiène organique: paleogéographie et milieus de dépot. *Rev. Inst. Fr. Petrol.*, 37:275–337.

Detrick, R. S., and Crough, S. T., 1978. Island subsidence, hot-spots, and lithospheric thinning. *J. Geophys. Res.*, 83:1236–1244.

Douglass, R. C., 1960. Revision of the Family Orbitolinidae. *Micropaleontology*, 6(3):249–270.

Duennebier, F. K., and Petersen, L. D., 1982. Summary report of IPOD site surveys in the western Pacific conducted by R/V *Kana Keoki*, Crusie KK810626 Leg 4, Guam to Majuro, 20 Sept.–25 Oct. 1981, Hawaii Institute of Geophysics.

Ellis, B. F., and Messina, A. R., 1967. *Catalogue of Index Foraminifera:* New York (The American Museum of Natural History), Spec. Publ. Vol. 2.

Espitalié, J., Laporte, J. L., Madec, M., Marquis, F., Leplat, P., Paulet, J., and Boutefeu, A., 1977. Méthode rapide de caractérisation des roches mères, de leur potential pétrolier et de leur degré d'évolution. *Rev. Inst. Fr. petrol.*, 32:23–42.

Foreman, H. P., 1973. Radiolaria from DSDP Leg 20. *In* Heezen, B. C., MacGregor, I. D., et al., *Init. Repts. DSDP*, 20: Washington (U.S. Govt. Printing Office), 249–305.

________, 1975. Radiolaria from the North Pacific, Deep Sea Drilling Project, Leg 32. *In* Larson, R. L., Moberly, R., et al., *Init. Repts. DSDP*, 32: Washington (U.S. Govt. Printing Office), 579–676.

Fujii, N., 1981. Anisotropy in compressional-wave velocities and wet-bulk densities of calcareous sedimentary rocks. Deep Sea Drilling Project Leg 62. *In* Thiede, J., Vallier, T. L., et al., *Init. Repts. DSDP*, 62: Washington (U.S. Govt. Printing Office), 995–997.

Haggerty, J. A., Schlanger, S. O., and Premoli Silva, I., 1982. Late Cretaceous and Eocene volcanism in the southern Line Islands and implications for hot-spot theory. *Geology*, 10:433–437.

Hardenbol, J., and Berggren, W. A., 1978. A new Paleogene numerical time scale. *Am. Assoc. Petrol. Geol. Studies Geol.*, 6:213–234.

Heezen, B. C., MacGregor, I. D., et al., 1973a. *Init. Repts. DSDP*, 20: Washington (U.S. Govt. Printing Office).

________, 1973b. Mesozoic chalks beneath the Caroline abyssal plain: DSDP Site 199. *In* Heezen, B. C., MacGregor, I. D., et al., *Init. Repts. DSDP*, 20: Washington (U.S. Govt. Printing Office), 65–74.

Hilde, T. W. C., Isezaki, N., and Wageman, J. M., 1976. Mesozoic seafloor spreading in the North Pacific. *In* Sutton, G. H., Manghnani, M. H., and Moberly, R. (Eds.), *Geophysical Monograph 19, The Geophysics of the Pacific Ocean Basin and Its Margins* (Woodard Vol.): Washington (Am. Geophys. Union), pp. 205–226.

Hilde, T. W. C., Uyeda, S., and Kroenke, L., 1976. Tectonic history of the western Pacific. *In* Drake, C. L. (Ed.), *Geodynamics: Progress and Prospects:* Washington (Am. Geophys. Union), pp. 1–15.

Jenkyns, H. C., 1980. Cretaceous anoxic events: from continents to oceans. *J. Geol. Soc. London*, 137:171–188.

Kagami, H., Karig, D. E., Coulbourn, W. T., et al., in press. *Init. Repts. DSDP*, 87: Washington (U.S. Govt. Printing Office).

Keating, B. H., and Helsley, C. E., 1978a. Magnetostratigraphic studies of Cretaceous sediments from DSDP Site 369. *In* Lancelot, Y., Seibold, E., et al., *Init. Repts. DSDP*, 41 (Supplement to Vol. 41): Washington (U.S. Govt. Printing Office), 983–986.

________, 1978b. Paleomagnetic results from DSDP Hole 391C and the magnetostratigraphy of Cretaceous sediments from the Atlantic Ocean floor. *In* Benson, W. E., Sheridan, R. E., et al., *Init. Repts. DSDP*, 44: Washington (U.S. Govt. Printing Office), 523–528.

Kono, M., 1980a. Paleomagnetism of DSDP Leg 55 basalts and implications for the tectonics of the Pacific Plate. *In* Jackson, E. D., Koizumi, I., et al., *Init. Repts. DSDP*, 55: Washington (U.S. Govt. Printing Office), 737–752.

________, 1980b. Statistics of paleomagnetic inclination data. *J. Geophys. Res.*, 85:3878–3882.

Kuenen, P. H., 1964. The shell pavement below oceanic turbidites. *Mar. Geol.*, 2:236–246.

Kulp, J. L., 1963. Potassium-argon dating of volcanic rocks. *Bull. Volcanologique*, 26:247–258.

Ladd, H. S., Ingerson, E., Townsend, R. C., Russel, M., and Stephenson, H. K., 1953. Drilling on Eniwetok Atoll, Marshall Islands. *Am. Assoc. Pet. Geol. Bull.*, 37:2257-2280.

Lanphere, M. A., and Jones, D. L., 1978. Cretaceous time scale from North America. *In* Cohee, G. V., Glaessner, M. F., and Hedberg, H. D. (Eds.), *Contributions to the Geologic Time Scale*. Am. Assoc. Pet. Geol. Studies in Geology, 6:259-268.

Larson, R. L., Schlanger, S. O., 1981. Cretaceous volcanism and Jurassic magnetic anomalies in the Nauru Basin, western Pacific Ocean. *Geology*, 9:480-484.

Larson, R. L., Schlanger, S. O., et al., 1981. *Init. Repts. DSDP*, 61: Washington (U.S. Govt. Printing Office).

Lowrie, W., Alvarez, W., Premoli Silva, I., and Monechi, S., 1980. Lower Cretaceous magnetic stratigraphy in Umbrian pelagic carbonate rocks. *Geophys. J. Roy. Astron. Soc.*, 60:263-281.

Martini, E., 1971. Standard Tertiary and Quaternary calcareous nannoplankton zonation. *Second Plankt. Conf., Rome*, pp. 739-785.

Okada, H., and Bukry, D., 1980. Supplementary modification and introduction of code numbers to the low-latitude coccolith biostratigraphic zonation (Bukry, 1973, 1975). *Mar. Micropaleontol.*, 5: 321-325.

Pechersky, D. M., Khramov, A. N., 1973. Mesozoic paleomagnetic scale of the U.S.S.R. *Nature*, 244:499-501.

Perch-Nielsen, K., 1979. Calcareous nannofossils from the Cretaceous between the North Sea and the Mediterranean. Aspekte der Kreide Europas. *IUGS Series A*, 6:223-272.

Pessagno, E. A., Jr., 1967. Upper Cretaceous planktonic foraminifera from the western Gulf coastal plain. *Paleontogr. Am.*, 37:1-445.

Premoli Silva, I., and Brusa, C., 1981. Shallow-water skeletal debris and larger foraminifers from Deep Sea Drilling Project Site 462, Nauru Basin, western equatorial Pacific. *In* Larson, R. L., Schlanger, S. O., et al., *Init. Repts. DSDP*, 61: Washington (U.S. Govt. Printing Office), 439-473.

Premoli Silva, I., and Sliter, W. V., 1981. Cretaceous planktonic foraminifers from the Nauru Basin, Leg 61, Site 462, western equatorial Pacific. *In* Larson, R. L., Schlanger, S. O., et al., *Init. Repts. DSDP*, 61: Washington (U.S. Govt. Printing Office), 423-437.

Riedel, W. R., 1974. Radiolaria from the southern Indian Ocean, DSDP Leg 26. *In* Davies, T. A., Luyendyk, B. P., et al., *Init. Repts. DSDP*, 26: Washington (U.S. Govt. Printing Office), 771-814.

Romein, A. J. T., 1979. Lineages in early Paleogene calcareous nannoplankton. *Utrecht Micropaleon. Bull.*, 22:1-231.

Schaaf, A., 1981. Late Early Cretaceous Radiolaria from Deep Sea Drilling Project Leg 62. *In* Thiede, J., Vallier, T. L., et al., *Init. Repts. DSDP*, 62: Washington (U.S. Govt. Printing Office), 419-470.

Schlanger, S. O., and Cita, M. B. (Eds.), 1982. *Nature and Origin of Cretaceous Organic Carbon-Rich Facies:* London (Academic Press).

Schlanger, S. O., and Jenkyns, H. C., 1976. Cretaceous oceanic anoxic events—causes and consequences. *Geologie en Mijnbouw*, 55: 179-184.

Schlanger, S. O., Jenkyns, H. C., and Premoli Silva, I., 1981. Volcanism and vertical tectonics in the Pacific basin related to the global Cretaceous transgressions. *Earth Planet. Sci. Lett.*, 52:435-449.

Schlanger, S. O., Arthur, M. A., Jenkyns, H. C., and Scholle, P. A., in press. The Cenomanian-Turonian oceanic anoxic event. I. Stratigraphy and distribution of organic carbon-rich beds and the marine $\delta^{13}C$ excursion. *In* Brooks, J., and Fleet, A. (Eds.), *Marine Petroleum Source Rocks:* Geol. Soc. London.

Schlanger, S. O., and Premoli Silva, I., 1981. Tectonic, volcanic, and paleogeographic implications of redeposited reef faunas of Late Cretaceous and Tertiary age from the Nauru Basin and the Line Islands. *In* Larson, R. L., Schlanger, S. O., et al., *Init. Repts. DSDP*, 61: Washington (U.S. Govt. Printing Office), 817-828.

Shipley, T. H., Whitman, J. M., Duennebier, F. K., and Peterson, L. D., 1983. Seismic stratigraphy and sedimentation history of the East Mariana Basin, western Pacific. *Earth Planet. Sci. Lett.*, 64: 257-275.

Sigal, J., 1977. Essai de zonation du Cretace Mediterranéen a l'aide des foraminiferes planctoniques. *Geol. Mediterranéene*, 4:99-108.

Steiner, M. B., 1981a. Paleomagnetism of the Cretaceous section, Site 462. *In* Larson, R. L., Schlanger, S. O., et al., *Init. Repts. DSDP*, 61: Washington (U.S. Govt. Printing Office), 711-716.

________, 1981b. Paleomagnetism of the igneous complex, Site 462. *In* Larson, R. L., Schlanger, S. O., et al., *Init. Repts. DSDP*, 61: Washington (U.S. Govt. Printing Office), 717-729.

Thiede, J., Dean, W. E., and Claypool, G. E., 1982. Oxygen-deficient depositional paleoenvironments in the mid-Cretaceous tropical and subtropical Pacific Ocean. *In* Schlanger, S. O., and Cita, M. B. (Eds.), *Nature and Origin of Cretaceous Organic Carbon-Rich Facies:* London (Academic Press).

Thiede, J., Vallier, T. L., et al., 1981. *Init. Repts. DSDP*, 62: Washington (U.S. Govt. Printing Office).

Thierstein, H., 1976. Mesozoic calcareous nannoplankton biostratigraphy of marine sediments. *Mar. Micropaleontol.*, 1:325-362.

Vandenberg, J., and Wonders, A. A. H., 1980. Paleomagnetism of late Mesozoic pelagic limestones from the Southern Alps. *J. Geophys. Res.*, 85:3623-3627.

van Hinte, J. E., 1976. A Cretaceous time scale. *Bull. Am. Assoc. Pet. Geol.*, 60:498-516.

Verbeek, J. W., 1977. Calcareous nannoplankton biostratigraphy of middle and Upper Cretaceous deposits in Tunisia, southern Spain, and France. *Utrecht Micropaleont. Bull.*, 16:1-157.

Vogt, P. R., and Einwich, A. M., 1979. Magnetic anomalies and seafloor spreading in the western North Atlantic, and a revised calibration of the Keathly (*M*) geomagnetic reversal chronology. *In* Tucholke, B. E., Vogt, P. R., et al., *Init. Repts. DSDP*, 43: Washington (U.S. Govt. Printing Office), 857-876.

Watts, A. B., Bodine, J. H., and Riber, N. M., 1980. Observations of flexure and the geologic evolution of the Pacific Ocean basin. *Nature*, 283:532-537.

Whitman, J. M., 1981. Tectonic and bathymetric evolution of the Pacific Ocean basin since 74 Ma (Master's thesis). University of Miami, Florida.

Winterer, E. L., 1976. Bathymetry and regional tectonic setting of the Line Island Chain. *In* Schlanger, S. O., Jackson, E. D., et al., *Init. Repts. DSDP*, 33: Washington (U.S. Govt. Printing Office), 731-748.

APPENDIX
Smear Slide Summary for Holes 585 and 585A

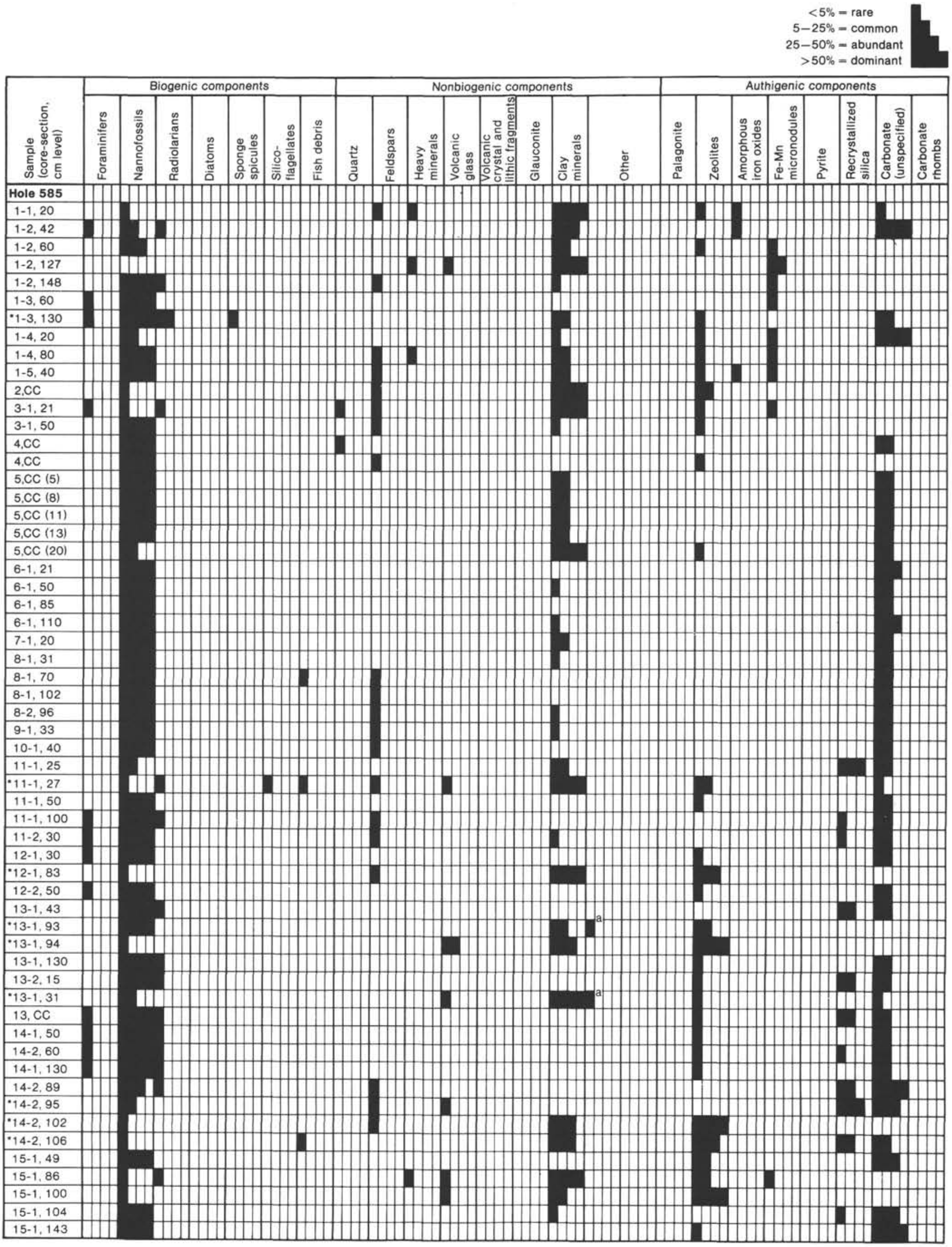

Appendix (continued).

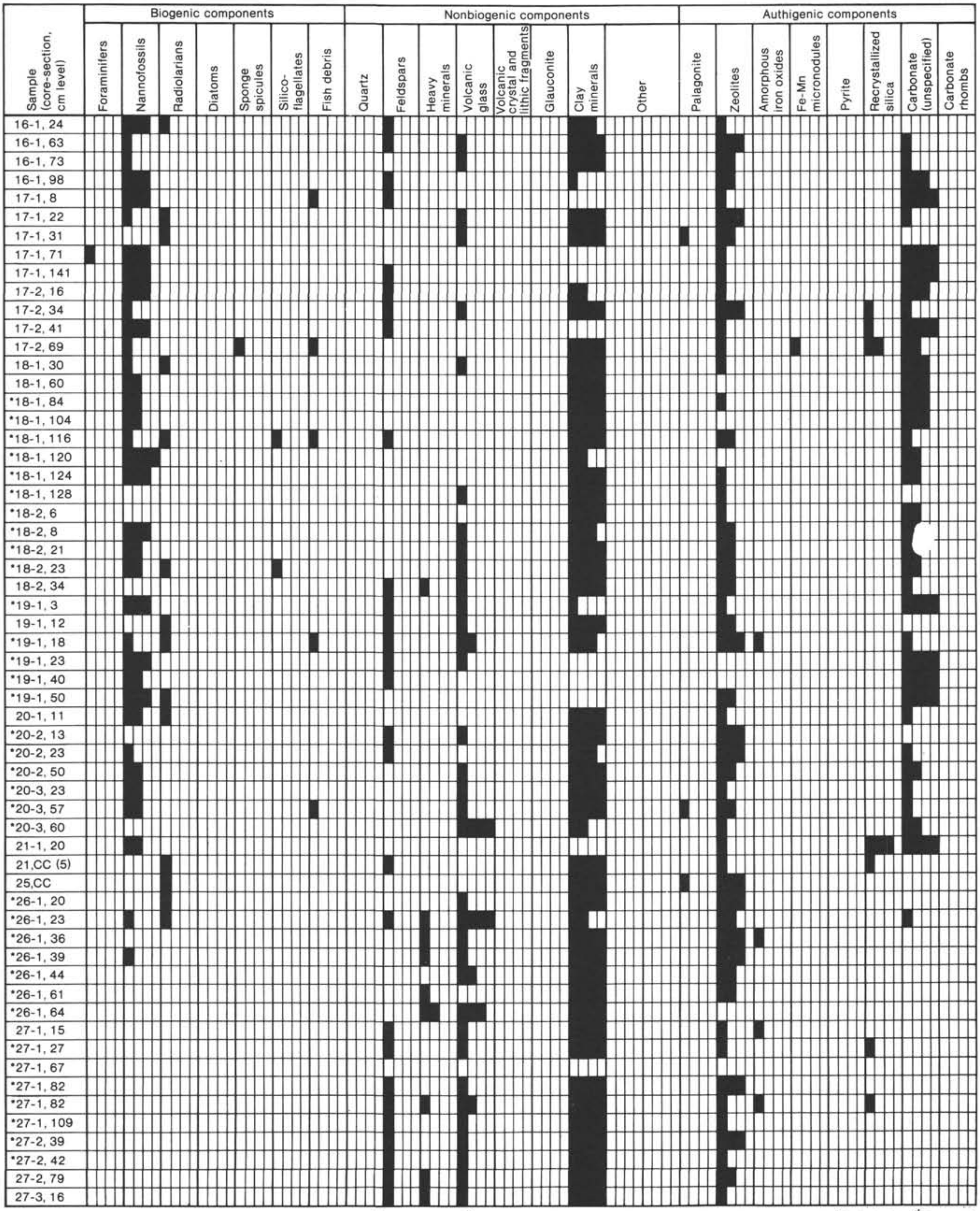

* = minor lithology

[a]Plant debris? [b]Lath-shaped (20–100 μm) polycrystalline carbonate mineral [c]Celadonite [d]Gypsum?

Appendix (continued).

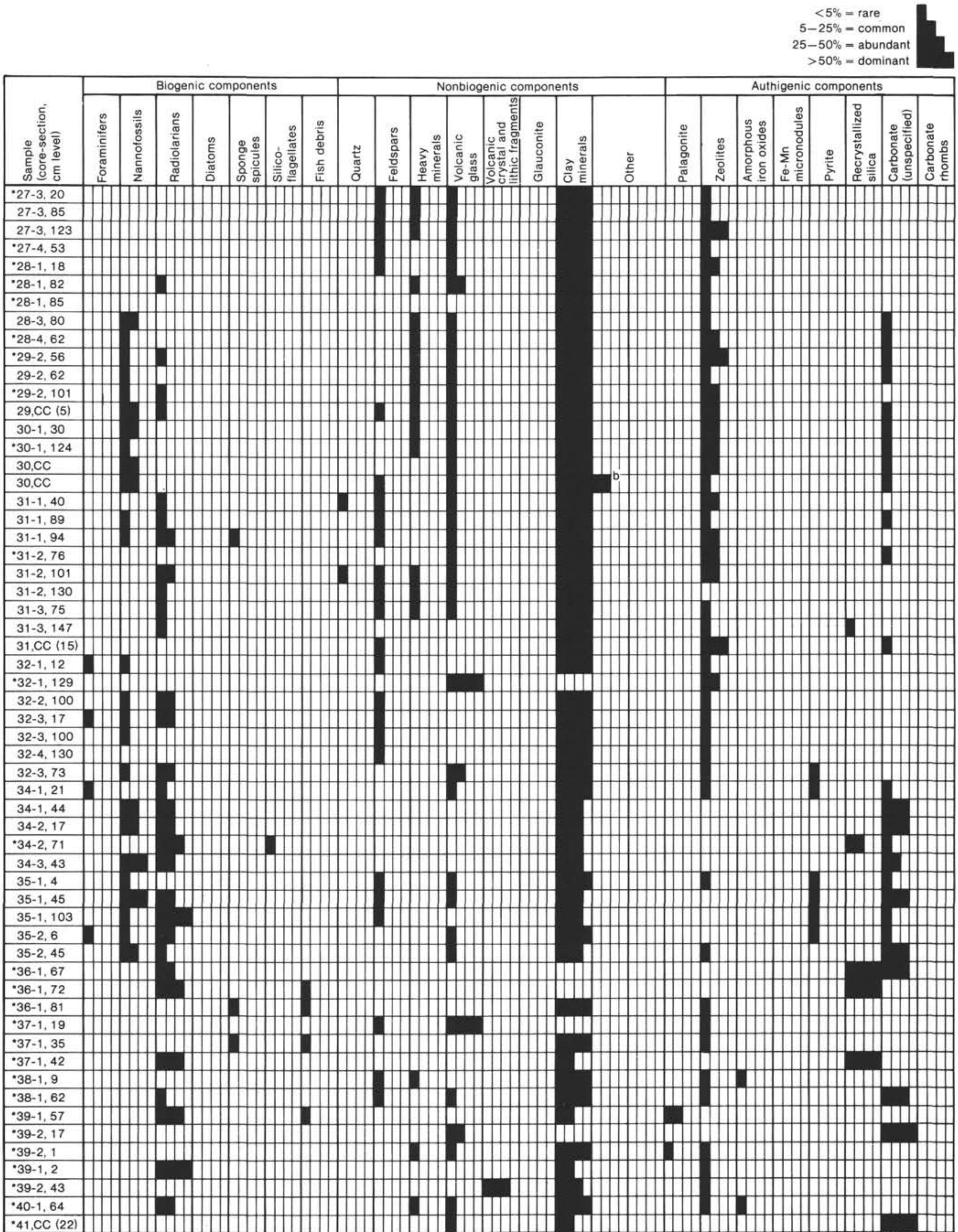

Appendix (continued).

* = minor lithology

[a]Plant debris? [b]Lath-shaped (20–100 μm) polycrystalline carbonate mineral [c]Celadonite [d]Gypsum?

Appendix (continued).

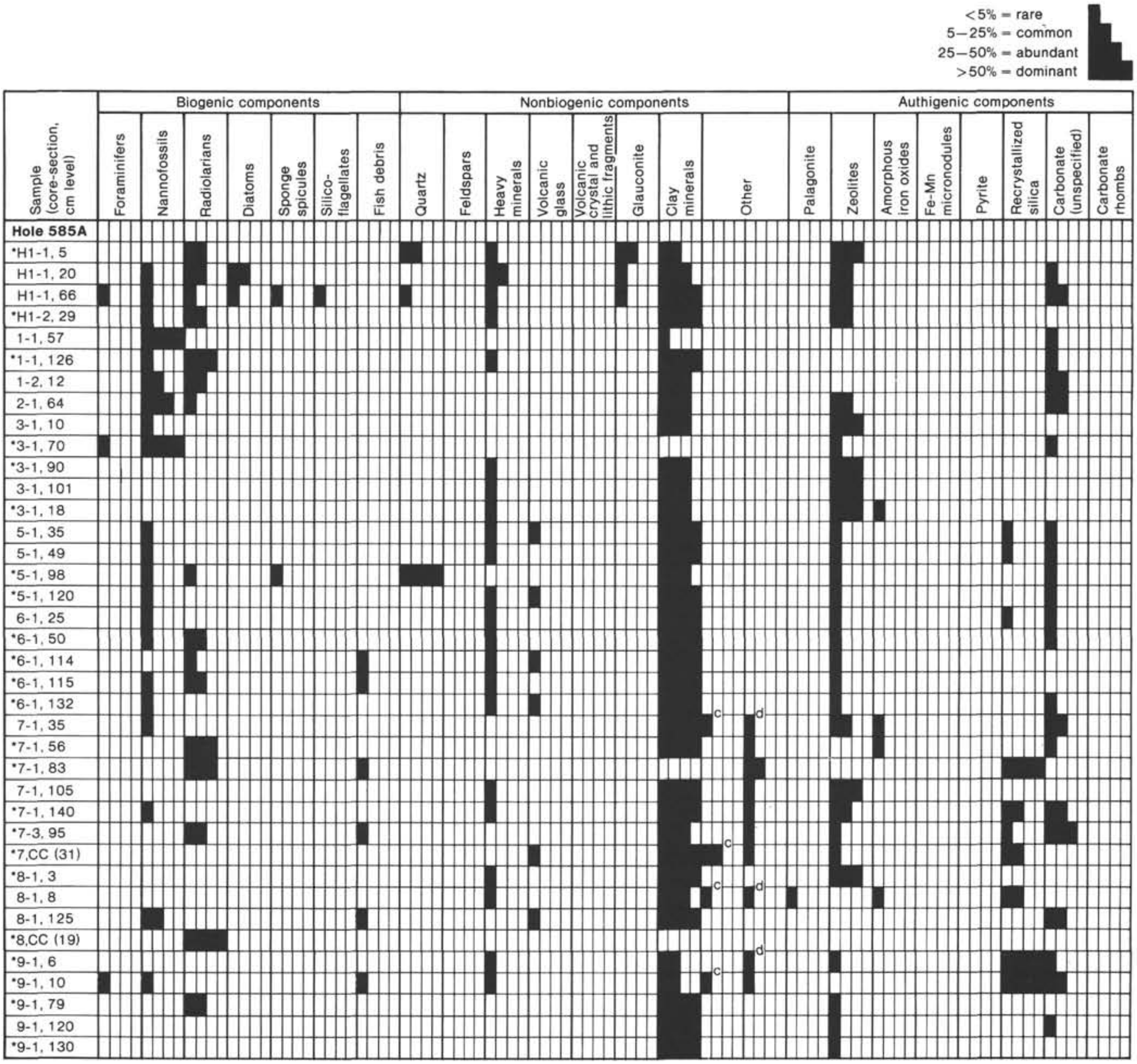

Appendix (continued).

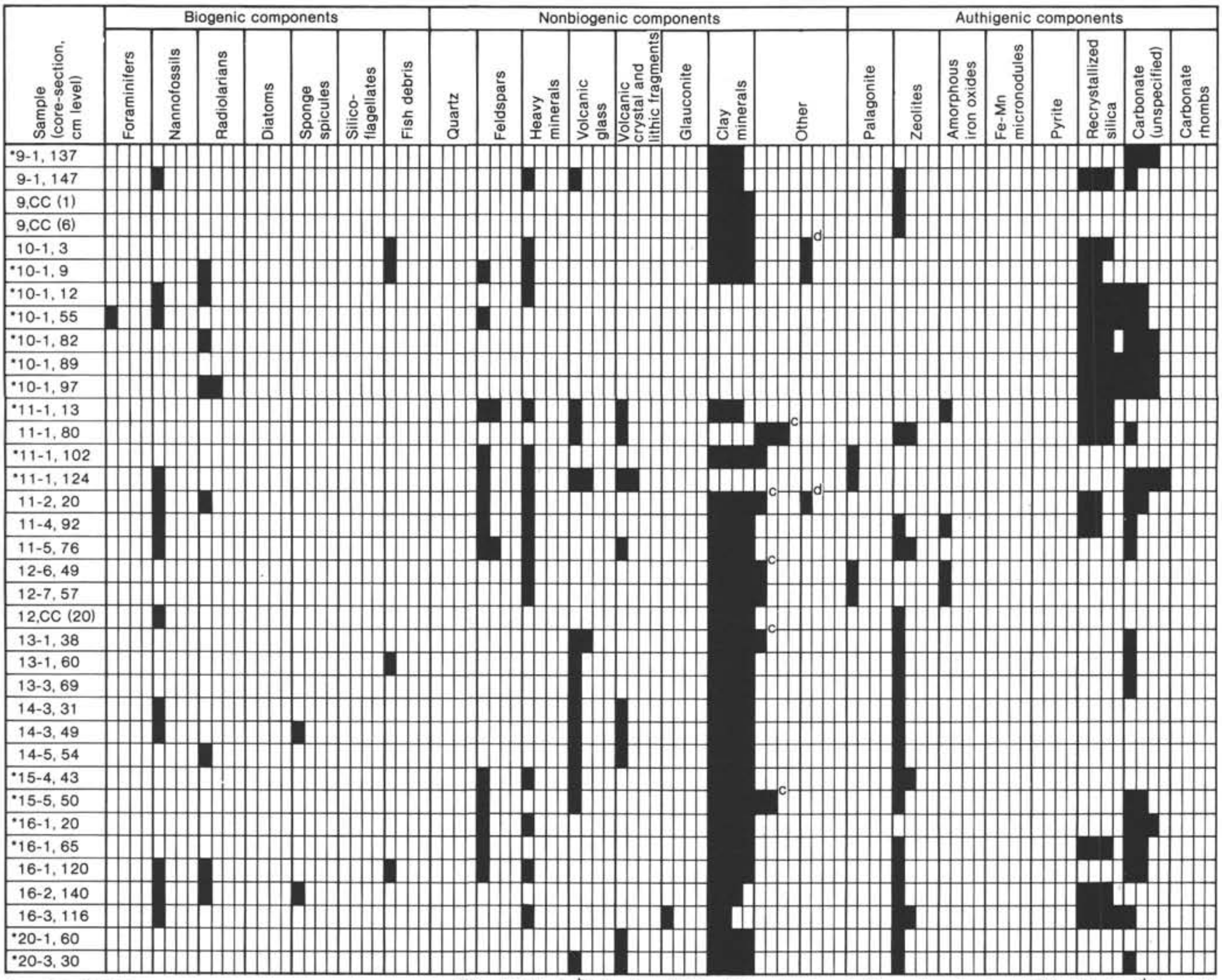

* = minor lithology

[a]Plant debris? [b]Lath-shaped (20–100 μm) polycrystalline carbonate mineral [c]Celadonite [d]Gypsum?

SITE 585 HOLE CORE 1 CORED INTERVAL 0.0–6.8 m sub-bottom; 6122.3–6129.1 m below rig floor

TIME – ROCK UNIT: Recent; early Pleistocene

BIOSTRATIGRAPHIC ZONE: N21–N22? (F)

FOSSIL CHARACTER (FORAMINIFERS, NANNOFOSSILS, RADIOLARIANS, DIATOMS): B B B; B; B; B; CM AM B; FM; B; B; RM B

SECTION: 1, 2, 3, 4, 5, CC — METERS: 0.5, 1.0

GRAPHIC LITHOLOGY

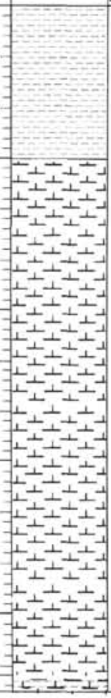

DRILLING DISTURBANCE / SEDIMENTARY STRUCTURES / SAMPLES

LITHOLOGIC DESCRIPTION

5YR 3/4; 10YR 5/4; 10YR 8/3; 10YR 5/3; 10YR 8/2; 10YR 3/2; 10YR 8/2; 10YR 7/2; 10YR 3/2; 10YR 8/3; 2.5Y 6/2; 10YR 4/3

NANNOFOSSIL OOZE AND CLAY-BEARING NANNOFOSSIL OOZE (>150 cm)

Mostly shades of light yellowish brown to brown interbedded; stiff to soft CLAY brown to moderate brown (0–150 cm and several thin beds in nannofossil ooze); soupy; homogeneous.

SMEAR SLIDE SUMMARY (%):

	1, 20	2, 42	2, 60	2, 127	2, 148
	D	D	D	D	D
Texture:					
Sand	2	3	–	–	–
Silt	10	5	2	25	1
Clay	88	92	98	75	99
Composition:					
Feldspar	1	–	–	–	2
Heavy minerals	2	–	–	1	–
Clay	88	43	10	63	–
Volcanic glass	–	–	–	<1	–
Micronodules	–	–	<1	8	–
Zeolite	4	–	1	13	–
Carbonate unspec.	1	50	–	–	–
Foraminifers	–	2	<1	–	–
Calc. nannofossils	3	5	88	5	98
Radiolarians	–	<1	–	–	<1
Hematite	1	–	<1	–	–

SMEAR SLIDE SUMMARY (%):

	3, 80	3, 130	4, 20	4, 80	5, 40
	D	D	D	D	D
Texture:					
Sand	–	–	2	–	–
Silt	5	35	8	1	1
Clay	95	65	90	99	99
Composition:					
Feldspar	–	–	–	1	1
Heavy minerals	–	–	–	1	–
Clay	<1	10	2	10	10
Micronodules	<1	–	2	2	2
Zeolite	–	3	1	–	2
Carbonate unspec.	–	20	85	–	–
Foraminifers	2	2	–	–	–
Calc. nannofossils	98	55	10	88	84
Radiolarians	–	8	–	–	–
Sponge spicules	–	<1	–	–	–
Hematite	–	–	–	–	1

ORGANIC CARBON AND CARBONATE (%):

	1, 21	2, 61	3, 61
Organic carbon	0.11	0.11	0.07
Carbonate (bomb)	1	52	83

(Wash core)

SITE 585 HOLE CORE H-1 CORED INTERVAL 6.8–255.9 m sub-bottom; 6129.1–6373.2 m below rig floor

TIME – ROCK UNIT: middle Eocene to early Miocene

BIOSTRATIGRAPHIC ZONE: *Thyrsocyrtis bromia* to *Buryella clinata* (R); *Helicosphaera ampliaperta* (CN3) (N); P11? to N7–N8 (F)

FOSSIL CHARACTER: FORAMINIFERS B, RP, AP, RP; NANNOFOSSILS AM; RADIOLARIANS AM

SECTION: 1, CC — METERS: 0.5

GRAPHIC LITHOLOGY

SAMPLES: T, T, T, T

LITHOLOGIC DESCRIPTION

Drilling breccia of fragments of LIMESTONE (grayish orange pink [5YR 7/2]), SILTSTONE and CLAYSTONE (medium dark gray [7.5YR 4/0]), and multicolored fragments of CHERT.

SITE 585 HOLE CORE 2 CORED INTERVAL 255.9–265.5 m sub-bottom; 6378.2–6387.8 m below rig floor

TIME – ROCK UNIT: ?

FOSSIL CHARACTER: FORAMINIFERS B; RADIOLARIANS FP

SECTION: CC

GRAPHIC LITHOLOGY

LITHOLOGIC DESCRIPTION

Drilling breccia consisting mainly of multicolored chips (<1 cm) and larger fragments (several cm) of CHERT. Dominant colors of chert are dark yellow brown (10YR 4/2), gray brown (10YR 5/2), and very pale brown (10YR 7/3).

One fragment of gray green NANNO-BEARING, ZEOLITIC MUDSTONE.

Several of the large chert fragments have partial rims of very pale orange (10YR 8/2) PORCELLANITE. Some of smaller fragments also consist of same material.

SMEAR SLIDE SUMMARY (%):

	CC
	M
Texture:	
Sand	–
Silt	20
Clay	80
Composition:	
Feldspar	2
Clay	80
Zeolite	16
Calc. nannofossils	2

Information on core description sheets, for ALL sites, represents field notes taken aboard ship under time pressure. Some of this information has been refined in accord with post-cruise findings, but production schedules prohibit definitive correlation of these sheets with subsequent findings. Thus the reader should be alerted to the occasional ambiguity or discrepancy.

SITE 585 HOLE CORE 3 CORED INTERVAL 265.5–275.1 m sub-bottom; 6387.8–6397.4 m below rig floor

Time-rock unit: middle Eocene. Biostratigraphic zone: CP12A? (N), P11? (F). Fossil character: Foraminifers RP, RP, CP, RP; Nannofossils CP; Radiolarians RP, B. Section 1, CC. Void.

LITHOLOGIC DESCRIPTION

Drilling breccia consisting mainly of multicolored chips (< 0.5 cm) and larger fragments (several cm) of CHERT. Dominant colors of chert are reddish brown (5YR 5/3–4/4), light reddish brown (5YR 5/6), and grayish orange (10YR 7/4). Most of the large chert fragments have partial rims of white porcellanite, which also comprises about 25% of smaller chips.

About 15% of smaller chips and several larger fragments are of ZEOLITE-BEARING CLAYSTONE (dusky blue green (5BG 3/2)).

One large fragment (~ 5 cm) and about 10% of smaller chips consist of NANNOFOSSIL CHALK.

SMEAR SLIDE SUMMARY (%):

	1, 21 D	1, 50 D
Texture:		
Sand	–	–
Silt	15	2
Clay	85	98
Composition:		
Quartz	1	–
Feldspar	2	1
Clay	85	–
Glauconite?	1	–
Micronodules	2	–
Zeolite	4	<1
Foraminifers	1	–
Calc. nannofossils	4	98
Radiolarians	<1	–

SITE 585 HOLE CORE 4 CORED INTERVAL 275.1–279.1 m sub-bottom; 6397.4–6401.4 m below rig floor

Time-rock unit: middle Eocene. Biostratigraphic zone: P10? (F). Fossil character: Foraminifers B, FP; Nannofossils CP. Section CC.

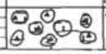

LITHOLOGIC DESCRIPTION

Fragments (several cm) and chips (< 0.5 cm) of CHERT[1]. Several fragments of chert have partial rims of white (N9) PORCELLANITE. Dominant color is light gray[1] (10YR 8/1) with several dark brown (10YR 3/2).

[1] The light gray chert is clearly SILICIFIED LIMESTONE and is "peppered" with sand-size silicified foraminifers "porcellanites" appears to be incompletely silicified limestone.

One fragment of white NANNOFOSSIL CHALK.

SMEAR SLIDE SUMMARY (%):

	CC M	CC M
Texture:		
Sand	–	–
Silt	–	1
Clay	–	99
Composition:		
Quartz	1	–
Feldspar	–	<1
Zeolite	–	<1
Carbonate unspec.	24	–
Calc. nannofossils	75	99

SITE 585 HOLE CORE 5 CORED INTERVAL 279.1–284.6 m sub-bottom; 6401.4–6406.9 m below rig floor

Time-rock unit: middle? Eocene. Fossil character: Nannofossils AM. Section CC.

LITHOLOGIC DESCRIPTION

0–15 cm: 1 piece white (10YR 9/1) nannofossil limestone with 0.5–1 cm cap of dark yellowish brown (10YR 3/4) CHERT; 1 piece of white (N9) NANNOFOSSIL CHALK; 1 piece of very pale yellowish brown (10YR 7/2) CLAY-BEARING NANNOFOSSIL LIMESTONE.

15–35 cm: drilling breccia of chips (< 0.5 cm) of yellow brown (10YR 7/2) to dark yellowish brown (10YR 4/2) CHERT; white (N9) to very pale yellowish brown (10YR 7/2) LIMESTONE; dark yellowish brown (10YR 4/4) CALCAREOUS CLAYSTONE; dark green gray (10G 3/2) CLAYSTONE.

SMEAR SLIDE SUMMARY (%):

	CC, 5 D	CC, 8 D	CC, 11 D	CC, 13 D	CC, 20 D
Texture:					
Sand	–	–	–	–	–
Silt	60	50	65	50	15
Clay	40	50	35	50	85
Composition:					
Clay	5	10	20	10	80
Zeolite	–	–	–	–	1
Carbonate unspec.	20	10	15	25	5
Calc. nannofossils	75	80	65	65	8

SITE 585 HOLE CORE 6 CORED INTERVAL 284.6–293.7 m sub-bottom; 6406.9–6416.0 m below rig floor

Time-rock unit: middle? Eocene. Biostratigraphic zone: P10? (F). Fossil character: Foraminifers RP, AP; Nannofossils CP; Radiolarians B, B. Sections 1, 2.

LITHOLOGIC DESCRIPTION

NANNOFOSSIL CHALK AND LIMESTONE; SILICIFIED LIMESTONE AND CHERT

Dominantly white (10YR 8/1) limestone with varying degree of diagenesis chalk to limestone to silicified limestone. Some faint laminations.

Numerous chips (< 1 cm) of multicolored CHERT (~ 58%), dark yellowish brown (10YR 3/4) and brown (7.5YR 5/6); NANNOFOSSIL LIMESTONE (35%) white; and PORCELLANITE (7%), light gray (10YR 7/2) chips mostly in intervals 135–150 cm, Section 1 and 0–50 cm Section 2; 50–83 cm, Section 2 consists of larger (>2 cm) fragments of brown chert and white limestone and chalk.

SMEAR SLIDE SUMMARY (%):

	1, 50	1, 85	1, 110	1, 21
Texture:				
Clay	100	100	100	100
Composition:				
Clay	3	–	2	–
Carbonate unspec.	20	15	43	35
Calc. nannofossils	77	85	55	65

ORGANIC CARBON AND CARBONATE (%):

	1, 28–32	1, 119–120
Organic carbon	0.01	0.03
Carbonate	63	29

SITE 585 HOLE CORE 7 CORED INTERVAL 293.7–302.9 m sub-bottom; 6416.0–6425.2 m below rig floor

TIME – ROCK UNIT	BIOSTRATIGRAPHIC ZONE	FORAMINIFERS	NANNOFOSSILS	RADIOLARIANS	DIATOMS	SECTION	METERS	GRAPHIC LITHOLOGY	DRILLING DISTURBANCE	SEDIMENTARY STRUCTURES	SAMPLES
middle Eocene	CP12A? (N) P9? (F)	FP	CP	B		1					T *

LITHOLOGIC DESCRIPTION

Five fragments (several cm each) of dark yellowish brown (10YR 3/4) CHERT with partial rims of white (N9) PORCELLANITE.

One fragment (3x5 cm) of white (N9) NANNOFOSSIL CHALK.

SMEAR SLIDE SUMMARY (%):

	1, 20
	D
Texture:	
Clay	100
Composition:	
Clay	5
Carbonate unspec.	5
Calc. nannofossils	90

SITE 585 HOLE CORE 8 CORED INTERVAL 302.9–312.0 m sub-bottom; 6425.2–6434.3 m below rig floor

TIME – ROCK UNIT	BIOSTRATIGRAPHIC ZONE	FORAMINIFERS	NANNOFOSSILS	RADIOLARIANS	DIATOMS	SECTION	METERS	GRAPHIC LITHOLOGY	DRILLING DISTURBANCE	SEDIMENTARY STRUCTURES	SAMPLES
early Eocene	P9? (F)	FP RP		B B		1 2 CC	0.5 1.0	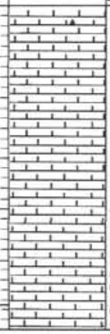			*

LITHOLOGIC DESCRIPTION

NANNOFOSSIL CHALK

White (N9); massive below 65 cm, Section 2. Recovery consist of fragments mostly >2 cm.

SMEAR SLIDE SUMMARY (%):

	1, 31	1, 70	1, 102	2, 96
	D	D	D	D
Texture:				
Clay	100	100	100	100
Composition:				
Feldspar	3	2	2	1
Clay	–	–	–	4
Carbonate unspec.	10	8	13	10
Calc. nannofossils	87	90	85	85
Fish remains	–	<1	–	–

ORGANIC CARBON AND CARBONATE (%):

	1, 16–17	2, 12–14	CC
Organic carbon	0.04	0.01	0.02
Carbonate	64	57	56

SITE 585 HOLE CORE 9 CORED INTERVAL 312.0–321.2 m sub-bottom; 6434.3–6443.5 m below rig floor

TIME – ROCK UNIT	BIOSTRATIGRAPHIC ZONE	FORAMINIFERS	NANNOFOSSILS	RADIOLARIANS	DIATOMS	SECTION	METERS	GRAPHIC LITHOLOGY	DRILLING DISTURBANCE	SEDIMENTARY STRUCTURES	SAMPLES
early Eocene	CP11 (N) P8–P9 (F)	CP	CP CP			1 CC	0.5	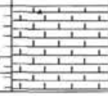			*

LITHOLOGIC DESCRIPTION

NANNOFOSSIL CHALK

White (N8); massive below 45 cm, Section 1, recovery consists of fragments, mostly >2 cm.

SMEAR SLIDE SUMMARY (%):

	1, 33
	D
Texture:	
Clay	100
Composition:	
Feldspar	1
Clay	3
Carbonate unspec.	8
Calc. nannofossils	88

SITE 585 HOLE CORE 10 CORED INTERVAL 321.2–330.3 m sub-bottom; 6443.5–6452.6 m below rig floor

TIME – ROCK UNIT	BIOSTRATIGRAPHIC ZONE	FORAMINIFERS	NANNOFOSSILS	RADIOLARIANS	DIATOMS	SECTION	METERS	GRAPHIC LITHOLOGY	DRILLING DISTURBANCE	SEDIMENTARY STRUCTURES	SAMPLES
early Eocene	P8–P9? (F)	CP				1 CC	0.5	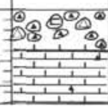			* *

LITHOLOGIC DESCRIPTION

0–40 cm = chips (< 0.5 cm) of: 1) white (N8) to light gray (5Y 7/1) SILICIFIED LIMESTONE (~35%), 2) brown (10YR 5/6 and 10YR 3/4) CHERT (~63%), and 3) green CLAYSTONE (2%). These chips also are packed around larger fragments below 40 cm.

40 cm through Core-Catcher = larger fragments (several cm) of white (N9) NANNOFOSSIL CHALK and 2 fragments of light gray (5Y 7/1) SILICIFIED LIMESTONE.

SMEAR SLIDE SUMMARY (%):

	1, 40
	D
Texture:	
Sand	–
Silt	1
Clay	99
Composition:	
Feldspar	<1
Carbonate unspec.	10
Calc. nannofossils	89

ORGANIC CARBON AND CARBONATE (%):

	1, 39–42	CC, 3–5
Organic carbon	0.02	0.01
Carbonate	77	32

SITE 585 HOLE CORE 11 CORED INTERVAL 330.3–339.5 m sub-bottom; 6452.6–6461.8 m below rig floor

TIME-ROCK UNIT: early Eocene
BIOSTRATIGRAPHIC ZONE: P8? (F)
FOSSIL CHARACTER: Foraminifers RP, RP
SECTION: 1, 2
METERS: 0.5, 1.0

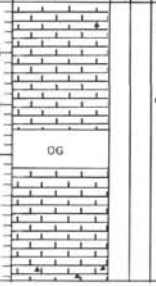

LITHOLOGIC DESCRIPTION

NANNOFOSSIL CHALK
Massive; white (N9)

Several fragments of SILICIFIED LIMESTONE, the core of one (25–28 cm, Section 1) consists of zeolite-bearing clay.

SMEAR SLIDE SUMMARY (%):

	1, 25 D	1, 27 M	1, 50	1, 100	2, 30
Texture:					
Sand	–	–	–	–	–
Silt	–	5	1	3	2
Clay	100	95	99	97	98
Composition:					
Feldspar	–	<1	–	2	1
Clay	10	80	–	2	1
Volcanic glass	–	<1	–	–	–
Zeolite	–	10	<1	–	–
Carbonate unspec.	15	–	10	25	10
Foraminifers	–	–	–	2	1
Calc. nannofossils	25	5	90	65	85
Radiolarians	–	<1	–	2	1
Silicoflagellates	–	<1	–	–	–
Fish remains	–	<1	–	–	–
Silica unspec.	50	–	–	2	1

ORGANIC CARBON AND CARBONATE (%):

	1, 98–100	2, 110–112
Organic carbon	0.02	0.06
Carbonate	78	34

SITE 585 HOLE CORE 12 CORED INTERVAL 339.5–348.6 m sub-bottom; 6461.8–6470.9 m below rig floor

TIME-ROCK UNIT: early Eocene
BIOSTRATIGRAPHIC ZONE: P7? (F)
FOSSIL CHARACTER: Foraminifers RP; Nannofossils RP; Radiolarians RP, B
SECTION: 1, 2
METERS: 0.5, 1.0

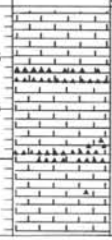

LITHOLOGIC DESCRIPTION

NANNOFOSSIL CHALK
Very light gray (5Y 7.5/1); massive with thin whisps and lenses of ZEOLITIC CLAY.

Forams present throughout mostly concentrated in zone (up to 10% estimated on core surface), but no distinct grading is noticeable.

Light gray (5Y 7/1) SILICIFIED LIMESTONE in several zones; some pieces contain subspherical cores of zeolitic clay, implying that silicification preceded compaction (which resulted in lenses of zeolitic clay in chalk).

SMEAR SLIDE SUMMARY (%):

	1, 30 D	2, 50 D	1, 83 M
Texture:			
Sand	–	–	–
Silt	2	2	2
Clay	98	98	98
Composition:			
Feldspar	–	–	1
Clay	–	–	57
Zeolite	<1	<1	40
Carbonate unspec.	10	10	–
Foraminifers	1	2	–
Calc. nannofossils	89	88	2

ORGANIC CARBON AND CARBONATE (%):

	2, 57–58
Organic carbon	0.18
Carbonate	83

SITE 585 HOLE CORE 13 CORED INTERVAL 348.6–357.8 m sub-bottom; 6470.9–6480.1 m below rig floor

TIME-ROCK UNIT: early Eocene
BIOSTRATIGRAPHIC ZONE: P7? (F)
FOSSIL CHARACTER: Foraminifers RP, B, VRP, B, RP; Nannofossils RP, RP
SECTION: 1, 2, CC
METERS: 0.5, 1.0

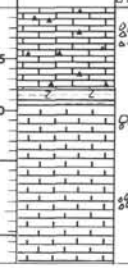

LITHOLOGIC DESCRIPTION

93 cm (5.1) to base of Core-Catcher = NANNOFOSSIL CHALK
Massive with a few thin, small lenses of ZEOLITIC CLAY; white (N9).

ZEOLITIC CLAY bed (82–94 cm); olive gray (5Y 4/2) containing black, organic?-rich clayey nannofossil chalk band with green reduction "halo" for 0.5 cm on either side of black band.

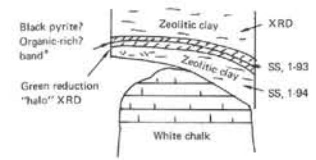

*A few grains of native Cu found in this band

Chalk above zeolitic clay bed has been silicified and is now silicfied limestone (0–82 cm); light gray (5Y 6/1); massive brown chert nodule at 16–21 cm.

SMEAR SLIDE SUMMARY (%):

	1, 43 D	1, 93 M	1, 94 M	1, 130 D	2, 15 D	CC D	1, 31 M
Texture:							
Sand	–	–	–	–	–	–	–
Silt	2	20	70	2	–	–	–
Clay	98	80	30	98	–	–	–
Composition:							
Clay	–	5	28	–	–	–	77
Volcanic glass	–	–	20	–	–	–	1
Zeolite	–	15	50	1	1	<1	2
Carbonate unspec.	10	–	–	10	10	7	5
Foraminifers	–	–	–	–	1	1	–
Calc. nannofossils	80	70	2	88	82	85	10
Radiolarians	<1	–	–	1	1	2	–
Plant debris?	–	10	–	–	–	–	5
Silica unspec.	10	–	–	–	5	5	–

ORGANIC CARBON AND CARBONATE (%):

	1, 94–95	CC, 3–7	1, 53–56
Organic carbon	0.1	0.07	0.09
Carbonate	0	74	52

SITE 585 HOLE CORE 14 CORED INTERVAL 357.8–366.9 m sub-bottom; 6480.1–6489.2 m below rig floor

TIME – ROCK UNIT: early Eocene
BIOSTRATIGRAPHIC ZONE: CP9 (N); P6b (F)
FOSSIL CHARACTER – FORAMINIFERS: FP; VRP; VRP
FOSSIL CHARACTER – NANNOFOSSILS: B; AM
FOSSIL CHARACTER – RADIOLARIANS: B
SECTION: 1; 2
METERS: 0.5; 1.0

GRAPHIC LITHOLOGY

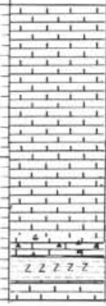

LITHOLOGIC DESCRIPTION

NANNOFOSSIL CHALK

Very light gray (5Y 7.5/1) massive appearing but peppered with coarser grains (= recrystallized radiolarians? and foraminifers?).

Minor lithologies:

1. SILICIFED NANNOFOSSIL LIMESTONE – light gray (5Y 7/1–7/2) (79–102 cm, Section 2); bioturbated at base.
2. ZEOLITIC CLAYSTONE – very dark grayish brown (2.5Y 3/2); moderately bioturbated with reduction halos around some burrows (102–110 cm, Section 2).

SMEAR SLIDE SUMMARY (%):

	1, 50 D	1, 130 D	2, 60 D	2, 89 D	2, 95 M	2, 102 M	2, 106 M
Texture:							
Sand	–	–	–	–	–	–	–
Silt	5	3	5	20	5	55	25
Clay	95	97	95	80	95	45	75
Composition:							
Feldspar	–	–	–	<1	2	1	–
Clay	–	–	–	–	38	44	48
Volcanic glass	–	–	–	–	1	–	–
Zeolite	1	1	<1	–	4	50	40
Carbonate unspec.	5	5	5	60	25	–	5
Foraminifers	2	2	2	–	–	–	–
Calc. nannofossils	90	91	88	25	10	1	2
Radiolarians	2	1	2	–	–	4	–
Fish remains	–	–	–	–	–	–	<1
Recry. silica	–	–	2	10	–	–	–

ORGANIC CARBON AND CARBONATE (%):

	1, 64–67	2, 75–79	2, 92–94	2, 105–108
Organic carbon	0.08	0.12	0.10	0.12
Carbonate	76	77	53	0

SITE 585 HOLE CORE 15 CORED INTERVAL 366.9–380.4 m sub-bottom; 6489.2–6502.7 m below rig floor

TIME – ROCK UNIT: late Paleocene; early Paleocene
BIOSTRATIGRAPHIC ZONE: CP5 (N); CP1b (N) P1b–c (F)
FOSSIL CHARACTER – FORAMINIFERS: FP; RP; RP FP
FOSSIL CHARACTER – NANNOFOSSILS: FP; CP
FOSSIL CHARACTER – RADIOLARIANS: B; B; B
SECTION: 1; 2; CC
METERS: 0.5; 1.0

GRAPHIC LITHOLOGY

LITHOLOGIC DESCRIPTION

NANNOFOSSIL CHALK AND SILICIFED LIMESTONE AND BROWN ZEOLITIC MUDSTONE

0–52 cm: NANNOFOSSIL CHALK AND SILICIFIED LIMESTONE; mostly light gray (10YR 6.5/1), pale brown (10YR 6/3) and zeolite-bearing at base; brown CHERT at several horizons.

52–95 cm: ZEOLITIC CLAYSTONE (dark brown [10YR 4/3]); harder at base than at top.

95–103 cm: ZEOLITIC CLAYSTONE soft; brown (7.5YR 4/4).

103 cm–base Section 2: NANNOFOSSIL CHALK AND SILICIFIED LIMESTONE; pinkish white (7.5YR 7.5/2); some bioturbation at top visible where silicified.

Core-Catcher: drilling breccia, mainly of pinkish white LIMESTONE and brown CHERT, with several larger clasts of pinkish gray (7.5YR 7/2) CHALK.

SMEAR SLIDE SUMMARY (%):

	1, 49 D	1, 86 D	1, 100 D	1, 104 D	1, 143 D
Texture:					
Sand	–	–	–	–	–
Silt	20	10	5	–	10
Clay	80	90	95	100	90
Composition:					
Feldspar	–	–	–	3	–
Heavy minerals	–	<1	–	–	–
Clay	–	84	20	–	–
Volcanic glass	–	<1	<1	–	–
Micronodules	–	<1	–	–	–
Zeolite	8	15	80	–	4
Carbonate unspec.	30	–	–	34	66
Calc. nannofossils	60	<1	<1	55	30
Radiolarians	–	<1	–	–	–
Other	2	–	–	4	–

ORGANIC CARBON AND CARBONATE (%):

	1, 34–36	1, 61–62	1, 86–88	1, 98–100
Organic carbon	0.06	0.09	0.08	0.11
Carbonate	18	0	0	0

	1, 113–114	1, 129–130
Organic carbon	0.04	0.03
Carbonate	41	85

SITE 585 HOLE CORE 16 CORED INTERVAL 380.4–389.5 m sub-bottom; 6502.7–6511.8 m below rig floor

TIME – ROCK UNIT: Maestrichtian early Paleocene

BIOSTRATIGRAPHIC ZONE: CP1a / CP1b; *Micula mura*; P1a to P1b (F)

FOSSIL CHARACTER: FORAMINIFERS | NANNOFOSSILS | RADIOLARIANS | DIATOMS

SECTION | METERS | GRAPHIC LITHOLOGY | DRILLING DISTURBANCE | SEDIMENTARY STRUCTURES | SAMPLES

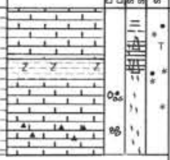

LITHOLOGIC DESCRIPTION

Dominant lithologies:

0–54 cm: NANNOFOSSIL CHALK AND CLAYEY NANNOFOSSIL CHALK (mostly white [N9] to light brown [5YR 6/4]); some faint, indistinct laminations; some coarser layers with foraminifer(?) and radiolarians(?); some indication of bioturbation.

54–78 cm: ZEOLITIC CLAYSTONE; brown (7.5YR 5/4), some bioturbation.

78–90 cm: drilling breccia with mixed lithologies – mostly zeolitic claystone and nannofossil chalk.

90–108 cm: NANNOFOSSIL OOZE; white (10YR 8/2); some bioturbation with burrows filled with brown zeolitic clay.

108–113 cm: dark brown (10YR 4/3) chert.

113–144 cm: NANNOFOSSIL CHALK; mostly light brown to very pale brown (5YR 6/4–10YR 7/4) clayey at base; some bioturbation.

SMEAR SLIDE SUMMARY (%):

	1, 24 D	1, 63 D	1, 73 D	1, 98 D
Texture:				
Clay	100	100	100	100
Composition:				
Feldspar	2	1	–	3
Clay	30	60	69	4
Volcanic glass	–	3	3	–
Zeolite	4	3	20	6
Carbonate unspec.	30	2	2	47
Calc. nannofossils	25	1	5	40
Radiolarians	3	–	–	–
Recrystal. SiO_2	6	–	–	–

ORGANIC CARBON AND CARBONATE (%):

	1, 22–23	1, 69–70
Organic carbon	0.04	0.16
Carbonate	49	0

SITE 585 HOLE CORE 17 CORED INTERVAL 389.5–398.7 m sub-bottom; 6511.8–6521.0 m below rig floor

TIME – ROCK UNIT: Maestrichtian

FOSSIL CHARACTER: FORAMINIFERS | NANNOFOSSILS | RADIOLARIANS | DIATOMS

SECTION | METERS | GRAPHIC LITHOLOGY | DRILLING DISTURBANCE | SEDIMENTARY STRUCTURES | SAMPLES

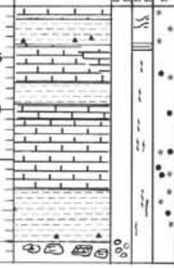

10YR 8/3
10YR 4/3
10YR 6/3
10YR 8/3
5Y 5/2
10YR 8/3
10YR 7/3
5YR 5/2

LITHOLOGIC DESCRIPTION

Dominant lithologies:

Section 1, 0–12 cm: NANNOFOSSIL CHALK.

Section 1, 12–27 cm: dark brown zeolitic claystone; black, whispy laminations throughout.

Section 1, 27–42 cm: pale brown ZEOLITIC CLAYSTONE, very hard.

Section 1, 42–75 cm: NANNOFOSSIL CHALK AND LIMESTONE (silicified?); highly variable degree of induration; very sharp contact with overlying and underlying claystones.

Section 1, 75–96 cm: pale brown CLAYSTONE; soft at top, very hard at base.

Section 1, 96–150 cm and Section 2, 0–30 cm: NANNOFOSSIL CHALK and (silicified?) LIMESTONE; faint hints of bioturbation.

Section 2, 30–80 cm: CLAYSTONE; mostly pale brown with several greenish gray bands; some bioturbation.

Core-Catcher: drilling breccia consisting mainly of green and brown claystone and pink chalk.

SMEAR SLIDE SUMMARY (%):

	1, 8 D	1, 22 D	1, 31 D	1, 71 D	1, 141 D	2, 16 D	2, 34 D	2, 41 D	2, 69 D
Texture:									
Sand	–	–	–	–	–	–	–	–	–
Silt	–	–	–	2	1	–	1	–	8
Clay	–	100	100	98	99	100	99	100	92
Composition:									
Feldspar	1	–	–	–	2	2	2	1	–
Clay	–	66	81	–	4	7	50	–	85
Volcanic glass	–	2	3	–	–	1	3	–	1
Palagonite	–	–	1	–	–	–	–	–	–
Micronodules	–	–	<1	<1	–	–	–	–	<1
Zeolite	2	30	15	3	3	5	35	2	–
Carbonate unspec.	72	1	–	50	54	48	3	60	5
Foraminifers	–	–	–	2	–	–	–	–	–
Calc. nannofossils	25	<1	–	45	35	37	3	35	2
Radiolarians	–	1	1	–	–	–	–	<1	–
Sponge spicules	–	–	–	–	–	–	–	–	<1
Fish remains	<1	–	–	–	–	–	–	–	<1
Recrystal. SiO_2	–	–	–	–	–	–	4	1	–

ORGANIC CARBON AND CARBONATE (%):

	1, 67–73	1, 104–105	1, 140–141	2, 7–9
Organic carbon	0.07	0.10	0.06	0.04
Carbonate	72	36	60	83

	2, 18–23	2, 52–53
Organic carbon	0.07	0.12
Carbonate	51	0

SITE 585 HOLE CORE 18 CORED INTERVAL 398.7–407.8 m sub-bottom; 6521.0–6530.1 m below rig floor

TIME-ROCK UNIT	BIOSTRATIGRAPHIC ZONE	FORAMINIFERS	NANNOFOSSILS	RADIOLARIANS	DIATOMS	SECTION	METERS
Maestrichtian	?	AP	FP			1	0.5
		CP		B			1.0
		RP		B			
		FP	FP	B		2	

GRAPHIC LITHOLOGY · DRILLING DISTURBANCE · SEDIMENTARY STRUCTURES · SAMPLES

LITHOLOGIC DESCRIPTION

Pale green (5G 7/2)

Drill breccia

10G 8/2 beds and mottling in 10YR 7/3 (dominant color)

Interbedded red and green CALCAREOUS CLAYSTONE with minor ZEOLITIC CLAYSTONE and CLAYEY NANNOFOSSIL CHALK.

Thin interbeds of dark brown (10YR 3/3) ZEOLITIC CLAYSTONE and pale green (10G 4/2) CLAYEY CHALK

Brown (5YR 3/4) CHERT nodules

Interbedded brown (10YR 4/2; 10YR 6/2; 10YR 8/1; 10G 6/2) ZEOLITIC CLAYSTONE and pale green CALCAREOUS CLAYSTONE with several brown CHERT nodules

SMEAR SLIDE SUMMARY (%):

	1, 30	1, 60	1, 84	1, 104	1, 116	1, 120	1, 124	1, 128	2, 6	2, 34
	D	D	M	M	M	M	M	M	M	D
Texture:										
Sand	–	–	–	–	–	–	–	–	–	–
Silt	–	–	–	–	10	–	–	–	–	–
Clay	100	100	100	100	90	100	100	100	100	100
Composition:										
Feldspar	–	–	–	–	<1	–	–	–	–	1
Heavy minerals	–	–	–	–	–	–	–	–	–	2
Clay	65	60	55	70	71	25	52	92	87	78
Volcanic glass	<1	–	–	–	–	–	–	3	3	5
Zeolite	<1	–	1	–	15	–	3	5	–	12
Carbonate unspec.	30	35	25	25	2	15	15	–	10	2
Calc. nannofossils	5	5	20	5	3	60	30	–	–	–
Radiolarians	<1	–	–	–	<1	–	–	–	–	–
Silicoflagellates	–	–	–	–	<1	–	–	–	–	–
Fish remains	–	–	–	–	<1	–	–	–	–	–

ORGANIC CARBON AND CARBONATE (%):

	1, 13–15	1, 53–56
Organic carbon	0.06	0.07
Carbonate	27	43

SITE 585 HOLE CORE 19 CORED INTERVAL 407.8–417.0 m sub-bottom; 6530.1–6539.3 m below rig floor

TIME-ROCK UNIT	BIOSTRATIGRAPHIC ZONE	FORAMINIFERS	NANNOFOSSILS	RADIOLARIANS	DIATOMS	SECTION	METERS
Maestrichtian?	?	B	CP	B		1	0.5
		CM		B			

GRAPHIC LITHOLOGY · DRILLING DISTURBANCE · SEDIMENTARY STRUCTURES · SAMPLES

LITHOLOGIC DESCRIPTION

5G 7/2

10YR 4/2; 10G 4/2

10YR 7/1–8/1

5G 7/2

Interbedded brown and green (10YR 4/3 and 5G 7/2) claystones

Interbedded brown, green, and tan ZEOLITIC CLAYSTONE and NANNOFOSSIL CHALK. A few brown CHERT nodules.

SMEAR SLIDE SUMMARY (%):

	1, 3	1, 12	1, 18	1, 23	1, 50
	M	D	M	M	M
Texture:					
Sand	–	–	–	–	–
Silt	–	1	–	–	–
Clay	100	99	100	100	–
Composition:					
Feldspar	1	1	3	1	–
Clay	4	78	42	2	–
Volcanic glass	–	5	9	2	–
Zeolite	3	15	41	–	7
Carbonate unspec.	51	–	–	56	63
Foraminifers	–	–	–	1	–
Calc. nannofossils	40	–	1	40	30
Radiolarians	–	1	<1	–	<1
Fish remains	–	–	<1	–	–

ORGANIC CARBON AND CARBONATE (%):

	1, 38–40	1, 48–49	1, 56–57
Organic carbon	0.15	0.01	0.10
Carbonate	57	76	0

SITE 585 HOLE CORE 20 CORED INTERVAL 417.0–426.1 m sub-bottom; 6539.3–6548.4 m below rig floor

TIME-ROCK UNIT	BIOSTRATIGRAPHIC ZONE	FORAMINIFERS	NANNOFOSSILS	RADIOLARIANS	DIATOMS	SECTION	METERS
Maestrichtian	*Tetralithus trifidus*? (N)	VRP				1	0.5
		AP	CP	RP			1.0
		RP				2	
		B					
		B		RP			
late Campanian	*Quadrum gothicum* (N)	CP		B		3	
			AM				
		FP					
		VRP					
		RP				4	
		CP		B			
		VRP					

GRAPHIC LITHOLOGY (Void; OG) · DRILLING DISTURBANCE · SEDIMENTARY STRUCTURES · SAMPLES

LITHOLOGIC DESCRIPTION

10YR 7/4

10YR 7/4

5YR 3/4

Interbedded dark brown (7.5YR 4/4) ZEOLITIC CLAYSTONE and light brown (7.5YR 6/4) ZEOLITE-BEARING CALCAREOUS CLAYSTONE, and, in extreme, NANNOFOSSIL CLAYSTONE or CLAYEY NANNOFOSSIL CHALK (pinkish white [7.5YR 8/2]).

Many of the units some grading apparent but very subtle. The bases of several $CaCO_3$-rich beds have thin laminae of silty, ashy material (see smear slide 3, 60) which usually are accompanied by thin green reduction "halos" around the laminae.

Interbedded 7.5YR 4/4 and 7.5YR 8/2

7.5YR 6/4

Interbedded brown (7.5YR 4/4) and pinkish white (7.5 8/2)

7.5YR 4/4

7.5YR 6/4

Interbedded brown (7.5YR 4/4) and pinkish white (7.5 8/2)

Mostly pinkish white (7.5YR 8/2)

Mostly 7.5YR 4/4

SMEAR SLIDE SUMMARY (%):

	1, 11	2, 23	2, 50	3, 57	3, 60
	D	M	M	M	M
Texture:					
Sand	–	–	–	–	–
Silt	–	4	1	7	60
Clay	–	96	99	93	40
Composition:					
Feldspar	–	2	–	–	–
Clay	81	44	71	71	20
Volcanic glass	–	4	1	2	60
Palagonite	–	–	–	1	–
Zeolite	3	44	10	7	5
Carbonate unspec.	5	2	8	–	10
Foraminifers	–	–	–	<1	–
Calc. nannofossils	10	4	10	13	5
Radiolarians	1	–	–	–	–
Fish remains	–	–	–	<1	–
Other	–	–	–	3	–

ORGANIC CARBON AND CARBONATE (%):

	1, 8–16	2, 12–18	3, 20–26
Organic carbon	0.02	0.09	0.03
Carbonate	66	0	79

SITE 585 HOLE CORE 21 CORED INTERVAL 426.1–435.8 m sub-bottom; 6548.4–6557.6 m below rig floor

TIME – ROCK UNIT	BIOSTRATIGRAPHIC ZONE	FORAMINIFERS	NANNOFOSSILS	RADIOLARIANS	DIATOMS	SECTION	METERS	GRAPHIC LITHOLOGY	DRILLING DISTURBANCE	SEDIMENTARY STRUCTURES	SAMPLES
late Campanian	*Ceratolithoides aculeus* (N)	B	FP			1					*
						CC	0.5				*

LITHOLOGIC DESCRIPTION

Fragments of dark brown (7.5YR 4/4) CLAYSTONE, light brown (7.5YR 4/4) SILICIFIED(?) CHALK, and pale green (5G 8/2) CHERT.

SMEAR SLIDE SUMMARY (%):

	1, 20	CC
	D	D
Texture:		
Sand	–	–
Silt	2	2
Clay	98	98
Composition:		
Clay	–	92
Zeolite	1	<1
Carbonate unspec.	54	–
Calc. nannofossils	5	–
Radiolarians	–	1
Sponge spicules	–	1
Recrystal. SiO_2	40	5

Core 22: 435.3–444.4 m sub-bottom (6557.6–6566.7 mbrf): No recovery.

SITE 585 HOLE CORE 23 CORED INTERVAL 444.4–453.6 m sub-bottom; 6566.7–6575.9 m below rig floor

TIME – ROCK UNIT	BIOSTRATIGRAPHIC ZONE	FORAMINIFERS	NANNOFOSSILS	RADIOLARIANS	DIATOMS	SECTION	METERS	GRAPHIC LITHOLOGY	DRILLING DISTURBANCE	SEDIMENTARY STRUCTURES	SAMPLES
?		RP	B			CC					T T

LITHOLOGIC DESCRIPTION

Three fragments of CHERT (silicified bioclastic limestone).

SITE 585 HOLE CORE 24 CORED INTERVAL 453.6–462.7 m sub-bottom; 6575.9–6585.0 m below rig floor

TIME – ROCK UNIT	BIOSTRATIGRAPHIC ZONE	FORAMINIFERS	NANNOFOSSILS	RADIOLARIANS	DIATOMS	SECTION	METERS	GRAPHIC LITHOLOGY	DRILLING DISTURBANCE	SEDIMENTARY STRUCTURES	SAMPLES
?		B	B			CC					

LITHOLOGIC DESCRIPTION

Four fragments of CHERT.

Lenticular laminations with mixing of various shades of brown: brown (10YR 4/3); yellowish brown (10YR 3/4), dark brown (10YR 3/3) plus intermediate shades.

Texture suggests that the chert formed by silicification of bioclastic granular limestone with fine lenticular banding.

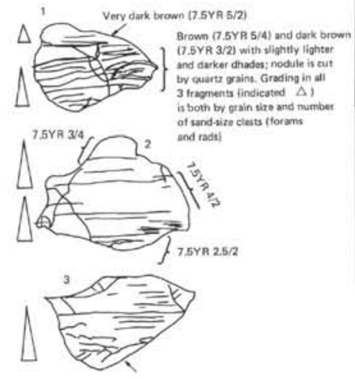

SITE 585 HOLE CORE 25 CORED INTERVAL 462.7–476.3 m sub-bottom m; 6585.0–6598.6 m below rig floor

TIME-ROCK UNIT	BIOSTRATIGRAPHIC ZONE	FORAMINIFERS	NANNOFOSSILS	RADIOLARIANS	DIATOMS	SECTION	METERS	GRAPHIC LITHOLOGY	DRILLING DISTURBANCE	SEDIMENTARY STRUCTURES	SAMPLES
Campanian	*Amphipyndax enessetti* (R)	B B	B	FM		CC		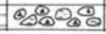			* T

LITHOLOGIC DESCRIPTION

Five fragments of CHERT; brown (7.5YR 4/6 to 7.5YR 5/4); laminated, parallel to wavy; some size-grading evident in several pieces.

Four fragments of ZEOLITIC CLAYSTONE.

SMEAR SLIDE SUMMARY (%):

	CC D
Texture:	
Sand	–
Silt	15
Clay	85
Composition:	
Clay	58
Palagonite	1
Micronodules	1
Zeolite	40
Radiolarians	<1

SITE 585 HOLE CORE 26 CORED INTERVAL 476.3–485.4 m sub-bottom; 6598.6–6607.7 m below rig floor

TIME-ROCK UNIT	BIOSTRATIGRAPHIC ZONE	FORAMINIFERS	NANNOFOSSILS	RADIOLARIANS	DIATOMS	SECTION	METERS	GRAPHIC LITHOLOGY	DRILLING DISTURBANCE	SEDIMENTARY STRUCTURES	SAMPLES
Santonian	*Amphipyndax enessetti* (R)	B B RP B	B	CM AM RM		1	0.5				T * *

LITHOLOGIC DESCRIPTION

Fragments of dark brown (7.5YR 4/4) and light olive gray (5Y 5/2) CHERT.

ZEOLITIC AND ZEOLITE-BEARING CLAYSTONE; mostly dark brown (7.5YR 3/2–4/2).

SMEAR SLIDE SUMMARY (%):

	1, 20 M	1, 23 M	1, 36 M	1, 39 M	1, 44 M
Texture:					
Sand	–	–	–	–	–
Silt	3	65	2	2	–
Clay	97	35	98	98	–
Composition:					
Feldspar	–	1	–	–	–
Heavy minerals	–	2	5	4	–
Clay	50	10	71	68	50
Volcanic glass	2	65	3	–	25
Zeolite	–	15	30	25	25
Carbonate unspec.	–	2	–	–	–
Calc. nannofossils	–	5	–	~1	–
Radiolarians	–	<1	–	–	–
Other	1	–	1	–	–

SITE 585 HOLE CORE 27 CORED INTERVAL 485.4–494.6 m sub-bottom; 6607.7–6616.9 m below rig floor

TIME-ROCK UNIT	BIOSTRATIGRAPHIC ZONE	FORAMINIFERS	NANNOFOSSILS	RADIOLARIANS	DIATOMS	SECTION	METERS
Santonian		B B B B RP B	B B B B B	B FP RP RP B B		1 2 3 4 CC	0.5 1.0

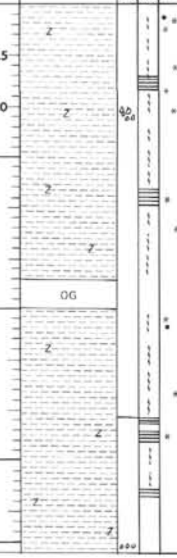

LITHOLOGIC DESCRIPTION

5YR 2.5/2 (dominant)

(5G 7/4)

(5G 7/4)

5Y 2/1 (dominant)

10G 4/2

(5G 7/4)

Interbedded moderate brown (5YR 3/4) and grayish green (5G 5/2) CLAYSTONE

Dominant lithology is ZEOLITE-BEARING CLAYSTONE Mostly dark reddish brown (5YR 2.5/2) in Sections 1 and 2 and olive black (5Y 2/1) in rest of core.

Zones of fine laminations of light green (5G 7/4) claystone occur throughout.

Plant fragments appear in foram-preparations from a dark band (~0.5 cm) at Section 3, 128 cm.

Claystone is moderately bioturbated throughout; most burrows are flattened and subparallel to bedding. Burrows are commonly filled with more-reduced claystone (usually green or black).

SMEAR SLIDE SUMMARY (%):

	1, 15 D	1, 27 M	1, 67 M	1, 82 M	1, 109 M
Texture:					
Sand	–	–	–	–	–
Silt	12	11	1	20	1
Clay	88	89	99	80	99
Composition:					
Feldspar	2	2	1	1	1
Heavy minerals	–	–	–	2	–
Clay	88	89	99	80	99
Volcanic glass	3	4	–	10	<1
Zeolite	3	2	<1	3	<1
Fe-oxides	4	2	–	2	–

	2, 42 M	2, 79 D	3, 16 D	3, 85 D	3, 123 D
Texture:					
Sand	–	–	–	–	–
Silt	7	5	3	5	14
Clay	93	95	97	95	86
Composition:					
Feldspar	2	1	2	2	4
Heavy minerals	–	1	1	–	–
Clay	93	91	92	91	86
Volcanic glass	2	2	3	2	2
Zeolite	3	5	2	3	5
Fe-oxides	–	1	–	2	2

ORGANIC CARBON AND CARBONATE (%):

	1, 13–19	3, 20–24
Organic carbon	0.09	0.14
Carbonate	1	2

SITE 585 HOLE CORE 28 CORED INTERVAL 494.6–503.7 m sub-bottom; 6616.9–6626.0 m below rig floor

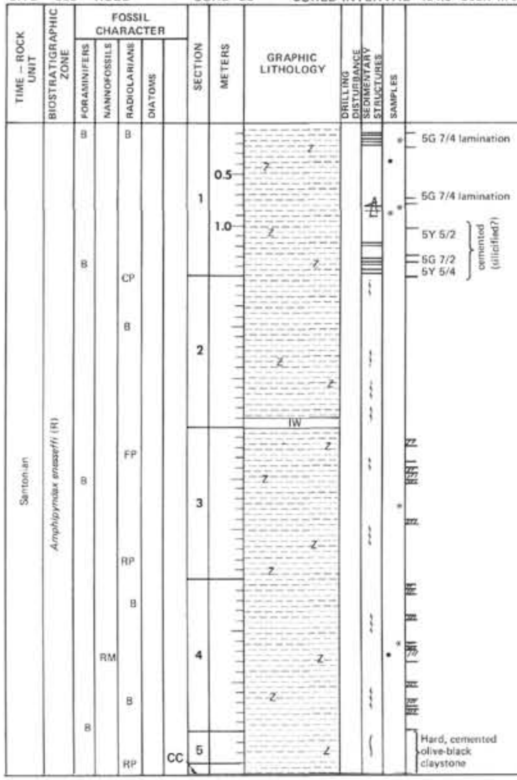

LITHOLOGIC DESCRIPTION

Dominant lithology is ZEOLITE-BEARING CLAYSTONE Mostly olive black (5Y 2/1); other colors as indicated.

Some bioturbation throughout but most is massive-appearing.

Laminations of light green (5G 7/4) occur at several horizons. Some appear to be bases of turbidites. Mottles and indistinct thin beds of pale green (10G 6/2) occur in Sections 3 and 4 (indicated to right of column as ~~~).

SMEAR SLIDE SUMMARY (%):

	1, 18	1, 82	1, 85	3, 80	4, 62
	M	M	M	D	M
Texture:					
Sand	–	–	–	–	–
Silt	9	7	7	2	4
Clay	91	93	93	98	96
Composition:					
Feldspar	2	–	–	–	–
Heavy minerals	–	1	–	3	1
Clay	91	72	95	76	86
Volcanic glass	3	10	–	4	1
Zeolite	2	15	5	10	8
Carbonate unspec.	–	–	–	1	2
Calc. nannofossils	–	–	–	6	2
Radiolarians	–	1	–	–	–

ORGANIC CARBON AND CARBONATE (%):

	1, 38–40	4, 76–78
Organic carbon	0.02	0.15
Carbonate	0	2

SITE 585 HOLE CORE 29 CORED INTERVAL 503.7–512.9 m sub-bottom; 6626.0–6635.2 m below rig floor

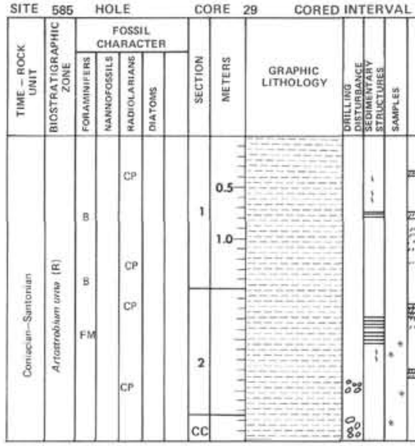

LITHOLOGIC DESCRIPTION

Dominant lithology is olive black (5Y 2/1) CLAYSTONE Some faint laminations; minor bioturbation; several intervals of radiolarian "sandstone" (indicated as "rad sand").

Pale green (10G 6/2) beds throughout indicated as ////.

SMEAR SLIDE SUMMARY (%):

	2, 56	2, 62	2, 101	CC, 5
	M	D	M	M
Texture:				
Clay	–	100	100	100
Composition:				
Heavy minerals	1	1	2	2
Clay	86	93	88	82
Volcanic glass	2	1	–	–
Zeolite	7	3	9	6
Carbonate unspec.	–	1	–	1
Calc. nannofossils	3	1	–	7
Radiolarians	<1	–	1	1

SITE 585 HOLE CORE 30 CORED INTERVAL 512.9–522.0 m sub-bottom; 6635.2–6644.3 m below rig floor

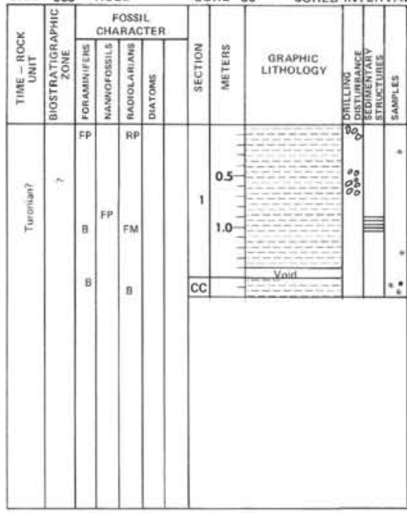

LITHOLOGIC DESCRIPTION

Dominant lithology is dark olive gray CLAYSTONE

Other colors as indicated.

Some indications of bioturbation, but most is massive-appearing.

SMEAR SLIDE SUMMARY (%):

	1, 30	1, 124	CC	CC
	D	M	D	D
Texture:				
Sand	–	–	–	3
Silt	–	–	5	10
Clay	100	100	95	87
Composition:				
Feldspar	–	–	–	<1
Heavy minerals	2	2	–	–
Clay	89	82	88	78
Zeolite	4	9	3	2
Carbonate unspec.	2	2	2	3
Calc. nannofossils	7	4	5	10
Polyxln. $CaCO_3$	–	–	–	10

ORGANIC CARBON AND CARBONATE (%):

	CC, 19–21
Organic carbon	0.07
Carbonate	6

SITE 585 HOLE CORE 31 CORED INTERVAL 522.0–531.2 m sub-bottom; 6644.3–6653.5 m below rig floor

TIME–ROCK UNIT: early Turonian

BIOSTRATIGRAPHIC ZONE: upper part of "*Obesacapsula somphedia*" Zone (R)

FOSSIL CHARACTER: Foraminifers: B, B; Nannofossils: B, B, FP; Radiolarians: FP, CP, CP, B, B

SECTION: 1, 2, 3, 4, CC

GRAPHIC LITHOLOGY: OG

LITHOLOGIC DESCRIPTION

Dominant lithology is dark greenish gray CLAYSTONE (5GY 4/1).

Abundant fine laminations throughout most of core (see sediment structure column).

Pale green (10G 6/2) laminae, thin beds, and burrow fill.

Several coarser, radiolarian-rich layers (mostly light gray [5Y 6/1]).

White calcite vein in Section 2, 21 cm, dipping at 75°.

SMEAR SLIDE SUMMARY (%):

	1, 40	1, 89	1, 94	2, 76	2, 101	2, 130	3, 75	3, 147	CC, 15
	D	D	M	M	M	D	D	D	D
Texture:									
Sand	–	–	3	2	20	–	–	–	–
Silt	10	10	10	8	10	10	5	2	10
Clay	90	90	87	90	70	90	95	98	90
Composition:									
Quartz	<1	<1	–	–	1	–	–	–	–
Feldspar	<1	–	<1	–	1	<1	–	–	<1
Heavy minerals	–	–	–	–	3	–	<1	–	–
Clay	87	85	84	85	70	87	91	95	70
Volcanic glass	–	–	–	–	2	2	4	1	–
Pyrite	–	–	–	–	1	–	–	–	–
Zeolite	7	1	8	7	7	10	2	2	30
Carbonate unspec.	–	1	–	1	–	–	–	–	<1
Calc. nannofossils	–	1	<1	–	–	–	2	–	–
Radiolarians	3	1	5	5	15	1	1	2	–
Sponge spicules	–	–	1	–	–	–	–	–	–

SITE 585 HOLE CORE 32 CORED INTERVAL 531.2–540.3 m sub-bottom; 6653.5–6662.6 m below rig floor

TIME–ROCK UNIT: Turonian; late Cenomanian

BIOSTRATIGRAPHIC ZONE: *Whiteinella archaeocretacea* / *Obesacapsula somphodia* (R); *Lithraphidites acutum* (N) *Rotalipora cushmani* / *Whiteinella aprica* Subzone (F)

FOSSIL CHARACTER: Foraminifers: B, RP, B, B, AM; Nannofossils: CP; Radiolarians: B, CP, B, CP

SECTION: 1, 2, 3, 4, 5, CC

LITHOLOGIC DESCRIPTION

CLAYSTONE

Dark gray (5Y 4/1; 5Y5.5/1; 2.5Y 4.5/2); slightly calcareous; forams and radiolarians in more or less distinct layers; black, pyritized flecks (plant fragments?) scattered throughout subparallel to stratification; black flecks increase in size (<1 to 3 mm) and abundance downward within a depositional unit; one fining-upwards depositional unit [probably turbidite] extends from Section 3, 33 cm through Section 11 Units usually have a siltstone at base.

Enlargement of 69–74 cm, Section 3:

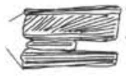

Cross-laminated bed sandwiched between parallel laminated units, and overlying black (N1), coarse, pyritic silty claystone layer

SMEAR SLIDE SUMMARY (%):

	1, 12	2, 100	3, 17	3, 100	4, 130
	D	D	D	D	D
Texture:					
Sand	–	–	–	–	–
Silt	–	5	6	1	1
Clay	–	95	94	99	99
Composition:					
Feldspar	1	1	1	<1	<1
Clay	90	91	91	98	99
Zeolite	3	2	2	1	<1
Foraminifers	<1	<1	1	–	–
Calc. nannofossils	1	1	1	1	–
Radiolarians	5	5	5	–	–

ORGANIC CARBON AND CARBONATE (%):

	1, 57–59	2, 35–39	3, 41–48
Organic carbon	0.13	0.33	0.22
Carbonate	6	12	7

	3, 13–18	3, 73–74	3, 72–73
Organic carbon	0.24	0.13	5.59
Carbonate	11	0	2

Calcite veins

XRD: 2, 140 cm = celadonite, smectite (minor), clinoptilolite, common christobalite, some quartz and calcite.

SITE 585 HOLE CORE 33 CORED INTERVAL 540.3–549.5 m sub-bottom; 6667.6–6671.8 m below rig floor

TIME–ROCK UNIT: late Cenomanian?

FOSSIL CHARACTER: Nannofossils: B

SECTION: 1

LITHOLOGIC DESCRIPTION

Fragments of gray (5Y 5/1) CLAYSTONE with drilling breccia (chips <1 cm) in between composed of gray (5Y 5/1) claystone, very dark grayish brown (10YR 3/2) chert, dark brown (10YR 3/3) claystone, pinkish gray (7.5YR 6/2) calcareous claystone, and dark gray (5Y 4/1) claystone.

SITE 585 HOLE CORE 34 CORED INTERVAL 549.5–558.6 m sub-bottom; 6671.5–6680.9 m below rig floor

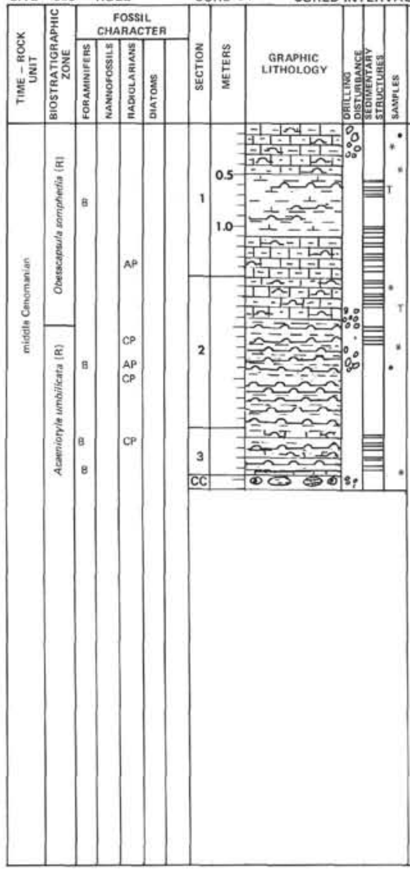

LITHOLOGIC DESCRIPTION

Interbedded CLAY-RADIOLARIAN-, and NANNOFOSSIL-BEARING LIMESTONE, CLAYEY RADIOLARITE, and NANNOFOSSIL-BEARING CLAYSTONE – multicolored.

Section 1, 0–57 cm: pale red (10R 6/2–5R 6/2) NANNOFOSSIL-BEARING CLAYEY LIMESTONE.

Section 1, 57–100 cm: pale red (5R 6/2) NANNOFOSSIL-BEARING CLAYSTONE with continuous, parallel laminations; several light greenish gray (5G 8/1) bands very rich in radiolarians.

Section 1, 100–150 cm: NANNOFOSSIL-BEARING CLAYEY LIMESTONE – reddish purple (5RP 6/2) and gray (N5–N7) with highly variable content of radiolarians.

Section 2, 0–38 cm: light gray (N7) CLAY-, RAD-, and NANNO-BEARING LIMESTONE with thin continuous laminations.

Section 2, 38–150 cm: grayish brown (10YR 5/2, 4/2, 4/1) CLAYEY RADIOLARITE; some zone very rich in radiolaria (see smear slide 2, 71). Several thin beds burrow fillings, and reduction halos along fractures of light greenish gray (5G 8/1).

Section 3, 0–45 cm: CLAYEY RADIOLARITE AND RADIOLARIAN-BEARING LIMESTONE with some fine, parallel laminations; multicolored but mostly shades of brown (10YR); zones with highly varying degrees of richness in rads.

SMEAR SLIDE SUMMARY (%):

	1, 21	1, 41	2, 17	2, 71	3, 43
	D	D	D	M	M
Texture:					
Sand	–	5	–	–	10
Silt	5	55	80	–	50
Clay	95	40	20	–	40
Composition:					
Quartz	–	–	3	–	–
Clay	88	28	10	30	30
Volcanic glass	2	–	–	–	–
Pyrite	1	–	–	–	–
Zeolite	2	2	–	–	–
Carbonate unspec.	3	40	45	2	20
Foraminifers	1	–	–	–	–
Calc. nannofossils	1	20	15	–	39
Radiolarians	1	7	15	50	10
Plant debris	–	–	–	1	–
Recrystal. SiO_2	–	–	–	18	–

ORGANIC CARBON AND CARBONATE (%):

	1, 11–12	2, 92–93
Organic carbon	0.06	0.05
Carbonate	29	0

SITE 585 HOLE CORE 35 CORED INTERVAL 558.6–572.1 m sub-bottom; 6680.9–6694.4 m below rig floor

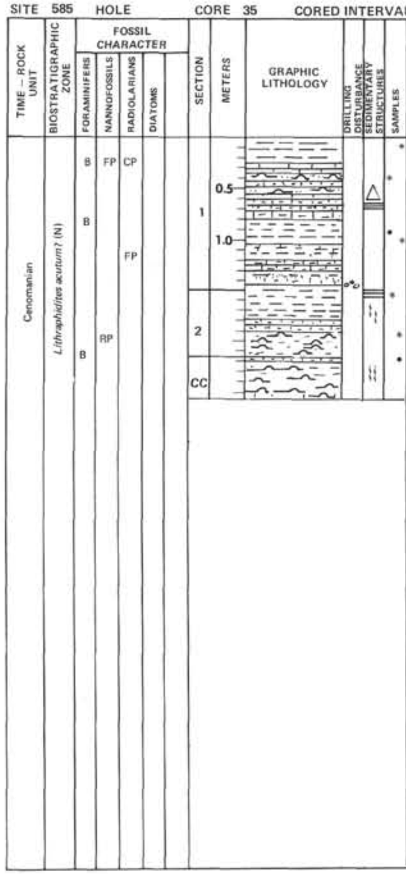

LITHOLOGIC DESCRIPTION

Mostly interbedded CALCAREOUS CLAYSTONE and CLAYEY LIMESTONE and RADIOLARIAN CLAY

Section 1, 0–12 cm: CLAYSTONE, dark gray (N4), massive-appearing.

Section 1, 12–17 cm: CHERT, yellow brown (10YR 5/4).

Section 1, 17–65 cm: CLAYEY LIMESTONE, mostly pale blue green (5BG 7/2) with several interbeds of yellow brown (10YR 6/2) rad-rich SANDY SILTSTONE.

Section 1, 65–80 cm: yellow brown (10YR 6/2) clayey limestone.

Section 1, 80–100 cm: CLAYSTONE, dark gray (N3), hard, massive-appearing.

Section 1, 100–130 cm: CLAYEY LIMESTONE or CALCAREOUS CLAYSTONE.

Section 1, 130–150 cm: CALCAREOUS SANDY SILTSTONE, rad-rich in some zone.

Section 2 and Core-Catcher: dominantly RADIOLARIAN CLAYSTONE, pale yellow brown (10YR 6/2), mostly massive-appearing with only slight bioturbation; faint laminations in upper part.

Several beds of CLAYEY LIMESTONE, light grayish green (5G 8/1).

SMEAR SLIDE SUMMARY (%):

	1, 4	1, 45	1, 103	2, 6	2, 45
	D	D		D	D
Texture:					
Sand	–	3	50	10	–
Silt	5	3	10	5	2
Clay	95	94	40	85	98
Composition:					
Feldspar	<1	<1	1	–	–
Clay	87	43	–	85	48
Volcanic glass	2	–	–	<1	1
Glauconite	–	–	<1	–	–
Pyrite	3	1	3	1	–
Zeolite	2	–	–	–	5
Carbonate unspec.	–	25	3	2	25
Foraminifers	–	–	–	1	–
Calc. nannofossils	3	25	2	1	–
Radiolarians	–	5	50	10	1

ORGANIC CARBON AND CARBONATE (%):

	1, 91–92	CC, 3–5
Organic carbon	0.05	0.04
Carbonate	6	32

SITE 585 HOLE CORE 36 CORED INTERVAL 572.1–581.2 m sub-bottom; 6694.4–6703.5 m below rig floor

TIME – ROCK UNIT	BIOSTRATIGRAPHIC ZONE	FORAMINIFERS	NANNOFOSSILS	RADIOLARIANS	DIATOMS	SECTION	METERS
late Albian	*Tic. breggiensis/praeticinensis* (F)	RP		CP		1	0.5
				CP			
		B				CC	1.0

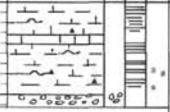

LITHOLOGIC DESCRIPTION

Most of material recovered is CALCAREOUS CLAYSTONE ± radiolarians. Most colors are various shades of yellow brown (2.5Y) with some thin beds of pale yellowish green (10GY 7/2); laminations are common throughout.

Note: recovery from Core 36 consisted of a jumbled series of poker-chip-like fragments in liner so there is no real or implied sequence or continuity of lithologies.

SMEAR SLIDE SUMMARY (%):

	1, 67 M	1, 72 M	1, 81 M
Texture:			
Clay	100	–	100
Composition:			
Clay	–	10	100
Zeolite	–	–	<1
Carbonate unspec.	25	<1	–
Radiolarians	10	30	–
Sponge spicules	–	–	<1
Fish remains	–	–	<1
Recrystal. SiO_2	65	60	–

SITE 585 HOLE CORE 37 CORED INTERVAL 581.2–590.4 sub-bottom; 6703.5–6712.7 m below rig floor

TIME – ROCK UNIT	BIOSTRATIGRAPHIC ZONE	FORAMINIFERS	NANNOFOSSILS	RADIOLARIANS	DIATOMS	SECTION	METERS
middle Albian	*Acaeniotyle umbilicata* (R)			CP		1	0.5
				CP			1.0

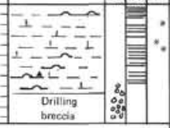

LITHOLOGIC DESCRIPTION

Fragments of CLAYSTONE highly variable in color and composition.

Most colors are shades of yellow brown (2.5Y) with mottles, thin beds, and reduction halos around fractures of pale green (10G 8/2).

Variable carbonate and radiolarian contents.

No significance in stratigraphic sequence or continuity because fragments were completely jumbled in liner.

SMEAR SLIDE SUMMARY (%):

	1, 19 M	1, 35 M	1, 42 M
Texture:			
Clay	100	100	100
Composition:			
Feldspar	<1	–	–
Clay	–	99	15
Volcanic glass	99	–	–
Zeolite	1	1	–
Radiolarians	–	–	25
Sponge spicules	<1	<1	–
Fish remains	<1	<1	–
Recrystal. SiO_2	–	–	60

SITE 585 HOLE CORE 38 CORED INTERVAL 590.4–599.5 m sub-bottom; 6712.7–6721.8 m below rig floor

TIME – ROCK UNIT	BIOSTRATIGRAPHIC ZONE	FORAMINIFERS	NANNOFOSSILS	RADIOLARIANS	DIATOMS	SECTION	METERS
middle Albian?		B	FP			1	0.5
		B					

LITHOLOGIC DESCRIPTION

CALCAREOUS CLAYSTONE in smaller fragments in upper and lower parts of recovered section. Dominant color is grayish brown (2.5Y 5/2).

22–47 cm = CALCAREOUS CLAYSTONE and SANDY CALCAREOUS CLAYSTONE with shallow-water debris in graded sequences (coarser debris includes oolites, benthic and planktonic forams, radiolarians, volcanogenic sand, and glauconite); fine-grained matrix contains volcanic glass altered to celladonite(?) or glauconite(?). Dominant color is grayish brown (2.5Y 5/2).

SMEAR SLIDE SUMMARY (%):

	1, 9 M	1, 62 M
Texture:		
Sand	–	–
Silt	3	<1
Clay	97	99
Composition:		
Feldspar	<1	<1
Heavy minerals	2	–
Clay	97	75
Volcanic glass	–	<1
Zeolite	<1	<1
Carbonate unspec.	–	25
Radiolarians	–	<1

ORGANIC CARBON AND CARBONATE (%):

	1, 24–28	1, 32–38
Organic carbon	0.04	0.03
Carbonate	25	9

SITE 585 HOLE CORE 39 CORED INTERVAL 599.5–608.7 m sub-bottom; 6721.8–6731.0 m below rig floor

TIME-ROCK UNIT: middle Albian ?

FOSSIL CHARACTER: Radiolarians CP, AP, B; Nannofossils RP; Foraminifers RP, B

SECTION: 1, 2, CC — METERS: 0.5, 1.0

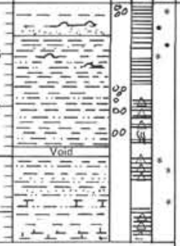

LITHOLOGIC DESCRIPTION

Fining-upward sequences, usually with very pale brown (10YR 7/3) CLAY-BEARING RADIOLARITE grading upward into dark brown (7.5YR 3/2) CLAYSTONE.

Other lithologies: white (N9) = CALCAREOUS SILTSTONE; dark gray (10YR 4/1) = SILTY CLAYSTONE; these lithologies also form the bases of fining-upward sequences.

Sequence contains several excellent examples of interlaminated coarse and fine material at the bases of fining-upward sequences, particularly in Section 2 and Core-Catcher.

SMEAR SLIDE SUMMARY (%):

	1, 2 M	1, 57 M	2, 17 M	2, 1 M	2, 43 M
Texture:					
Sand	–	–	–	–	–
Silt	80	60	85	–	60
Clay	20	40	15	100	40
Composition:					
Heavy minerals	–	–	–	1	–
Clay	16	16	–	95	40
Volcanic fragments	–	–	20	1	35
Palagonite	–	20	–	<1	–
Zeolite	4	–	–	3	5
Carbonate unspec.	–	–	80	–	–
Radiolarians	80	60	–	–	–
Fish remains	–	4	–	–	–

ORGANIC CARBON AND CARBONATE (%):

	1, 25–27	1, 42–44
Organic carbon	0.05	0.07
Carbonate	3	0

SITE 585 HOLE CORE 40 CORED INTERVAL 608.7–617.8 m sub-bottom; 6731.0–6740.1 m below rig floor

TIME-ROCK UNIT: middle Albian?

FOSSIL CHARACTER: Foraminifers B; Radiolarians B

SECTION: 1 — METERS: 0.5

LITHOLOGIC DESCRIPTION

Fining-upward sequences consisting mainly of white (N9) coarse CLAYEY CALCAREOUS siltstone bases with many thin laminae, which decrease in frequency and thickness upward as the sediment gets darker and finer. Grading into gray (5Y 6/1) CLAYSTONE.

SMEAR SLIDE SUMMARY (%):

	1, 40
Texture:	
Sand	–
Silt	12
Clay	88
Composition:	
Heavy minerals	1
Clay	86
Volcanic glass	4
Zeolite	<1
Radiolarians	8

SITE 585 HOLE CORE 41 CORED INTERVAL 617.8–627.0 m sub-bottom; 6740.1–6749.3 m below rig floor

TIME-ROCK UNIT: middle Albian

FOSSIL CHARACTER: Foraminifers B; Nannofossils RP; Radiolarians B

SECTION: CC

LITHOLOGIC DESCRIPTION

Graded sequences consisting of interlayered dark gray (2.5Y 4/0 CLAYSTONE, light gray (2.5Y 7/0) SILTY CLAYSTONE, dark greenish gray (5G 4/1) CLAYSTONE, and coarse basal beds of white (2.5Y 8/0) CARBONATE GRAINSTONE and CONGLOMERATIC VOLCANICLASTIC SANDSTONE with clasts up to 6 mm.

SMEAR SLIDE SUMMARY (%):

	CC, 6 M	CC, 22 M	CC, 32 M
Texture:			
Sand	70	20	–
Silt	15	70	–
Clay	15	10	–
Composition:			
Feldspar	3	–	–
Heavy minerals	–	1	1
Clay	–	–	96
Volcanic glass	60	–	–
Glauconite	4	–	–
Zeolite	2	–	<1
Carbonate unspec.	4	89	–
Foraminifers	5	–	–
Radiolarians	2	–	1

SITE 585 HOLE CORE 42 CORED INTERVAL 627.0–636.1 m sub-bottom; 6749.3–6758.4 m below rig floor

TIME-ROCK UNIT: middle Albian

BIOSTRATIGRAPHIC ZONE: *Tic. primula?* (F)

FOSSIL CHARACTER: Foraminifers B, B, FP; Nannofossils RP; Radiolarians B, RP

SECTION: 1, 2, 3, CC — METERS: 0.5, 1.0

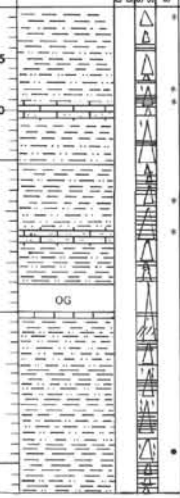

LITHOLOGIC DESCRIPTION

Graded sequences that consist dominantly of dark gray (N4) SILTY CLAYSTONE or CLAYEY SILTSTONE that contain abundant volcanogenic material. As basal units grading up into dark gray (N4) CLAYSTONE, and, finally, in several sequences, into bioturbated greenish gray (5G 6/1; 5Y 6/1) CLAYSTONE or CALCAREOUS CLAYSTONE or LIMESTONE. The coarse basal layer may be massive or laminated; coarser laminae consist of an interlamination of N4 siltstone and dark greenish gray (5G 4/1) siltstone. Most basalt units of graded sequences are N4 siltstone, but a few are white (N9) limestone.

SMEAR SLIDE SUMMARY (%):

	1, 10 M	1, 80 D	1, 99 M	2, 41 D	2, 70 M
Texture:					
Sand	2	–	–	–	40
Silt	10	8	1	10	40
Clay	88	92	99	90	20
Composition:					
Feldspar	1	1	–	1	2
Heavy minerals	3	3	1	2	–
Clay	86	89	3	88	–
Volcanic glass	3	–	1	1	35
Zeolite	2	3	<1	3	10
Carbonate unspec.	–	–	95	1	–
Foraminifers	–	–	–	–	30
Calc. nannofossils	–	–	–	<1	–
Radiolarians	3	2	–	4	3
Pyroxene	2	–	–	–	–

ORGANIC CARBON AND CARBONATE (%):

	3, 140–142
Organic carbon	0.06
Carbonate	34

SITE 585 HOLE CORE 43 CORED INTERVAL 636.1–645.3 m sub-bottom; 6758.4–6767.6 m below rig floor

TIME – ROCK UNIT	BIOSTRATIGRAPHIC ZONE	FORAMINIFERS	NANNOFOSSILS	RADIOLARIANS	DIATOMS	SECTION	METERS
middle Albian	VRP					1	0.5, 1.0
		RP		B		2	
						3	
				B		4	
						5	

GRAPHIC LITHOLOGY — DRILLING DISTURBANCE — SEDIMENTARY STRUCTURES — SAMPLES

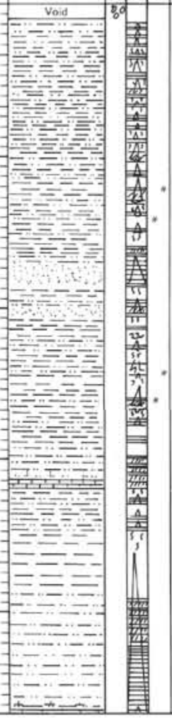

LITHOLOGIC DESCRIPTION

Numerous graded sequences of olive black (5Y 2/1) to dark olive gray (5Y 3/1), CLAYEY SILTSTONE to CLAYSTONE. Bases of graded sequences common and are massive, sandy (granular), laminated, an (or) cross-laminated. The finer-grained tops of the sequences commonly are bioturbated, calcareous, and olive gray (5Y 4/1).

As in the previous 10± cores, all laminae have an apparent dip of about 4–6°.

SMEAR SLIDE SUMMARY (%):

	2, 33 M	2, 68 D	3, 66 M	3, 94 M
Texture:				
Sand	–	–	–	–
Silt	25	20	22	–
Clay	75	80	78	–
Composition:				
Quartz	1	–	2	–
Mica	–	–	1	1
Heavy minerals	3	7	9	9
Clay	66	78	–	–
Volcanic glass	–	–	–	2
Zeolite	2	10	6	–
Carbonate unspec.	20	2	1	77
Calc. nannofossils	5	1	–	2
Radiolarians	3	–	3	3

SITE 585 HOLE CORE 44 CORED INTERVAL 645.3–654.4 m sub-bottom; 6767.6–6776.7 m below rig floor

TIME – ROCK UNIT	BIOSTRATIGRAPHIC ZONE	FORAMINIFERS	NANNOFOSSILS	RADIOLARIANS	DIATOMS	SECTION	METERS
middle Albian?		B		RP		1	0.5, 1.0
				B		2	
				B		3	
				B		4	
						5	
		RP				CC	

GRAPHIC LITHOLOGY — DRILLING DISTURBANCE — SEDIMENTARY STRUCTURES — SAMPLES

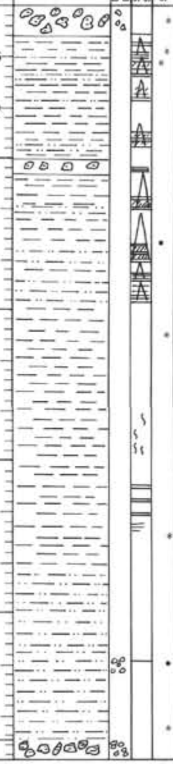

LITHOLOGIC DESCRIPTION

Graded sequences of dark greenish gray (5G 4/1) SILTSTONE and CLAYEY SILTSTONE bases and dusky brown (5YR 2/2), reddish black (10R 2.5/1), or black (2.5YR 2.5/0) CLAYSTONE tops.

SMEAR SLIDE SUMMARY (%):

	1, 16 M	1, 48 M	1, 55 M	3, 25 D	4, 72 D	5, 115 D
Texture:						
Sand	–	–	–	–	–	10
Silt	–	–	25	–	–	50
Clay	100	100	75	–	100	40
Composition:						
Quartz	–	–	2	–	–	–
Feldspar	–	1	–	–	–	1
Mica	–	–	1	–	–	–
Heavy minerals	2	–	–	–	–	4
Clay	–	5	68	18	26	30
Volcanic glass	3	–	–	–	2	–
Palagonite	–	90	–	–	9	–
Zeolite	18	4	3	5	–	48
Carbonate unspec.	–	–	18	2	3	8
Calc. nannofossils	–	–	5	–	<1	–
Radiolarians	<1	–	2	–	–	7
Sponge spicules	–	–	–	1	–	–
Fish remains	–	–	1	–	–	–
Volcanic material	3	–	–	74	50	–

ORGANIC CARBON AND CARBONATE (%):

	2, 84–85	5, 50–51
Organic carbon	0.08	0.06
Carbonate	5	3

SITE 585 HOLE CORE 45 CORED INTERVAL 654.4–667.8 m sub-bottom; 6776.7–6790.1 m below rig floor

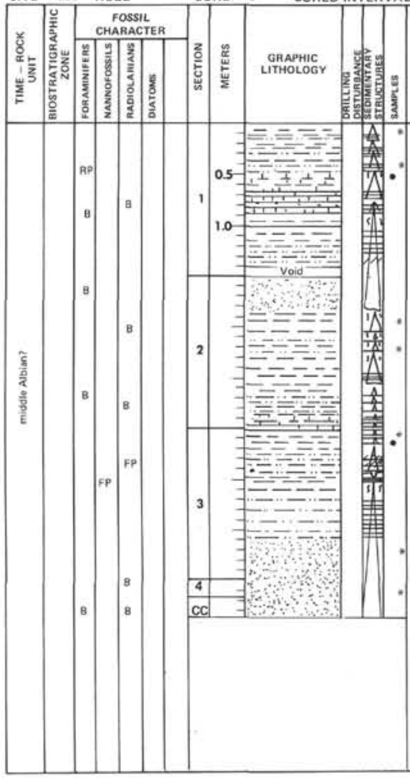

LITHOLOGIC DESCRIPTION

Graded sequences of dark gray (N4) siltstone-claystone with a few carbonate-rich graded units. Bases of graded sequences are mostly SILTY CLAYSTONE or CLAYEY SILTSTONE (N4) grading upward into CLAYSTONE (N4 or, in extreme cases, olive gray (5Y 4/1), in the upper, usually bioturbated, part of a graded unit (Bauma "E"). Several units show well developed Bauma sequences, particularly laminated (B and D) and ripple laminated (C) units of an ideal sequence. Several graded units are $CaCO_3$-rich with COARSE CLASTIC LIMESTONE grading up into CLAYEY MICRITIC LIMESTONE. The base of one unit is a sandstone (top Section 2).

SMEAR SLIDE SUMMARY (%):

	1, 9	1, 46	2, 49	2, 77	3, 9	3, 128	4, 12
	D	D	D	D	D	D	D
Texture:							
Sand	–	75	5	–	5	35	–
Silt	5	15	5	–	50	45	100
Clay	95	10	90	–	45	20	–
Composition:							
Quartz	–	<1	<1	<1	–	1	–
Feldspar	<1	1	1	2	1	3	–
Mica	–	–	–	1	–	–	–
Heavy minerals	–	3	–	–	5	8	–
Clay	76	10	75	50	50	20	–
Volcanic glass	7	3	9	14	15	20	86
Glauconite	1	1	2	1	2	2	–
Micronodules	–	–	–	2	–	2	–
Zeolite	7	2	10	7	9	7	–
Carbonate unspec.	–	80	2	–	–	20	7
Foraminifers	–	–	–	–	–	2	–
Calc. nannofossils	1	–	–	2	–	–	–
Radiolarians	–	–	1	15	15	15	–
Sponge spicules	–	–	–	1	–	1	–
Volcanic fragments	–	–	–	–	–	–	7

ORGANIC CARBON AND CARBONATE (%):

	1, 54–55	3, 18–19
Organic carbon	0.08	0.07
Carbonate	3	0

SITE 585 HOLE CORE 46 CORED INTERVAL 667.8–676.9 m sub-bottom; 6790.1–6799.2 m below rig floor

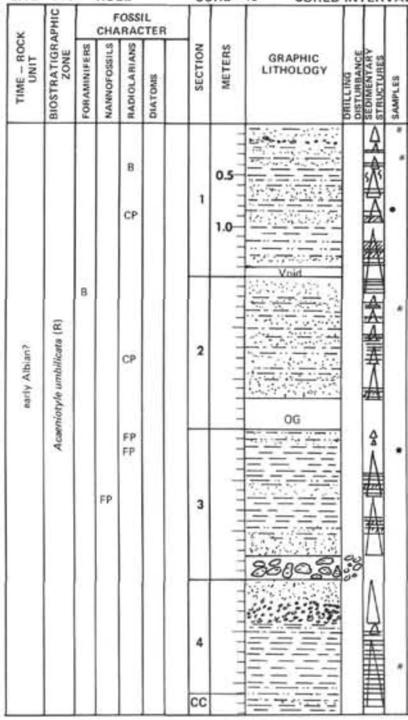

LITHOLOGIC DESCRIPTION

Graded sequences with bases mostly of dark greenish gray (5GY 4/1) or greenish black (5GY 2/1) volcanogenic SILTSTONE or SANDSTONE grading up into very dark gray (N4 or 5Y 4.5/1), brownish-gray (5YR 4/1), or dark greenish gray (5GY 4/1) MUDSTONE. Several sequences are complete Bauma (A–E) sequences. Fine to coarse parallel- and current-ripple-lamination are common. Bioturbation of uppermost fine top of a sequence is rare. Bases of several sequences have pebble-size clasts (up to 6 cm) rounded and flattened. Several water escape structures also are present. Volcanogenic components in units include volcanic lithic and crystal fragments, celadonite, and altered volcanic glass.

SMEAR SLIDE SUMMARY (%):

	1, 2	1, 35	2, 30	4, 85
	M	M	D	D
Texture:				
Sand	–	–	–	–
Silt	–	85	3	–
Clay	100	15	97	100
Composition:				
Feldspar	–	–	–	1
Heavy minerals	–	<1	2	1
Clay	9	5	81	74
Volcanic glass	<1	–	–	2
Zeolite	5	7	–	5
Carbonate unspec.	1	1	9	4
Calc. nannofossils	<1	–	–	–
Volcanic fragments	3	–	3	5
Celadonite	–	85	4	2

ORGANIC CARBON AND CARBONATE (%):

	1, 82–83	3, 24–25
Organic carbon	0.12	0.10
Carbonate	5	3

SITE 585 HOLE CORE 47 CORED INTERVAL 676.9–686.1 m sub-bottom; 6799.2–6808.4 m below rig floor

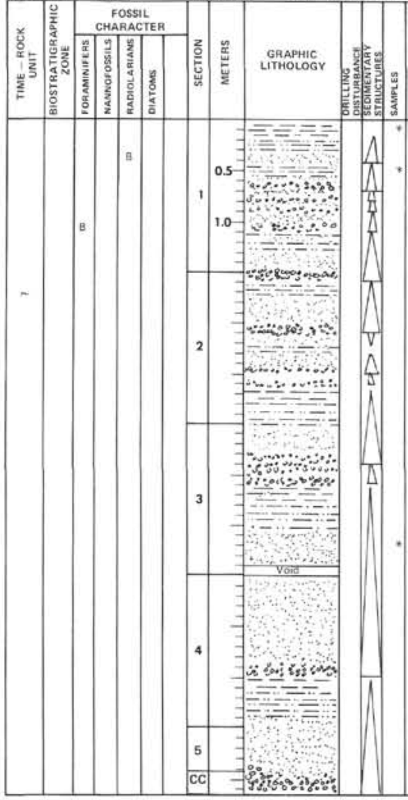

LITHOLOGIC DESCRIPTION

VERY COARSE VOLCANICLASTICS in graded sequences grading from COARSE SANDSTONE (usually conglomeratic, with fragments up to several cm but most are several mm) to SILTSTONE. Larger clasts are angular to rounded, but most are subrounded to rounded. Volcanic debris comprises most of all lithologies, and includes volcanic lithic and crystal fragments, celadonite, and highly altered volcanic glass.

Dominant colors of coarser bases of graded sequences are grayish green (10G 4/2) and dusky green (5G 3/2), and of finer tops are grayish green (10G 4/2), very dark gray (5Y 3/1), and dark grayish brown (10YR 3/2).

Veins of white (N9) calcite occur at several horizons.

SMEAR SLIDE SUMMARY (%):

	1, 10	1, 50	3, 120
	M	D	D
Texture:			
Sand	–	75	91
Silt	–	25	9
Clay	–	–	–
Composition:			
Feldspar	1	1	–
Clay	–	10	9
Volcanic glass	2	1	–
Palagonite	–	1	–
Carbonate unspec.	6	2	–
Fish remains	<1	–	–
Volcanic fragments	3	35	20
Celadonite	5	–	62

SITE 585 HOLE CORE 48 CORED INTERVAL 686.1–695.2 m sub-bottom; 6808.4–6817.5 m below rig floor

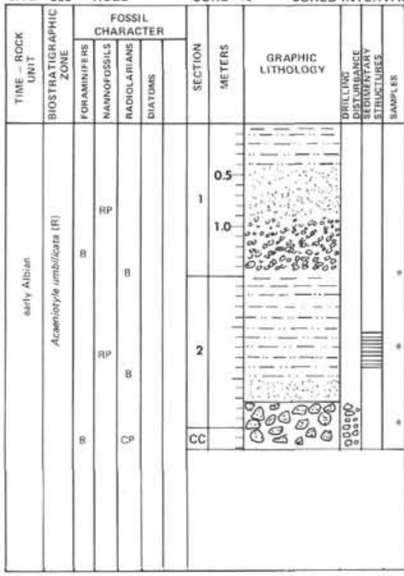

LITHOLOGIC DESCRIPTION

Thick graded sequences of volcaniclastics grading from conglomeratic sandstone bases, grading up into very coarse sandstone, sandstone, siltstone, and claystone.

Dominant colors are dusky green (5G 3/2) (= most), dark greenish gray (5G 4/1), grayish green (10G 4/2), olive gray (5Y 4/2), and grayish olive (GY 3/2) (= finer upper parts of graded sequences).

Larger clasts (up to 5 cm) at bases of units are subrounded to angular.

SMEAR SLIDE SUMMARY (%):

	1, 149	2, 70	2, 149
	M	D	M
Texture:			
Sand	–	–	–
Silt	15	–	10
Clay	85	–	90
Composition:			
Heavy minerals	1	2	5
Clay	50	–	–
Zeolite	2	3	–
Carbonate unspec.	45	9	81
Calc. nannofossils	<1	–	–
Radiolarians	–	–	<1
Sponge spicules	–	–	3
Volcanic fragments	–	50	10
Celadonite	3	5	–

SITE 585 HOLE CORE 49 CORED INTERVAL 695.2–704.4 m sub-bottom; 6817.5–6826.7 m below rig floor

TIME-ROCK UNIT	BIOSTRATIGRAPHIC ZONE	FORAMINIFERS	NANNOFOSSILS	RADIOLARIANS	SECTION
early Albian	*Hedbergella planispira?* (F)	B		CP	1
		CM		CP, B	2
			RP		3
				B	4
		B		CP	5
		RP		CP, CP	6

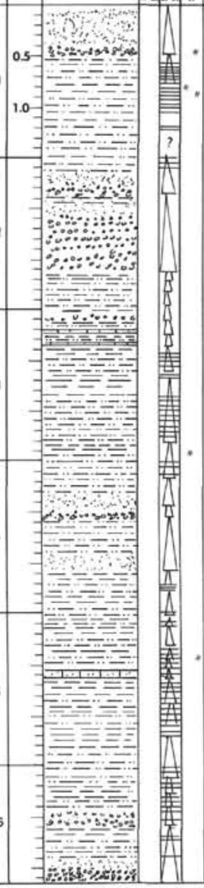

LITHOLOGIC DESCRIPTION

Graded sequences of volcaniclastics consisting of greenish black (5GY 2/1) SANDSTONE grading upward into SILTSTONE, and finally (but not in all sequences) into dark grayish brown (2.5Y 4/2) CLAYSTONE. Some sequences have CLASTIC LIMESTONE bases (white, N9) that grade upward into dark grayish brown (2.5Y 4/2) CLAYSTONE.

SMEAR SLIDE SUMMARY (%):

	1, 49	1, 81 D	1, 88 M	3, 143 D	5, 46 D
Texture:					
Sand	–	20	–	5	5
Silt	10	50	10	20	20
Clay	90	30	90	75	75
Composition:					
Feldspar	2	1	–	1	1
Heavy minerals	2	2	2	3	2
Clay	87	30	88	75	75
Volcanic glass	8	30	4	10	10
Glauconite	–	3	–	1	–
Zeolite	–	5	5	–	–
Carbonate unspec.	1	–	–	–	–
Calc. nannofossils	–	–	1	–	–
Radiolarians	<1	4	4	<1	2
Sponge spicules	–	–	–	<1	–
Volcanic fragments	–	24	–	–	11

SITE 585 HOLE CORE 50 CORED INTERVAL 704.4–713.5 m sub-bottom; 6826.7–6835.8 m below rig floor

TIME-ROCK UNIT	BIOSTRATIGRAPHIC ZONE	FORAMINIFERS	NANNOFOSSILS	RADIOLARIANS	SECTION
early Albian?				B	1
		RP		B	2
		RP, B		B	3
				B	4
					CC

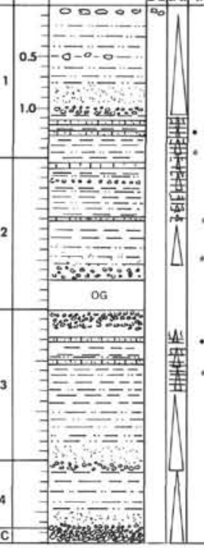

This unit probably continues into top of Core 51

LITHOLOGIC DESCRIPTION

Graded sequences of volcaniclastics, with COARSE SANDSTONES and CONGLOMERATIC SANDSTONES grading upward into SILTSTONES and finally CLAYSTONES; or CLASTIC LIMESTONES grading upward into CALCAREOUS CLAYSTONES (much less common). Claystones at the tops of graded sequences commonly are bioturbated.

Dominant colors are: greenish black (5GY 2/1) and olive black (5Y 2/1) for coarse basal layers; dark grayish brown (2.5Y 4/2) for top claystones; white (2.5Y 8/2) and light gray (2.5Y 7/2) for clastic limestones.

SMEAR SLIDE SUMMARY (%):

	1, 142 D	2, 62 M	2, 99 M	3, 65 D
Texture:				
Sand	10	–	–	20
Silt	30	15	50	40
Clay	60	85	50	40
Composition:				
Feldspar	3	<1	–	1
Heavy minerals	5	3	1	2
Clay	–	85	–	40
Volcanic glass	25	5	–	15
Glauconite	<1	<1	<1	<1
Zeolite	7	7	–	2
Carbonate unspec.	–	–	96	–
Calc. nannofossils	–	–	<1	–
Radiolarians	<1	<1	–	<1
Volcanic fragments	–	–	–	40

ORGANIC CARBON AND CARBONATE (%):

	1, 128–130	3, 31–32
Organic carbon	0.10	0.10
Carbonate	3	3

SITE 585 HOLE CORE 51 CORED INTERVAL 713.5–722.7 m sub-bottom; 6835.8–6845.0 m below rig floor

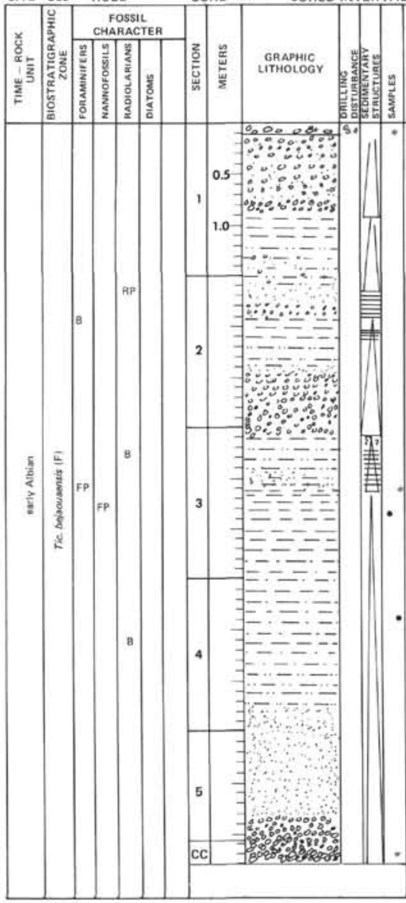

LITHOLOGIC DESCRIPTION

Graded sequences of VOLCANICLASTICS with COARSE SANDSTONES and CONGLOMERATIC SANDSTONES grading upward into SILTSTONES and finally CLAYSTONES. Bases of a few graded sequences are clastic limestones that grade upward into calcareous claystones.

Dominant colors are: SANDSTONES AND SILTSTONES – greenish black (5GY 2/1) and greenish gray (5G 2/1 and 5G 4/1), CLAYSTONES – greenish black (5GY 2/1) and dark greenish gray (5GY 4/1), and CARBONATES – white (2.5Y 8/2).

Conglomeratic sandstone at top of core probably is base of graded sequence at bottom of Core 50.

SMEAR SLIDE SUMMARY (%):

	1, 7	3, 61	CC, 21
	D	D	D
Texture:			
Sand	–	30	35
Silt	5	30	30
Clay	95	40	35
Composition:			
Quartz	–	3	–
Feldspar	–	<1	1
Clay	78	40	35
Volcanic glass	5	3	7
Glauconite	<1	–	65
Zeolite	3	–	–
Carbonate unspec.	15	52	–
Radiolarians	–	3	2
Volcanic fragments	–	3	–

ORGANIC CARBON AND CARBONATE (%):

	3, 81–88	4, 37–38
Organic carbon	0.09	0.08
Carbonate	5	4

Base of this graded unit continues into Core 52

SITE 585 HOLE CORE 52 CORED INTERVAL 722.7–731.8 m sub-bottom; 6845.0–6854.1 m below rig floor

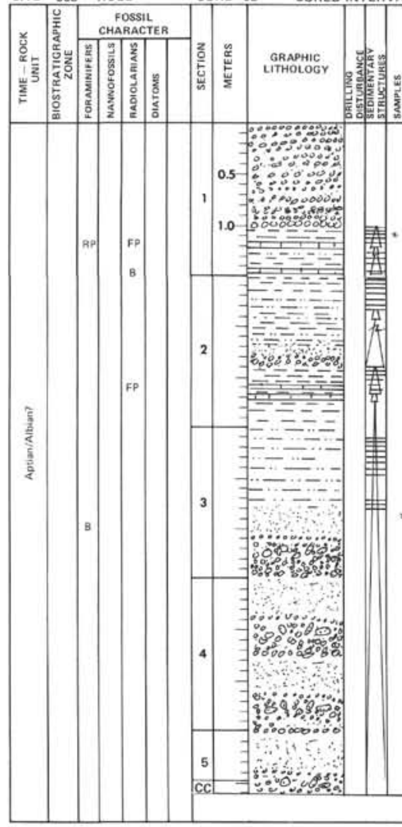

LITHOLOGIC DESCRIPTION

Graded sequences of volcaniclastics with coarse sandstones and conglomeratic sandstones (greenish black [5GY 2/1] and dark greenish gray [5GY 4/1]) grading upward into siltstones and finally claystones (very dark gray [5Y 3/1] and very dark grayish brown [10YR 3/2]). Bases of a few graded sequences are clastic limestones (light gray [2.5Y 7/2] and white [10YR 2/2]) that grade upward into claystone.

Top of core is probably the basal part of graded sequence at bottom of Core 51.

SMEAR SLIDE SUMMARY (%):

	1, 112	3, 88
	D	D
Texture:		
Sand	–	20
Silt	5	40
Clay	95	40
Composition:		
Feldspar	–	<1
Clay	50	40
Volcanic glass	1	10
Glauconite	<1	<1
Zeolite	–	3
Carbonate unspec.	44	6
Calc. nannofossils	2	–
Radiolarians	<1	1
Volcanic fragments	3	40

Base of this graded sequence continues in Core 53

SITE 585 HOLE CORE 53 CORED INTERVAL 731.8–741.0 m sub-bottom; 6854.1–6863.3 m below rig floor

TIME-ROCK UNIT: Aptian/Albian?

FOSSIL CHARACTER: B (Section 2)

SECTIONS: 1, 2, CC

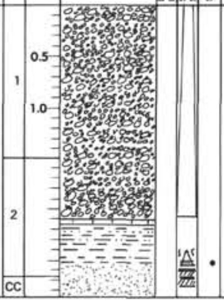

LITHOLOGIC DESCRIPTION

Graded sequences of VOLCANICLASTICS. COARSE SANDSTONE in Core 53, Section 1 to Section 2, 65 cm is the base of a graded sequence that started in Core 52, Section 2, 120 cm.

Rest of recovered section consists of CLASTIC LIMESTONE (light olive gray [5Y 7/1]), VOLCANICLASTIC SILTSTONE and SANDSTONE (greenish black [5GY 2/1]) and CLAYSTONE (dark greenish gray [5G 4/1] and olive black [5Y 4/1]).

ORGANIC CARBON AND CARBONATE (%):

	2, 105–106
Organic carbon	0.06
Carbonate	7

SITE 585 HOLE CORE 54 CORED INTERVAL 741.0–750.1 m sub-bottom; 6863.3–6872.4 m below rig floor

TIME-ROCK UNIT: late Aptian

BIOSTRATIGRAPHIC ZONE: lower part of "*Acaeniotyle umbilicata*" (R)

FOSSIL CHARACTER: RP FP (Section 2); RP, RP, B / FP (Section 3)

SECTIONS: 1, 2, 3, CC

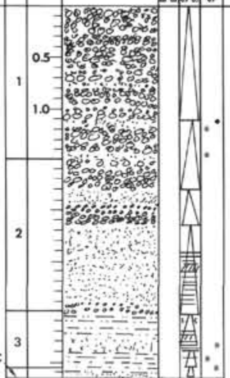

LITHOLOGIC DESCRIPTION

Graded sequences of volcaniclastics, mostly coarse sandstone and volcanic-rock-fragment conglomerates that grade up into siltstones.

Dominant colors are greenish black (5GY 2/1 and 5G 2/1).

SMEAR SLIDE SUMMARY (%):

	1, 144 D	1, 114 M	3, 35 M	3, 48 M	CC, 2 M
Texture:					
Sand	60	15	–	–	–
Silt	40	85	–	–	–
Clay	–	–	100	100	100
Composition:					
Heavy minerals	–	–	–	–	1
Clay	–	–	91	–	22
Palagonite	–	–	1	3	1
Zeolite	9	9	–	8	7
Carbonate unspec.	2	–	–	11	5
Calc. nannofossils	< 1	–	–	–	<1
Volcanic fragments	24	15	8	6	63
Celadonite	65	75	–	–	–
Recrystallized SiO_2	–	–	–	73	–

ORGANIC CARBON AND CARBONATE (%):

	1, 119–120
Organic carbon	0.05
Carbonate	5

SITE 585 HOLE CORE 55 CORED INTERVAL 750.1–763.7 m sub-bottom; 6872.4–6886.0 m below rig floor

TIME-ROCK UNIT: late Aptian?

FOSSIL CHARACTER: B, FP (Section 1); FP, RP, B, B (Section 2); CP, B (Section 4)

SECTIONS: 1, 2, 3, 4, 5, 6, CC

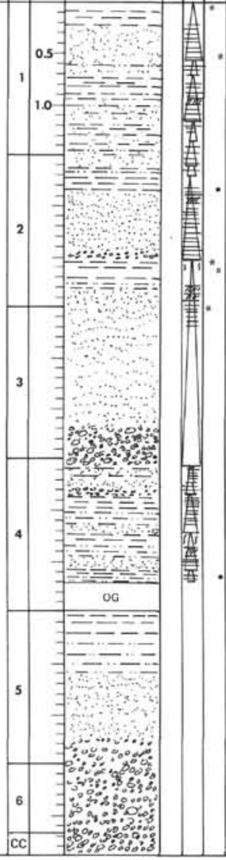

LITHOLOGIC DESCRIPTION

Graded sequences of greenish black (5GY 2/1 and 5G 2/1) VOLCANOGENIC COARSE-GRAINED SANDSTONES grading upward into FINER SANDSTONES and, in some sequences, SILTY CLAYSTONE (brownish gray [5YR 4/1]).

SMEAR SLIDE SUMMARY (%):

	1, 5 M	1, 59 M	2, 107 M	2, 113 M	3, 1 D
Texture:					
Sand	–	–	–	–	–
Silt	–	–	–	–	95
Clay	100	100	100	100	5
Composition:					
Heavy minerals	4	–	4	–	–
Clay	86	9	68	40	6
Volcanic glass	–	–	–	–	4
Palagonite	1	–	2	–	–
Zeolite	2	9	5	37	5
Carbonate unspec.	5	–	1	2	–
Celadonite	2	2	4	–	30
Volcanic fragments	–	80	7	20	55

ORGANIC CARBON AND CARBONATE (%):

	2, 36–37	4, 119–120
Organic carbon	0.04	0.04
Carbonate	6	18

SITE 585 HOLE A CORE H-1 (Wash core) CORED INTERVAL 0.0–363.7 m sub-bottom; 6122.3–6486.0 m below rig floor

TIME-ROCK UNIT: late Oligocene to Pleistocene

FOSSIL CHARACTER: Foraminifers RP, FM; Radiolarians B, B, B, B, B

SECTION: 1, 2, CC — METERS: 0.5, 1.0

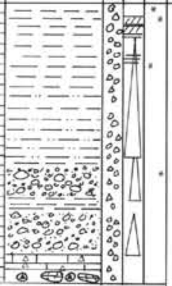

LITHOLOGIC DESCRIPTION

Mostly drilling breccia, but recovered fragments from Section 1, 5–150 cm appear to be from the same graded sequence, grading from dusky green (5G 3/2) SILTSTONE to dusky green nannofossil-, radiolarian-, and zeolite-bearing CLAYSTONE.

Section 2 contains fragments of green (5GY 4/1) CLAYSTONE at top. Recovered fragments from 13–50 cm appear to be from the same graded unit, grading from a CONGLOMERATE with pebbles of ZEOLITE-BEARING CLAYSTONE up to 3 cm in diameter at base to 1 mm in diameter at top of unit. A similar graded unit occurs from 60–95 cm. 95–110 cm consists of SILICIFIED NANNOFOSSIL LIMESTONE. The Core Catcher contains fragments of SILICIFIED NANNOFOSSIL LIMESTONE and CHERT.

SMEAR SLIDE SUMMARY (%):

	1,5 M	1,20 D	1, 66 D	2, 29 M
Texture:				
Sand	5	–	–	–
Silt	75	–	15	–
Clay	20	–	85	–
Composition:				
Quartz	15	–	–	–
Heavy minerals	5	10	2	5
Clay	20	40	62	70
Glauconite	10	5	3	–
Zeolite	40	20	7	18
Carbonate unspec.	–	2	6	–
Foraminifers	–	–	<1	–
Calc. nannofossils	–	–	4	1
Diatoms	–	10	Tr	–
Radiolarians	15	11	5	6
Sponge spicules	–	–	Tr	–
Silicoflagellates	–	–	Tr	–
Celadonite	–	–	4	–

SITE 585 HOLE A CORE 1 CORED INTERVAL 363.7–373.3 m sub-bottom; 6486.0–6495.6 m below rig floor

TIME-ROCK UNIT: early Eocene; late Paleocene

BIOSTRATIGRAPHIC ZONE: P6b? (F), CP9a (N); CP4 (N)

FOSSIL CHARACTER: Foraminifers VRP; Nannofossils CP, FP; Radiolarians B, B, B, B

SECTION: 1, 2, CC — METERS: 0.5, 1.0

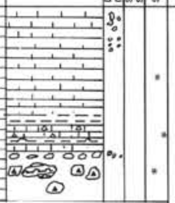

LITHOLOGIC DESCRIPTION

White (N9) NANNOFOSSIL CHALK, pinkish gray (5YR 7/2) SILICIFIED LIMESTONE, brown (5YR 4/1) RADIOLARIAN CLAYSTONE, and pinkish gray (5YR 7/2) SILICEOUS-BEARING CLAYEY LIMESTONE and, oh yes, the ever-present pale yellowish brown (10YR 6/2) CHERT.

SMEAR SLIDE SUMMARY (%):

	1, 57 D	1, 126 M	2, 12 D
Texture:			
Sand	–	–	–
Silt	95	50	50
Clay	5	50	50
Composition:			
Heavy minerals	–	<1	–
Clay	5	50	45
Volcanic glass	–	<1	–
Carbonate unspec.	5	<1	20
Calc. nannofossils	90	–	25
Radiolarians	–	–	10
Sponge spicules	–	49	–

SITE 585 HOLE A CORE 2 CORED INTERVAL 373.3–382.8 m sub-bottom; 6495.6–6505.1 m below rig floor

TIME-ROCK UNIT: early Paleocene

BIOSTRATIGRAPHIC ZONE: P1c (F), CP2 (N)

FOSSIL CHARACTER: Foraminifers CM, B, B; Nannofossils CP; Radiolarians B, B, B

SECTION: 1 — METERS: 0.5, 1.0

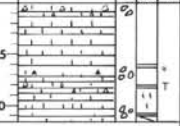

LITHOLOGIC DESCRIPTION

Pinkish gray (5YR 8/1), massive, micritic CHALK, moderate orange pink (5YR 8/4) SILICIFIED LIMESTONE, light brown (5YR 6/4) CLAYEY CHALK and CHERT.

SMEAR SLIDE SUMMARY (%):

	1, 64
Texture:	
Sand	–
Silt	60
Clay	40
Composition:	
Clay	30
Zeolite	10
Carbonate unspec.	15
Calc. nannofossils	42
Radiolarians	3

SITE 585 HOLE A CORE 3 CORED INTERVAL 382.8–392.3 m sub-bottom; 6505.1–6514.6 m below rig floor

TIME-ROCK UNIT: early Paleocene; Maestrichtian

BIOSTRATIGRAPHIC ZONE: "eugubina"? (F), Unzoned (R)/CP1a (N); *T. contusa* (R)

FOSSIL CHARACTER: Foraminifers FM, FP, FP, B, RP, CP, RP, B, RP; Nannofossils FP, CP; Radiolarians FP, FP, FP, CP

SECTION: 1, 2, CC — METERS: 0.5, 1.0

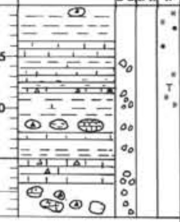

LITHOLOGIC DESCRIPTION

Interbedded light moderate brown (5YR 5/4) ZEOLITIC CLAY and very pale orange (10YR 8/2) CLAYEY NANNOFOSSIL CHALK. Some intervals of chalk have been silicifed, one fragment of moderate brown (5YR 3/4) CHERT was recovered in the Core Catcher, and at several horizons in Section 1.

SMEAR SLIDE SUMMARY (%):

	1, 10 D	1, 18 M	1, 70 M	1, 90 M	1, 101 D
Texture:					
Clay	100	100	–	–	–
Composition:					
Heavy minerals	–	3	–	1	<1
Clay	50	47	–	50	50
Zeolite	50	47	1	49	50
Carbonate unspec.	–	–	3	–	–
Foraminifers	–	–	<1	–	–
Calc. nannofossils	–	–	96	–	–
Hematite?	–	3	–	–	–

ORGANIC CARBON AND CARBONATE (%):

	1, 40–43	1, 21–26
Organic carbon	.05	.11
Carbonate	29	0

Wash core

SITE 585 HOLE A CORE H-2 CORED INTERVAL 392.3–438.2 m sub-bottom; 6514.6–6560.5 m below rig floor

TIME-ROCK UNIT	BIOSTRATIGRAPHIC ZONE	FORAMINIFERS	NANNOFOSSILS	RADIOLARIANS	DIATOMS	SECTION	METERS	GRAPHIC LITHOLOGY	DRILLING DISTURBANCE	SEDIMENTARY STRUCTURES	SAMPLES
?				B		1					

LITHOLOGIC DESCRIPTION

Drilling breccia consisting of fragments of bioturbated NANNOFOSSIL CHALK, SILICIFIED LIMESTONE, CLAYEY NANNOFOSSIL CHALK, CLAYSTONE, and CHERT.

SMEAR SLIDE SUMMARY (%):

	1, 1	1, 14
	M	M
Texture:		
Clay	100	100
Composition:		
Heavy minerals	<1	–
Clay	25	50
Carbonate unspec.	70	15
Calc. nannofossils	5	–

SITE 585 HOLE A CORE 4 CORED INTERVAL 438.2–447.7 m sub-bottom; 6560.5–6570.0 m below rig floor

TIME-ROCK UNIT	BIOSTRATIGRAPHIC ZONE	FORAMINIFERS	NANNOFOSSILS	RADIOLARIANS	DIATOMS	SECTION	METERS	GRAPHIC LITHOLOGY	DRILLING DISTURBANCE	SEDIMENTARY STRUCTURES	SAMPLES
?						1					

LITHOLOGIC DESCRIPTION

Four lovely fragments of dark brown (10YR 4/3) chert set in a matrix of chips (<1 cm) of chert, silicified limestone, and claystone.

Wash core

SITE 585 HOLE A CORE H-3 CORED INTERVAL 447.7–502.6 m sub-bottom; 6570.0–6624.9 m below rig floor

TIME-ROCK UNIT	BIOSTRATIGRAPHIC ZONE	FORAMINIFERS	NANNOFOSSILS	RADIOLARIANS	DIATOMS	SECTION	METERS	GRAPHIC LITHOLOGY	DRILLING DISTURBANCE	SEDIMENTARY STRUCTURES	SAMPLES
?		B				CC					
		B									

LITHOLOGIC DESCRIPTION

Drilling breccia consisting mainly of CHERT fragment in various shades of dark brown, with one interval of clay (brownish gray and dark yellowish brown). Chert is laminated, graded, bioturbated, and cut by veins of drusy quartz crystals growing into vugs.

SMEAR SLIDE SUMMARY (%):

	CC, 17
	M
Texture:	
Silt	4
Clay	96
Composition:	
Heavy minerals	2
Clay	95
Zeolite	1
Radiolarians	2

SITE 585 HOLE A CORE 5 CORED INTERVAL 502.6–511.8 m sub-bottom; 6624.9–6634.1 m below rig floor

TIME-ROCK UNIT	BIOSTRATIGRAPHIC ZONE	FORAMINIFERS	NANNOFOSSILS	RADIOLARIANS	DIATOMS	SECTION	METERS	GRAPHIC LITHOLOGY	DRILLING DISTURBANCE	SEDIMENTARY STRUCTURES	SAMPLES
Santonian	*A. urna* to *A. enesseffi* (R)	B				1	0.5, 1.0				
				CP		2					
		FP	RP	CP		3					

LITHOLOGIC DESCRIPTION

Interbedded greenish gray (5G 5/2) and greenish black (5GY 2/1) (= "light and dark" green) CLAYSTONE with minor beds of yellowish brown (10YR 2/2) and light olive gray (5Y 6/1) CLAYSTONE.

All units are hard and massive with only slight hints of bioturbation. Contacts between different-colored lithologies are fairly sharp.

SMEAR SLIDE SUMMARY (%):

	1, 35	1, 49	1, 98	1, 120
	D	D	M	M
Texture:				
Sand	–	–	10	–
Silt	1	1	60	1
Clay	99	99	30	99
Composition:				
Quartz	–	–	60	–
Heavy minerals	1	1	–	<1
Clay	94	95	30	96
Volcanic glass	<1	–	–	–
Zeolite	2	3	2	2
Carbonate unspec.	1	–	4	<1
Calc. nannofossils	1	1	<1	1
Radiolarians	1	1	2	–
Sponge spicules	–	–	<1	–

ORGANIC CARBON AND CARBONATE (%):

	1, 80–81	2, 59–60
Organic carbon	.01	.07
Carbonate	3	7

SITE 585 HOLE A CORE 6 CORED INTERVAL 511.8–520.9 m sub-bottom; 6634.1–6643.2 m below rig floor

TIME-ROCK UNIT	BIOSTRATIGRAPHIC ZONE	FORAMINIFERS	NANNOFOSSILS	RADIOLARIANS	DIATOMS	SECTION	METERS	GRAPHIC LITHOLOGY	DRILLING DISTURBANCE	SEDIMENTARY STRUCTURES	SAMPLES
?		B		FP		1	0.5, 1.0				
		FP				2					
						CC					

LITHOLOGIC DESCRIPTION

Dominant lithology is dark gray CLAYSTONE (2.5YR 3/0) with numerous mottles and several beds of grayish green (5G 5/2) CLAYSTONE.

One layer of olive gray (5Y 4/1) radiolarian-bearing.

SMEAR SLIDE SUMMARY (%):

	1, 25	1, 50	1, 114	1, 115	1, 132
Texture:	D	M			
Sand	–	2	–	2	<1
Silt	2	10	1	12	3
Clay	98	88	99	86	97
Composition:					
Heavy minerals	1	1	<1	<1	1
Clay	93	85	97	83	90
Zeolite	3	2	2	2	2
Carbonate unspec.	1	<1	–	–	1
Calc. nannofossils	1	<1	–	<1	3
Radiolarians	–	12	<1	15	–
Fish remains	–	–	<1	<1	–
Recryst. SiO_2	1	–	–	–	–

ORGANIC CARBON AND CARBONATE (%):

	1, 54–57
Organic carbon	.48
Carbonate	10

SITE 585 HOLE A CORE 7 CORED INTERVAL 520.9–532.4 m sub-bottom; 6643.2–6654.7 m below rig floor

TIME – ROCK UNIT: Turonian

BIOSTRATIGRAPHIC ZONE: *Obesacapsula somphedia*

FOSSIL CHARACTER (FORAMINIFERS, NANNOFOSSILS, RADIOLARIANS, DIATOMS): Section 1 – Foraminifers B; Radiolarians FP, CP, CP. Section 3 – Radiolarians CP; Nannofossils RP, Radiolarians CP. CC – Nannofossils B.

SECTION: 1, 2, 3, CC

METERS: 0.5, 1.0

GRAPHIC LITHOLOGY / DRILLING DISTURBANCE / SEDIMENTARY STRUCTURES / SAMPLES

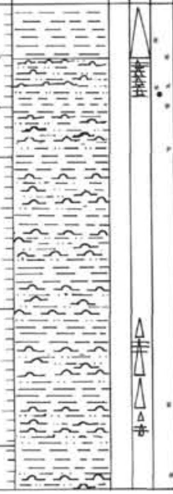

LITHOLOGIC DESCRIPTION

Dominant lithology is massive dark gray (N4) ZEOLITE CLAYSTONE, with a RADIOLARIAN CLAYEY SILTSTONE-laminated medium gray (N5) SILTY CLAYSTONE (light olive gray [5Y 6/1]) series of graded sequences between 58 and 85 cm, Section 1 (probably corresponds to greenish laminated interval in 585-31-2, 73–104 cm). A 2-cm bed of gypsiferous(?) SILICEOUS SILTSTONE occurs at the base of this series (83–85 cm; see smear slide 1, 83).

Graded sequences of gray (N6) silty claystone and N5 claystone are well developed in Section 3.

SMEAR SLIDE SUMMARY (%):

	1, 35 D	1, 56 M	1, 83 M	1, 105 D	1, 86 M
Texture:					
Sand	–	–	–	–	–
Silt	2	50	93	–	–
Clay	98	50	7	100	–
Composition:					
Heavy minerals	–	–	–	1	4
Clay	72	55	–	60	85
Palagonite	–	–	–	–	11
Zeolite	13	–	–	35	–
Carbonate unspec.	9	5	–	–	–
Calc. nannofossils	<1	–	–	–	–
Radiolarians	–	38	30	–	–
Recryst. silica	–	–	50	–	–
Fish remains	–	–	<1	1	
Gypsum?	<1	1	20	2	–
Barite?	2	–	–	–	–
Celadonite	2	–	–	1	–
Hematite	2	1	–	–	–

	1, 140 M	3, 95 M	CC, 31 M
Texture:			
Sand	–	–	–
Silt	–	55	–
Clay	100	45	100
Composition:			
Heavy minerals	2	–	–
Clay	61	36	64
Volcanic glass	–	–	1
Zeolite	10	2	1
Carbonate unspec.	20	36	–
Radiolarians	–	18	–
Recryst. SiO_2	7	5	20
Gypsum	<1	3	1
Celadonite	–	–	13

ORGANIC CARBON AND CARBONATE (%):

	1, 94–100
Organic carbon	.41
Carbonate	0

SITE 585 HOLE A CORE 8 CORED INTERVAL 532.4–543.5 m sub-bottom; 6654.7–6665.8 m below rig floor

TIME – ROCK UNIT: Turonian

BIOSTRATIGRAPHIC ZONE: *Obesacapsula somphedia* (R)

FOSSIL CHARACTER (FORAMINIFERS, NANNOFOSSILS, RADIOLARIANS, DIATOMS): Section 1 – Radiolarians FP; Foraminifers FP. Section 3 – Radiolarians CP. CC – Radiolarians CP.

SECTION: 1, 2, 3, CC

METERS: 0.5, 1.0

GRAPHIC LITHOLOGY / DRILLING DISTURBANCE / SEDIMENTARY STRUCTURES / SAMPLES

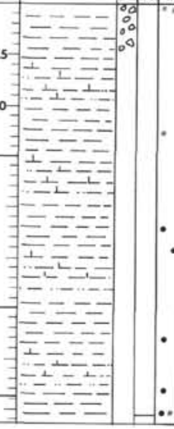

LITHOLOGIC DESCRIPTION

Thick (about 1 m) graded sequences of medium gray (N5) SILTSTONE grading into a SLIGHTLY CALCAREOUS SILTY CLAYSTONE or CLAYSTONE most of the material contains black flecks or flakes that are oriented parallel to stratification. Coarser bases of some graded sequences contain concentrations of radiolarians and foraminifera. Some parallel laminations are present but most of the material is massive-appearing.

Top 50 cm of core consists of drilling breccia of dusky yellowish brown (10YR 2/2) CLAYSTONE.

SMEAR SLIDE SUMMARY (%):

	1, 3 M	1, 8 D	1, 125 D	CC, 19 M
Texture:				
Sand	–	–	–	–
Silt	–	–	10	100
Clay	100	100	90	100 –
Composition:				
Feldspar	–	33	2	–
Heavy minerals	1	4	–	–
Clay	50	50	86	–
Volcanic glass	–	–	2	–
Palagonite	–	2	–	–
Zeolite	49	–	–	–
Carbonate unspec.	–	–	10	–
Calc. nannofossils	–	–	7	–
Radiolarians	–	–	–	100
Fish remains	–	–	<1	–
Celadonite	–	1	–	–
Gypsum?	–	–	1	–
Recryst. SiO_2	–	9	–	–

ORGANIC CARBON AND CARBONATE (%):

	2, 75–76	2, 95–96	3, 32–33
Organic carbon	.33	.04	.43
Carbonate	21	13	15

	3, 80–81	CC, 19–20
Organic carbon	.09	1.45
Carbonate	8	1

[a] Black band consists almost entirely of black flecks of organic matter and radiolarite

SITE 585 HOLE A CORE 9 CORED INTERVAL 543.5–552.6 m sub-bottom; 6665.8–6674.9 m below rig floor

Time-rock unit: Turonian / late Cenomanian (Rotalipora cushmani/Whiteinella aprica (F))

Biostratigraphic zone: Obesacapsula somphedia; Whiteinella archaeocretacea (F); Rotalipora cushmani/Whiteinella aprica

Fossil character: Foraminifers FM, FM, FP, B; Nannofossils RP, FP; Radiolarians CP, CP, AP

Section: 1, CC — Meters: 0.5, 1.0

LITHOLOGIC DESCRIPTION

Dominant lithologies include slightly calcareous SILICEOUS SILTSTONE and SILICEOUS CLAYSTONE or SILTY CLAYSTONE, mostly in shades of greenish gray (5GY 5/1–5GY 4/1), in which the coarser material occurs at the base of an upward-fining graded sequence, or as lenses, beds, or stringers within finer lithologies (especially in the upper 15 cm of Section 1). The coarser material contains abundant recrystallized radiolarians. Overall, the dominant lithology is toward the finer size range, i.e. CLAYSTONE. All lithologies contain abundant silica cement and are quite hard.

An interesting sequence of multicolored chert and laminated radiolarian-bearing siltstone occurs between 80–100 cm, Section 1. Three chert fragments recovered are brightly-colored shades of red, brown, and yellow. They all contain abundant blebs and lenses of pyrite. The laminated rad-bearing siltstone underlying the chert contains a thin (about 2 mm) band of organic matter, which is overlain by multicolored laminae of green, yellow, gray, and tan siltstone.

The Core Catcher contains interbedded reddish brown (5YR 5/3) and light greenish gray (5G 7/1) CLAYSTONE.

SMEAR SLIDE SUMMARY (%):

	1, 6 M	1, 10 M	1, 79 M	1, 120 D	1, 130 M
Texture:					
Sand	–	–	5	–	–
Silt	–	15	10	1	–
Clay	–	85	85	99	100
Composition:					
Feldspar	<1	9	–	–	–
Heavy minerals	<1	1	–	–	–
Clay	14	10	83	99	100
Zeolite	1	–	5	1	<1
Carbonate unspec.	5	6	–	<1	–
Foraminifers	–	1	–	–	–
Calc. nannofossils	<1	<1	–	–	–
Radiolarians	–	–	12	–	–
Fish remains	–	<1	–	–	–
Gypsum	<1	1	–	–	–
Recryst. SiO_2	80	72	–	–	–
Celadonite	1	1	–	–	–

	1, 137 D	1, 147 D	CC, 1 D	CC, 6 D
Texture:				
Sand	–	5	–	–
Silt	1	50	–	–
Clay	99	45	100	100
Composition:				
Heavy minerals	–	1	–	–
Clay	50	44	100	100
Volcanic glass	–	2	–	–
Zeolite	–	<1	<1	<1
Carbonate unspec.	50	2	–	–
Calc. nannofossils	–	1	–	–
Recryst. SiO_2	–	50	–	–

ORGANIC CARBON AND CARBONATE (%):

	1, 27–29	1, 82–83	1, 93–94
Organic carbon	.04	.01	.22
Carbonate	14	0	4

	1, 140–141	CC, 17–19
Organic carbon	.1	.06
Carbonate	14	21

SITE 585 HOLE A CORE 10 CORED INTERVAL 552.6–561.8 m sub-bottom; 6674.9–6684.1 m below rig floor

Time-rock unit: late Albian?

Biostratigraphic zone: O. somphedia (R)

Fossil character: Foraminifers B, B; Nannofossils FP, RP; Radiolarians CP, FP

Section: 1 — Meters: 0.5, 1.0

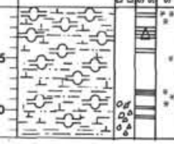

LITHOLOGIC DESCRIPTION

Interbedded dark brown (10YR 4/1) SILICEOUS CLAYSTONE, light to medium brown (10YR 6/2–5/2) CALCITE-BEARING SILICEOUS CLAYSTONE, light greenish gray (5G 7/1) CALCAREOUS AND SILICEOUS CLAYSTONE, with some coarsening to CLAYEY SILTSTONE and SILTSTONE in some layers.

One definite fining-upward sequence is apparent, but most of the core is too brecciated to identify graded sequences.

SMEAR SLIDE SUMMARY (%):

	1, 3 D	1, 9 M	1, 12 M	1, 55 M	1, 82 M	1, 89 M	1, 97 M
Texture:							
Sand	–	–	–	–	–	–	–
Silt	–	–	5	–	2	–	40
Clay	100	100	95	100	98	100	60
Composition:							
Feldspar	–	<1	–	<1	–	–	–
Heavy minerals	1	1	<1	–	–	–	–
Clay	69	79	–	–	–	–	–
Carbonate unspec.	–	–	20	24	49	–	–
Foraminifers	–	–	–	<1	–	–	–
Calc. nannofossils	–	–	1	<1	1	–	–
Radiolarians	–	<1	<1	–	2	–	10
Fish remains	1	<1	–	–	–	–	–
Gypsum	<1	<1	–	–	–	–	–
Recryst. SiO_2	29	20	79	76	48	60	60

SITE 585 HOLE A Wash core CORE H-4 CORED INTERVAL 561.8–658.0 m sub-bottom; 6684.1–6780.3 m below rig floor

Time-rock unit: late Albian?

Biostratigraphic zone: O. somphedia (R)

Fossil character: Radiolarians CP, CP, CP, CP

Section: 1, 2, CC — Meters: 0.5, 1.0

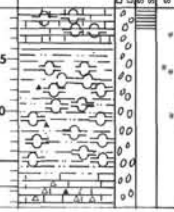

LITHOLOGIC DESCRIPTION

Fragments of:

Section 1, 0–40 cm: very light bluish gray (5B 8/1) clayey SILICEOUS LIMESTONE; some fine laminations.

Section 1, 40–150 cm: olive gray (5Y 4/1) to bluish gray (5B 6/1) SILICEOUS SILTY CLAYSTONE and minor brownish gray (5YR 4/1) CHERT.

Section 2: greenish black (5GY 2/1) VOLCANICLASTIC SILTSTONE and light gray (N7.5) coarse CLASTIC LIMESTONE.

Core Catcher: medium brownish gray (5YR 5/1) to yellowish gray (5Y 8/1) SILICEOUS LIMESTONE and brownish gray (5YR 4/1) CHERT.

SMEAR SLIDE SUMMARY (%):

	1, 26 M	1, 61 M	1, 62 M	1, 107 M
Texture:				
Sand	5	1	–	–
Silt	65	69	40	25
Clay	30	30	60	75
Composition:				
Quartz	–	–	1	–
Heavy minerals	3	3	3	1
Clay	25	29	60	75
Zeolite	–	1	2	6
Carbonate unspec.	30	5	4	10
Calc. nannofossils	20	2	1	3
Radiolarians	–	60	–	–
Recryst. SiO_2	25	–	29	5

SITE 585 HOLE A CORE Wash core H-5 CORED INTERVAL 658.0–772.1 m sub-bottom; 6780.3–6894.4 m below rig floor

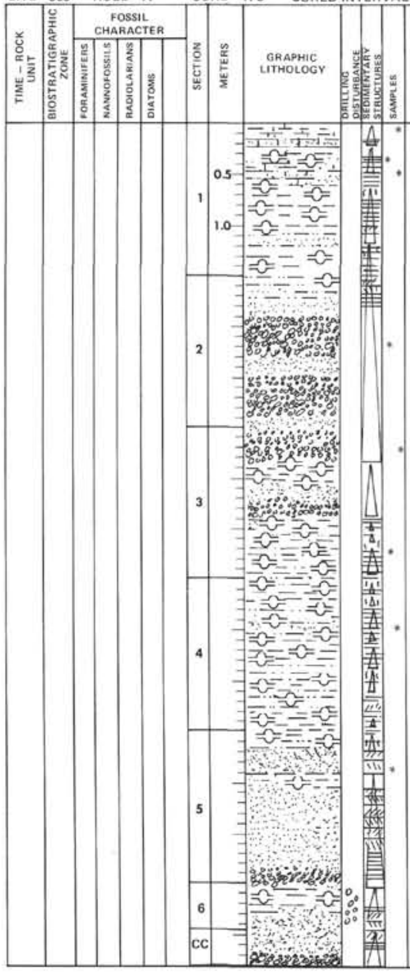

LITHOLOGIC DESCRIPTION

Graded sequences of volcaniclastic and carbonate. Finer-grained tops of sequences are mostly medium gray (N4) CLAYSTONE, massive, laminated, or sometimes bioturbated. Coarser bases of graded sequence are mainly very coarse volcaniclastic debris with clasts up to 1 cm, usually dark greenish gray (5GY 4/1), greenish black (5GY 2/1), or dark gray (N3). Some coarser units consist of interlaminated volcaniclastic and coarse carbonate debris.

SMEAR SLIDE SUMMARY (%):

	1, 8 M	1, 38 M	1, 46 M	2, 70 M	3, 25 M	3, 126 M	4, 50	5, 40
Texture:								
Sand	–	–	–	20	–	–	–	–
Silt	–	–	10	80	100	2	55	95
Clay	100	100	90	–	–	98	45	5
Composition:								
Feldspar	1	–	1	5	5	–	3	7
Heavy minerals	2	3	1	–	3	2	–	3
Clay	53	65	5	8	5	40	30	43
Volcanic glass	–	–	–	7	–	–	6	20
Zeolite	7	–	–	9	4	–	9	9
Carbonate unspec.	–	1	78	8	9	1	3	4
Calc. nannofossils	<1	<1	–	–	–	–	–	–
Radiolarians	<1	3	–	–	–	5	–	<1
Sponge spicules	–	7	–	–	–	–	<1	–
Fish remains	1	–	–	–	–	–	–	–
Celadonite	2	–	–	9	54	–	–	–
Hematite	–	–	–	–	–	1	–	<1
Gypsum	1	–	–	–	–	1	–	–
Recryst. SiO_2	33	20	15	34	20	60	9	–
Volc. xl. fr.	–	–	–	–	–	–	–	5

SITE 585 HOLE A CORE 11 CORED INTERVAL 772.1–781.3 m sub-bottom; 6894.4–6903.6 m below rig floor

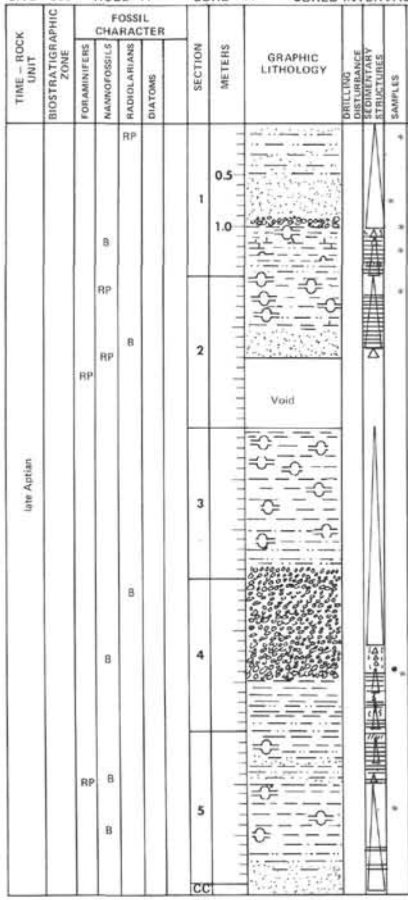

LITHOLOGIC DESCRIPTION

Graded sequences of volcaniclastic and coarse carbonate debris. Finer-grained tops are mostly very dark gray (10YR 3/1) laminated, massive, or bioturbated.

SMEAR SLIDE SUMMARY (%):

	1, 13 M	1, 80 D	1, 102 M	1, 124 M	2, 20 D	4, 92 D	5, 76 D
Texture:							
Sand	–	–	–	–	–	–	–
Silt	–	99	–	100	–	–	5
Clay	100	1	100	–	100	100	95
Composition:							
Feldspar	6	–	3	4	1	2	6
Heavy minerals	4	–	3	2	2	–	2
Clay	50	–	72	–	78	81	80
Volcanic glass	5	5	–	8	–	–	–
Palagonite	–	–	<1	1	–	–	–
Zeolite	–	9	–	–	–	2	6
Carbonate unspec.	–	5	–	72	8	3	3
Calc. nannofossils	–	–	–	<1	<1	–	<1
Radiolarians	–	–	–	–	<1	–	–
Hematite	2	–	1	–	–	1	–
Recryst. SiO_2	30	31	–	–	9	9	–
Volc. frags.	3	5	–	13	–	–	3
Celadonite	–	45	2	–	2	–	–

ORGANIC CARBON AND CARBONATE (%):

	4, 84–86
Organic carbon	.25
Carbonate	1

SITE 585 HOLE A CORE 12 CORED INTERVAL 781.3–790.4 m sub-bottom; 6903.6–6912.7 m below rig floor

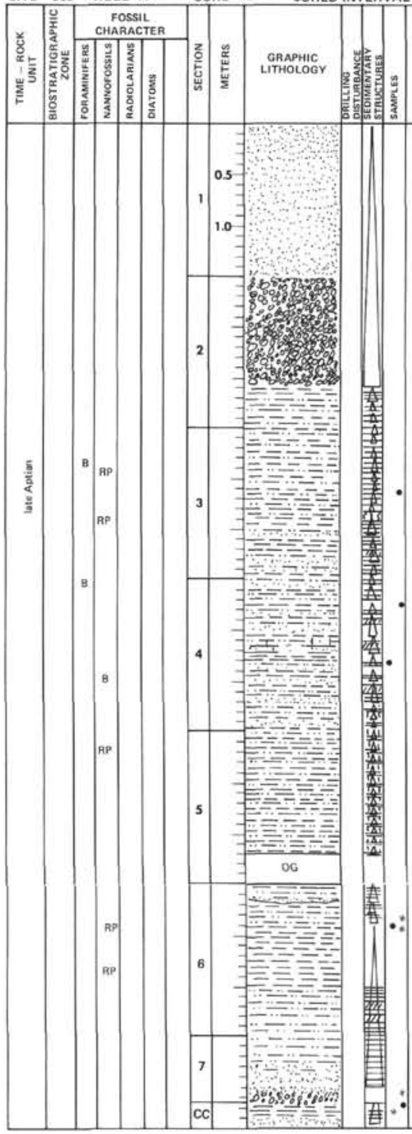

LITHOLOGIC DESCRIPTION

Graded sequences of very dark brown (5YR 3/1) CLAYSTONE at top, coarsening downward to greenish gray (5GY 2/1) VOLCANICLASTIC FINE SANDSTONE and SILTSTONE, and occasionally coarsening downward into an interlamination of dark volcaniclastic sandstone and light gray CLASTIC CARBONATE. The sandstone base of one graded sequence, that includes all of Section 1 and 110 cm of Section 2, is conglomeratic with clasts up to 2 cm.

SMEAR SLIDE SUMMARY (%):

	6, 49	4, 57	CC, 12	6, 31
	D	D	D	M
Texture:				
Silt	2	5	–	–
Clay	98	95	100	100
Composition:				
Heavy minerals	3	5	–	–
Clay	93	87	98	99
Volcanic glass	–	<1	–	–
Palagonite	<1	1	–	–
Zeolite	3	5	2	1
Calc. nannofossils	–	–	<1	–
Hematite	<1	<1	–	–
Celadonite	<1	2	–	–

ORGANIC CARBON AND CARBONATE (%):

	3, 68–74	4, 27–28	4, 84–85	6, 42–43	CC, 3–4
Organic carbon	.09	.11	.25	.25	.44
Carbonate	13	8	1	3	3

SITE 585 HOLE A CORE 13 CORED INTERVAL 799.6–808.7 m sub-bottom; 6921.9–6931.0 m below rig floor

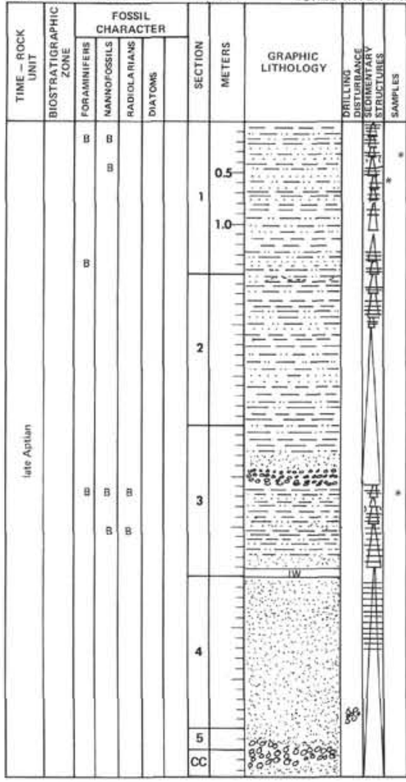

LITHOLOGIC DESCRIPTION

Graded sequences of olive black (5Y 2/1) VOLCANICLASTIC SILTSTONE and FINE- to MEDIUM-GRAINED SANDSTONE grading up into dark reddish brown (5YR 3/2) SLIGHTLY CALCAREOUS CLAYSTONE that is variously laminated, cross-bedded, scoured, and sometimes bioturbated. Basal contacts of coarser beds often contain concentrations of coarse celadonite.

Several zones are cemented by $CaCO_3$.

Several graded sequences with conglomeratic sandstone bases at the bottom of the core (Sections 4, 5, and Core Catcher).

SMEAR SLIDE SUMMARY (%):

	1, 38	1, 60	1, 69
	D	D	D
Texture:			
Sand	–	–	–
Silt	–	–	5
Clay	–	–	95
Composition:			
Clay	83	95	93
Volcanic glass	12	1	2
Zeolite	3	3	3
Carbonate unspec.	1	1	2
Fish remains	–	<1	–
Celadonite	1	–	–

SITE 585 HOLE A CORE 14 CORED INTERVAL 808.7–817.9 m sub-bottom; 6931.0–6940.2 m below rig floor

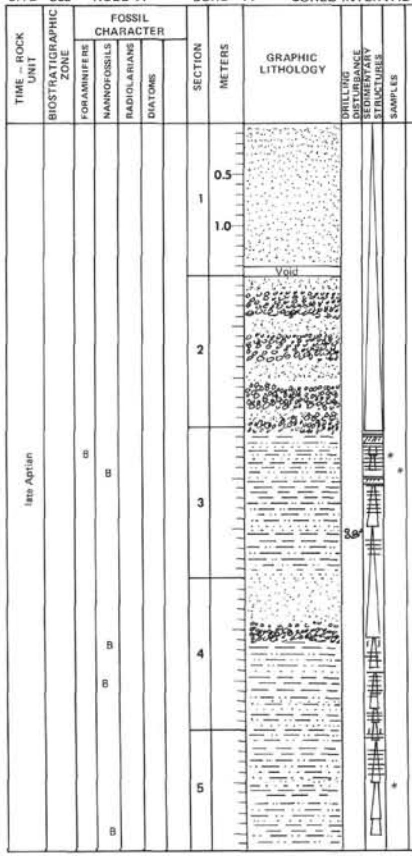

LITHOLOGIC DESCRIPTION

Graded sequences of volcaniclastics, with coarse clastic greenish black (5GY 2/1) SANDSTONE bases (two of which are conglomeratic) grading upward into dark green gray (10G 4/1) CLAYSTONE and, in a few cases, very dark gray (10YR 3/1) or dark reddish gray (5YR 4/2) CLAYSTONE.

SMEAR SLIDE SUMMARY (%):

	3, 31	3, 49	5, 54
	D	D	D
Texture:			
Silt	5	10	5
Clay	95	90	95
Composition:			
Clay	95	90	94
Volcanic glass	1	5	1
Zeolite	<1	–	1
Calc. nannofossils	<1	<1	1
Radiolarians	–	–	<1
Sponge spicules	–	<1	–
Volc. frags.	4	3	3

SITE 585 HOLE A CORE 15 CORED INTERVAL 817.9–827.0 m sub-bottom; 6940.2–6949.3 m below rig floor

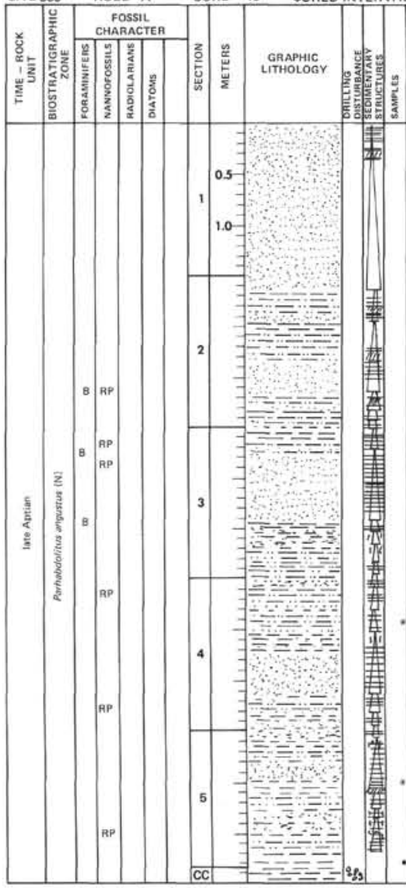

LITHOLOGIC DESCRIPTION

Graded sequences of volcaniclastic SANDSTONE and CLAYSTONE. The whole core is, in general, more homogeneous in texture than above (overlying) cores in that the coarse bases of sequences are not so coarse, and the claystone tops are more often silty claystone.

The dominant overall color is greenish black (5GY 2/1).

Basal contacts of many graded sequences are scoured.

SMEAR SLIDE SUMMARY (%):

	4, 43	5, 50
	M	M
Texture:		
Clay	100	100
Composition:		
Feldspar	1	1
Clay	91	70
Volcanic glass	<1	9
Zeolite	7	–
Carbonate unspec.	–	9
Calc. nannofossils	–	<1
Celadonite	–	10

ORGANIC CARBON AND CARBONATE (%):

	5, 136–137
Organic carbon	.10
Carbonate	14

SITE 585 HOLE A CORE 16 CORED INTERVAL 827.0–838.6 m sub-bottom; 6949.3–6960.9 m below rig floor

TIME – ROCK UNIT | BIOSTRATIGRAPHIC ZONE | FOSSIL CHARACTER (FORAMINIFERS, NANNOFOSSILS, RADIOLARIANS, DIATOMS) | SECTION | METERS | GRAPHIC LITHOLOGY | DRILLING DISTURBANCE | SEDIMENTARY STRUCTURES | SAMPLES

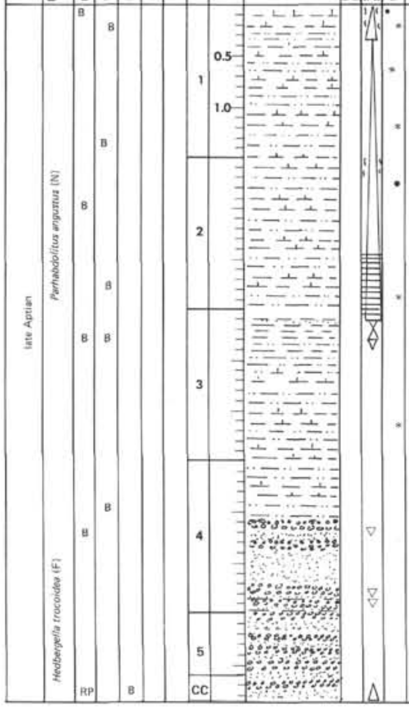

LITHOLOGIC DESCRIPTION

Graded sequences of volcaniclastics, mainly fine-grained sandstone, siltstone, and silty, calcareous claystone.

Silicified burrows are common throughout, but especially in Section 2.

Layer, lenses, and stringers rich in celadonite are common in the lower part of the recovered section.

Many of the units are quite hard and appear to be well cemented with silica cement.

There appear to be several fining-downward graded sequences, particularly in Section 4.

Calcareous material seems to be mostly from carbonate goids in with volcanigenic debris.

SMEAR SLIDE SUMMARY (%):

	1, 20	1, 85	1, 120	2, 140	3, 116
	M	M	D	D	D
Texture:					
Silt	–	15	1	5	85
Clay	100	85	99	95	15
Composition:					
Feldspar	<1	<1	<1	1	–
Mica	–	–	–	–	1
Heavy minerals	1	–	<1	1	3
Clay	69	50	80	50	10
Glauconite	–	–	–	–	5
Zeolite	–	1	1	5	10
Carbonate unspec.	30	9	18	–	5
Calc. nannofossils	–	–	1	<1	<1
Radiolarians	–	–	1	<1	–
Sponge spicules	–	–	–	<1	–
Fish remains	–	–	<1	–	–
Recryst. SiO_2	–	40	–	43	56

ORGANIC CARBON AND CARBONATE (%):

	1, 8–9	2, 31–34
Organic carbon	.16	.16
Carbonate	15	7

SITE 585 HOLE A CORE 17 CORED INTERVAL 838.6–847.6 m sub-bottom; 6960.9–6970.1 m below rig floor

TIME – ROCK UNIT | BIOSTRATIGRAPHIC ZONE | FOSSIL CHARACTER (FORAMINIFERS, NANNOFOSSILS, RADIOLARIANS, DIATOMS) | SECTION | METERS | GRAPHIC LITHOLOGY | DRILLING DISTURBANCE | SEDIMENTARY STRUCTURES | SAMPLES

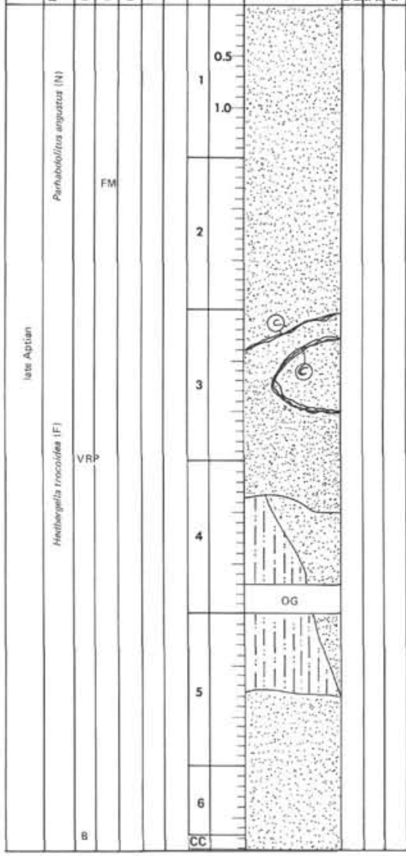

LITHOLOGIC DESCRIPTION

A single very gradually fining-upward sequence of volcaniclastic sandstone, grading from medium-size sand at the base to fine sand at the top. What appears to be a slice of a vertical "vein" of siltstone that cuts across sandstone in Sections 4 and 5.

Thin calcite veins cut core in Section 3 (indicated " (c) " on graphic column).

Dominant color is dark greenish gray (5G 4/1).

Carbonate ooids observed along with volcaniclastics on cut surface of core.

SITE 585 HOLE A CORE 18 CORED INTERVAL 847.6–857.8 m sub-bottom; 6970.1–6980.1 m below rig floor

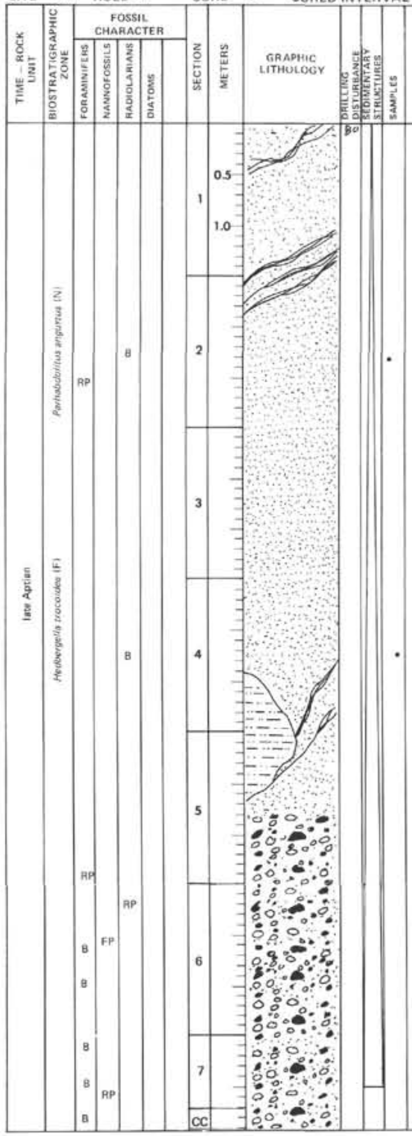

LITHOLOGIC DESCRIPTION

Entire core is part of a graded sequence that consists of MEDIUM-SIZED SANDSTONE of volcaniclastics and carbonate ooids at the top of the core grading downward into COARSE SANDSTONE becoming CONGLOMERATIC and poorly sorted (debris flow?) by Section 5 with clasts up to 5 cm of VOLCANICS, CLAYSTONE, and SILTY CLAYSTONE, and also coarse carbonate fragments (mainly rudistid fragments and benthic foram Orbitalina) in addition to the ooids which are present throughout.

= "veins" of finer material (siltstone) cut across the sandstone as almost vertical anastomosing stringers at several places and as a thicker "dike?", truncated by the core, in Sections 4 and 5.

Dominant color throughout is greenish black (5GY 2/1).

ORGANIC CARBON AND CARBONATE (%):

	2, 81–82	4, 79–80
Organic carbon	.21	.23
Carbonate	16	21

SITE 585 HOLE A CORE 19 CORED INTERVAL 857.8–866.9 m sub-bottom; 6980.1–6989.2 m below rig floor

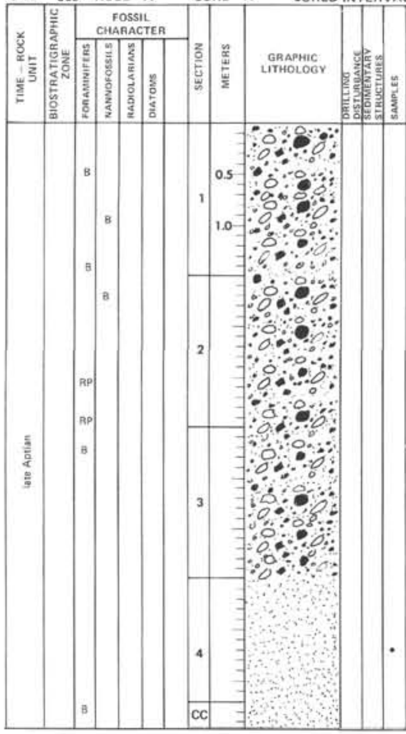

LITHOLOGIC DESCRIPTION

Entire core is a CONGLOMERATIC, COARSE-SAND VOLCANICLASTIC SANDSTONE with some clasts larger than the diameter of the core consisting of claystone, siltstone, basalt, and limestone. Many of the larger clasts are rounded to sub-rounded although most of the volcaniclastic debris is angular with green reaction rims (celadonite). Matrix clasts consist mainly of basalt, volcanic glass, red lithic fragments, and carbonate debris (ooids, benthic forams, and rudistids).

The unsorted nature of the clasts and rounding of many of the mudstone clasts suggest that this material is part of a debris-flow deposit.

ORGANIC CARBON AND CARBONATE (%):

	4, 71–72
Organic carbon	.26
Carbonate	6

SITE 585 HOLE A CORE 20 CORED INTERVAL 866.9–876.1 m sub-bottom; 6989.2–6998.4 m below rig floor

TIME – ROCK UNIT: late Aptian

FOSSIL CHARACTER (Foraminifers / Nannofossils / Radiolarians / Diatoms): B, B, B RP, RP B, B, B, RP, RP B, B, B B, B, B

SECTION: 1, 2, 3 — METERS: 0.5, 1.0

GRAPHIC LITHOLOGY:

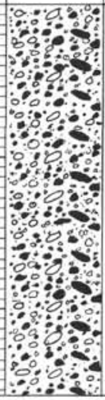

LITHOLOGIC DESCRIPTION

Entire core consists of a VOLCANICLASTIC SANDSTONE matrix with larger clasts (up to at least[a] 5 cm) of SILTSTONE, CLAYSTONE, BASALT, VOLCANIC GLASS and LITHIC FRAGMENTS, and SHALLOW-WATER CARBONATE DEBRIS (benthic forams, ooids, rudistid fragments). Many of the larger clasts, especially claystone and siltstone, are sub-rounded to rounded.

Overall color of sandstone matrix is greenish black (5GY 2/1).

Vugs in clasts at base of Section 2 lined with zeolites (henlandite?). One 15-cm piece? clast? of amigoaloidal basalt.

Most volcanic fragments are rimmed by celadonite.

[a] Some clasts are truncated by core but are probably boulders.

SMEAR SLIDE SUMMARY (%):

	1, 60 M	3, 30 M
Texture:		
Silt	15	10
Clay	85	90
Composition:		
Clay	83	90
Volcanic glass	15	2
Zeolite	2	–
Carbonate unspec.	1	–
Volc. frags.	4	–
Celadonite	1	–

ORGANIC CARBON AND CARBONATE (%):

	2, 102–103	3, 67–68
Organic carbon	.19	.18
Carbonate	3	3

SITE 585 HOLE A CORE 21 CORED INTERVAL 876.1–885.2 m sub-bottom; 6998.4–7007.5 m below rig floor

TIME – ROCK UNIT: late Aptian

FOSSIL CHARACTER: B, B, RP

SECTION: 1, CC — METERS: 0.5, 1.0

GRAPHIC LITHOLOGY:

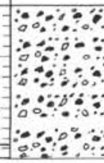

LITHOLOGIC DESCRIPTION

Debris-flow deposit consisting mainly of a coarse greenish black (5GY 2/1) SANDSTONE matrix with poorly sorted, angular to sub-rounded fragments of SILTSTONE, CLAYSTONE, and BASALT. Matrix contains grains of red lithic fragments, volcanic glass, and basalt. No carbonate grains. Some clasts are actually boulders >10 cm in diameter truncated by core. Many volcanic fragments in matrix have a celadonite alteration rim.

SMEAR SLIDE SUMMARY (%):

	1, 82 M	1, 87 M
Texture:		
Silt	15	5
Clay	85	95
Composition:		
Heavy minerals	1	1
Clay	85	89
Volcanic glass	<1	8
Zeolite	7	2
Carbonate unspec.	1	1
Pyroxene	3	–
Celadonite	3	–

ORGANIC CARBON AND CARBONATE (%):

	CC, 10–11
Organic carbon	0.1
Carbonate	0

SITE 585 HOLE A CORE 22 CORED INTERVAL 885.2–892.9 m sub-bottom; 7007.5–7015.2 m below rig floor

TIME – ROCK UNIT: late Aptian

SECTION: 1, 2, CC — METERS: 0.5, 1.0

GRAPHIC LITHOLOGY:

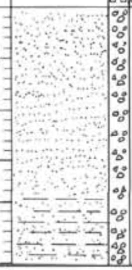

LITHOLOGIC DESCRIPTION

Section 1, 0–95 cm: fine drill cuttings, mostly of chert, claystone, and chalk.

Section 1, 95–150 cm: greenish black (5GY 2/1 to 5GY 3/1) coarse VOLCANICLASTIC SANDSTONE; poorly sorted with pebble-sized clasts in a sand matrix.

Core Catcher: 62 cm of greenish black (5GY 2/1) volcaniclastic silty sandstone and coarse sandstone.


0 cm
25
50
75
100
125
150
1-1
1-2
1-3
1-4
1-5
1,CC
H-1
H1,CC
2,CC
3-1
3,CC
4,CC
5,CC
6-1
6-2

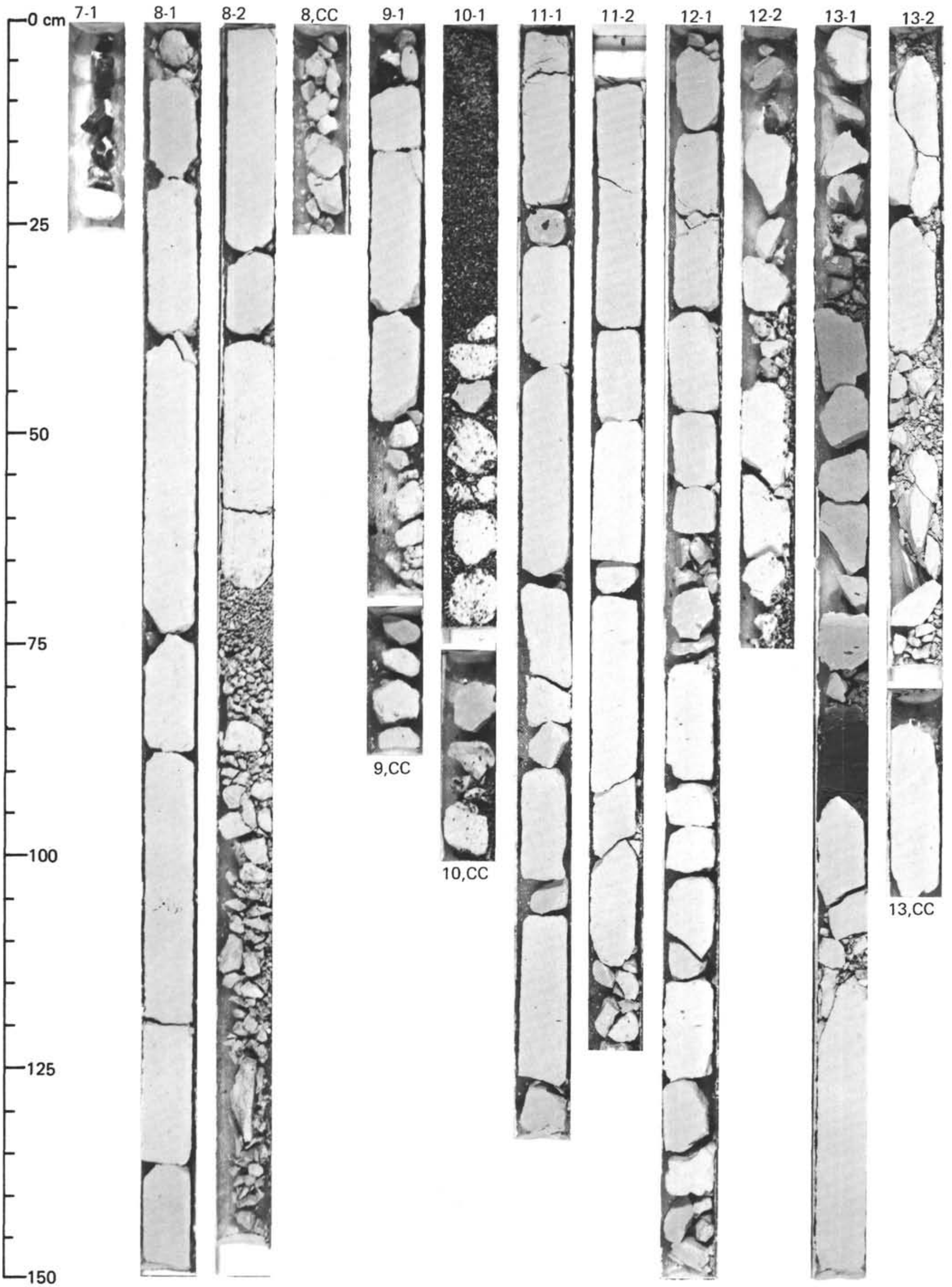
0 cm
25
50
75
100
125
150
7-1
8-1
8-2
8,CC
9-1
9,CC
10-1
10,CC
11-1
11-2
12-1
12-2
13-1
13-2
13,CC

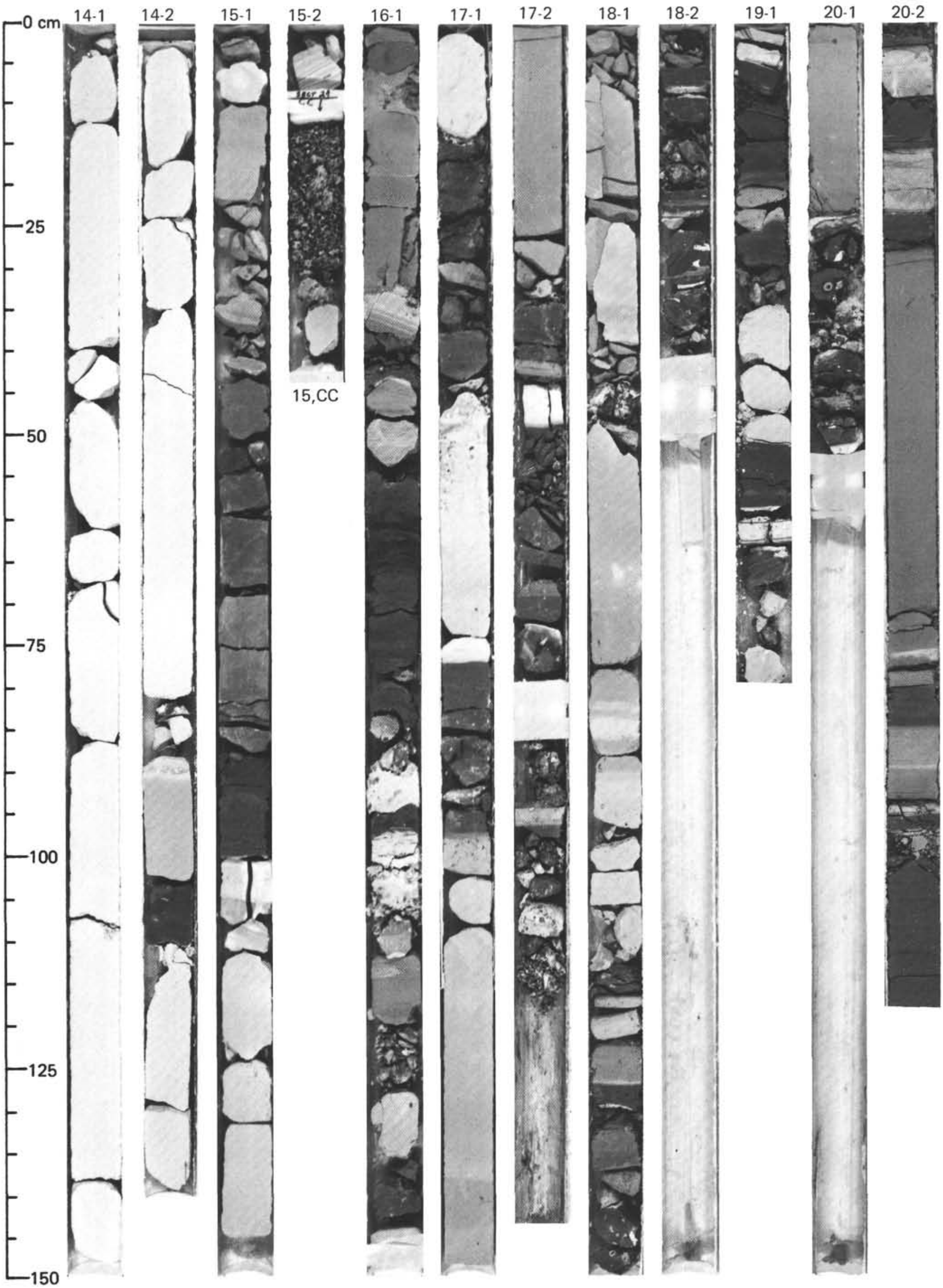
0 cm
25
50
75
100
125
150
14-1
14-2
15-1
15-2
16-1
17-1
17-2
18-1
18-2
19-1
20-1
20-2
15,CC


0 cm
25
50
75
100
125
150
20-3
20-4
21-1
21,CC
22
NO RECOVERY
23,CC
24,CC
25,CC
26-1
27-1
27-2
27-3
27-4
27,CC

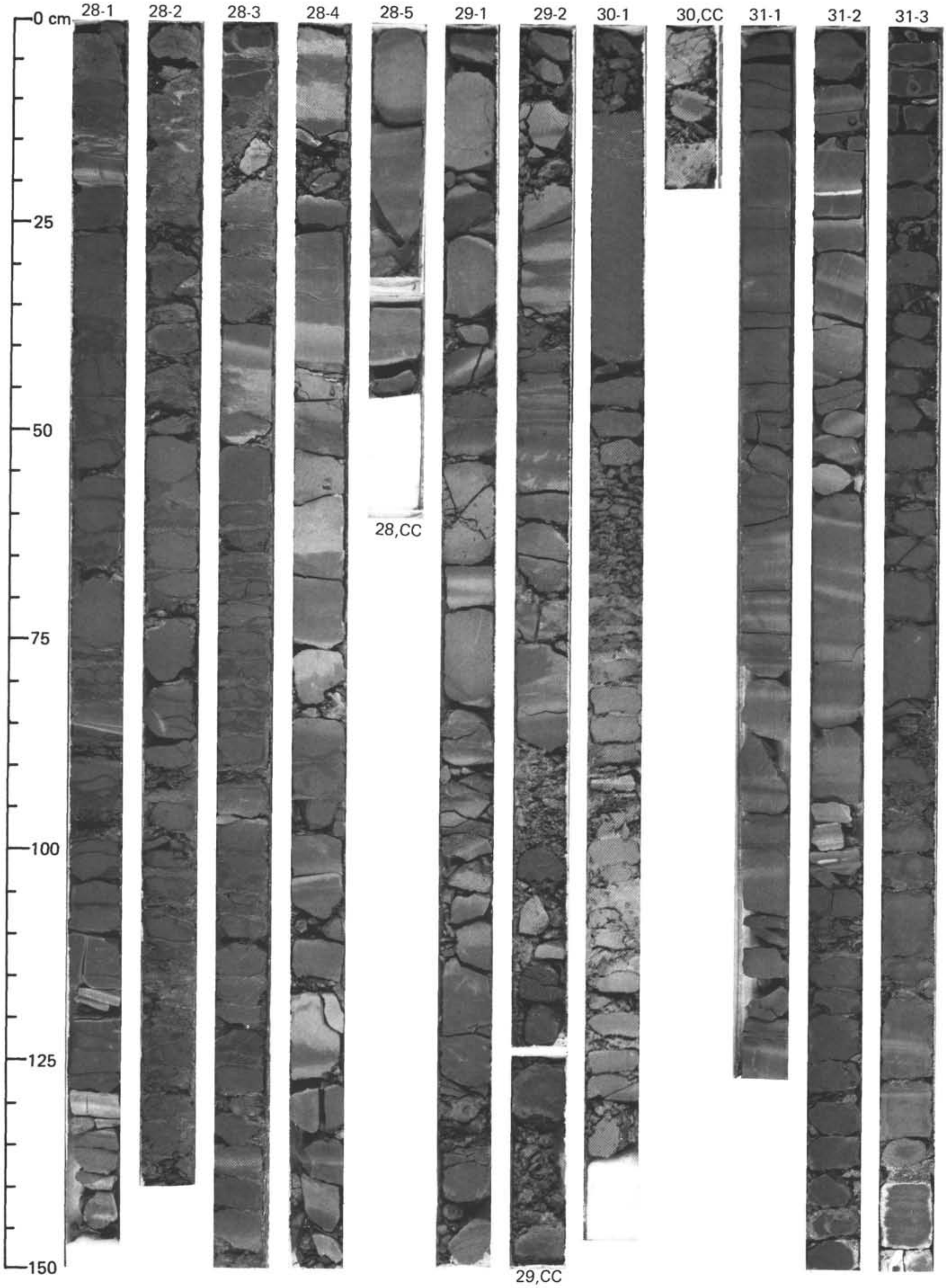
0 cm
25
50
75
100
125
150
28-1
28-2
28-3
28-4
28-5
28,CC
29-1
29-2
29,CC
30-1
30,CC
31-1
31-2
31-3

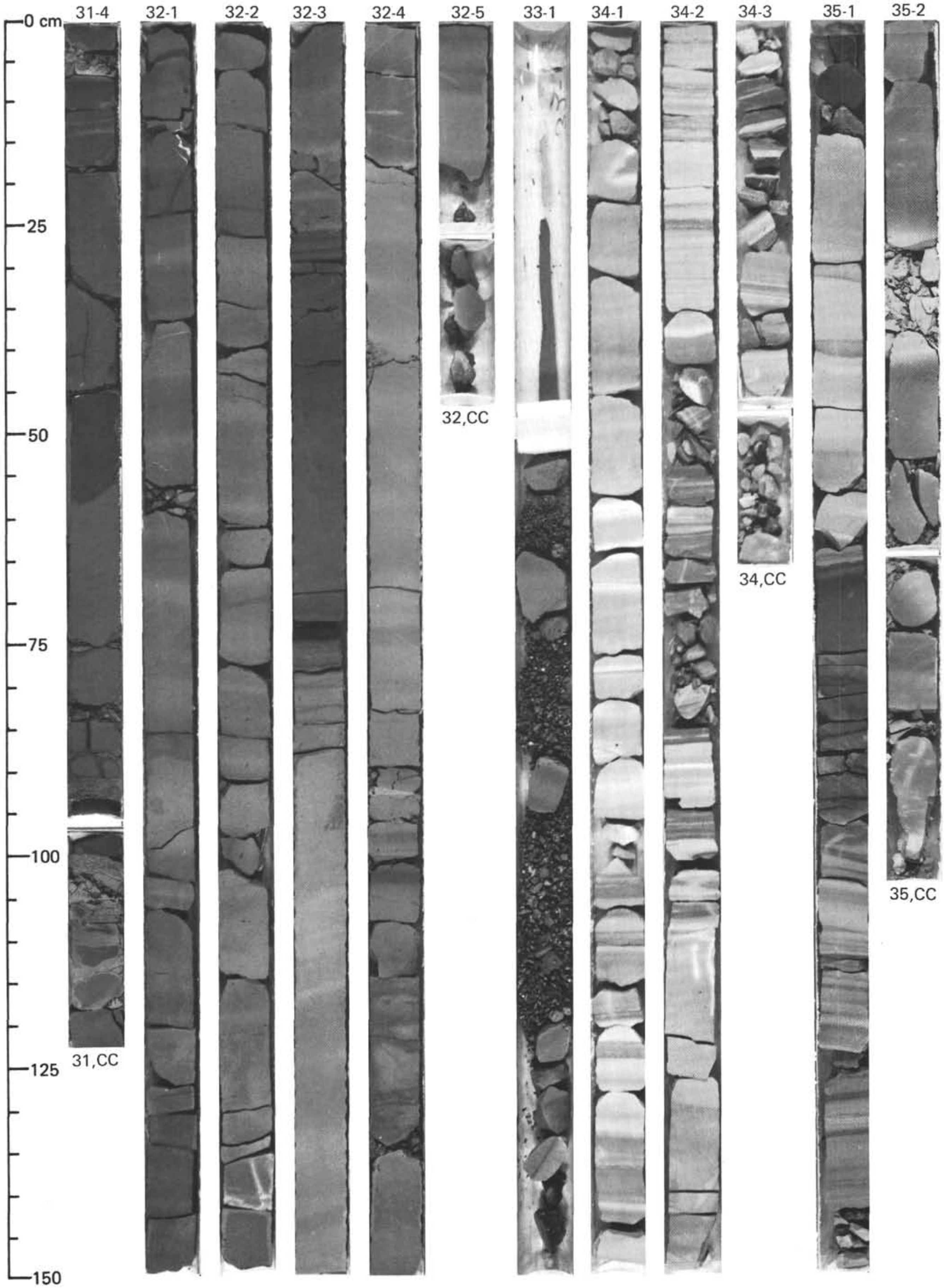
0 cm
25
50
75
100
125
150
31-4
32-1
32-2
32-3
32-4
32-5
33-1
34-1
34-2
34-3
35-1
35-2
32,CC
34,CC
35,CC
31,CC

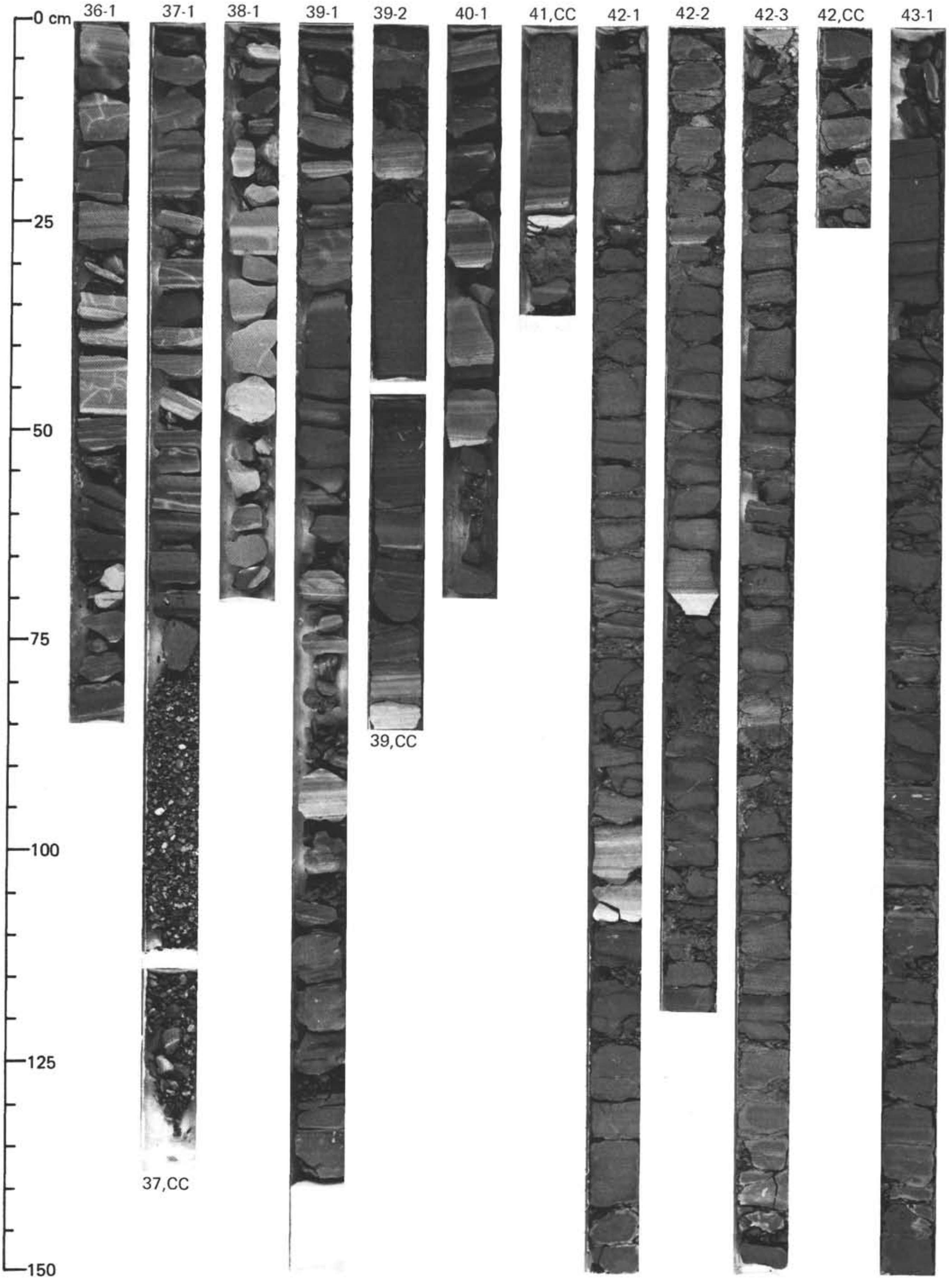
0 cm
25
50
75
100
125
150
36-1
37-1
38-1
39-1
39-2
40-1
41,CC
42-1
42-2
42-3
42,CC
43-1
39,CC
37,CC

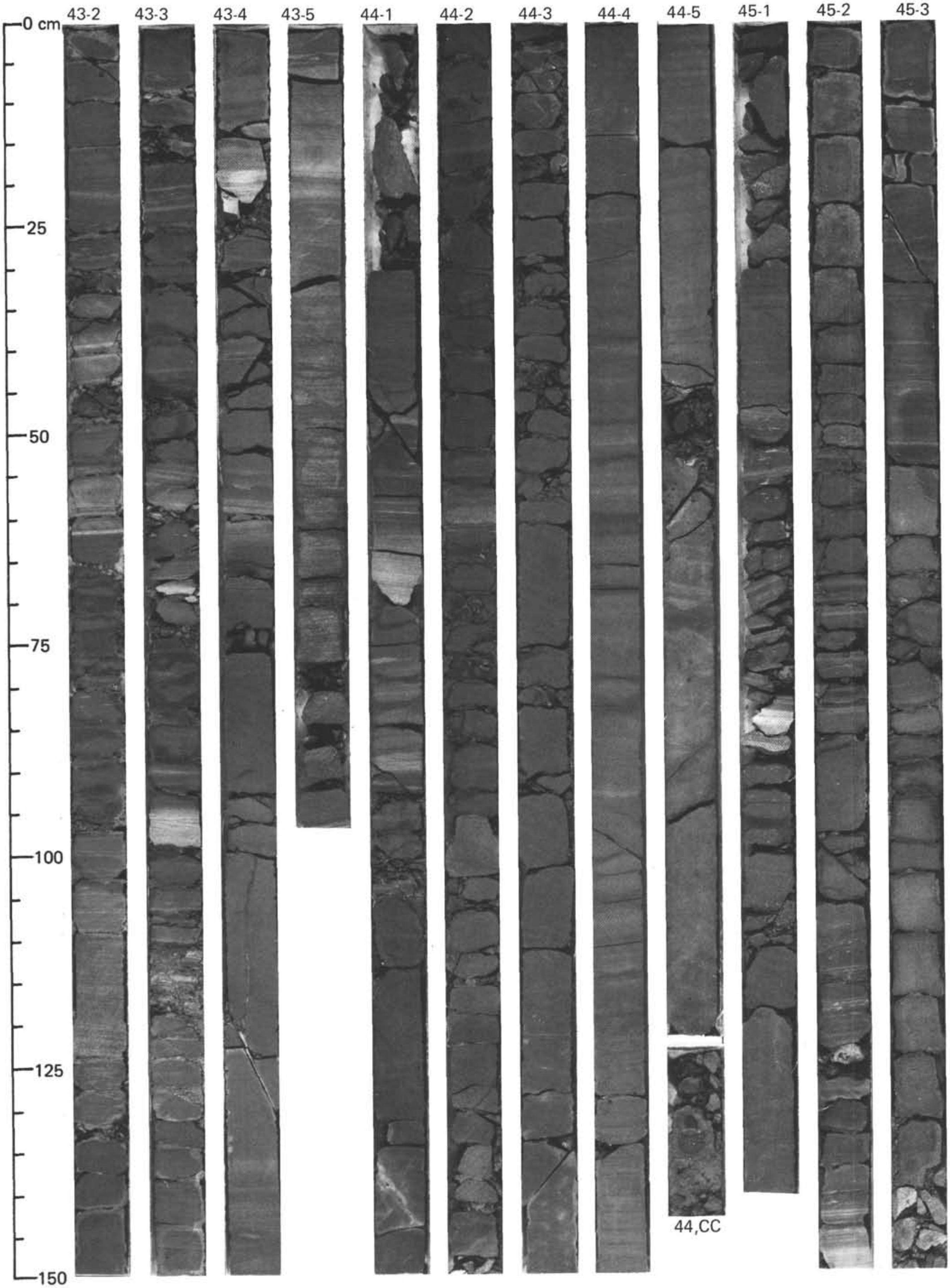
0 cm
25
50
75
100
125
150
43-2
43-3
43-4
43-5
44-1
44-2
44-3
44-4
44-5
44,CC
45-1
45-2
45-3

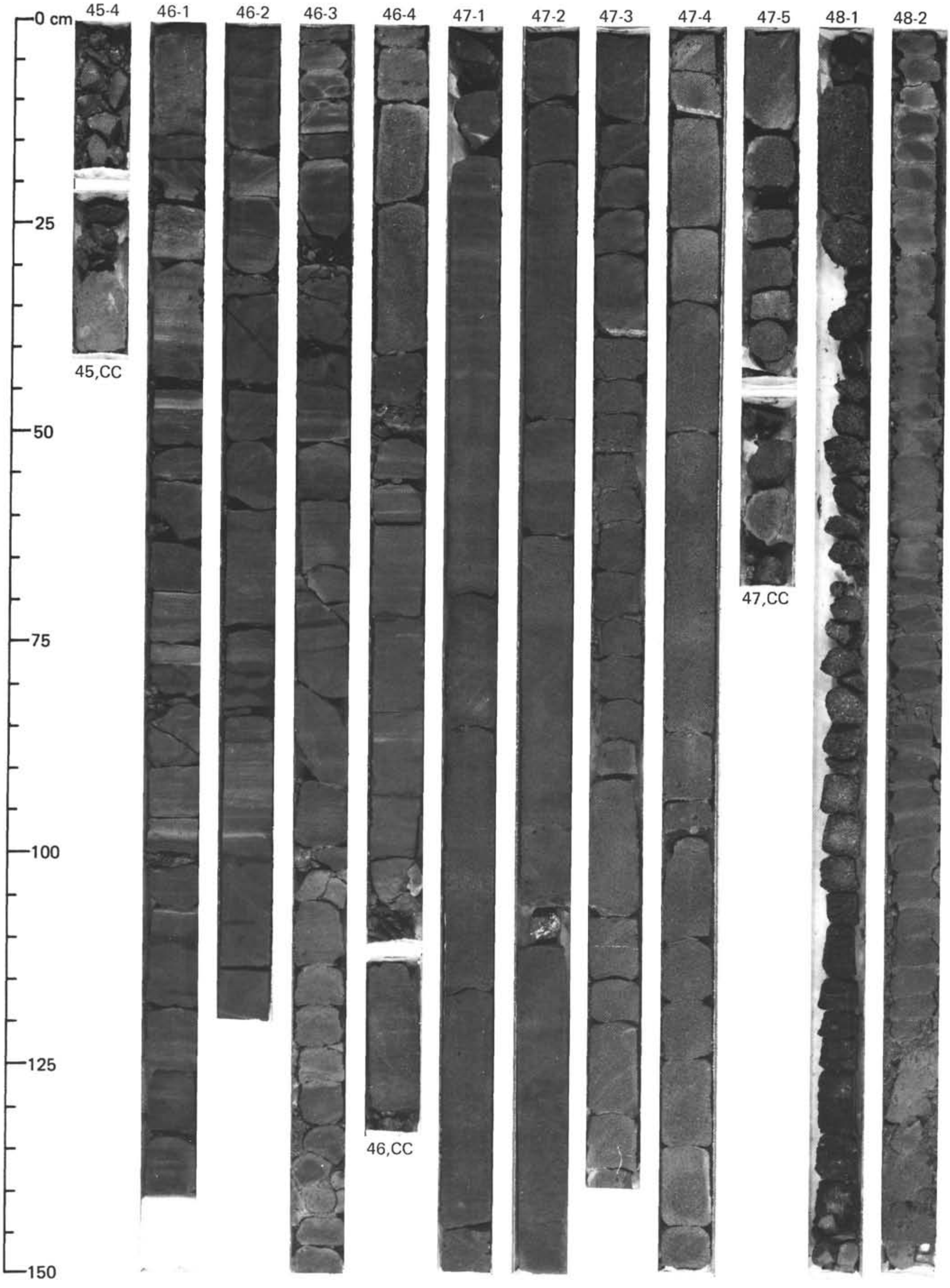
0 cm
25
50
75
100
125
150
45-4
46-1
46-2
46-3
46-4
47-1
47-2
47-3
47-4
47-5
48-1
48-2
45,CC
46,CC
47,CC

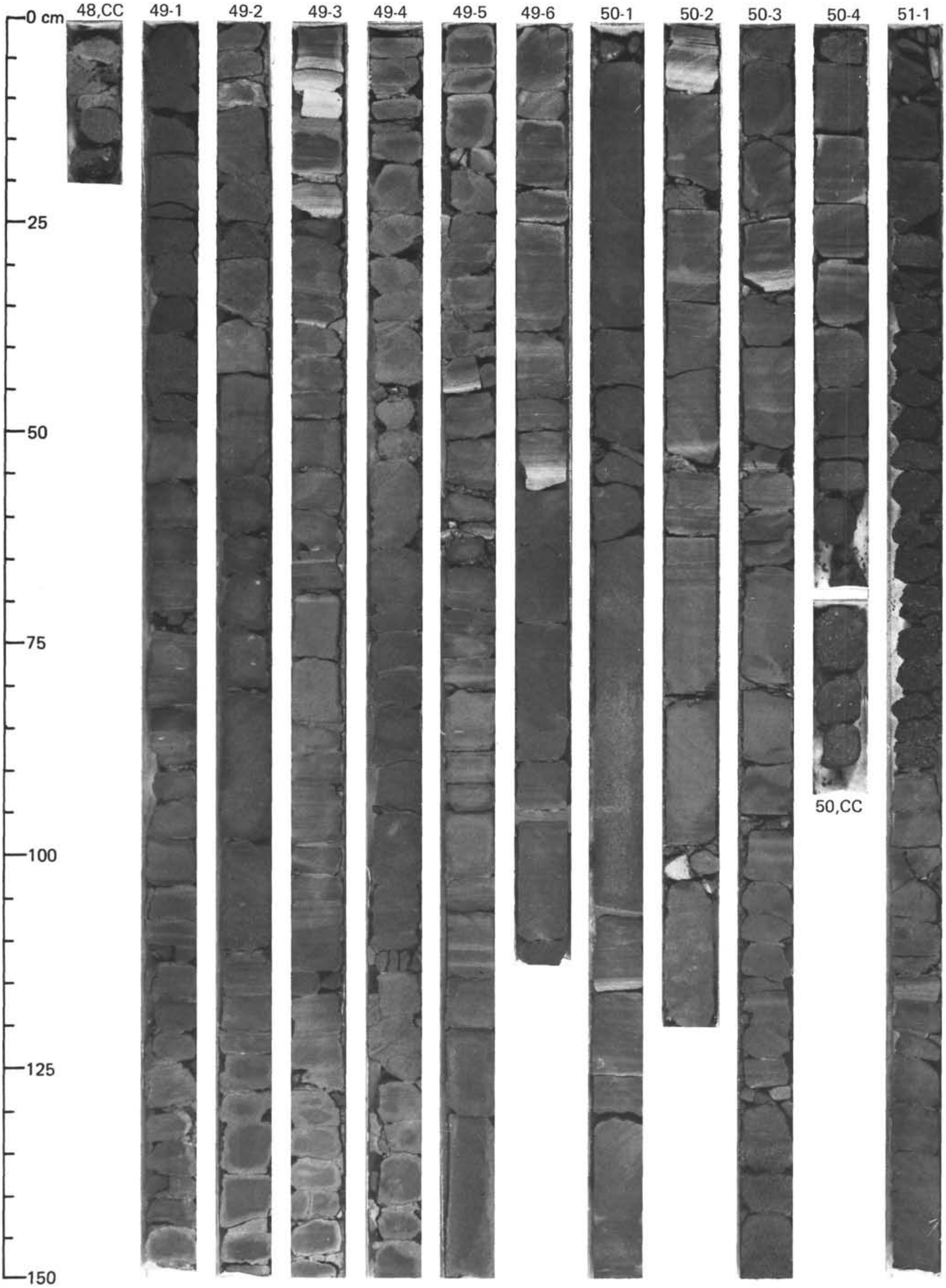
0 cm
25
50
75
100
125
150
48,CC
49-1
49-2
49-3
49-4
49-5
49-6
50-1
50-2
50-3
50-4
50,CC
51-1

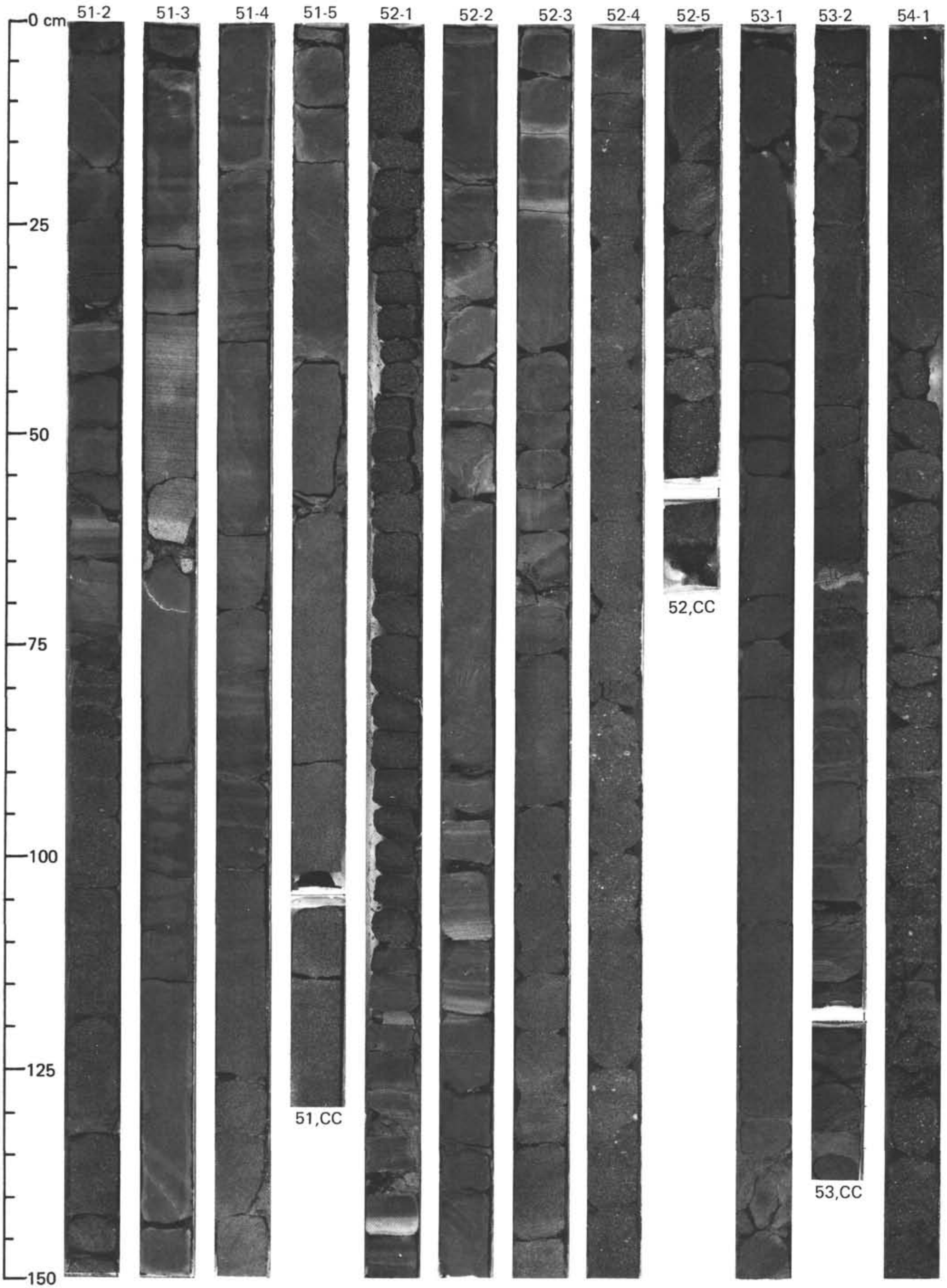
0 cm
25
50
75
100
125
150
51-2
51-3
51-4
51-5
52-1
52-2
52-3
52-4
52-5
53-1
53-2
54-1
51,CC
52,CC
53,CC

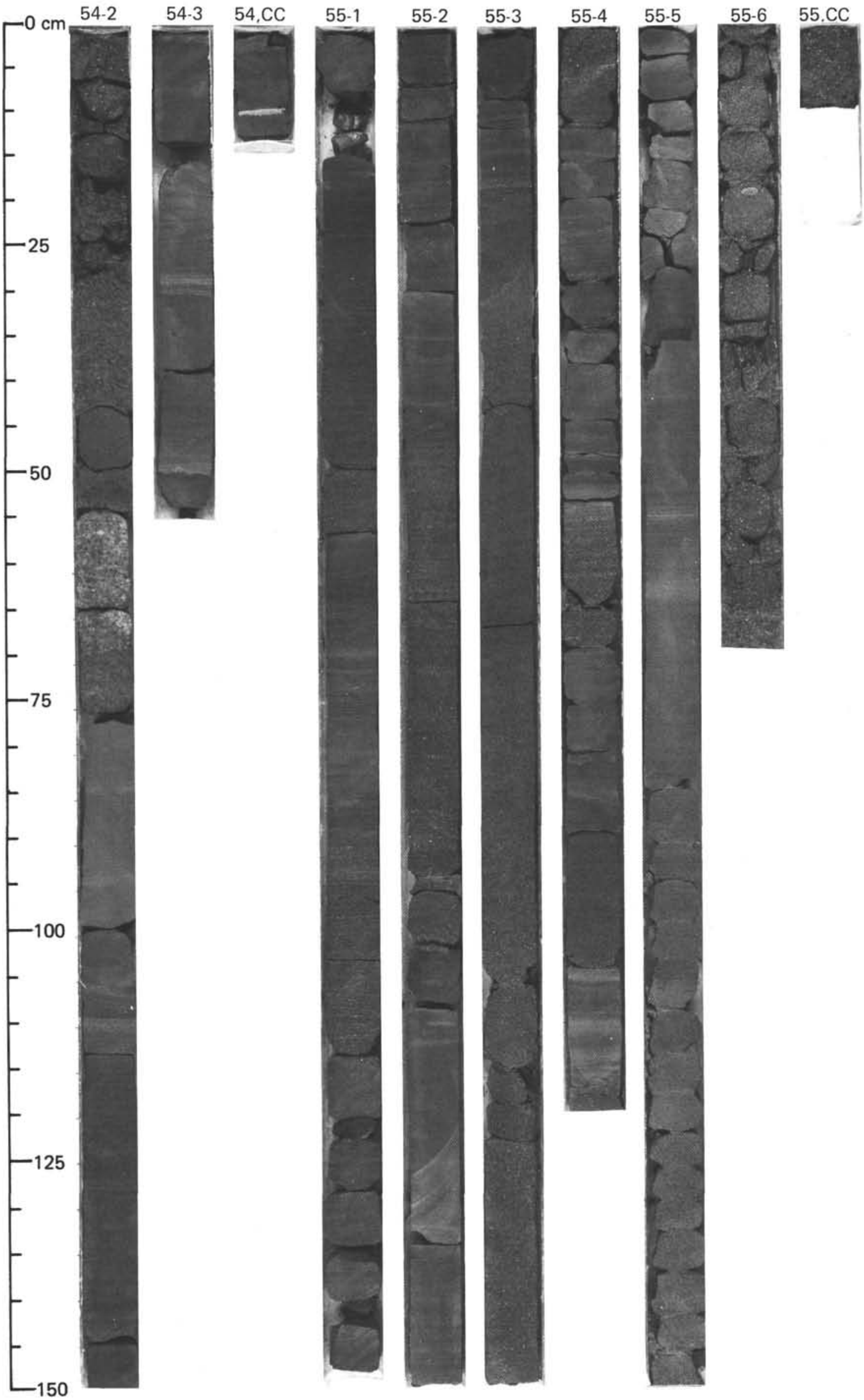
54-2
54-3
54,CC
55-1
55-2
55-3
55-4
55-5
55-6
55,CC
0 cm
25
50
75
100
125
150

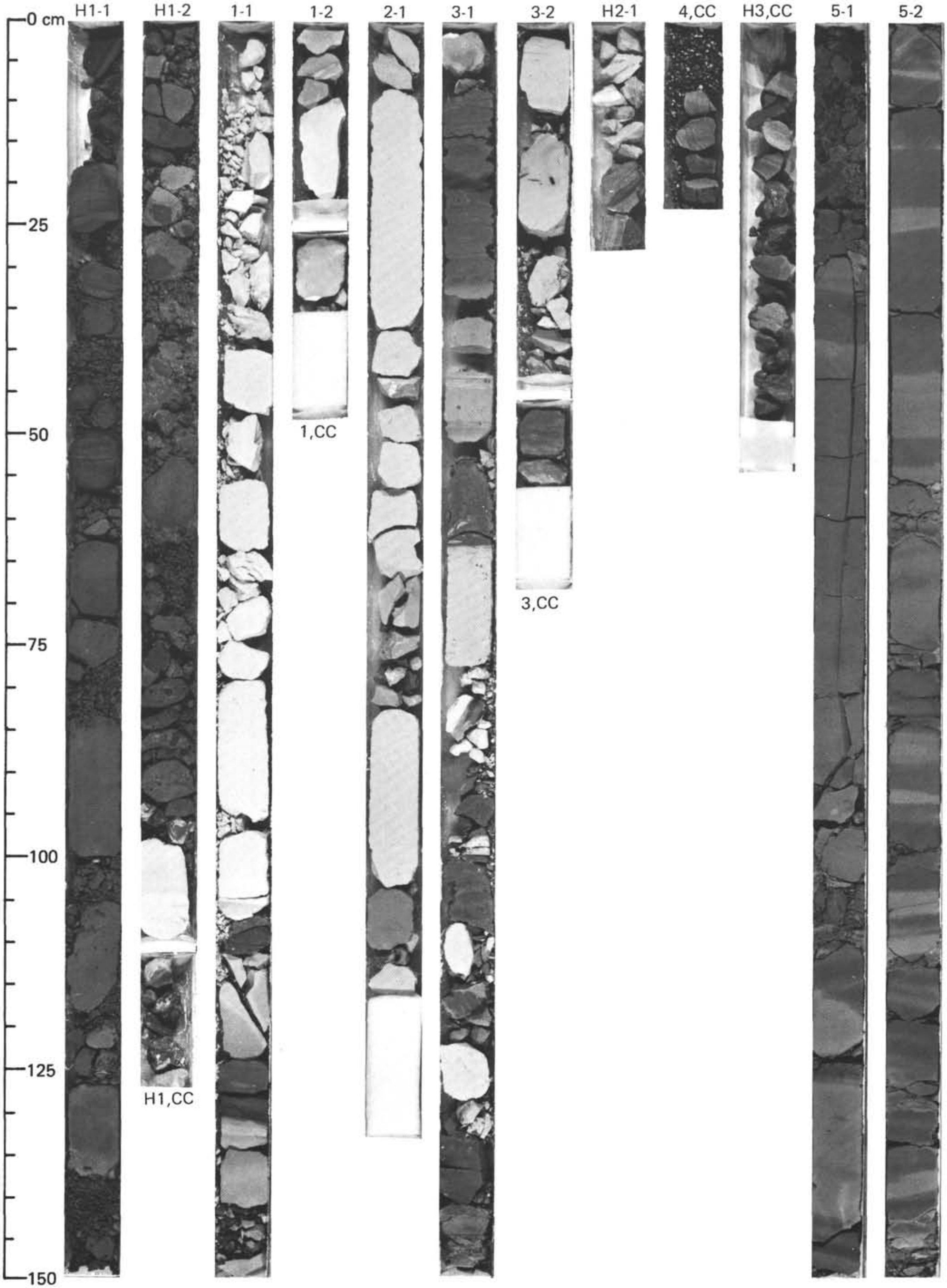
0 cm
25
50
75
100
125
150
H1-1
H1-2
H1,CC
1-1
1-2
1,CC
2-1
3-1
3-2
3,CC
H2-1
4,CC
H3,CC
5-1
5-2

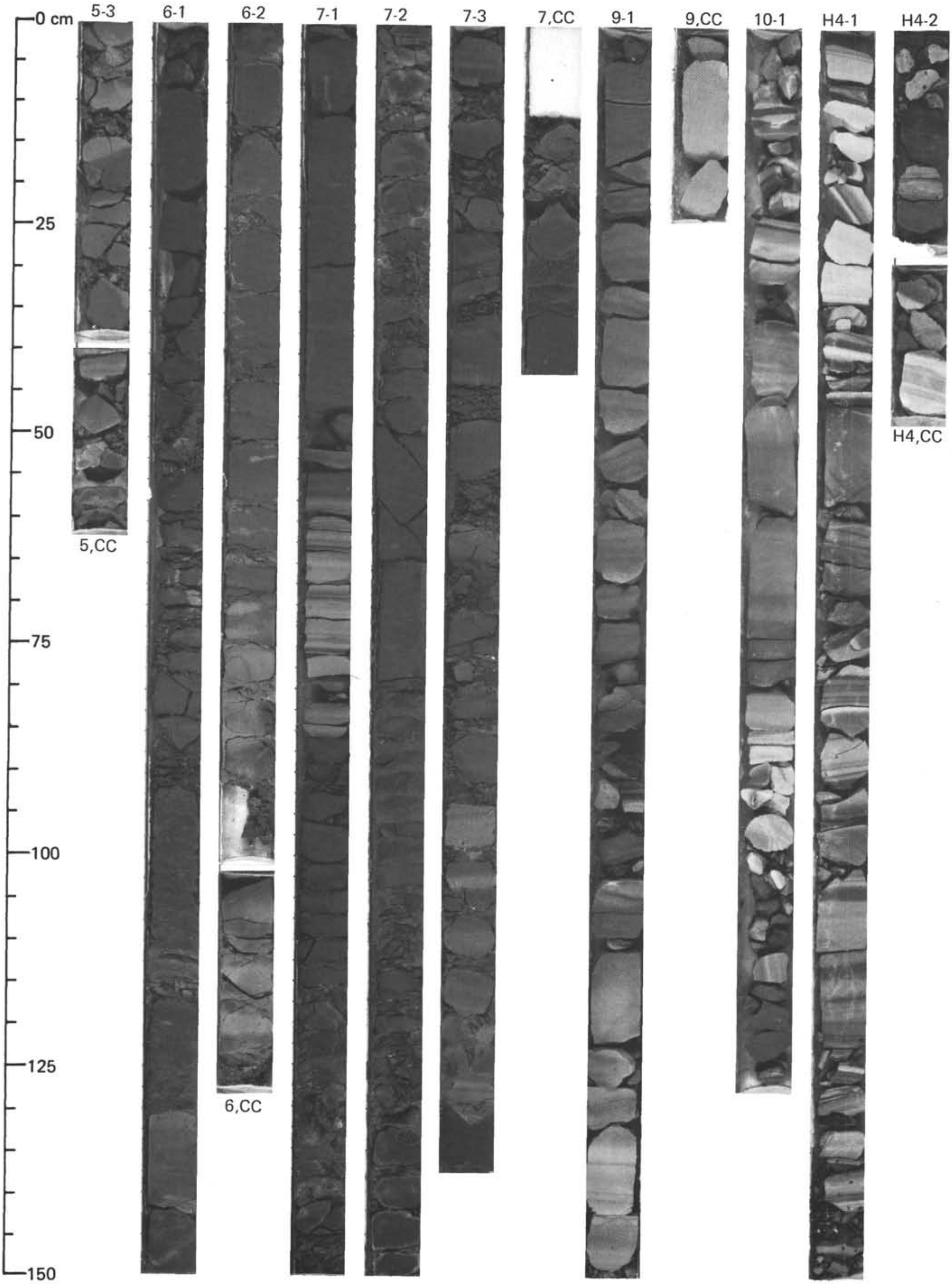
0 cm
25
50
75
100
125
150
5-3
6-1
6-2
7-1
7-2
7-3
7,CC
9-1
9,CC
10-1
H4-1
H4-2
5,CC
6,CC
H4,CC

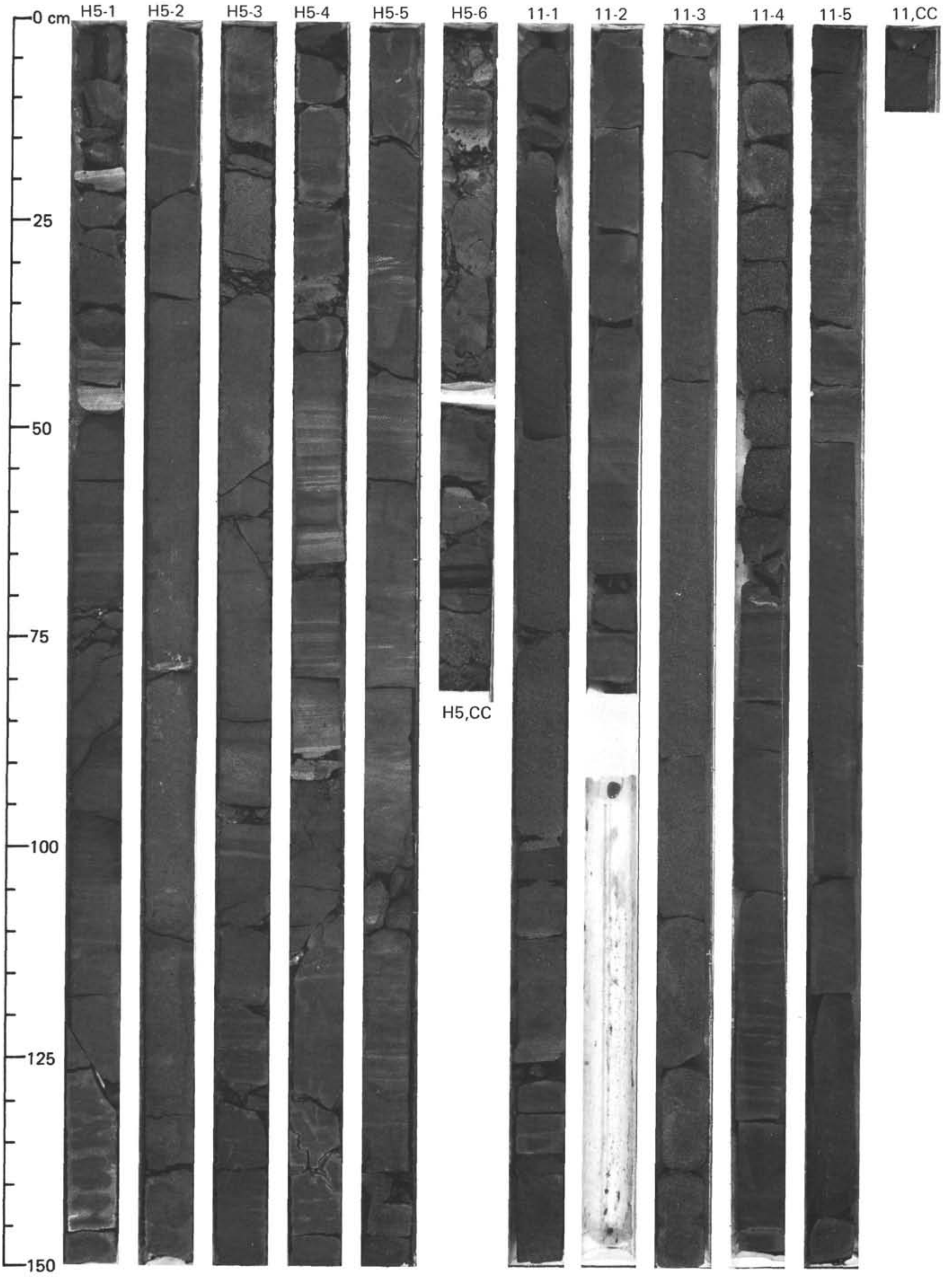
0 cm
25
50
75
100
125
150
H5-1
H5-2
H5-3
H5-4
H5-5
H5-6
H5,CC
11-1
11-2
11-3
11-4
11-5
11,CC

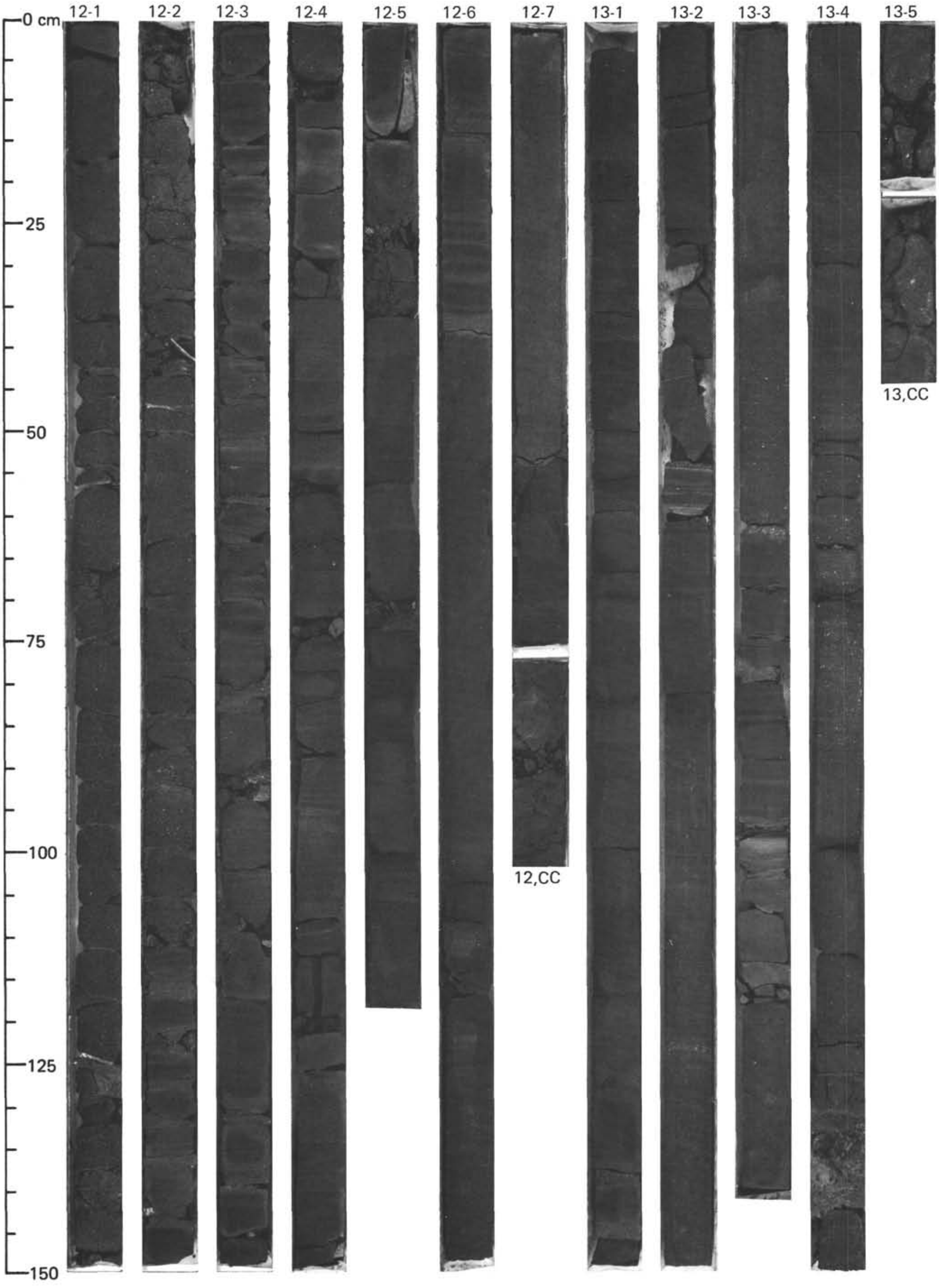
0 cm
25
50
75
100
125
150
12-1
12-2
12-3
12-4
12-5
12-6
12-7
13-1
13-2
13-3
13-4
13-5
12,CC
13,CC

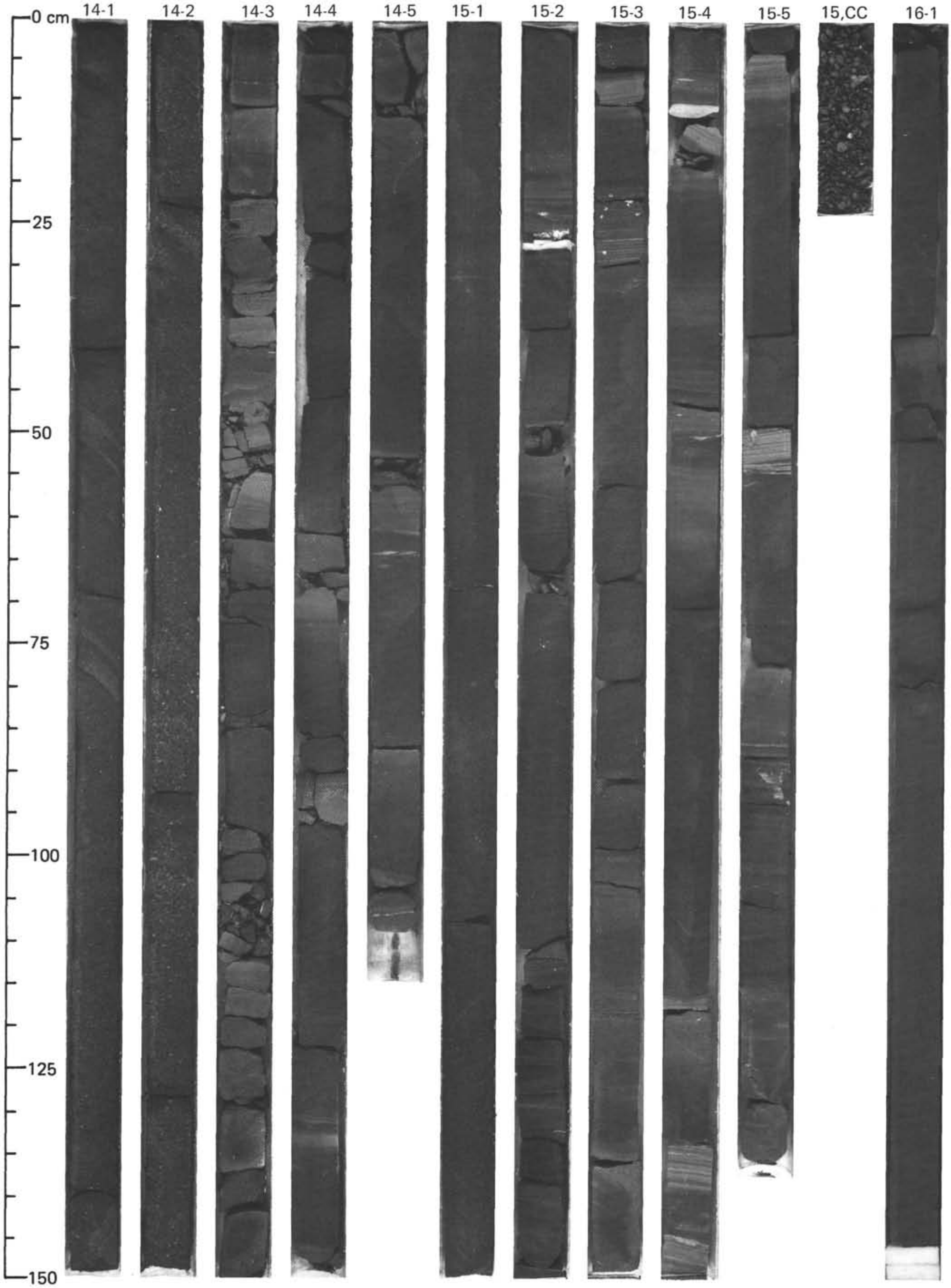
0 cm
25
50
75
100
125
150
14-1
14-2
14-3
14-4
14-5
15-1
15-2
15-3
15-4
15-5
15,CC
16-1

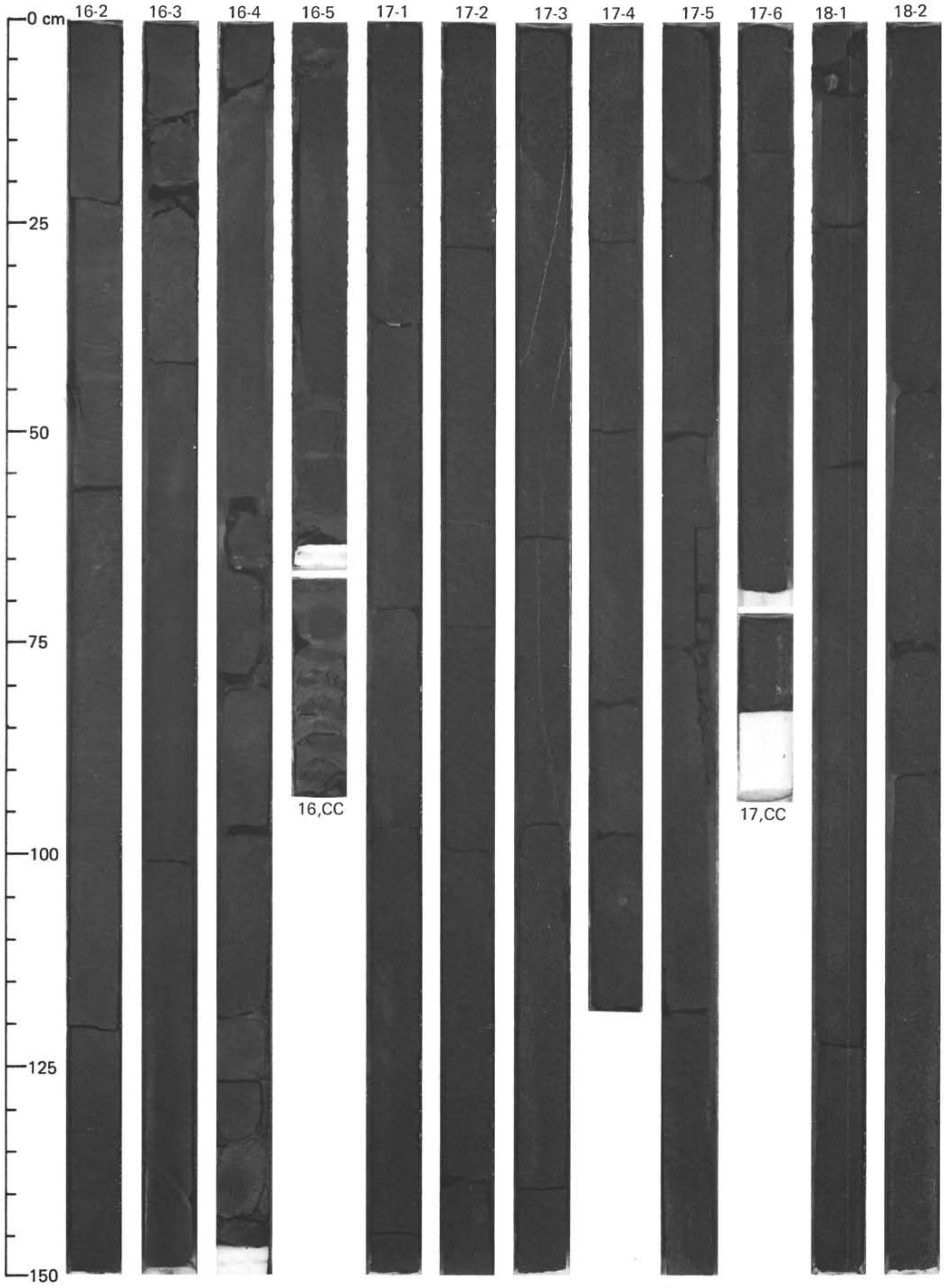
0 cm
25
50
75
100
125
150
16-2
16-3
16-4
16-5
17-1
17-2
17-3
17-4
17-5
17-6
18-1
18-2
16,CC
17,CC

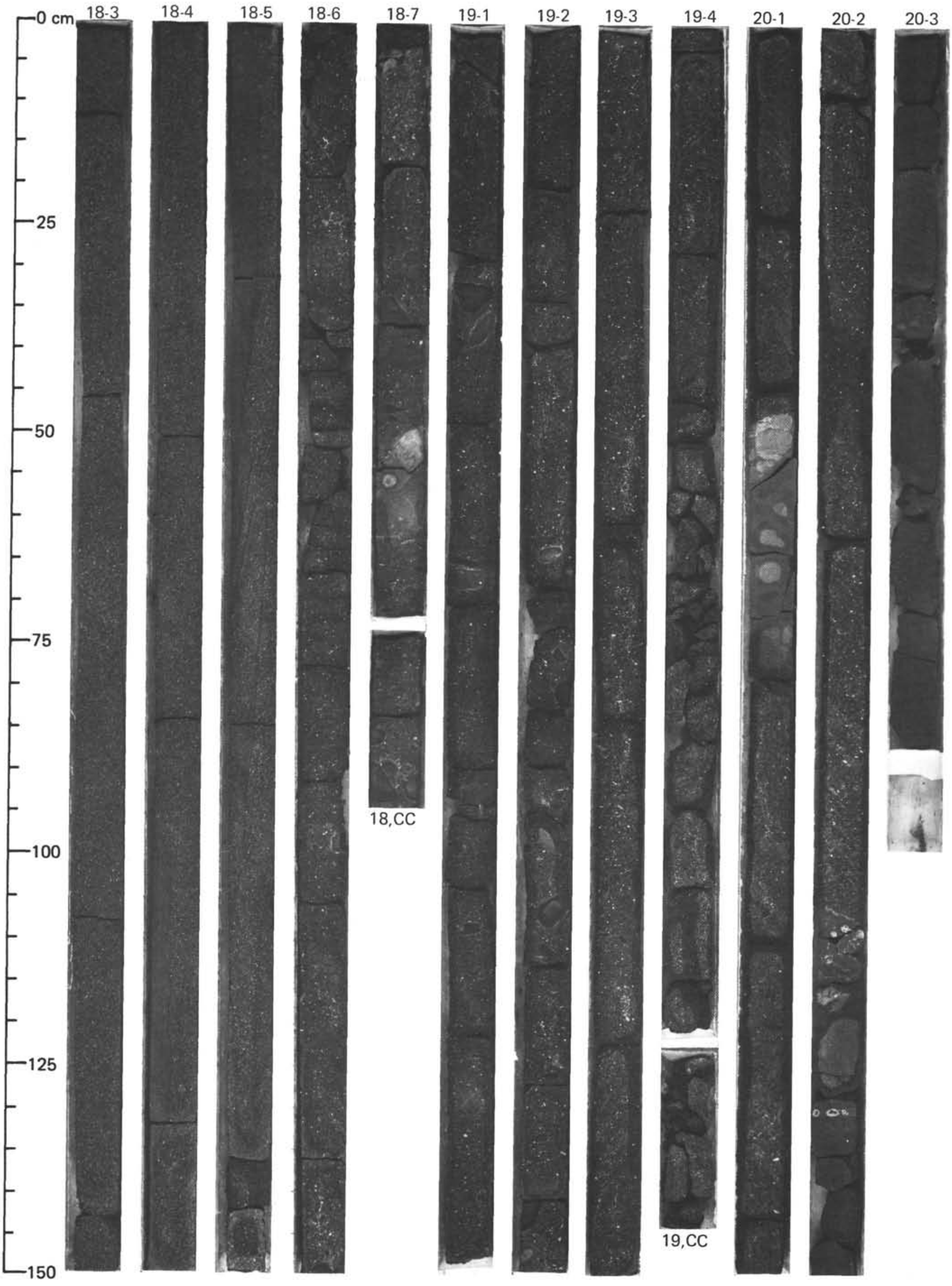
0 cm
25
50
75
100
125
150
18-3
18-4
18-5
18-6
18-7
19-1
19-2
19-3
19-4
20-1
20-2
20-3
18,CC
19,CC

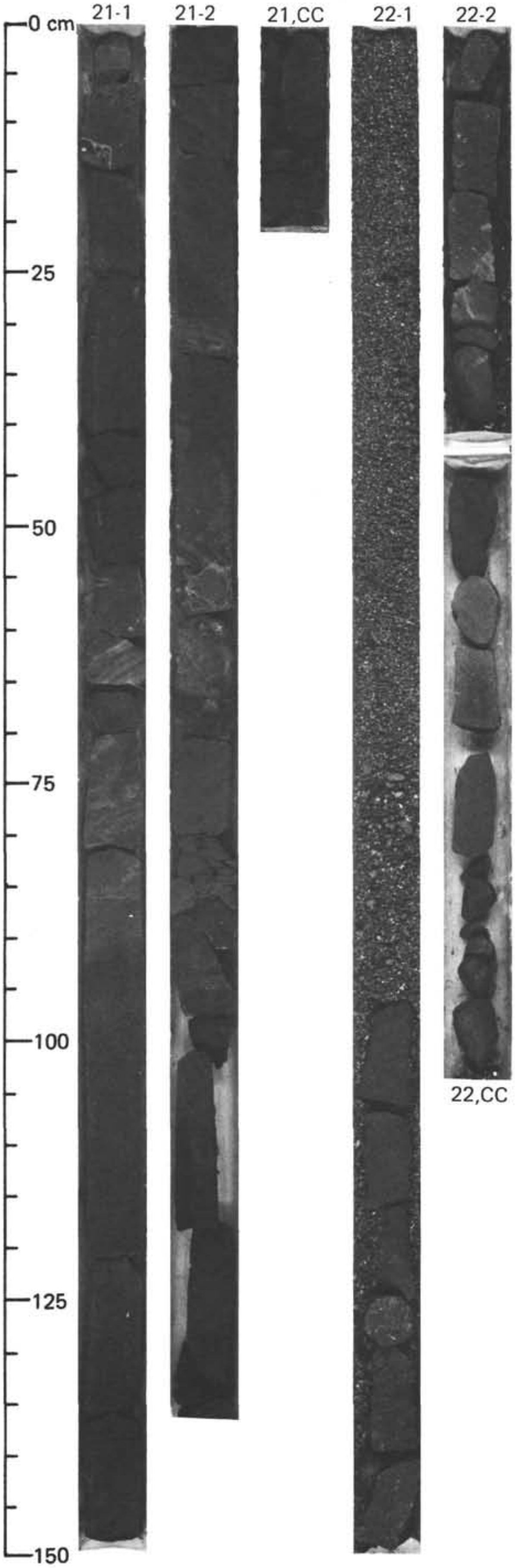

0 cm
25
50
75
100
125
150
21-1
21-2
21,CC
22-1
22-2
22,CC